

EVALUATION OF THE INTERACTION OF  
MECHANICAL DAMAGE AND WELDS

FINAL REPORT

July 2006

Submitted to:

Materials Committee  
Pipeline Research Committee International

and

Pipeline & Hazardous Materials Safety Administration (PHMSA)  
U.S. Department of Transportation

Submitted by:

BMT FLEET TECHNOLOGY LIMITED  
311 Legget Drive  
Kanata, ON  
K2K 1Z8

BMT FTL Contact: A Dinovitzer  
Tel: 613-592-2830, Ext.203  
Fax: 613-592-4950  
Email: [adinovitzer@fleetech.com](mailto:adinovitzer@fleetech.com)

*BMT Fleet Technology Limited accepts no liability for any errors or omissions or for any loss, damage, claim or other demand in connection with the usage of this report, insofar as those errors and omissions, claims or other demands are due to any incomplete or inaccurate information supplied to BMT Fleet Technology Limited for the purpose of preparing this report.*

## BMT FTL DOCUMENT QUALITY CONTROL DATA SHEET

**REPORT:** Evaluation of the Interaction of Mechanical Damage and Welds

**DATE:** July, 2006

**PREPARED BY:**



\_\_\_\_\_  
L.B. Carroll, Senior Engineer

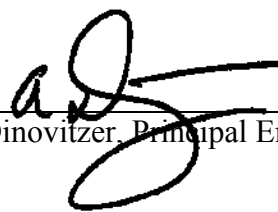


\_\_\_\_\_  
Abdelfettah Fredj, Structures Specialist



\_\_\_\_\_  
Vlado Semiga, Structures Specialist

**REVIEWED AND APPROVED BY:**



\_\_\_\_\_  
A. Dinovitzer, Principal Engineer, President

**Project Team:**

A. Dinovitzer  
B. Carroll  
M. Asavare

A. Fredj  
V. Semiga  
S. Tiku

TABLE OF CONTENTS

1.	INTRODUCTION .....	1
1.1	Project Scope and Objective .....	3
1.2	References .....	4
2.	FATIGUE PERFORMANCE ESTIMATION .....	5
2.1	References .....	6
3.	DENT – WELD INTERACTION CRITERIA .....	7
3.1	Assumptions used to Generate the Dent – Weld Interaction Criteria .....	7
3.1.1	Pipe Geometry .....	7
3.1.2	Material Properties .....	7
3.1.3	Dent Depth and Shape .....	7
3.1.4	Dent Restraint Condition .....	8
3.1.5	Weld Type and Location .....	8
3.1.6	Internal Pressure and Pressure Fluctuations .....	9
3.2	Intended Application of the Dent – Weld Interaction Criteria .....	10
3.3	Description of FE Models used to Develop the Criteria .....	10
3.3.1	Model Boundary Conditions .....	10
3.3.2	Element Type and Size .....	14
3.3.3	Material Properties .....	14
3.4	Numerical Model Matrix .....	16
3.5	Model Data Post-Processing .....	17
3.6	Criteria Development .....	20
3.6.1	Interaction with Dents and Long Seam Welds .....	20
3.6.2	Interaction of Dents with Girth Welds .....	21
3.7	Dent-Weld Interaction Summary .....	30
3.8	References .....	31
4.	OVALITY – WELD INTERACTION CRITERIA .....	32
4.1	Pipeline Ovality .....	32
4.2	Assumptions used to Generate the Ovality – Weld Interaction Criteria .....	32
4.2.1	Weld Seam .....	33
4.2.2	Pipe Geometry .....	33
4.2.3	Material Properties .....	33
4.2.4	Ovality .....	33
4.2.5	Weld Type and Location .....	34
4.2.6	Internal Pressure and Pressure Fluctuations .....	34
4.2.7	Fatigue Life Ratio .....	34
4.3	Intended Application of the Ovality – Weld Interaction Criteria .....	34
4.4	Description of FE Models used to Develop the Criteria .....	35
4.4.1	Finite Element Model .....	35
4.4.2	Material Model .....	35
4.4.3	Boundary Conditions and Load Sequence .....	36
4.5	Finite Element Model Matrix .....	36
4.6	Finite Element Model Results Post-Processing .....	37

4.7	Ovality-Weld Interaction Criteria Development.....	42
4.7.1	Identification of Scenarios of Interest.....	42
4.7.2	Regression Analysis.....	44
4.8	Application of Ovality-Weld Interaction Criteria.....	49
4.9	Ovality-Weld Interaction Summary.....	49
4.10	References.....	50
5.	WRINKLE – WELD INTERACTION CRITERIA.....	51
5.1	Local Buckling.....	51
5.1.1	Bending Moment Capacity.....	53
5.2	Assumptions Used to Generate the Wrinkle – Weld Interaction Criteria.....	53
5.2.1	Pipe Geometry.....	54
5.2.2	Material Properties.....	54
5.2.3	Wrinkle Amplitude.....	54
5.2.4	Weld Type and Location.....	56
5.2.5	Internal Pressure and Pressure Fluctuations.....	56
5.3	Intended Application of the Wrinkle – Weld Interaction Criteria.....	56
5.4	Non-Linear FE Model of Pipeline Buckling.....	57
5.4.1	Finite Element Model Geometry Details.....	58
5.4.2	Finite Element Model Material Properties.....	59
5.4.3	Finite Element Model Loading.....	59
5.5	Finite Element Model Matrix.....	61
5.6	Wrinkle/Weld Interaction Criteria.....	61
5.6.1	Interaction of Wrinkle and Long Seam Welds.....	61
5.6.2	Interaction of Wrinkles with Girth Welds.....	66
5.7	Wrinkle-Weld Interaction Summary.....	69
5.8	References.....	72
6.	CONCLUSIONS.....	73
6.1	Dent-Weld Interaction Criteria.....	74
6.2	Ovality-Weld Interaction Criteria.....	76
6.3	Wrinkle-Weld Interaction Criteria.....	78
7.	RECOMMENDATIONS.....	81
7.1	Dent-Weld Criteria Recommendations.....	81

**APPENDICES****APPENDIX A: FE MODEL SENSITIVITY STUDIES FOR DENTED PIPE****APPENDIX B: PLOTS OF RESIDUAL STRESS FIELDS FOLLOWING DENT ROUNDING FOR DIFFERENT PIPE MODEL ELEMENT SIZES****APPENDIX C: RESULTS OF SENSITIVITY STUDY TO EVALUATE BOUNDARY CONDITIONS EFFECTS ON STRESS FLUCTUATIONS IN PIPE WITH RESTRAINED DENTS****APPENDIX D: WRINKLE FE MODEL DEVELOPMENT, VALIDATION AND SENSITIVITY****APPENDIX E: PIPE SOIL INTERACTION****APPENDIX F: APPLICATION OF THE DENT-WELD INTERACTION CRITERIA****APPENDIX G: APPLICATION OF THE OVALITY-WELD INTERACTION CRITERIA****APPENDIX H: APPLICATION OF THE WRINKLE-WELD INTERACTION CRITERIA**

LIST OF FIGURES

Figure 1.1: Comparison of BMT Model with Full Scale Trial Results ..... 3

Figure 3.1: Dent Shoulder Shape Change with Changes in Internal Pressure..... 9

Figure 3.2: Example of Nonlinearity of the Hoop Stress Fluctuations Associated with Undented and Dented Pipe Segments (200 mm from the dent peak) ..... 10

Figure 3.3: (a) Hemispherical End Cap and (b) Axially Restrained Boundary Condition Models ..... 12

Figure 3.4: Vertical Boundary Restraint Scenarios for the ¼ Symmetry Models, (a) 450 mm from Center of Dent and (b) Along Full Length of Pipe Section ..... 12

Figure 3.5: Comparison of the (a) Membrane and (b) Bending Stress Fluctuations in the Axial Orientation from a 3% Deep Dent in NPS12 Pipe using 10 mm ANSYS SHELL181 and SHELL93 Elements for a 50% to 100% MOP Internal Pressure Fluctuation .... 15

Figure 3.6: Relative Life Estimates vs. Radial Displacement for the (a) Axial and (b) Circumferential Profiles from Model SR1\_12\_45\_6\_X52 for an Internal Pressure Fluctuation of 50% to 100% MOP ..... 18

Figure 3.7: Axial Profile Data from Figure 3.6(a) before Axial Orientation End Restraint Correction ..... 19

Figure 3.8: Circumferential Profile Data for Model SR1\_12\_45\_X52 with a Vertical Dashed Line Indicating the Intersection of the “OD Life” and “No Dent” Curves for a 50% to 100% MOP Pressure Fluctuation..... 20

Figure 3.9: Illustration of the Region on a Dented Pipe Segment where a Symmetrical Dent and Long Seam Weld would Interact to Reduce the Fatigue Life of the Pipe Segment .. 21

Figure 3.10: Axial Orientation Radial Displacement and Relative Life Estimate Plots for Model SR1\_12\_45\_6 for Pressure Fluctuations of (a) 75% to 100% MOP and (b) 50% to 100% MOP ..... 22

Figure 3.11: Axial Orientation Radial Displacement and Relative Life Estimate Plots for Model SR1\_12\_45\_6 for Pressure Fluctuations of (a) 25% to 100% MOP and (b) 0% to 100% MOP ..... 23

Figure 3.12: Dent Geometry Parameters used for the Axial Interaction Criteria ..... 25

Figure 3.13: Dent Girth Weld Interaction Criteria Performance for (a) 75% to 100% MOP and (b) 50% to 100% MOP Pressure Fluctuation Ranges..... 28

Figure 3.14: Dent Girth Weld Interaction Criteria Performance for (a) 25% to 100% MOP and (b) 0% to 100% MOP Pressure Fluctuation Ranges..... 29

Figure 4.1: Ovalized Pipe Cross-section..... 32

Figure 4.2: ANSYS Finite Element Model - Ovality ..... 35

Figure 4.3: Residual Ovality at End of Finite Element Analysis – X52..... 37

Figure 4.4: Residual Ovality at End of Finite Element Analysis – X65..... 38

Figure 4.5: Percentage of Residual Zero Pressure Ovality vs. Internal Pressure ..... 39

Figure 4.6: Relative Fatigue Life vs. Circumferential Position..... 40

Figure 4.7: Critical Angle and Acceptable Region..... 41

Figure 4.8: Critical Angles..... 41

Figure 4.9: Comparison of Regression Prediction vs. Finite Element Prediction – 100% MOP Pressure Range..... 45

Figure 4.10: Comparison of Regression Prediction vs. Finite Element Prediction – 75% MOP Pressure Range..... 46

Figure 4.11: Comparison of Regression Prediction vs. Finite Element Prediction – 50% MOP Pressure Range..... 46

Figure 4.12: Comparison of Scaled Regression Equation vs. Finite Element Prediction – 100% MOP Pressure Range..... 47

Figure 4.13: Comparison of Scaled Regression Equation vs. Finite Element Prediction – 75% MOP Pressure Range..... 48

Figure 4.14: Comparison of Scaled Regression Equation vs. Finite Element Prediction – 50% MOP Pressure Range..... 48

Figure 5.1: Typical Moment Curvature (M-κ) Relationship for Pipe under Constant Pressure and Axial Force [5.2]..... 52

Figure 5.2: Wrinkle Height and Length..... 55

Figure 5.3: Axial Profile through the Wrinkle Apex for Four Different Wrinkles (D=508 mm, t=7.14 mm, D/t=71) ..... 55

Figure 5.4: Transverse Profile along the Apex of Four Different Wrinkles (D=762 mm, t=7.14 mm, D/t=107) ..... 56

Figure 5.5: Parametric Study - 1/4 Symmetry Finite Element Model..... 58

Figure 5.6: Schematic Transverse Cross-section through the Apex of a Pipe Wrinkle..... 62

Figure 5.7: Normalized Critical Angle vs. H/Lw ..... 63

Figure 5.8: Normalized Critical Angle vs. H/Lw: Effect of Material Grade..... 65

Figure 5.9: Normalized Critical angle vs. H/Lw: Effect of pressure fluctuation -X52 ..... 65

Figure 5.10: Normalized Critical Angle vs. H/Lw: Effect of Pressure Fluctuation -X65 ..... 65

Figure 5.11: Fatigue Life Estimate for Model D20\_t281\_x52\_A8 at Various Locations along an Axial Section through the Wrinkle Apex ..... 66

Figure 5.12: Life estimate for model D30\_t375\_X65\_A9 at Various Locations along an Axial Section through the Wrinkle Apex ..... 67

Figure 5.13: Wrinkle Girth Weld Interaction Criteria Performance for 100% to 75% MOP Pressure Fluctuations..... 69

Figure 5.14: Wrinkle Girth Weld Interaction Criteria Performance for 100% to 50% MOP Pressure Fluctuations..... 69

Figure 5.15: Wrinkle Girth Weld Interaction Criteria Performance for 100% to 25%MOP Pressure Fluctuations..... 70

Figure 5.16: Wrinkle Girth Weld Interaction Criteria Performance for 100% to 0% MOP Pressure Fluctuations..... 70

Figure 6.1: Illustration of the Region on a Dented Pipe Segment where a Symmetrical Dent and Long Seam Weld would Interact to Reduce the Fatigue Life of the Pipe Segment.. 76

Figure 6.2: Wrinkle Height and Length..... 78

**LIST OF TABLES**

Table 3.1: Restrained Dent Models used in the Boundary Condition Sensitivity Study .....	12
Table 3.2: Dent Depths Observed for the Restrained Dent Models used to Evaluate Model Boundary Condition Effects.....	13
Table 3.3: Numerical Model Matrix used to Develop the Dent-Weld Interaction Criteria.....	16
Table 3.4: Summary of FE Model Data used to Generate Regression Equations to Estimate Interaction Distances between Dents and Girth Welds.....	26
Table 3.5: Equation Coefficients to Estimate Dent-Girth Weld Interaction Distances .....	27
Table 3.6: Summary of Dent-Girth Weld Regression Analysis Sensitivity Study .....	27
Table 4.1: Finite Element Model Input Parameter Range .....	36
Table 4.2: Summary of Regression Cases .....	44
Table 4.3: Regression Equation Constants .....	45
Table 4.4: Summary of Mean and Maximum Regression Errors .....	47
Table 5.1: Pipe Wrinkling - Parameter Ranges .....	54
Table 5.2: Modeling Matrix Used to Estimate Interaction Distances Between Wrinkles and Long Seam Welds .....	64
Table 5.3: Summary of FE Results Used to Estimate Interaction Distances between Wrinkles and Girth Welds Seam .....	68
Table 6.1: Details of Regression Equations to Estimate Maximum Dent-Girth Weld Interaction Distances .....	76
Table 6.2: Regression Equation Constants .....	77
Table G.2: Regression Equation Constants .....	6

## 1. INTRODUCTION

Failures in transmission pipelines are often the result of mechanical damage. The US DOT has indicated that 20 to 40 percent of the serious pipeline incidents in any given year are related to mechanical damage. This damage is due to third party activities, mishandling during construction, pipeline bedding material consolidation, or ground movement.

In this project, the definition of mechanical damage is defined in terms of damage that has caused a change in the pipe shape that may be associated with plastic deformation. Based upon this definition, mechanical damage to a pipeline can include a number of damage mechanisms that may be deformation or metallurgical/metal loss related including dents, ovality, and wrinkling or buckling. Damage associated with gouges and/or corrosion related metal loss have not been included within the scope of the damage mechanisms considered in this project. The scope has been limited specifically to the following forms of mechanical damage that are present within the vicinity of girth welds or long seam welds:

- Restrained rock dents
- Pipe ovality
- Wrinkles

The significance of mechanical damage may be identified in terms of post damage life or damage accumulation rate and the process that may eventually lead to a loss of containment:

- Immediately after damage formation (e.g., a gouge formed by excavation equipment that will fail as the pipe re-bounds with the removal of the indenter), and
- Following a time-dependent process (i.e., fatigue, environmental cracking, creep, continued ground movement and settling) that results in a gradual damage accumulation due to post formation loading events.

In general, pipeline design standards require the repair of dents with depths exceeding 6% of the pipeline's outside diameter and those that interact with weld seams. This cautious damage disposition approach is based upon numerical and full-scale trials [1.1, 1.2, 1.3, 1.4, 1.5] demonstrating the significant impact that weld seams have on the life of the mechanically damaged pipe segments. Weld seams are considered less damage tolerant than the line pipe base material due to:

- Range of weldment mechanical properties;
- Potential for weld faults promoting failure – welds have a greater potential to contain fabrication faults (lack of fusion, inclusions, etc.) than the linepipe base material;
- Weld geometry stress concentration effects – even welds without flaws contain notches and discontinuities that reduce effective fatigue lives; and
- Weld residual stress fields - while the weld and fabrication residual stresses, of greater magnitude in and immediately adjacent to weld seams, have only a secondary effect on fatigue crack growth, they promote fracture in welded connections.

Recent advances in the understanding of mechanical damage failure suggest that the regulatory requirements could be made less restrictive for a specific pipeline if consideration is given to:

- The operating pressure history;
- The type and extent of the mechanical damage; and
- The position of the weld with respect to the mechanical damage.

A reduction in the conservatism associated with the existing repair criteria would eliminate costs to pipeline operators associated with unnecessary repairs. These savings could then be better channelled to address more significant pipeline integrity issues.

BMT has developed a numerical modelling process, which uses the dent profile and in-service pressure history as inputs [1.6]. This approach is useful in evaluating the effects of the pipe deformation on the longer term performance of a pipeline system. The BMT model relies on well-defined parameters including:

- The pipe characteristics (e.g., dimensions and mechanical properties);
- The dent description which may consist of a 3-dimensional dent profile from in-line inspection (ILI);
- A description of the operating conditions including pipeline fluid pressure or load history and indenter contact condition (e.g., is the dent stabilized by the indenter remaining in contact with the pipe).

Related research and development efforts at BMT have developed a numerical model to predict the formation and behaviour of pipeline buckles and wrinkles. A buckle or a wrinkle form in linepipe is due to a combination of axial, flexural and lateral applied loads. In this report, and in the research by others, the primary difference between a buckle and wrinkle is the deformed geometry of the pipe segment. A wrinkle is characterized by an outward deflection of the pipe wall, whereas, a buckle is typically described as having an inward or diamond type of wall deflection. While a buckle or a wrinkle may form in the absence of a lateral load (mechanically applied loads or construction loads) their formation is facilitated by the application of lateral loads.

The buckle/wrinkle formation model considers the continued growth and damage accumulation of the buckle and wrinkle. The model was developed to simulate the behaviour of a pipe before, during, and after the formation of a buckle/wrinkle and considers:

- Internal pressure (static or cyclic);
- Axial loads (due to thermal or ground movement);
- Flexural loads (due to pipe curvature or ground movement); and
- Pipe imperfections (out of roundness, ovality or wall thickness variations).

The wrinkle formation model has been validated through comparison with full-scale trials, as shown in Figure 1.1 illustrating the agreement of the “FTL LS-Dyna” model with the “Experimental” trial results.

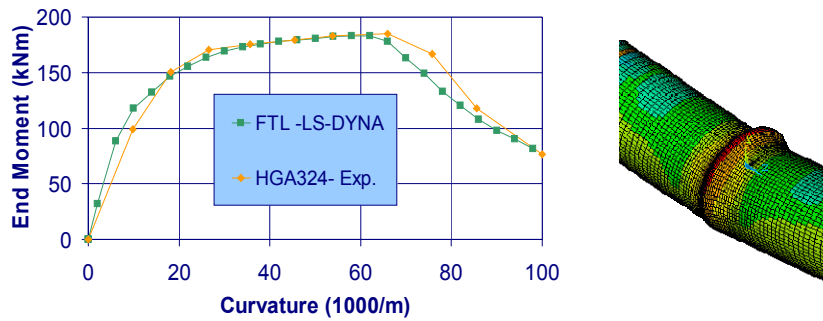


**Figure 1.1: Comparison of BMT Model with Full Scale Trial Results**

### 1.1 Project Scope and Objective

This project was completed to support the development of a guidance note for the disposition of welds interacting with pipe wall mechanical damage (dents, wrinkles and ovality) and thus allow a more rational treatment of these forms of damage. The intent is not to evaluate the life of welds interacting with dents wrinkles and ovality, but rather to identify when the interaction is significant and needs to be considered explicitly. Based upon the criteria developed in this project, inspection results that indicate the presence of pipe wall deformation in the vicinity of a girth weld or long seam weld can be used to assess if the interaction is significant and must be treated as a repairable defect.

This project report includes a discussion of the following work:

- Development of a criteria for weld interaction with restrained rock dents, pipe ovality and wrinkles;
- Development of a means of considering pressure fluctuation severity in these criteria, and
- Development of guidance and recommendations on how to consider the effects of soil confinement

The criteria do not predict the actual life of a mechanical damage feature, but instead present a means of defining the interaction distance between damage feature and a weld. The processes have been established based upon numerical modeling results with a detailed consideration of the effects of both physical and numerical variables. Due to the virtually limitless combination of weld seam geometries, weld quality, and residual stress fields, these parameters were not explicitly included in the numerical models. Instead, potential weld quality issues and residual stresses are addressed using an appropriate and conservative fatigue design curve while the weld geometry effects have been included with the selection of a stress concentration factor applied to the numerical modeling results.

In all cases, the pipe was assumed to be straight prior to the introduction of the mechanical damage process. The criteria are not applicable for damage occurring at pipe bends.

This scope of work was funded jointly by the Pipeline Research Committee International (PRCI) and US DOT.

## 1.2 References

- 1.1 Fowler, J.R., Alexander, C.R., Kovach, P.J., Connelly, L.M., 1995, “Fatigue Life of Pipelines with Dents and Gouges Subjected to Cyclic Internal Pressure”, PD Vol. 69, Pipeline Engineering, ASME.
- 1.2 Alexander, C.R., Kiefner, J.F., “Effects of Smooth and Rock Dents on Liquid Petroleum Pipelines”, American Petroleum Institute, API Publication 1156, November 1997.
- 1.3 Kiefner, J.F., Alexander, C.R., , “Effects of Smooth and Rock Dents on Liquid Petroleum Pipelines (Phase II)”, American Petroleum Institute, Addendum to API Publication 1156, October 1999.
- 1.4 Wang, K.C., Smith, E.D., “The Effect of Mechanical Damage on Fracture Initiation in Line Pipe: Part 1 – Dents”, ERP/PMRL 82-11(TR), Physical Metallurgy Research Laboratories, CANMET, Jan 1982.
- 1.5 Evaluation of a Composite System for Repair of Mechanical Damage in Gas Transmission Lines, GRI, Dec. 1998, GRI-97/0413.
- 1.6 Dinovitzer, A., Lazor, R., Walker, R., 1999, “A Pipeline Dent Assessment Model”, OMAE’99.

## 2. FATIGUE PERFORMANCE ESTIMATION

A variety of methodologies has been proposed or is currently under development to assess the potential for an immediate or short-term failure for a variety of mechanical damage features. The interaction criteria developed under this project has been based upon the premise that the deformation under evaluation does not pose an immediate threat to the integrity of the pipeline, but there is a need to evaluate the long term integrity under continued operation.

The primary loading mechanism considered was the fluctuation of internal pressure and fatigue life reductions resulting from the interaction of the pipe deformation and girth or long seam welds have been estimated using the fatigue design curve for low carbon steel weldments in the ASME Boiler and Pressure Vessel Code, Section VIII, Division 3 [2.1]. The fatigue evaluation has been conducted in accordance with Article KD-3. The fatigue life calculations have been restricted to regions where the principal stress axes are aligned with the hoop and axial orientations of the pipe. In highly deformed regions, the principal stress axes may rotate as the internal pressure changes, however, it would be undesirable to have weld seams located within these regions due to the complex loading scenarios and it would be impractical to assume that these scenarios could be accurately numerically modeled without validating the models against a series of detailed full scale tests. Such data does not exist in the public domain at this time.

The principal stresses must be determined in order to carry out fatigue calculations in accordance with Article KD-3 [2.1]. Three stress differences are first calculated using Equations 2.1 to 2.3 for the minimum and maximum applied loads in the fluctuating load scenario.

$$S_{12} = \sigma_1 - \sigma_2 \quad \text{Eqn. 2.1}$$

$$S_{23} = \sigma_2 - \sigma_3 \quad \text{Eqn. 2.2}$$

$$S_{31} = \sigma_3 - \sigma_1 \quad \text{Eqn. 2.3}$$

The alternating stress intensities,  $S_{alt\ ij}$ , are then calculated using Equation 2.4 for the combinations of stress differences.

$$S_{alt\ ij} = 0.5(S_{ij\ max} - S_{ij\ min}) \quad \text{Eqn. 2.4}$$

The design fatigue curve for welds in low carbon steel incorporates mean stress effects and therefore treatment of the mean stress in addition to the alternating stress amplitude was not required. The equivalent stress,  $S_{eq}$ , is set equal to the maximum alternating stress amplitude and the number of design load cycles required to cause a fatigue failure,  $N$ , is calculated according to Equations 2.5 to 2.7.

$$\text{For } S_{eq} \geq 38 \text{ ksi:} \quad \frac{1}{N} = -(7.125E-4) + (4.4692E-8)(S_{eq}^2) \ln(S_{eq}) + \frac{3.561E-3}{S_{eq}^2} \quad \text{Eqn. 2.5}$$

$$\text{For } 12.5 \text{ ksi} < S_{eq} < 38 \text{ ksi:} \quad \ln(N) = \frac{18.0353 - 1.3663 S_{eq} - 0.01549 S_{eq}^2}{1 - 0.04031 S_{eq} + (1.816E-3) S_{eq}^2} \quad \text{Eqn. 2.6}$$

$$\text{For } S_{eq} \leq 12.5 \text{ ksi:} \quad \ln(N) = -20 \ln\left(\frac{S_{eq}}{24.94}\right) \quad \text{Eqn. 2.7}$$

Since the weld seam was not explicitly included in the numerical models, for reasons discussed later, the equivalent stress estimates from the FE models were multiplied by a weld toe stress concentration factor of 3 prior to calculating  $N$ . The ASME design curve is only valid for low carbon steels with ultimate tensile strengths less than 80 ksi, therefore, when material property effects were considered in the interaction criteria Grade X65 was the strongest grade of material considered.

The number of design cycles was calculated for undeformed and deformed pipe having the same nominal material properties and geometry with consideration given to welds in a variety of positions with respect to the mechanical deformation. This process provided a means of determining the minimum interaction distance between the deformation and the weld seam based upon the relative fatigue life estimates for deformed and undeformed pipe. This process will be elaborated upon in the sections related to each form of pipe deformation considered.

## **2.1 References**

- 2.1 American Society of Mechanical Engineers, Boiler and Pressure Vessel Code, Section VIII, Division 3, “Alternative Rules for the Construction of High Pressure Vessels”.

### **3. DENT-WELD INTERACTION CRITERIA**

The premise behind the dent-weld interaction criteria developed under this project is based upon the pressure fluctuation response of the deformed pipeline as predicted by finite element models of dented pipe segments. A matrix of FE models was generated to consider a range of influential parameters which could impact such predictions. The parameters considered in this study included:

- Pipe geometry;
- Material properties;
- Dent depth and shape;
- Dent restraint;
- Weld type and location; and
- Internal pressure and pressure fluctuations.

#### **3.1 Assumptions used to Generate the Dent-Weld Interaction Criteria**

It was impractical to consider modeling every possible combination of the influential parameters within the scope of this project. Therefore, a matrix was devised to cover a range of combinations to identify trends that could be used to generate interaction criteria.

##### 3.1.1 Pipe Geometry

The pipe diameter and wall thickness combinations used in the modeling study were restricted to pipe diameters larger than 324 mm (NPS 12) and wall thicknesses in excess of 4.78 mm (0.188 inches) typical of larger transmission pipelines.

##### 3.1.2 Material Properties

Extensive material testing would be required in order to characterize the work hardening and cyclic loading behaviour of pipeline steels and it is impractical to assume that such data exists for most pipelines. A detailed treatment of the pipe material performance has been excluded from the current program. Instead, pipe material behaviour was based solely on minimum specified material properties assuming kinematic hardening behaviour. Models have been developed using Grade 359 (X52) and Grade 448 (X65) properties. These assumptions may lead to errors in stress predictions in the highly deformed region of the pipe, but the region of interest for the purposes of developing the interaction criteria is outside of the highly deformed region where the internal pressure to pipe wall stress relationship is linear-elastic.

##### 3.1.3 Dent Depth and Shape

The depth and shape of a dent depends upon the pipe geometry and material properties and the process of formation of the dent, whether it can be attributed to pipeline settlement, third party contact, etc. Most pipeline maintenance standards [3.1, 3.2] consider any plain dent deeper than 6% of the pipe OD an automatic repair, therefore, for the purposes of this study, the dent depth will be limited to a maximum value of 6%. Dents used in the criteria were formed in the FE model with spherical shaped indenters having three diameters, 25 mm (1 inch), 50 mm (2 inches) and 100 mm (4 inches). The dent profiles will, therefore, be symmetrical and exclude sharp stress risers.

#### 3.1.4 Dent Restraint Condition

Dents interacting with weld seams can be generated by several means, and while this investigation considers fatigue damage accumulation, all forms of damage accumulation need to be considered in assessing these damage features. A pipe segment may come to rest on a rock during initial construction or at some point during the service life of a pipeline. In that scenario, the rock normally remains in contact with the pipe and the amount of pipe wall movement with changes in internal pressure is limited by the restraint provided by the indenter, the weight of the pipe and the surrounding backfill. Alternatively, a dent may be formed due to third party contact with a pipeline. In that scenario, if the dent survived the initial indentation and re-rounding, the pipe wall would be free to flex when subjected to pressure fluctuations.

In this study, only the restrained dent condition has been considered. An in-service dent in the restrained condition presents a significant level of complexity, however, the complexity increases substantially for unrestrained dents formed by mechanical contact with the pipeline. Plastic deformation is a path dependent process so the final stress-strain state associated with an unrestrained dent is difficult to characterize unless the exact formation process is known or some means of measuring the stress-strain state exists. Since neither option is likely for most unrestrained in-service dents, it was decided that this initial research effort would focus on dents in the restrained condition where the variability should be significantly reduced. While the plastic deformation associated with these dents is also path dependent it normally follows a similar process especially if the dents can be attributed to original construction when the dent is formed when the pipeline comes to rest on a foreign object (i.e., a rock), the pipeline is subjected to a commissioning hydrostatic test and then the pipeline is placed into service. This formation process has been assumed for the dent models used in this project.

#### 3.1.5 Weld Type and Location

Variability in welding procedures can influence the fatigue performance of a welded connection. In this study, generic girth and long seam welds were considered, with no special attention paid to specific welding procedures. The interaction criteria are based upon fatigue calculations using the ASME design fatigue curve applicable to welded carbon steel parts [3.3]. This design curve contains an inherent level of conservatism considering the range of weld types and quality used in its development, therefore, it should be conservative for the majority of girth and long seam welds in in-service pipelines.

The FE models were generated using shell elements and neither weld seam geometries nor material property variations were explicitly included. While the slight increase in wall thickness associated with a weld and the material property variations could influence the resulting dent shape, these variations would be relatively minor compared to the gross deformation causing the dent and the allowable weld positions. This study focuses on the region surrounding a dent where the amount of plasticity is limited. To account for stress concentration effects associated with weld toe geometries a stress concentration factor of 3 was applied to the FE model stress fluctuation predictions.

### 3.1.6 Internal Pressure and Pressure Fluctuations

Even restrained dents will experience shape changes with internal pressure fluctuations. While the dent depth does not change if the indenter is held rigidly in place, the length of the dent (i.e., the length of deformation in the axial orientation with respect to the original pipe diameter) does change. As illustrated in Figure 3.1, at the maximum operating pressure, the half length of the dent (distance from the peak to the point of zero radial deflection) is 1200 mm (47.2 inches), while the length increases to 2150 mm (85.6 inches) when there is no internal pressure. Therefore, the dent profile measured by an in-line inspection tool can vary due to the internal pressure, if the ILI tool is sufficiently sensitive. The variability in dent dimensions with pressure has been considered in the development of the interaction criteria.

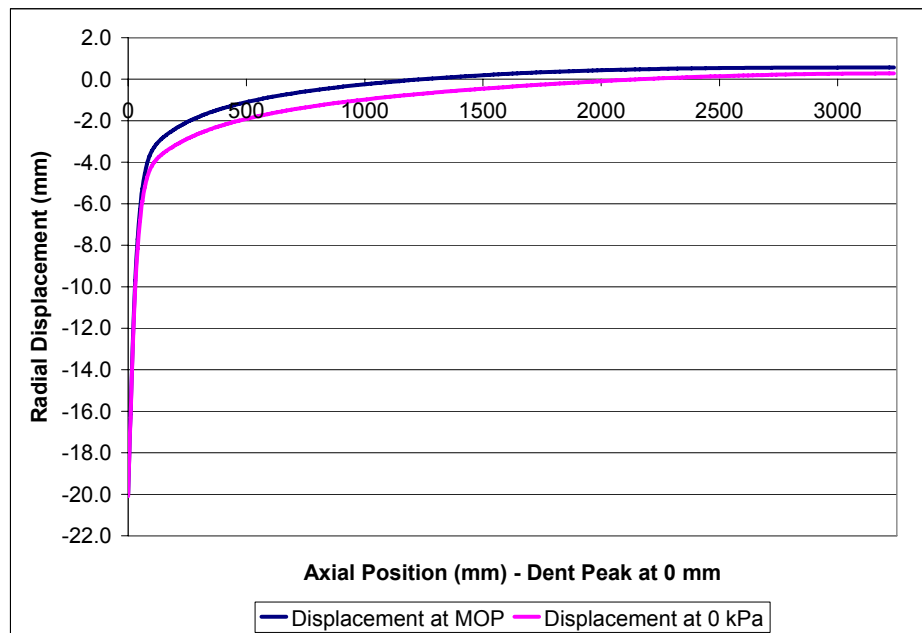


**Figure 3.1: Dent Shoulder Shape Change with Changes in Internal Pressure**

The pipe wall stress response to internal pressure change may not be linear because of the nonlinear geometry associated with the dent. Figure 3.2 provides the hoop stress fluctuation results of an FE model solution for a dented pipe segment with the stress fluctuations calculated at four pressure increments: 75% to 100% MOP, 50% to 100% MOP, 25% to 100% MOP and 0 to 100% MOP, where MOP is the internal pressure that generates 72% SMYS pipe wall hoop stresses in an undented pipe. The hoop stress fluctuations were extracted at a distance of 200 mm from the dent peak along the axial centreline through the dent profile.

In this example, the MOP level hoop stress would be 258 MPa (37.4 ksi) and assuming linear elastic material and geometry response for an undented pipe the stress fluctuations at each of the listed pressure fluctuation ranges would be 64.5 MPa (9.4 ksi), 129 MPa (18.7 ksi), 193.5 MPa (28.0 ksi) and 258 MPa (37.4 ksi), respectively, but with the dent applied to the pipe segment this is not the case. While the magnitude of the stress fluctuation increases in a nonlinear manner as the internal pressure fluctuation increases, the behaviour is repeatable from cycle to cycle.

Therefore, the scenario is one of nonlinear elastic behaviour, where the nonlinearity arises from the geometry effects. The developed interaction criteria account for these nonlinear effects, however, the operating pressure regime of the pipeline should be known. Characterizing the operating pressure regime will be discussed later in this document.

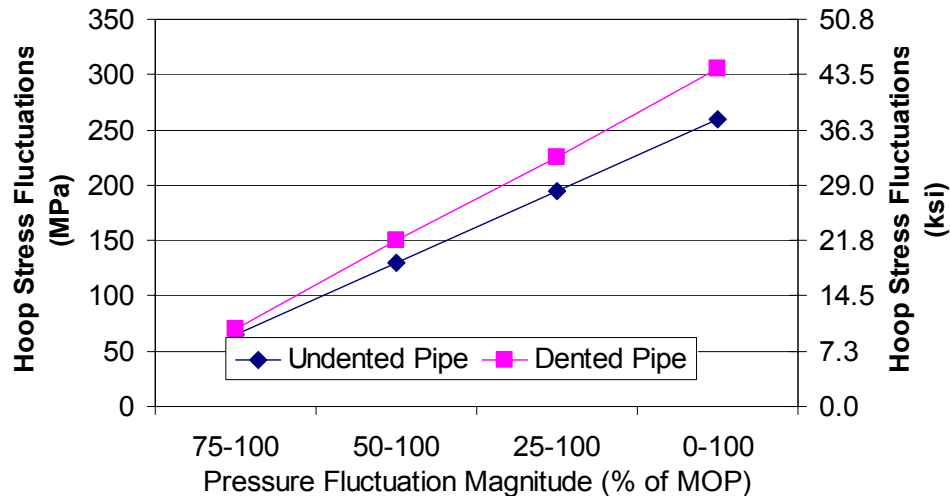


**Figure 3.2: Example of Nonlinearity of the Hoop Stress Fluctuations Associated with Undented and Dented Pipe Segments (200 mm from the dent peak)**

### 3.2 Intended Application of the Dent – Weld Interaction Criteria

The criteria developed under this program is intended for use with restrained dents (i.e., rock dents) in pipelines where the operating pressure regime has been characterized. The interaction criteria is not intended to replace the strain based criteria presented in ASME B31.8 [3.1], but instead it is intended to compliment that assessment procedure. The ASME procedure provides a means of characterizing the acceptability of a dent based upon an assessment of pipe wall strain in terms of the potential for fracture, however, it does not account for pressure cycling events which could contribute to a time-dependent failure. The proposed dent-weld criteria should only be employed for dents that satisfy the strain based criteria to estimate the safe distance between the peak of a dent and a weld seam to determine whether a cyclic load-dependant (fatigue) related failure is likely.

### 3.3 Description of FE Models used to Develop the Criteria

#### 3.3.1 Model Boundary Conditions

Sensitivities to the pipe model length and support conditions are discussed in Appendix A based upon the observed stresses in the pipe wall in the highly deformed region following indentation. Further analysis was undertaken to examine the impact of the model restraint conditions on the post dent formation pipe wall stress fluctuations under conditions specific to the model matrix used in developing the interaction criteria. The goal of this study was to determine the effect of model boundary conditions on the deformation and subsequently on the stress state (in particular the stress fluctuations) observed in a dented pipe segment.

This phase of the study examined:

- The influence of the pipe end boundary conditions on the stress fluctuations in the pipe and compared results from:
  - Pipe with hemispherical end caps;
  - Pipe without end caps and axial restraint; and
  - Pipe without end caps and no axial restraint.
- All three axial constraint cases were supported along the bottom of the pipe in two ways:
  - Vertical restraints applied for 450 mm from the center of the dent; and
  - Vertical restraints applied along the entire length of the pipe

The boundary conditions are illustrated in Figures 3.3 and 3.4.

The modeling parameters were based upon the UD12A-3 test in the API 1156 study [3.4], except the pipe geometry and grade were modified to represent nominal properties instead of the measured properties from the pipe used in the full scale test and both restrained and unrestrained dents were evaluated.

- Pipe OD = NPS 12 (323.85 mm);
- Pipe WT = 0.188 inches (4.78 mm);
- Pipe Grade = X52 (SMYS = 52 ksi or 359 MPa, UTS = 66 ksi or 455 MPa);
- Length of pipe segment = 5\*OD;
- Indenter diameter = 8.625 inches or 219 mm; and
- Initial indentation depth = 12% of OD.

For the restrained dent models the following load scenario was used:

- Load Step 1: Pipe indented with no internal pressure;
- Load Step 2: Internal pressure increased to generate 100% SMYS hoop stress in undeformed pipe;
- Load Step 2: Internal pressure reduced to zero;
- Load Step 4: Internal pressure increased to generate 72% SMYS hoop stress in undeformed pipe; and
- Load Step 5: Internal pressure reduced to zero.

The pressures used to generate 72% and 100% SMYS hoop stresses were calculated using Barlow's equation.

$$P_{100} = \frac{2 \sigma_{SMYS} t}{D} = \frac{2(359MPa)(4.77mm)}{323.85mm} = 10.572 MPa$$

$$P_{100} = f \frac{2 \sigma_{SMYS} t}{D} = (0.72) \frac{2(359MPa)(4.77mm)}{323.85mm} = 7.612 MPa$$

This scenario is consistent with a dent that is formed during initial construction and remains restrained by the indenter in service. The stress fluctuations were calculated using loads steps 4 and 5. The models used to evaluate the effects of the different end restraint conditions are summarized in Table 3.1.

**Table 3.1: Restrained Dent Models used in the Boundary Condition Sensitivity Study**

Model ID	End Restraint	Vertical Restraint
RD12_ec	End cap	450 mm from dent center
RD12_ec_a	End cap	Entire length of pipe
RD12_ncr	No cap, restrained axially	450 mm from dent center
RD12_ncr_a	No cap, restrained axially	Entire length of pipe

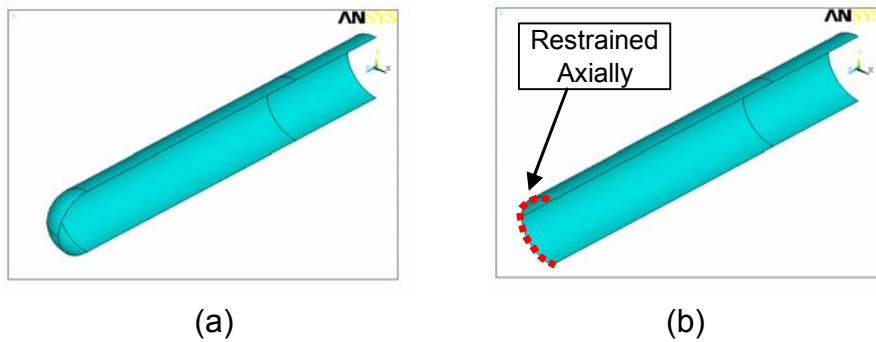


**Figure 3.3: (a) Hemispherical End Cap and (b) Axially Restrained Boundary Condition Models**

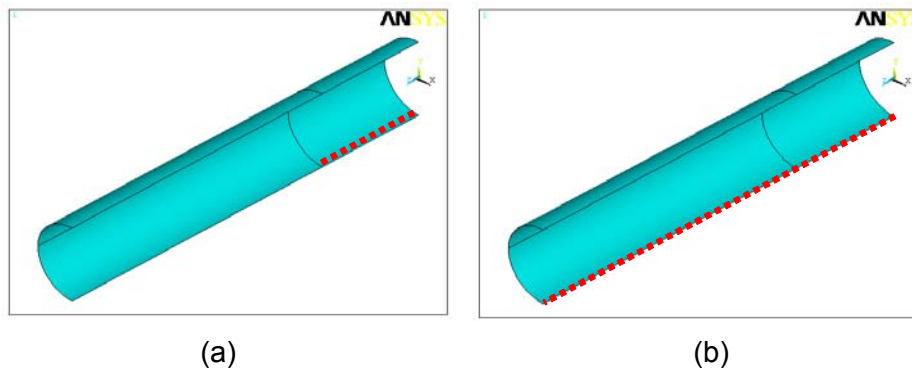


**Figure 3.4: Vertical Boundary Restraint Scenarios for the  $\frac{1}{4}$  Symmetry Models, (a) 450 mm from Center of Dent and (b) Along Full Length of Pipe Section**

The dent depth for the restrained models was set to 2.5 mm (0.10 inches) or 0.8% of the pipe wall thickness. Perfect contact is difficult to achieve in such highly complex nonlinear material models unless the surfaces are assumed to be bonded. It is practically impossible to prevent some penetration of the rigid target element by the contact elements therefore there was some variation in dent depth at different internal pressures. The observed dent depths are presented in Table 3.2. The fact that the pipe wall position changes slightly, will have some effect on the predicted stress fluctuations, but in the scheme of this project, this variability is negligible.

**Table 3.2: Dent Depths Observed for the Restrained Dent Models used to Evaluate Model Boundary Condition Effects**

Model	Dent Depth at Each Load Step									
	LS1		LS2		LS3		LS4		LS5	
	(mm)	%OD	(mm)	%OD	(mm)	%OD	(mm)	%OD	(mm)	%OD
RD12_ec	2.27	0.70	2.29	0.70	2.41	0.74	2.26	0.70	2.41	0.74
RD12_ec_a	2.26	0.70	2.30	0.71	2.40	0.74	2.31	0.71	2.40	0.74
RD12_ncr	2.26	0.70	2.26	0.70	2.44	0.75	2.30	0.71	2.44	0.75
RD12_ncr_a	2.26	0.70	2.32	0.72	2.45	0.76	2.32	0.72	2.45	0.76

The hoop ( $\sigma_{fh}$ ) and axial ( $\sigma_{fa}$ ) direction stress fluctuations were calculated using the Load Step 4 and Load Step 5 results:

$$\sigma_f = \sigma_{Load\ Step\ 4} - \sigma_{Load\ Step\ 5}$$

For an ideal thin-walled pressurized cylinder with end caps the hoop and axial stress fluctuations would be:

$$\sigma_{fh} = 0.72(359\ MPa) - 0 = 258\ MPa$$

$$\sigma_{fa} = \frac{1}{2} \sigma_{fa} = 129\ MPa$$

Surface plots for the axial and hoop stress fluctuations were generated for the ¼ symmetry pipe models with the X-axis equal to the axial distance from the center of the dent and the Y-axis equal to the distance from the center of the dent along the pipe circumference. The stress fluctuation plots are provided in Figures B.1 to B.4. As expected, the end capped cylinder models yielded stress fluctuations remote from the dent that best matched the theoretical values for a thin-walled pressurized cylinder. In the models without end caps, the axial stress fluctuation magnitudes decreased compared to the end capped models and these models showed slightly more variability in the hoop stress fluctuations remote from the dent. To reduce the computational requirements associated with additional elements required to produce end caps, restrained end models were used to generate the dent criteria. In reality, the axial restraint applied to a segment of an in-service pipeline would fall somewhere in between the end cap scenario and a completely unrestrained scenario. The exact restraint conditions could vary from location to location.

The interaction criteria developed in this project uses a relative comparison in fatigue life predictions between undeformed and dented pipe segments. The boundary conditions would influence life predictions in both the dented and undeformed scenarios, but as long as the boundary conditions were consistent the goal of this project could be met.

### 3.3.2 Element Type and Size

The 5 mm element sizes used in the sensitivity studies were impractical for meshing larger diameter pipe segments used to develop the interaction criteria based upon the required computational power. Therefore, a decision was made to increase the element size to 10 mm with a 1:1 aspect ratio under the indenter and 500 mm from the indenter in the axial direction switch to a 1:2 aspect ratio element size. It was observed in the results presented in Appendix A that the 10 mm SHELL181 elements did not provide consistent stress results within the 30 mm axial by 100 mm circumferential region immediately under the indenter so a further evaluation of the elements type and size effects was completed.

Two NPS12 models were generated with a wall thickness of 8.74 mm (0.344 inches) and a 25 mm (1 inch) indenter impressed to a depth of 3% of the OD. The element mesh described in the preceding paragraph was used in both models except in one case the 4-noded SHELL181 elements were used and in the second the 8-noded SHELL93 elements were used. Axial and circumferential stress fluctuations and dent shapes from both models w

ere compared (Figures C.1 to C.3). While the dent shapes were very similar, the stiffer SHELL181 elements resulted in slightly higher stress fluctuations at a greater distance from the dent peak as illustrated in Figure 3.5. As expected, immediately in the contact region, the stress fluctuations differed quite significantly, however, it should be kept in mind that there is no data available to confirm what the exact stress fluctuations would be that close to the indenter and the criteria developed in this project focuses on the stress fluctuations farther away where the stress fluctuations are more easily predicted.

Beyond approximately 200 mm from the dent peak, the membrane (or mean) stress fluctuations vary by about 4 MPa. The stiffer SHELL181 elements appear to accentuate the bending stress fluctuations, albeit slightly, at a distance farther from the dent peak. It was decided that the higher order SHELL93 elements were better able to handle the bending associated with the denting process so they were incorporated into the models used to generate the interaction criteria.

### 3.3.3 Material Properties

The ASME design fatigue curve [3.3] used in this project is applicable to welds in low carbon steel with an ultimate tensile strength of less than 552 MPa (80 ksi). Therefore, to assess the impact of material grade on the interaction criteria, the highest strength pipeline material that could be considered was Grade 448 (X65). Grade 359 (X52) and Grade 448 (X65) material properties were selected.

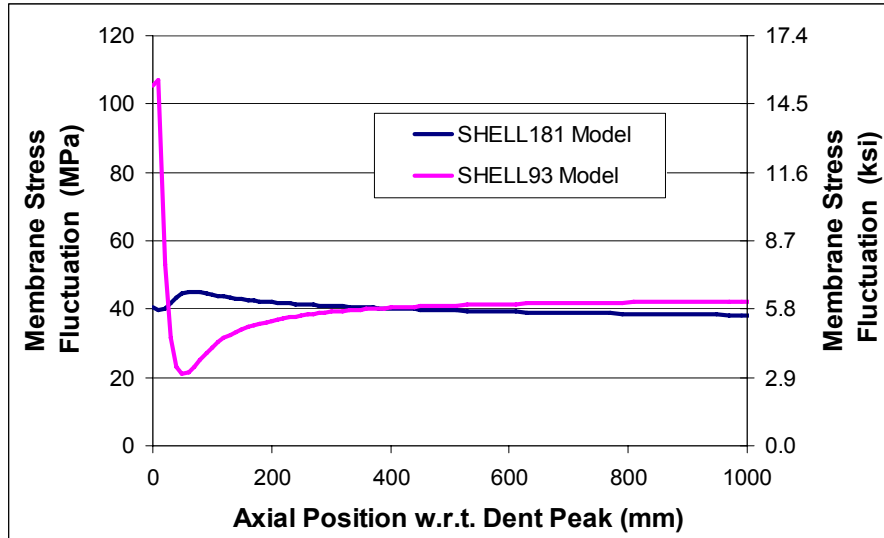
The actual yield and ultimate strength may vary significantly for pipe material meeting a specified grade. Some of the effects of pipe material property assumptions used in numerical modeling of dents were demonstrated in Appendix A. The following assumptions were used for the criteria development matrix:

Grade 359 (X52) Pipe Properties:

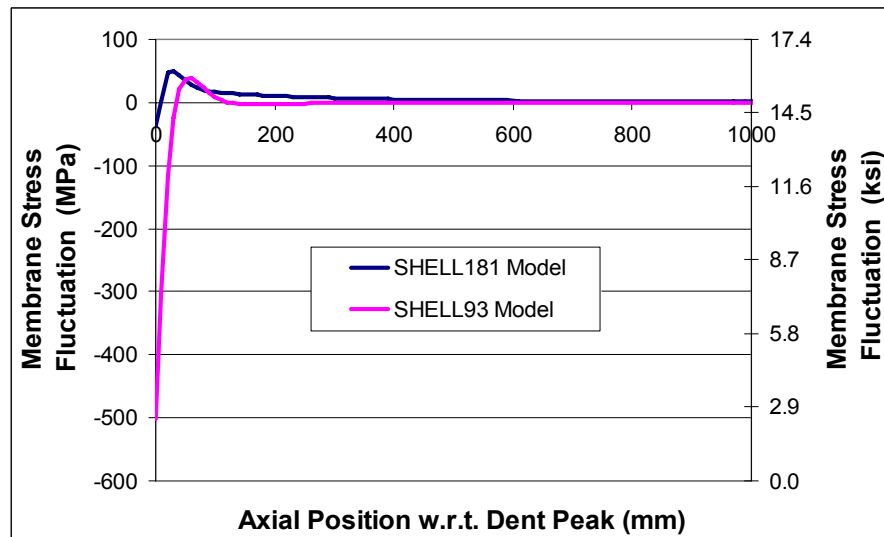
- Linear proportionality limit at strain = 0.0015 and stress = 311 MPa (45 ksi)
- SMYS at strain = 0.005 and stress = 359 MPa (52ksi)
- UTS at strain = 0.10 and stress = 455 MPa (66 ksi)

Grade 448 (X65) Pipe Properties:

- Linear proportionality limit at strain = 0.0019 and stress = 386 MPa (56 ksi)
- SMYS at strain = 0.005 and stress = 448 MPa (65 ksi)
- UTS at strain = 0.10 and stress = 531 MPa (77 ksi)



(a)



(b)

**Figure 3.5: Comparison of the (a) Membrane and (b) Bending Stress Fluctuations in the Axial Orientation from a 3% Deep Dent in NPS12 Pipe using 10 mm ANSYS SHELL181 and SHELL93 Elements for a 50% to 100% MOP Internal Pressure Fluctuation**

The strain and stress values at the linear proportionality limit and the strain at UTS were based upon typical stress strain curve data observed during BMT testing programs and ensure a material elastic modulus of approximately 207 GPa (30,000 ksi). Poisson's ratio for the material was assumed to be 0.30.

The engineering stress and strain values were converted to true stress and true strain for incorporation into the numerical models and kinematic hardening was assumed. Material anisotropy was ignored.

### 3.4 Numerical Model Matrix

The FE model matrix was comprised of 21 models and designed to cover a range of pipe and indenter geometries and dent depths for both material models used. The matrix is summarized in Table 3.3. The maximum pipe diameter included in this data set was restricted to 610 mm (24 inch) to limit the computational time associated with each model solution. The maximum dent depth was restricted to 6% of the nominal pipe diameter since deeper dents automatically require repair in accordance with existing pipeline codes.

**Table 3.3: Numerical Model Matrix used to Develop the Dent-Weld Interaction Criteria**

Model Identifier	Pipe Grade (MPa (ksi))	Outside Diameter (mm)	Wall Thickness (mm)	D/t Ratio	Indenter Diameter (mm)	Target Indentation Depth (%OD)	
SR1 12 37 3 X52	359 (52)	324	8.74	37	25.4	3	
SR1 12 45 6 X52			7.14	45		6	
SR1 12 68 3 X52			4.78	68		3	
SR1 12 68 6 X52			4.78	68	6		
SR2 12 45 3 X52			7.14	45	50.8	3	
SR2 12 45 6 X52			7.14	45		6	
SR2 12 68 3 X52		4.78	68	3			
SR4 12 37 3 X52		101.6	610	8.74	37	3	
SR4 12 45 6 X52				7.14	45	6	
SR4 12 68 3 X52				4.78	68	3	
SR1 24 70 3 X52		610	610	8.74	70	25.4	3
SR1 24 70 6 X52				8.74	70		6
SR1 24 96 3 X52				6.35	96		3
SR1 24 96 6 X52				6.35	96	6	
SR2 24 70 3 X52	8.74			70	50.8	3	
SR2 24 70 6 X52	8.74			70	50.8	3	
SR1 12 45 6 X65	448 (65)	324	7.14	45	25.4	6	
SR1 12 68 3 X65			4.78	68		3	
SR2 12 45 3 X65			7.14	45	50.8	3	
SR2 12 68 3 X65			4.78	68		3	
SR4 12 37 3 X65			8.74	37	101.6	3	
SR4 12 45 6 X65			7.14	45		6	

The model solutions used the following process to simulate a restrained rock dent that occurred during original construction:

- Load Step 1: Indented with no internal pressure

- Load Step 2: Internal pressure increased to generate SMYS level hoop stresses to simulate a hydrostatic test condition
- Load Step 3: Internal pressure reduced to zero
- Load Step 4: Internal pressure increased to 100% MOP (assuming MOP generates 72% SMYS level hoop stresses in undeformed pipe)
- Load Step 5: Internal pressure reduced to 90% MOP
- Load Step 6: Internal pressure reduced to 75% MOP
- Load Step 7: Internal pressure reduced to 50% MOP
- Load Step 8: Internal pressure reduced to 25% MOP
- Load Step 9: Internal pressure reduced to zero

### 3.5 Model Data Post-Processing

Load steps 4 to 9 were used to determine the equivalent stress for each of the following pressure cycle combinations:

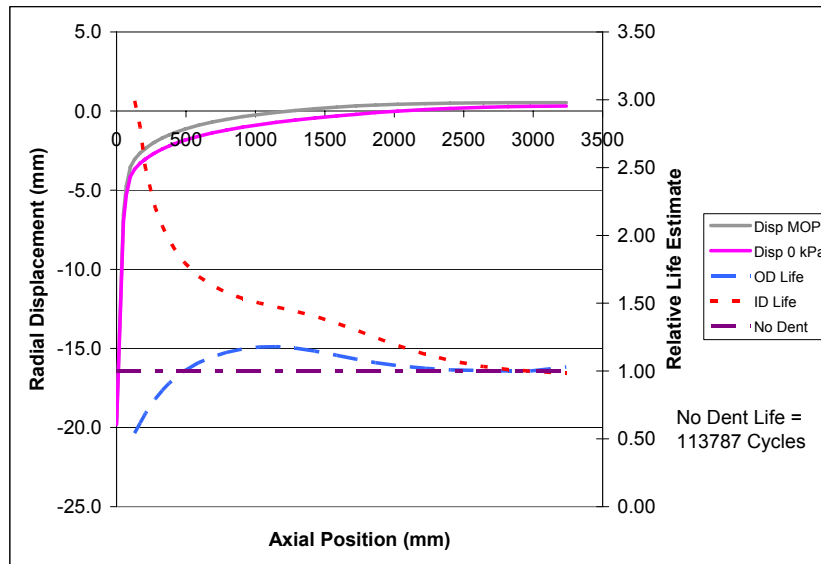
- 90% to 100% MOP
- 75% to 100% MOP
- 50% to 100% MOP
- 25% to 100% MOP
- 0% to 100% MOP

This permitted an evaluation of the number of design cycles estimated to generate fatigue failures for five internal pressure fluctuation scenarios. Nodal stress values were extracted from the FE models along the axial and circumferential centrelines through the dent peaks. The equivalent stress values (see Section 2) were calculated for the OD and ID surfaces for each node along the profiles where the maximum and minimum principal stresses remained aligned with the hoop and axial orientations. The equivalent stress values were multiplied by a stress concentration factor of 3 to account for weld toe stress concentration effects.

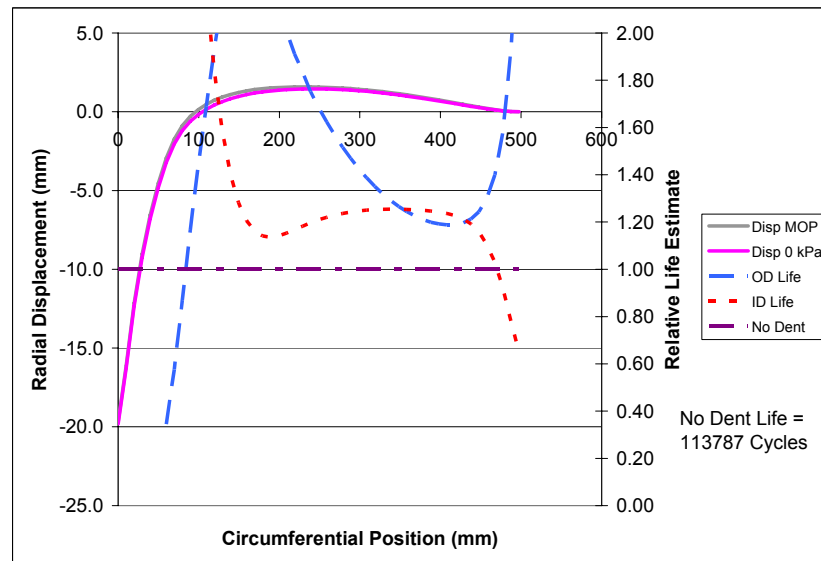
Close to the dent peak, the principal stress orientations could rotate significantly between minimum and maximum pressure, invalidating the simple methodology for calculating the equivalent stress presented in Section 2. In this region, the validity of the FE model solution also comes into question without significantly detailed full scale test data that can be used for calibration. Within the region close to the dent peak it would be undesirable to have a weld.

The equivalent stress values were used to calculate the number of design cycles for the applied loading in the dented pipe which was compared to the design cycles for the same internal pressure fluctuation in an undeformed pipe segment. The ASME design curve [3.3] for carbon steel weldments is truncated at a life of  $1 \times 10^8$  cycles, therefore, whenever a value in excess of  $1 \times 10^8$  was calculated it was assumed to be equal to  $1 \times 10^8$ . This information was used to plot curves for each dent model similar to that shown in Figure 3.6. The solid lines show the radial deflection of the pipe wall at the maximum operating pressure and at zero internal pressure along the axial or circumferential orientation with respect to the dent peak. The position  $X = 0$  is the peak of the dent. The difference between these two lines illustrates the pipe wall flexing that occurs as the pressure fluctuates. The dot-dash line illustrates a relative life estimate of 1.0 (plotted with respect to the secondary Y-axis) and represents the life of an undeformed pipe segment subjected to pressure fluctuations between 50% and 100% SMYS. This would equate to 113,787 cycles according to the design curve.

The dotted line presents the relative life estimate based upon the ID surface stresses from the dented pipe model and the dashed line shows the relative life estimate calculated using the OD surface stresses. Whenever either of these two lines drops below the 1.0 relative life line the dented pipe would be expected to have a shorter fatigue life at that axial or circumferential position. Figure 3.6(a) suggests that a crack would initiate on the OD surface and the dented pipe segment would have a shorter life than an undented segment within a distance 490 mm axially from the dent peak. Beyond 490 mm, the life of the dent pipe would be as least as long as the undented pipe.



(a)



(b)

**Figure 3.6: Relative Life Estimates vs. Radial Displacement for the (a) Axial and (b) Circumferential Profiles from Model SR1\_12\_45\_6\_X52 for an Internal Pressure Fluctuation of 50% to 100% MOP**

The circumferential position in Figure 3.6(b) starts at the peak of the dent ( $X=0$ ) and extends around half of the pipe circumference 180 degrees from the peak of the dent. At that location the model is restrained using symmetry boundary conditions and in the vertical direction along the axial orientation of the pipe. The drop in the ID life estimate and increase in the OD life estimate at the 180 degree location is an artifact of the model boundary conditions applied along a single line opposite the dent. In reality, a pipe would be supported by a distributed pressure due to the surrounding backfill and this concentration in bending load would not exist so this effect was ignored when evaluating allowable interaction distances between the long seam weld and the dent.

In some examples (particularly for the deeper dents, larger pressure fluctuation magnitudes and stronger pipe materials), the axial length of the pipe segment of 10D was not sufficient to completely cancel out the bending due to the axial end effects applied to the pipe segment and resulted in reductions in dented pipe life predictions remote from the dent. A correction was applied to the FE model life predictions by shifting the affected OD or ID life curve to match the undeformed pipe curve at the end of the pipe segment by correcting the stress estimates at the end of the dented pipe. In the case of Figure 3.6(a), this correction has been applied and Figure 3.7 presents the data before correction to illustrate the results of the process. There was a 20% correction in the “ID Life” curve between the data in Figure 3.7 and the data in Figure 3.6(a) at the end of the pipe. While this may appear significant, in actual fact, the difference was the result of a stress correction (including the stress concentration factor) of only 15 MPa (2 ksi) for an equivalent stress of 300 MPa (44 ksi), which equates to a variability in stress fluctuations of only 5% between the “No Dent” and “ID Life” calculations. Towards the peak of the dent where the stress fluctuation magnitudes increased, the 15 MPa (2.2 ksi) stress correction was significantly less than 5% of the equivalent stress.

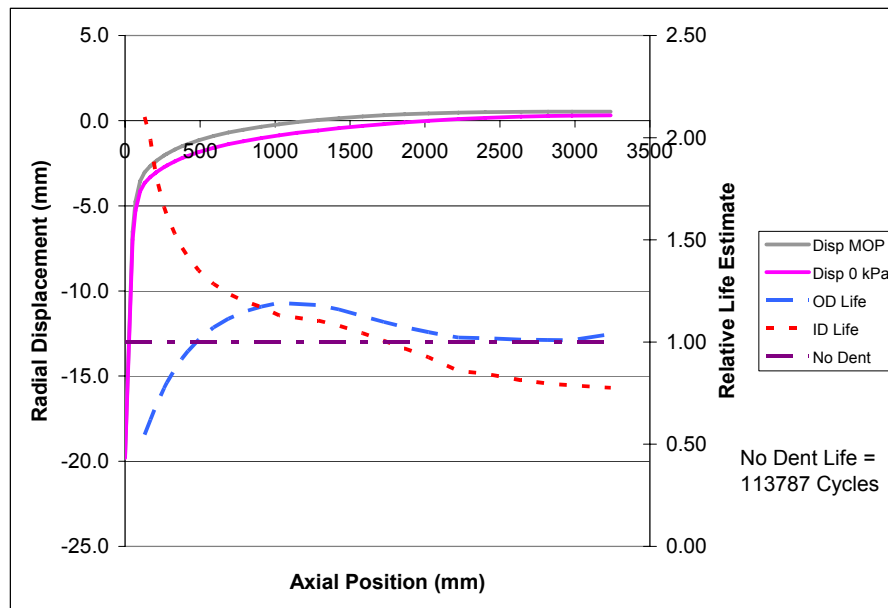


**Figure 3.7: Axial Profile Data from Figure 3.6(a) before Axial Orientation End Restraint Correction**

The life curves do not start at the zero position (i.e., dent peaks) in Figures 3.6 and 3.7. Instead they start at the position where the equivalent stress calculations are valid based upon the principal stress orientations. The exact starting position depended upon pipe D/t ratio, the material properties, the dent depth and the indenter diameter, but generally it was within 150 mm from the peak in the axial orientation and 75 mm in the circumferential orientation.

### 3.6 Criteria Development

The criteria developed in this project is intended for use with data from in-line inspection technologies capable of determining the three dimensional profile of a dent. Such tools would be required in order to carry out a dent strain analysis in accordance with the ASME B31.8 [3.1] procedures. The criteria have been developed for restrained dents which are symmetrical about the axial and circumferential orientations through the dent peak. Further work will be required to validate the procedures for dents that are significantly unsymmetrical in nature.

#### 3.6.1 Interaction with Dents and Long Seam Welds

By far the interaction distance between a dent and long seam weld was the easiest to characterize. Figure 3.6(b) is reproduced in Figure 3.8 with a vertical dashed line positioned at the intersection of the “OD Life” and “No Dent” curves. To the right of the vertical line, the dented pipe segment has a fatigue life estimate equal to or higher than the undeformed pipe. To the left of the vertical line, the life estimate is less than the undeformed pipe and drops quickly as the distance to the dent peak is reduced. The vertical line intersects the radial displacement plots at MOP and 0 kPa (0 psi) internal pressures close to the location where the radial displacement is zero. This behavior was consistent for all dent models and the 75% to 100%, 50% to 100%, 25% to 100% and 0 to 100% MOP pressure fluctuation ranges. In the case of the 90% to 100% pressure fluctuation ranges, the resulting pipe wall stress values were so low that the dented pipe life never dropped below the undeformed pipe life within the circumferential distance analyzed with the maximum cycle limit of  $1 \times 10^8$  implemented.

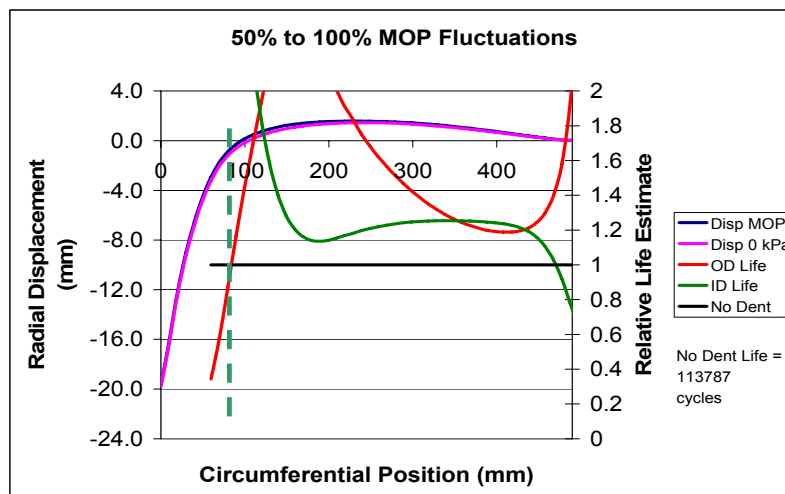


**Figure 3.8: Circumferential Profile Data for Model SR1\_12\_45\_X52 with a Vertical Dashed Line Indicating the Intersection of the “OD Life” and “No Dent” Curves for a 50% to 100% MOP Pressure Fluctuation**

The aforementioned observations lead to the development of the proposed dent long seam interaction criteria:

“For a symmetrical dent profile, a long seam weld does not interact with a dent to reduce the fatigue life of the pipe segment if the long seam is located beyond outside the zero deflection position of the circumferential profile through the dent.”

This criterion is illustrated schematically in Figure 3.9. Further study considering a wider range of indenter shapes and alignment positions with respect to the pipe axes will be required to expand the applicability of this criterion to highly unsymmetrical dent profiles.

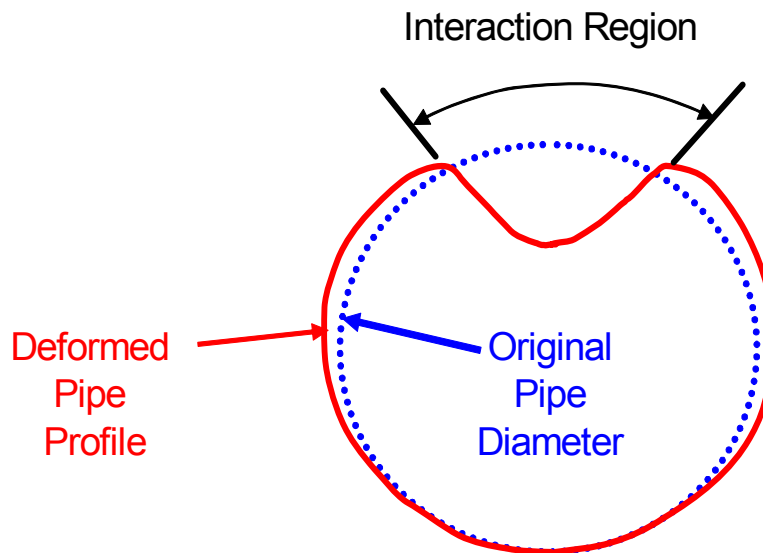
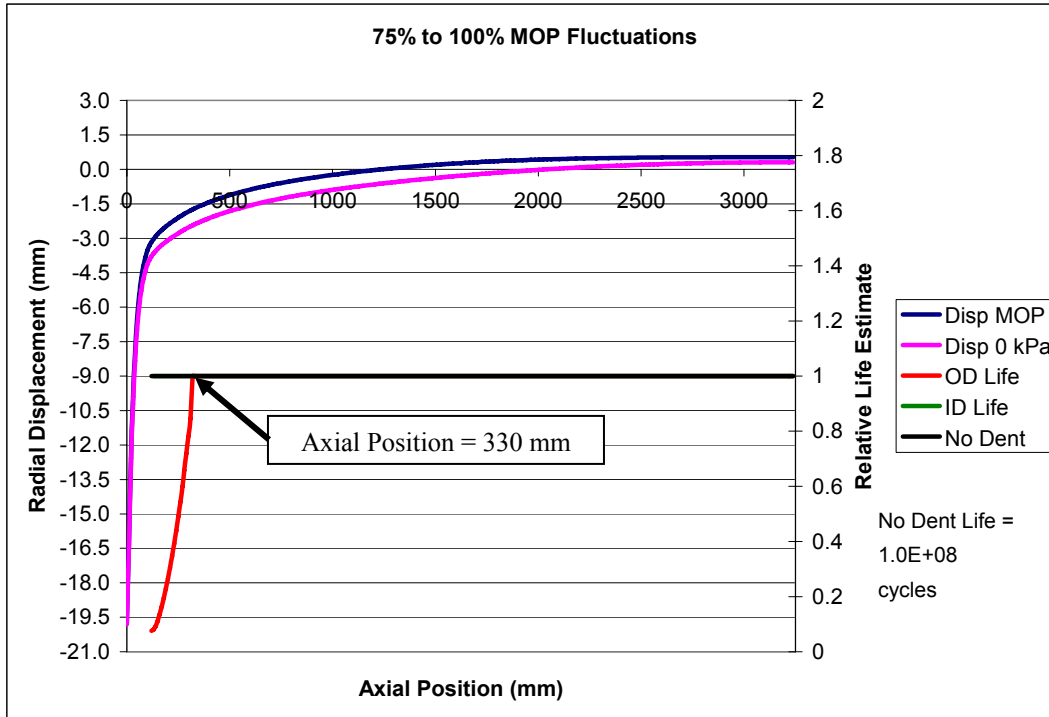


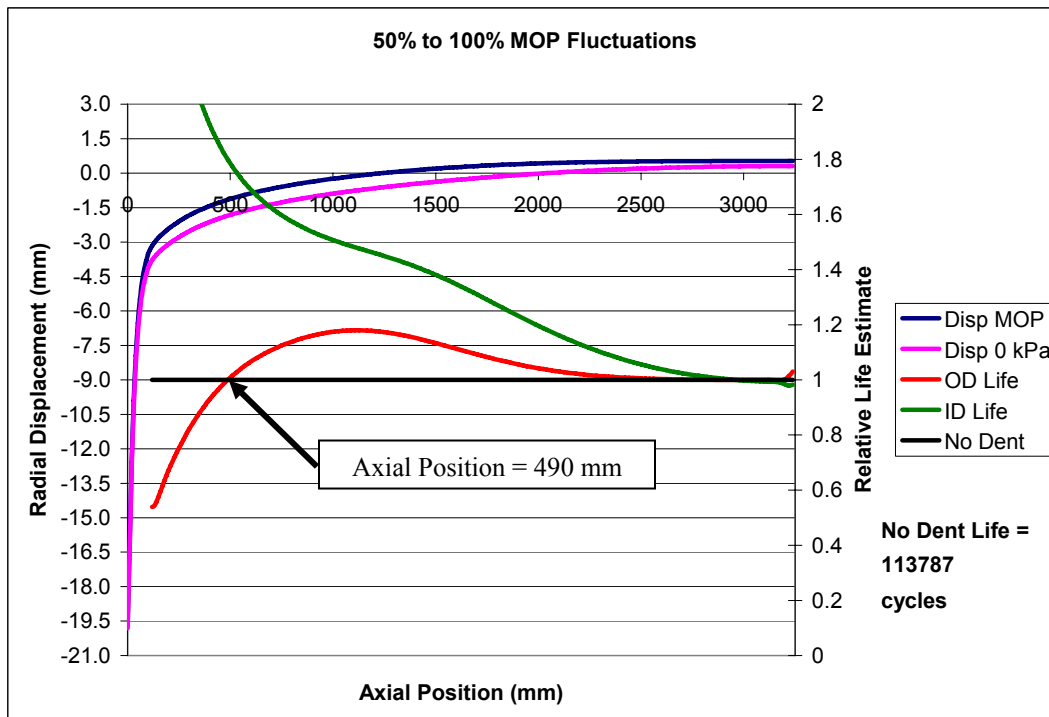
**Figure 3.9: Illustration of the Region on a Dented Pipe Segment where a Symmetrical Dent and Long Seam Weld would Interact to Reduce the Fatigue Life of the Pipe Segment**

### 3.6.2 Interaction of Dents with Girth Welds

The development of the girth weld interaction criteria was not as straightforward as the long seam weld interaction criteria for several reasons. The 90% to 100% pressure fluctuation cases generated the same results as the long seam weld cases with no reduction in fatigue life estimates using  $1 \times 10^8$  cycle limit. However, as illustrated in Figures 3.10 and 3.11, the relative position of the crossing point of the dented life curves and the “No Dent” life curve varied with the remaining internal pressure fluctuation cases. As the magnitude of the pressure fluctuation increased, the curve intersection point usually moved farther away from the peak of the dent. To further complicate the situation, the internal pressurization level had a bigger impact on the shape of the axial profile of the dent. At lower internal pressures, the zero displacement point moved farther away from the peak and could vary by as much as 1000 mm (40 inches) for a pipe pressurized to MOP and a pipe with no internal pressure.

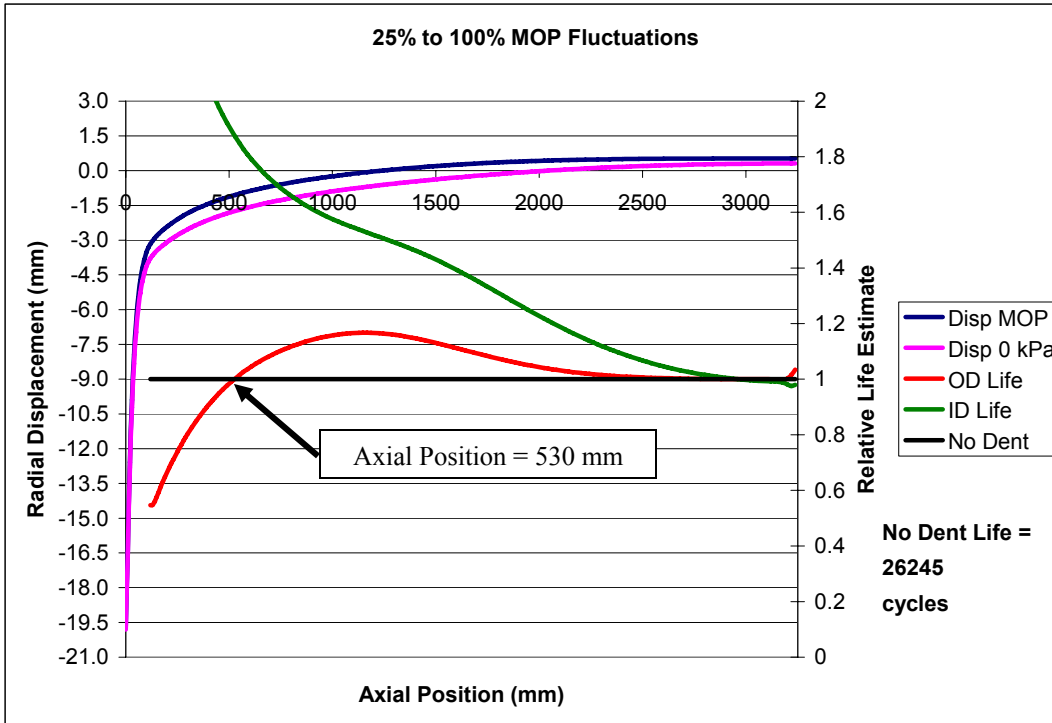


(a)

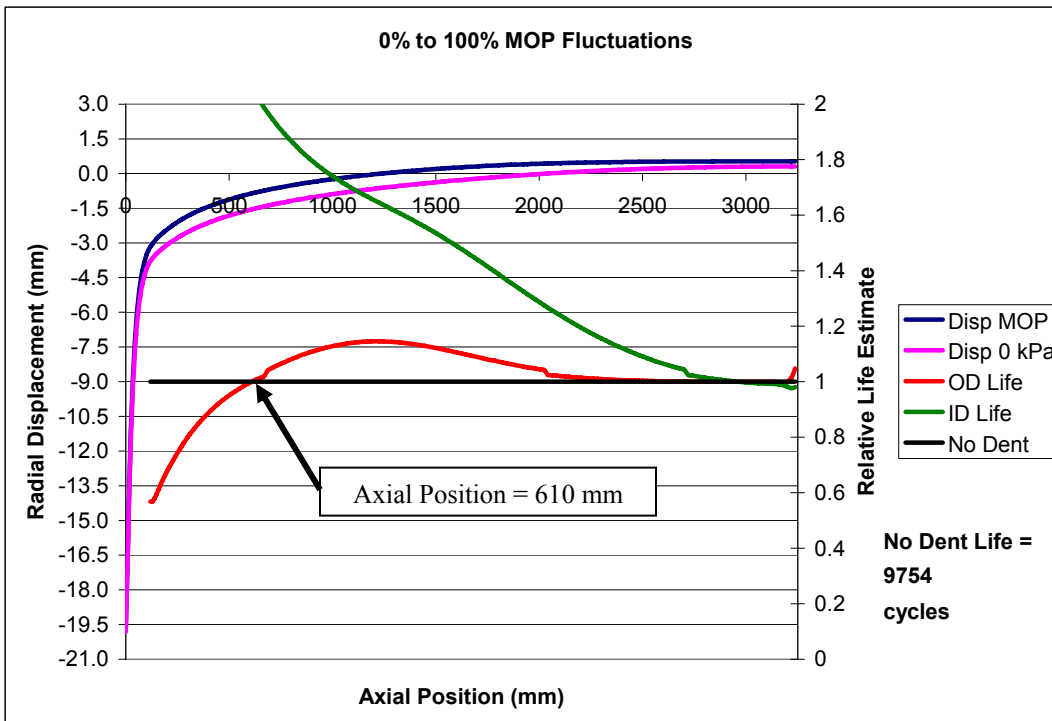


(b)

**Figure 3.10: Axial Orientation Radial Displacement and Relative Life Estimate Plots for Model SR1\_12\_45\_6 for Pressure Fluctuations of (a) 75% to 100% MOP and (b) 50% to 100% MOP**



(a)



(b)

**Figure 3.11: Axial Orientation Radial Displacement and Relative Life Estimate Plots for Model SR1\_12\_45\_6 for Pressure Fluctuations of (a) 25% to 100% MOP and (b) 0% to 100% MOP**

During the initial planning stages of the criteria development process, some thought was given to developing criteria for different levels of life reduction. For example, a dented pipe segment with a fatigue life of 80% of the undeformed pipe segment may be acceptable for continued service. However, when it came to some of the scenarios (particularly the 75% to 100% MOP pressure fluctuations) the distance between the relative life estimate points of 1.0 and 0.8 was so close (i.e., less than 10 mm) that this option did not seem practical and the interaction criteria was based solely upon the intersection of the dented life estimates and the “No Dent” life estimate curves.

The first step in the criteria development was to obtain the relative distance between the dent peak and the point of intersection between the dented pipe life estimate curves and the undeformed pipe curves (the life reduction point) for each pressure fluctuation case. After this information was obtained, the dent profile information was reviewed to determine if the life reduction point could be related to the shape of the axial profile of the dent as was the case for the circumferential orientation profiles. While there appeared to be a correlation between the pipe wall displacement and the life reduction points it was clear that this information could not be used from a practical standpoint. The life reduction points all fell within a band between 0 mm and 5 mm of radial displacement. Determining radial pipe wall displacements to that level of accuracy from in-line inspection tool data was unrealistic so another approach was required.

The methodology that was finally decided upon was based on a non-dimensional characterization of the pipe grade and geometry along with the dent’s axial profile geometry. These non-dimensional parameters were used to develop a series of regression equations that could be applied to estimate the minimum acceptable interaction distance between the peak of a dent and a girth weld in the axial orientation. Several possible parameters were investigated and the following appeared to be the most useful:

- Strength Ratio (SR): A material property parameter calculated using the ratio of the pipe material ultimate tensile strength (in practical terms the specified minimum ultimate strength) and the 552 MPa (80 ksi) maximum value applicable for materials evaluated using the ASME design fatigue curve [3.3].
- Pipe D/t Ratio (D/t): A pipe geometry parameter calculated using the ratio of the nominal pipe outside diameter (D) to the nominal pipe wall thickness (t).
- Dent Depth (d): A dent geometry parameter defined as the dent depth as a percentage of the pipe’s nominal outside diameter (d).
- Depth/Length Ratio ( $d/\sqrt{L}$ ): A dent geometry parameter defined as the depth of the dent (d) in mm divided by the square root of the length of the dent shoulder in mm (L).
- Axial Sharpness ( $l/\sqrt{L}$ ): A dent geometry parameter defined as the distance from the dent peak to the location of the half peak height (l) divided by the square root of length of the dent shoulder (L).

The parameters  $d$ ,  $d/\sqrt{L}$  and  $l/\sqrt{L}$  are used to define the dent profile in the axial orientation and are illustrated in Figure 3.12. As mentioned the length of the dent shoulder varies with internal pressure level and the actual internal pressure at a specific dent location along a pipeline may not be known. Even if the pressure is known, the accuracy of an in-line inspection tool may not be sufficient to distinguish subtle changes in the dent shoulder length. For the purposes of developing the interaction criteria,  $L$  was determined using the length of the dent shoulder at zero internal pressure since this would generate the longest shoulder length. At higher internal pressure levels, the shoulder length would be shorter and the  $l/\sqrt{L}$  ratio would be smaller, which would make the dent appear to have a sharper profile and increase the interaction distance thus adding conservatism to the assessment.

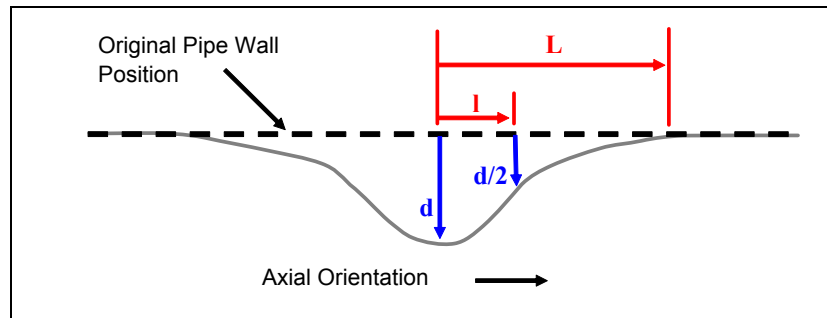


**Figure 3.12: Dent Geometry Parameters used for the Axial Interaction Criteria**

Table 3.4 summarizes the data from the FE models used to generate the interaction criteria. For Model SR1\_12\_37\_3\_X52 an intersection for the “No Dent” and dent life curves could not be obtained for the 75% to 100% MOP pressure range. The point appears to pass too close to the peak of the dent, within the region where the principal stress orientations do not remain aligned with the axial and hoop directions. Regression equations were developed for each pressure fluctuation scenario to calculate the estimated permissible interaction distance between the peak of the dent and the location of a girth weld. A combination of quadratic equations provided the best results in terms of a calculation of the mean squared error (Equation 3.1) between the interaction distances measured in the FE models and the estimated values from the regression equations. The regression results are summarized in Table 3.5.

$$MSE = \sqrt{\frac{\sum_i^n ((Interaction\ Length\ from\ FE\ Model) - (Interaction\ Length\ from\ Equation))^2}{n}} \quad \text{Eqn. 3.1}$$

$n$ : the total number of models used

Table 3.5 also provides the maximum and minimum prediction errors from the regression equations in terms of a percentage of the measured length in the FE models. A negative prediction error value implies that the regression equations underestimate the interaction length. Based upon prediction variability, it appears prudent to multiply the interaction length obtained from the regression equations by a factor of 1.2 to determine a suitable allowable interaction distance. The general form of the final regression equation is given in Equation 3.2.

**Table 3.4: Summary of FE Model Data used to Generate Regression Equations to Estimate Interaction Distances between Dents and Girth Welds**

Model	UTS MPa (ksi)	Strength Ratio	D (mm)	t (mm)	D/t	d		l (mm)	L (mm)	l/√L	d/√L	Axial Position of Life Intersection Point (mm)			
						(mm)	(%)					100%-75%	100%-50%	100%-25%	100%-0%
						OD	OD					OD	OD		
SR1_12_37_3_X52	455 (66.0)	-0.82	324	8.74	37	9.5	2.9	25	2070	0.549	0.209	ND	300	340	710
SR1_12_45_6_X52	455 (66.0)	-0.82	324	7.14	45	19.7	6.1	30	2030	0.666	0.437	330	490	530	610
SR1_12_68_3_X52	455 (66.0)	-0.82	324	4.78	68	10.1	3.1	25	2250	0.527	0.213	180	360	440	530
SR1_12_68_6_X52	455 (66.0)	-0.82	324	4.78	68	20.0	6.2	30	2170	0.644	0.429	230	360	390	450
SR2_12_45_3_X52	455 (66.0)	-0.82	324	7.14	45	9.8	3.0	30	2090	0.656	0.214	260	440	490	610
SR2_12_45_6_X52	455 (66.0)	-0.82	324	7.14	45	19.6	6.1	35	2030	0.777	0.435	340	490	530	610
SR2_12_68_3_X52	455 (66.0)	-0.82	324	4.78	68	10.0	3.1	25	2270	0.525	0.210	190	390	430	500
SR4_12_37_3_X52	455 (66.0)	-0.82	324	8.74	37	9.7	3.0	35	2070	0.769	0.213	270	530	550	750
SR4_12_45_6_X52	455 (66.0)	-0.82	324	7.14	45	19.7	6.1	40	2030	0.888	0.437	330	500	550	610
SR4_12_68_3_X52	455 (66.0)	-0.82	324	4.78	68	9.8	3.0	30	2290	0.627	0.205	200	420	450	510
SR1_24_70_3_X52	455 (66.0)	-0.82	610	8.74	70	18.2	3.0	40	4330	0.608	0.277	310	730	850	1010
SR1_24_70_6_X52	455 (66.0)	-0.82	610	8.74	70	36.4	6.0	50	4170	0.774	0.564	390	690	770	890
SR1_24_96_3_X52	455 (66.0)	-0.82	610	6.35	96	18.6	3.0	35	4850	0.503	0.267	230	630	690	890
SR1_24_96_6_X52	455 (66.0)	-0.82	610	6.35	96	36.7	6.0	45	4630	0.661	0.539	310	570	630	770
SR2_24_70_3_X52	455 (66.0)	-0.82	610	8.74	70	18.2	3.0	45	4290	0.687	0.278	320	730	810	990
SR1_12_45_6_X65	455 (66.0)	-0.82	324	7.14	45	19.7	6.1	30	2030	0.666	0.437	430	450	490	590
SR1_12_68_3_X65	455 (66.0)	-0.82	324	4.78	68	10.1	3.1	20	2310	0.416	0.210	340	360	440	530
SR2_12_45_3_X65	455 (66.0)	-0.82	324	7.14	45	9.8	3.0	30	2110	0.653	0.213	400	360	470	650
SR2_12_68_3_X65	455 (66.0)	-0.82	324	4.78	68	10.0	3.1	25	2310	0.520	0.208	360	380	430	530
SR4_12_37_3_X65	455 (66.0)	-0.82	324	8.74	37	9.6	3.0	35	2050	0.773	0.212	520	470	570	770
SR4_12_45_6_X65	455 (66.0)	-0.82	324	7.14	45	19.7	6.1	40	2030	0.888	0.437	440	480	530	610

ND - Not determined within stress assessment range.

$$I_{axial} = 1.2 \left[ A_{SR} (SR)^2 + B_{SR} (SR) + C_{SR} \right] + \left[ A_{D/t} \left( \frac{D}{t} \right)^2 + B_{D/t} \left( \frac{D}{t} \right) + C_{D/t} \right] + \left[ A_d (d)^2 + B_d (d) + C_d \right] + \left[ A_{d/\sqrt{L}} \left( \frac{d}{\sqrt{L}} \right)^2 + B_{d/\sqrt{L}} \left( \frac{d}{\sqrt{L}} \right) + C_{d/\sqrt{L}} \right] + \left[ A_{l/\sqrt{L}} \left( \frac{l}{\sqrt{L}} \right)^2 + B_{l/\sqrt{L}} \left( \frac{l}{\sqrt{L}} \right) + C_{l/\sqrt{L}} \right] \quad \text{Eqn. 3.2}$$

**Table 3.5: Equation Coefficients to Estimate Dent-Girth Weld Interaction Distances**

Pressure Range (% MOP)	Regression Equation Coefficients						Mean Error (mm)	Max Error (%)	Min Error (%)
	Coeff	SR	D/t	d	d/√L	l/√L			
75 – 100	A	415.82	0.02	66.46	265.25	-406.98	22	15	-11
	B	336.06	-4.56	-698.62	-350.33	1689.98			
	C	233.33	233.33	233.33	233.33	233.33			
50 – 100	A	87.16	-0.02	-157.18	-299.73	-7435.48	31	19	-12
	B	-252.71	2.23	1180.18	776.62	8277.58			
	C	-682.75	-682.75	-682.75	-682.75	-682.75			
25 – 100	A	183.85	-0.03	-167.01	-274.63	-8206.91	28	16	-9
	B	-225.83	4.11	1218.56	737.45	9402.45			
	C	-743.21	-743.21	-743.21	-743.21	-743.21			
0 – 100	A	-16.15	0.05	43.98	470.19	-7448.47	18	8	-4
	B	115.58	-10.07	-811.53	-600.68	10166.21			
	C	265.54	265.54	265.54	265.54	265.54			

Figures 3.13 and 3.14 present comparisons between the interaction distances measured from the FE models and the estimated values using the regression equations. An illustration of the calculation process used to estimate the permissible interaction distance,  $I_{axial}$ , is provided below for model SR2\_12\_45\_3\_X52 assuming a 75% to 100% pressure fluctuation range:

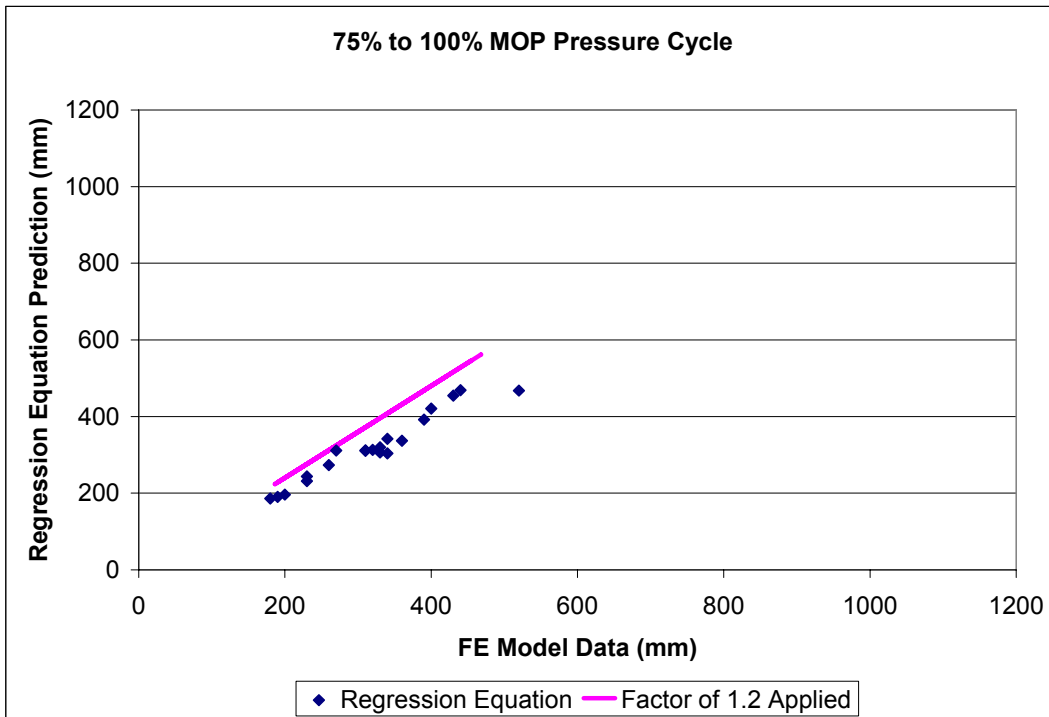
$$I_{axial} = 1.2 \left[ 415.85(0.82)^2 + 336.06(0.82) + 233.33 \right] + \left[ 0.02(45)^2 - 4.56(45) + 233.33 \right] + \left[ -66.46(3.0)^2 - 698.62(3.0) + 233.33 \right] + \left[ 265.25(0.656)^2 - 350.33(0.656) + 233.33 \right] + \left[ -406.98(0.214)^2 + 1689.98(0.214) + 233.33 \right] = 333 \text{ mm}$$

The actual regression equation value in this case was 278 mm, but recall that based upon the variability in the regression equation results it was recommended that  $I_{axial}$  be calculated using an additional factor of 1.2 to ensure that the estimate of interaction distance is conservative.

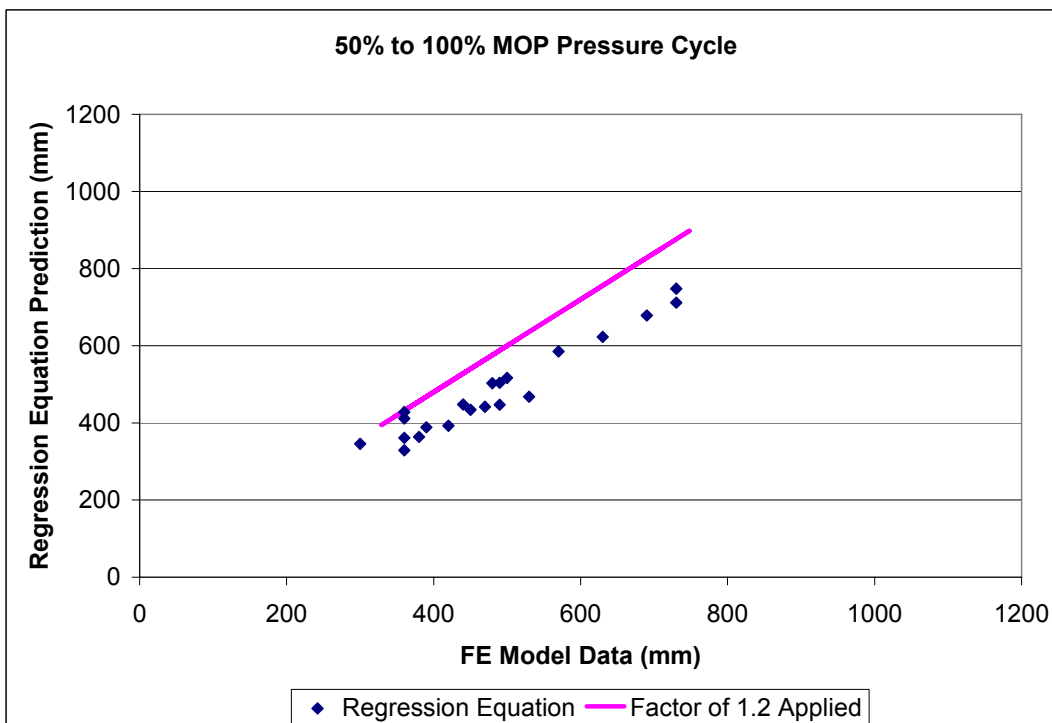
An analysis was undertaken to evaluate the sensitivity of the regression equation results to the input data. The regression process was repeated except one model result was excluded and the resulting equations were used to estimate the interaction distance for the omitted model. The results are presented in Table 3.6 and there was some sensitivity to the input data, however the results were still reasonable. This sensitivity could likely be improved upon by expanding the FE model data set to include more pipe and dent geometry combinations. The multiplication factor of 1.2 was omitted from the sensitivity analysis.

**Table 3.6: Summary of Dent-Girth Weld Regression Analysis Sensitivity Study**

Pressure Range (% MOP)	Model Omitted from Regression	Interaction Distance from Model (mm)	Full Regression Distance Estimate for Omitted Model (mm)	Distance Prediction with Model Omitted from Regression (mm)	Mean Error Full Data Set Regression (mm)	Mean Error Reduced Data Set Regression (mm)
75 – 100	SR4_12_37_3_X52	270	311	338	22	20
50 – 100	SR4_12_45_6_X65	480	503	497	31	33
25 – 100	SR1_24_96_3_X52	690	689	767	28	28
0 – 100	SR1_12_68_6_X52	450	446	503	18	17

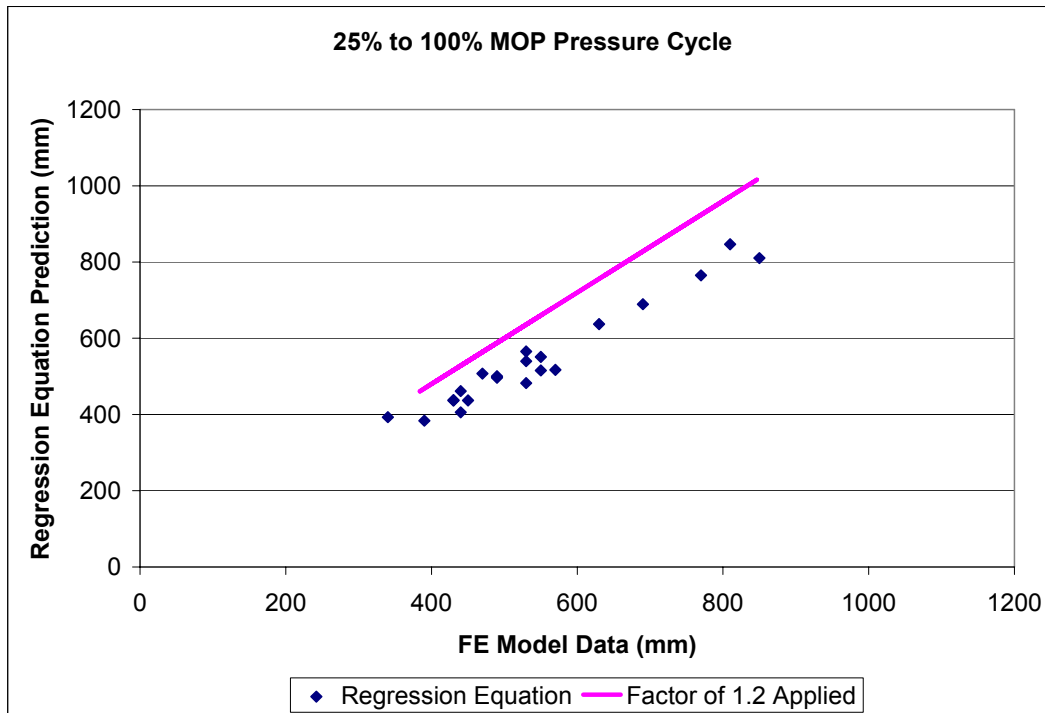


(a)

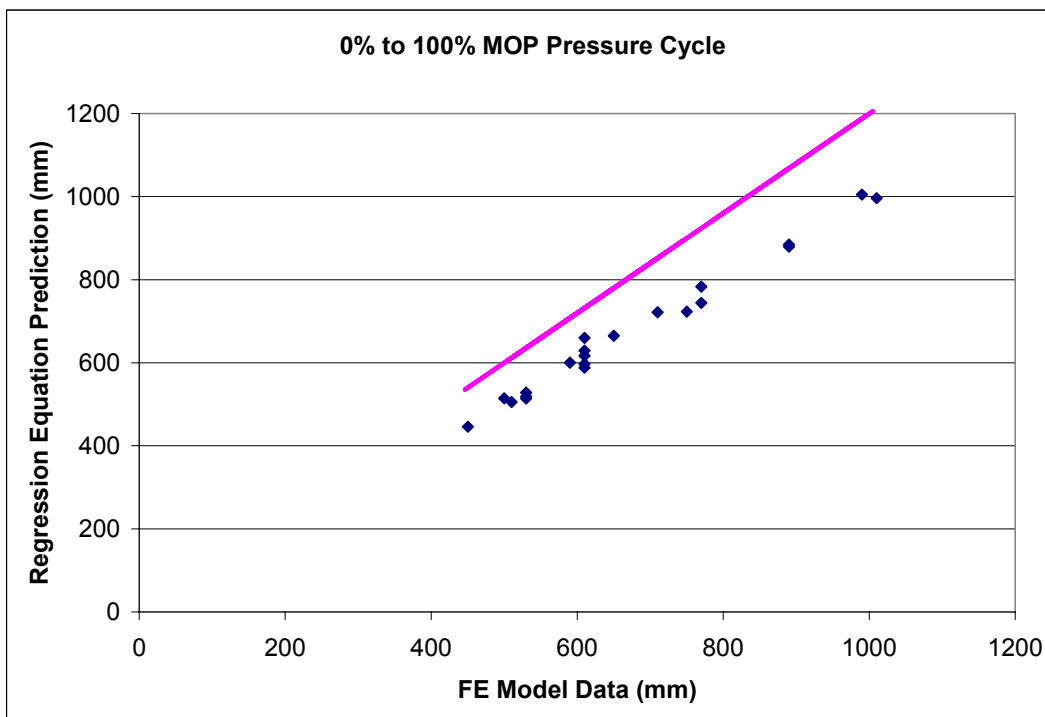


(a)

**Figure 3.13: Dent Girth Weld Interaction Criteria Performance for (a) 75% to 100% MOP and (b) 50% to 100% MOP Pressure Fluctuation Ranges**



(a)



(b)

**Figure 3.14: Dent Girth Weld Interaction Criteria Performance for (a) 25% to 100% MOP and (b) 0% to 100% MOP Pressure Fluctuation Ranges**

### 3.7 Dent-Weld Interaction Summary

Procedures have been developed to estimate acceptable distances between the peak of a dent and a long seam or girth weld subjected to the following inputs:

- The dents are restrained rock dents and acceptable in terms of strain based criteria like that presented in ASME B31.8 [3.1]
- The criteria assume time-based failure modes due to internal pressure fluctuations (fatigue failures)
- The dent geometries are such that they are symmetrical (or in practical terms nearly symmetrical) about the axial and circumferential orientations through the dent peak.
- The criteria have considered pipe geometries in the range of 324 mm (NPS12) to 610 mm (NPS24) OD with D/t ratios between 37 and 96.
- The pipe material properties ranged from Grade 359 (X52) to 448 (X65) and the fatigue calculations are limited to materials with UTS values below 552 MPa (80 ksi).

Given the consistency in the results generated to establish the dent-long seam weld interaction criteria no further work should be required to validate the criteria for symmetrical dents for a wider range of pipe and symmetrical dent geometries. Provided that the long seam is located outside of the region of inward radial deformation (as shown in Figure 4.9) the dented pipe should behave in a similar manner to an undeformed pipe segment in terms of its response to internal pressure fluctuations. Further work should be undertaken to confirm this observation for unsymmetrical dent profiles.

A consistent rule of thumb approach could not be considered for the axial direction interaction between a dent and a girth weld. Regression equations have been established to estimate acceptable distances between a dent peak and a girth weld based upon the pipe material properties, pipe geometry and dent geometry. These regression equations have demonstrated a slight variability depending upon the input data set and further numerical modeling could be considered to reduce this variability. Within such a carry on project, it may be worthwhile to add examples of larger diameter pipe and an additional material grade (possibly Grade 290) to confirm the trends observed for the existing data set hold for a wider range of input parameters. It would also be prudent to add examples of unsymmetrical dent profiles.

In order to apply the dent-girth weld interaction criteria, an analysis of the pipeline operating pressure data should be conducted to determine the typical pressure fluctuation regime for the pipeline system so that the appropriate regression equation can be applied. In the absence of this information the 0% to 100% MOP pressure fluctuation equation could be used to ensure a conservative estimate of the allowable distance between the dent peak and the girth weld.

It is acknowledged that the weld geometry and weld material properties have not been incorporated directly into the FE models used to develop these criteria. However, the pipe wall in the models at the allowable weld positions experience very little, if any, plastic deformation or radial deflection, therefore the geometry, stiffening or material property mismatch effects due to the weld would be minimal.

### **3.8 References**

- 3.1 American Society of Mechanical Engineers, ASME B31.8-2003, “Gas Transmission and Distribution Piping Systems.”
- 3.2 Canadian Standards Association, CAN-CSA Z662-03, “Oil and Gas Pipeline Systems.”
- 3.3 American Society of Mechanical Engineers, Boiler and Pressure Vessel Code, Section VIII, Division 3, “Alternative Rules for the Construction of High Pressure Vessels.”
- 3.4 API Publication 1156, “Effects of Smooth and Rock Dents on Liquid Petroleum Pipelines”, First Edition, November, 1997.

## 4. OVALITY – WELD INTERACTION CRITERIA

The following section summarizes the development of the ovality-weld interaction criteria. As with the dent-weld interaction criteria, the premise behind the ovality criteria is based upon the pressure fluctuation response of the ovalized pipe as predicted by finite element modeling, but it is only applicable to long seam interaction. The interaction criteria, (circumferential distance between oval peak and a long seam weld), is based on the location at which the ovalized pipe behaves similarly to a nominal circular pipe, where the estimated fatigue life, based on the ASME design curve [4.1] is used to compare ovalized and circular pipe behaviours.

### 4.1 Pipeline Ovality

Pipe ovality (out-of-roundness) can be described as the maximum difference between the smallest and largest diameter that exists at a given pipe cross section as defined in Figure 4.1.

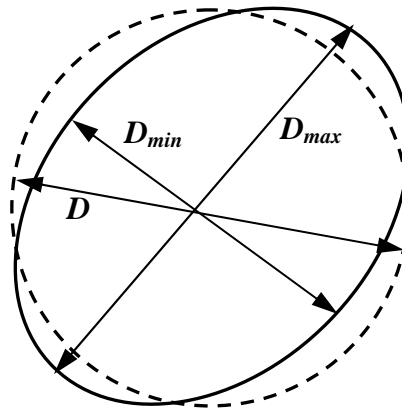


**Figure 4.1: Ovalized Pipe Cross-section**

When an oval pipe is pressurized, in addition to the normal circumferential membrane stress ( $\sigma = pr/t$ ) associated with internal pressure, there exists a circumferential bending stress due to the local re-rounding of the pipe wall associated with the ovalized section. The addition of the local circumferential bending stress can detrimentally affect the fatigue performance of the pipe. Affects of ovality on the pipe wall longitudinal stresses are minimal.

### 4.2 Assumptions used to Generate the Ovality – Weld Interaction Criteria

The ovality-weld interaction criteria were developed using a matrix of finite element models, (used to estimate the pipe wall stresses for the fatigue performance predictions). The matrix was assembled to include a range of parameters that could influence the response of ovalized pipe, including:

- Pipe geometry ( $D/t$ )
- Ovality
- Internal Pressure Fluctuations
- Material Properties
- Desired fatigue life ratio

Due to the large number of variables considered in the analysis, it was not deemed practical to consider modeling every possible combination of influential parameters within the scope of this project. Therefore, a matrix was assembled to cover a wide range of scenarios, the results of which could be used to identify trends and generate an ovality-weld interaction criterion. The complete numerical modeling matrix used in the analysis is presented in Table 4.3. Brief descriptions of the major assumptions and idealizations used in developing the weld interaction criteria are presented in the following sub-sections.

#### 4.2.1 Weld Seam

The ovality-weld interaction criteria developed in this project is primarily aimed at the long seam weld in an ovalized pipe. Based upon the critical angle definition, these criteria may also be used to identify areas in a girth weld, in an ovalized pipe that deserve additional inspection scrutiny when a pipe is unearthed.

#### 4.2.2 Pipe Geometry

The pipe diameters were larger than 324 mm (NPS 12) and wall thicknesses in excess of 4.78 mm (0.188 inches) typical of larger transmission pipelines. A total of four pipe diameters, with three pipe wall thickness each were included in the analysis matrix.

#### 4.2.3 Material Properties

In order to understand the potential effect of pipeline material grade on the ovality-weld interaction criteria, the same two material grades used in the dent-weld interaction criteria have been included in the analysis matrix, Grade 359 (X52) and Grade 448 (X65). As discussed previously during the development of the dent-weld interaction criteria, pipe material behaviour was based solely on minimum specified material properties assuming kinematic hardening behaviour.

#### 4.2.4 Ovality

Six levels of initial pipeline ovality were considered in the analysis; 1, 2, 4, 6, 8 and 10% where the level of ovality ( $\omega$ ) is expressed as:

$$\omega = \frac{D_{\max} - D_{\min}}{D_{av}} \times 100$$

where  $D_{\max}$  = maximum pipe diameter (at the major axis of the ovalized pipe)  
 $D_{\min}$  = minimum pipe diameter (at the minor axis of the ovalized pipe)  
 $D_{av}$  = average (nominal) pipe diameter

For the purposes of the analysis, the level of ovality refers to the ovalization that exists under zero internal pressure, following initial re-rounding of the pipe. In addition, the ovalized pipes are considered to be in a stress free state when ovalized (i.e., no residual stress exists in the pipe due to the process that caused the ovalization), and the re-rounding of the pipe due to internal pressure is conservatively assumed to occur in air (i.e., no soil restraint is considered in the analysis).

#### 4.2.5 Weld Type and Location

The assumptions stated in Section 3.1.5 are also applicable to the long seam welds in the ovality-weld interaction criteria. Weld quality and residual stress issues are incorporated into the design curve [4.1] and a factor of 3 is applied to the stress fluctuation ranges as an estimate of weld geometry effects.

#### 4.2.6 Internal Pressure and Pressure Fluctuations

Pipelines operate within different pressure regimes, where the internal operating pressure is a function of a number of variables including product, distance from discharge and suction stations, elevation etc. As the internal pressure fluctuations have a direct impact on the pipe wall stress fluctuations, and hence fatigue life predictions, it was considered paramount that the ovality-weld interaction criteria account for various pressure fluctuation regimes. Therefore, the numerical modeling matrix includes four internal pressure fluctuation ranges: 75% to 100% MOP, 50% to 100% MOP, 25% to 100% MOP and 0 to 100% MOP.

#### 4.2.7 Fatigue Life Ratio

In addition to the nominal membrane stress that exists in the pipe wall due to internal pressurization, re-rounding of an ovalized pipe results in a bending stress through the pipe wall thickness. At the peak of minor axis of an ovalized pipe, the combination of the membrane and bending stresses results in an increase in the extreme fibre stress on the outer surface of the pipe wall and a decrease in stress on the inner surface of the pipe wall. At the peak of the major axis, the scenario is reversed, with an increase on the inner surface of the pipe wall, and a decrease on the outer surface. Due to the distribution of the through thickness bending stresses in an ovalized pipe, at all points around the circumference of the pipe, either the inner or the outer surface extreme fibre stress is greater than the extreme fibre stress in an equivalent circular pipe (except at one point along the circumference where the bending stress is zero, which nominally occurs at the 45° point between the major and minor axes). Therefore, the fatigue lives calculated based on the extreme fibre stress will always be less for an ovalized pipe than for a circular pipe. Therefore, in order to provide a basis for comparison, three different life ratios were considered in the development of the interaction criteria, 90%, 75% and 50%, where the life ratio is expressed as a portion of the circular pipe fatigue life.

### **4.3 Intended Application of the Ovality – Weld Interaction Criteria**

CSA Z662 recommends a maximum ovality of 3% in order to avoid sectional collapse. If sectional collapse is not considered to occur, the maximum recommended ovality is 6% based on the unhindered passage of inspection instruments. The ovality-weld interaction criteria developed in this project is not intended to supersede existing standards or recommendations (i.e., CSA Z662, etc), but instead it is intended to be used in addition to current practices, for ovalities up to and including 6%.

The ASME based fatigue life procedure provides a means of characterizing the acceptability of an ovalized pipe interacting with a weld, based upon an assessment of the pipe fatigue life due to pressure cycling. Therefore, it represents an additional criterion which may be used to evaluate ovalized pipe scenarios.

#### 4.4 Description of FE Models used to Develop the Criteria

The following sections describe the finite element model used to develop the ovality-weld interaction criteria. The analysis was carried out using the ANSYS 10.0 finite element software.

##### 4.4.1 Finite Element Model

A typical finite element model used in analyzing ovalized pipes is shown in Figure 4.2. The model is constructed with the ovalized shape being considered. The  $\frac{1}{4}$  symmetry model is approximately 100 mm long and assumes that the ovalization exists along the entire length of the pipe. The model uses 4-noded, shell elements with reduced integration (9 integration points through the thickness) to model the entire pipe length. The elements are 5mm long along the axis of the pipe and approximately 2.5mm along the circumference of the pipe wall.

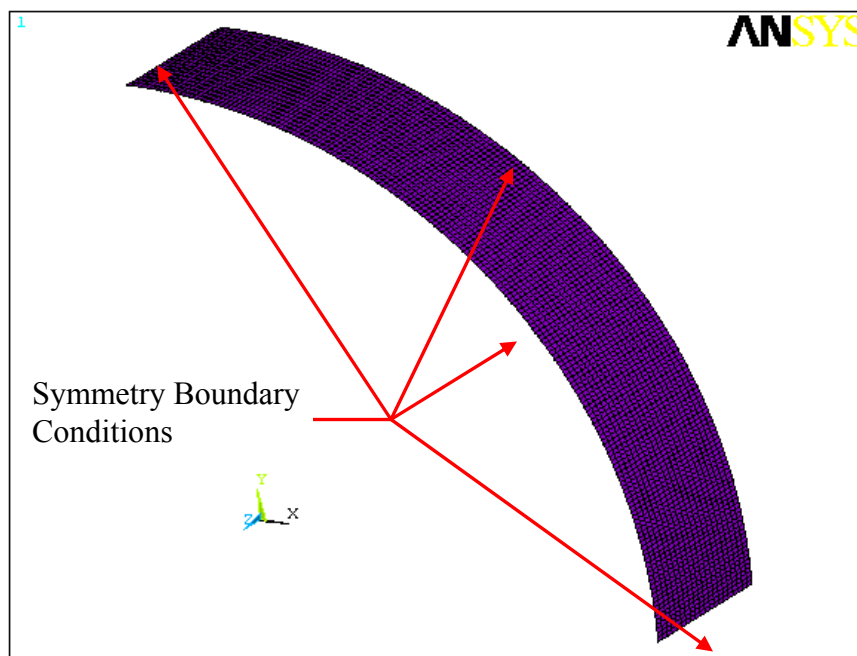


**Figure 4.2: ANSYS Finite Element Model - Ovality**

##### 4.4.2 Material Model

The ASME design fatigue curve [4.1] used in this project is applicable to welds in low carbon steel with an ultimate tensile strength of less than 552 MPa (80 ksi). Therefore, to assess the impact of material grade on the ovality-weld interaction criteria, the highest strength pipeline material that could be considered was Grade 448 (X65). Grade 359 (X52) and Grade 448 (X65) material properties were selected.

The following material property assumptions were used for the criteria development matrix:

Grade 359 (X52) Pipe Properties:

- Linear proportionality limit at strain = 0.0015 and stress = 311 MPa (45 ksi)
- SMYS at strain = 0.005 and stress = 359 MPa (52ksi)
- UTS at strain = 0.10 and stress = 455 MPa (66 ksi)

#### Grade 448 (X65) Pipe Properties:

- Linear proportionality limit at strain = 0.0019 and stress = 386 MPa (56 ksi)
- SMYS at strain = 0.005 and stress = 448 MPa (65 ksi)
- UTS at strain = 0.10 and stress = 531 MPa (77 ksi)

The strain and stress values at the linear proportionality limit and the strain at UTS were based upon typical stress strain curve data observed during BMT testing programs and ensure a material elastic modulus of approximately 207 GPa (30,000 ksi). Poisson's ratio for the material was assumed to be 0.30.

The engineering stress and strain values were converted to true stress and true strain for incorporation into the numerical models and kinematic hardening was assumed. Material anisotropy was ignored.

#### 4.4.3 Boundary Conditions and Load Sequence

The boundary conditions used in the finite element model are illustrated in Figure 4.2, and consist of symmetry boundary conditions on all four free edges of the ¼ symmetry model.

The load sequence used in the finite element analysis consists of five stages, designed to mimic the typical service loading experienced by pipelines. The five step load sequence is summarized as follows:

1. Increase the pipe internal pressure to 100% of MOP
2. Reduce pipe internal pressure to 75% of Case 3 pressure ( $0.72 \times 0.75 = 0.54 \times \text{MOP}$ )
3. Reduce pipe internal pressure to 50% of Case 3 pressure ( $0.72 \times 0.50 = 0.36 \times \text{MOP}$ )
4. Reduce pipe internal pressure to 25% of Case 3 pressure ( $0.72 \times 0.25 = 0.18 \times \text{MOP}$ )
5. Reduce pipe internal pressure to zero pressure.

#### 4.5 **Finite Element Model Matrix**

The finite element model matrix used to develop the ovality-weld interaction criteria was comprised of a total of 144 separate models which represents all the combinations of the four major input parameters. The range of input parameters is summarized in Table 4.1.

**Table 4.1: Finite Element Model Input Parameter Range**

<b>Parameter</b>	<b>Range of Values</b>	
Pipe Material Grade	X52, X65	
Pipe Diameter (mm)	323.85	608, 914, 1219
(in)	12.75	24, 36, 48
Pipe Wall Thickness (mm)	4.78, 7.14, 8.74	7.14, 8.74, 12.5
(in)	0.188, 0.281, 0.344	0.281, 0.344, 0.492
Ovality (%)	1, 2, 4, 6, 8, 10	

## 4.6 Finite Element Model Results Post-Processing

### 4.6.1 Residual Pipe Ovality

As stated previously, the ovality-weld interaction criteria have been developed based on the ovality at zero internal pressure, following initial re-rounding of the pipe. This condition represents the ovality a pipe will experience in-service, following the initial ovalization process and re-rounding due to internal pressurization.

The residual ovality at the end of load case five in the finite element analysis for the X52 and X65 finite element models are presented in Figures 4.3 and 4.4, respectively. The figures relate the residual ovality to the initial ovality and the pipe D/t ratio. As can be seen, higher D/t ratio pipes re-round less than lower D/t ratio pipes, and therefore result in larger residual ovalities.

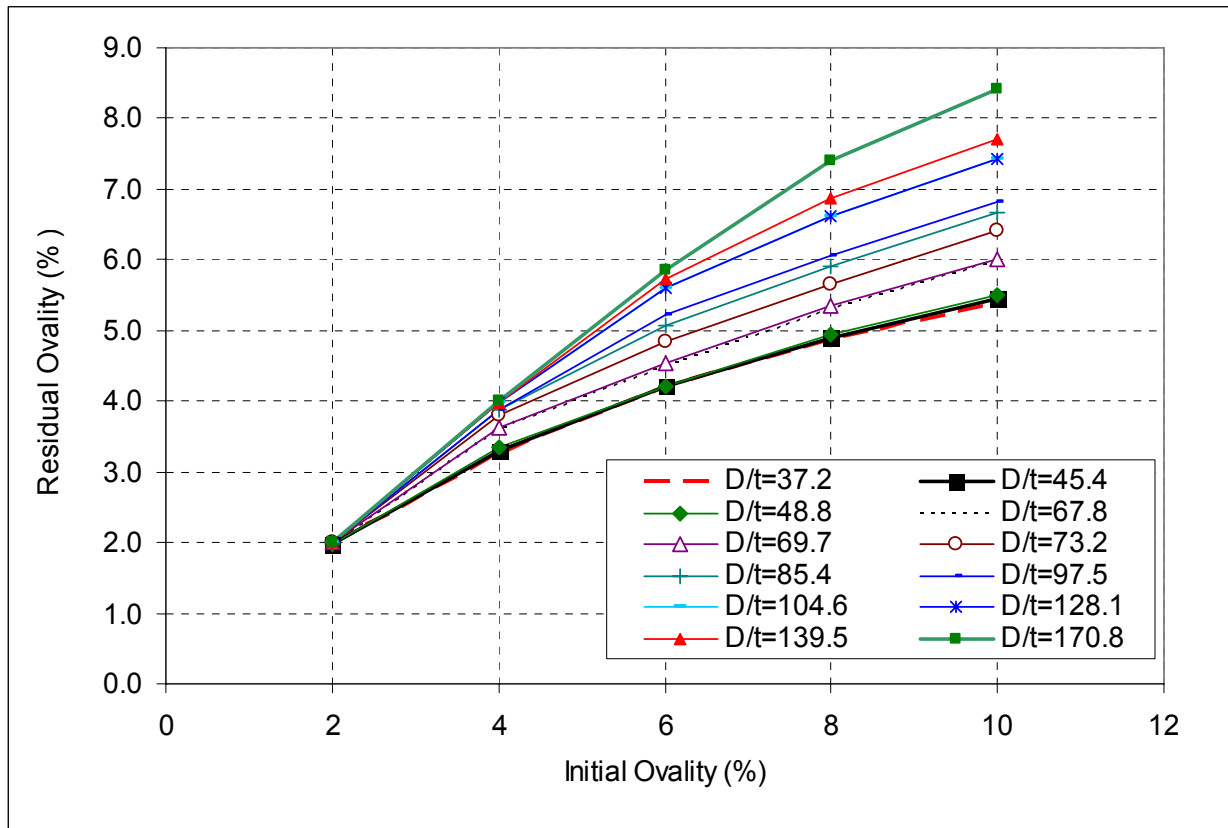
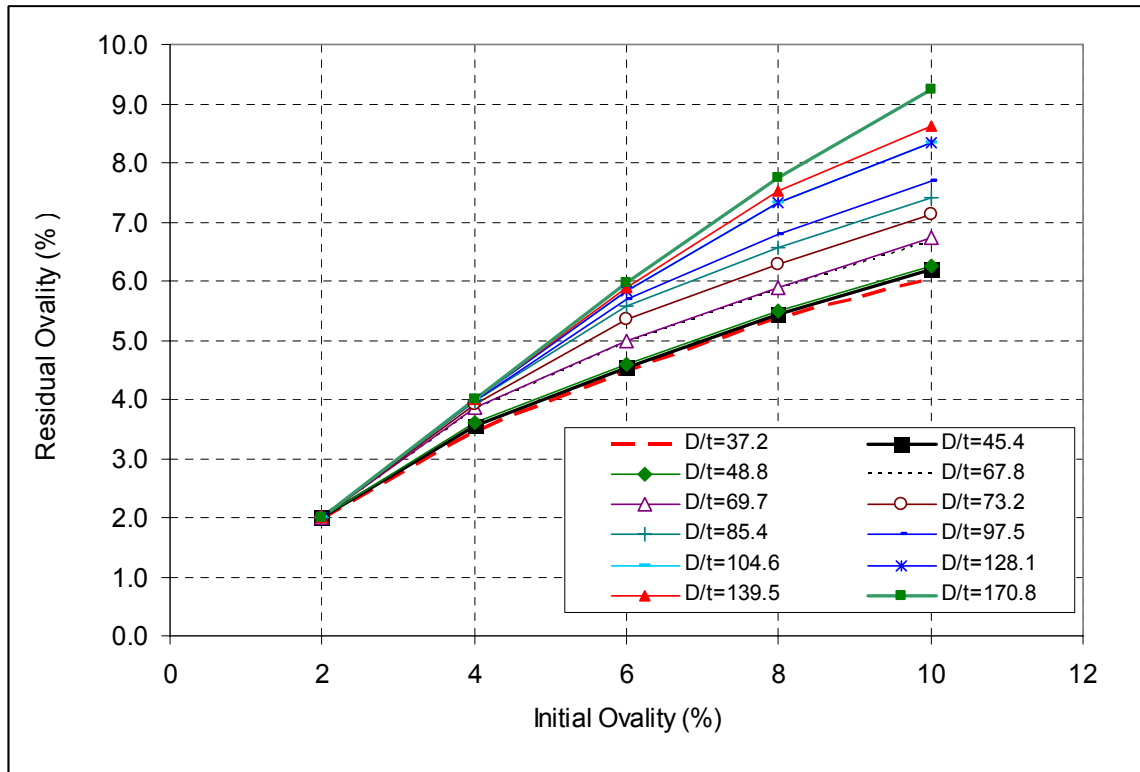


Figure 4.3: Residual Ovality at End of Finite Element Analysis – X52



**Figure 4.4: Residual Ovality at End of Finite Element Analysis – X65**

The ovality-weld interaction criteria have been developed based on the residual ovalities shown in Figures 4.3 and 4.4. In order to remain consistent with current practices and guidelines, residual ovalities greater than 6% have not been included in the development of the criteria. In addition, results of the finite element analysis indicate that plasticity occurs at the peak locations in the ovalized pipes for ovalities greater than 6%, and therefore are not considered valid for use in a stress based fatigue life calculation.

#### 4.6.2 Determination of Effective Residual Ovality at Zero Pressure

Pipeline ovality is generally detected in in-service pipelines through the use of internal inspection tools. As it is the internal pressure in the pipeline that propels these inspection tools through the pipeline, ovality detected by inspection tools will generally be detected while the pipeline is pressurized. The ovality detected upon inspection will not be equal to the zero pressure ovality, therefore a means of relating the ovality at a given pressure to the zero pressure residual ovality, used in developing the interaction criteria, is required.

In lieu of a formal relationship between ovality and internal pressure, Figure 4.5 presents the results of the finite element analysis, relating the ovality (as a % of the residual ovality) to the internal pressure (% of MOP) and the pipe geometry (D/t).

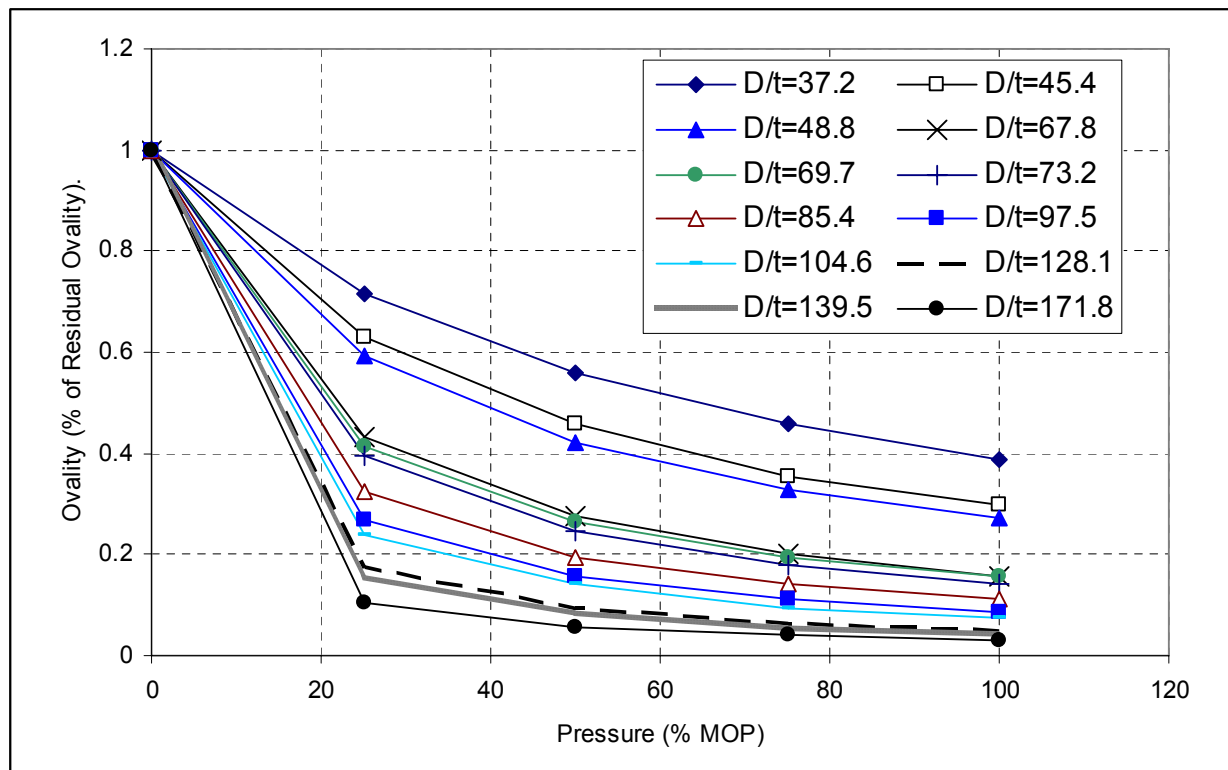


**Figure 4.5: Percentage of Residual Zero Pressure Ovality vs. Internal Pressure**

Figure 4.5 can be used to estimate the zero pressure residual ovality, based on the internal pressure at the time of inspection, the measured ovality under pressure and the pipe D/t ratio.

#### 4.6.3 Critical Angle Determination

The post processing carried out on the finite element model results was similar to that described in relation to the dent-weld interaction criteria. The main focus of the post processing was to estimate the fatigue life for each of the nodes along the circumference of the ovalized pipe wall and compare these to the estimated fatigue life for a circular pipe.

A summary of the major post processing steps is presented below:

- Determine the OD and ID surface equivalent stress levels (as defined in Section 2.0) for each of the nodes along the circumference of the pipe wall, for each of the pressure levels in load steps 1 to 5. (The equivalent stress values were multiplied by a stress concentration factor of 3 to account for potential weld toe stress concentration effects).
- Use these stress levels to calculate the equivalent stress range at the OD and the ID for each node, resulting from each of the following pressure fluctuations:
  - 75% to 100% MOP
  - 50% to 100% MOP
  - 25% to 100% MOP
  - 0% to 100% MOP

- Based on the ovalized pipe equivalent stress ranges, the number of pressure cycles of the applied pressure range was determined using the ASME fatigue design curve [4.1] for each of the nodes around the circumference of the pipe wall. (The design curve for carbon steel weldments is truncated at a life of  $1 \times 10^8$  cycles, therefore, whenever a value in excess of  $1 \times 10^8$  was calculated it was assumed to be equal to  $1 \times 10^8$ ).
- The fatigue life of a circular pipe was estimated based on the ASME design curve [4.1].
- The relative fatigue life (ratio of the ovalized pipe fatigue life to the circular pipe fatigue life) was determined for each node along the circumference of the pipe wall.

The results of the post processing were used to relate the relative fatigue lives to the circumferential position of the node, an example of which is shown in Figure 4.6. The circumferential position, in degrees, is measured from the peak of the minor axis.

A relative fatigue life of 1.0 indicates the life estimate for an ovalized pipe is the same as that for a circular pipe. The location where the OD or ID life prediction curves drop below a value of 1.0 indicates locations where the ovality and the weld are considered to interact, which reduces the life estimate for the pipe segment.

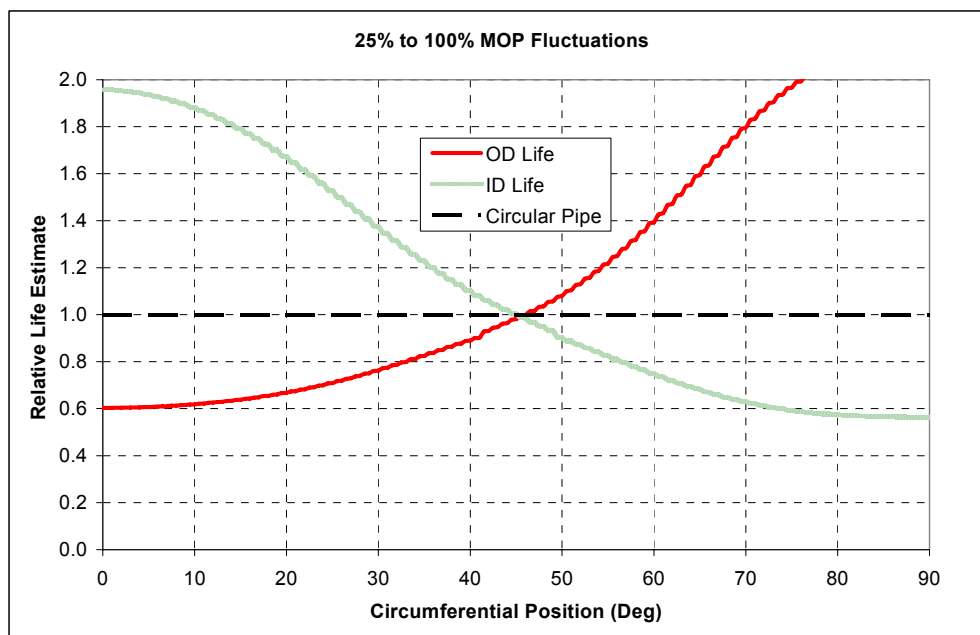


**Figure 4.6: Relative Fatigue Life vs. Circumferential Position**

As can be seen in Figure 4.6, there is only one point along the circumference of the pipe where both the OD and the ID life are equal to the life of a circular pipe. Based on this fact, it can be said that a long seam weld will interact with ovality and therefore reduce the pipe life, at all points along the pipe circumference. In order to develop a more practical ovality-weld interaction criterion, three fatigue life ratios were considered (90%, 75% and 50%). For each fatigue life ratio, a critical maximum angle, see Figure 4.7, was determined which defines the area where a weld cannot be located to achieve the desired relative fatigue life when compared to a nominal circular pipe. The critical angle is measured from either the peak of the major or the minor axis of the ovalized pipe.

An illustration of the critical angles for a relative fatigue life of 75% is presented in Figure 4.8 for the example results shown in Figure 4.6. The acceptable region is bounded between 27° and 59° from the minor axis of the ovalized pipe. For the purposes of the interaction criteria development, the maximum critical angle is taken to be the maximum angle from either the major or the minor axis. For the example case the critical angle,  $\alpha_{crit}$ , is calculated as follows:

$$\text{Critical angle: } \alpha_{crit} = \text{MAX}(27, 90-59) = 31^\circ$$

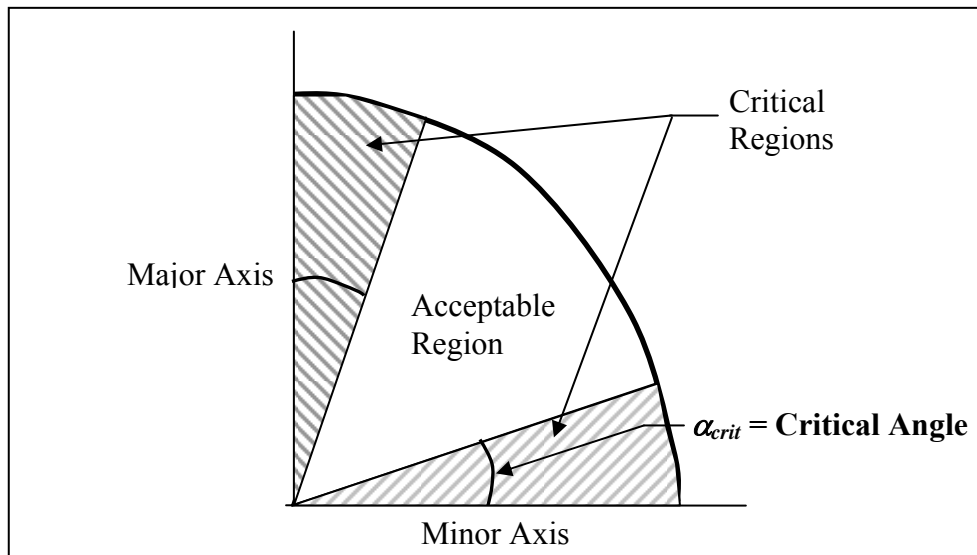


Figure 4.7: Critical Angle and Acceptable Region

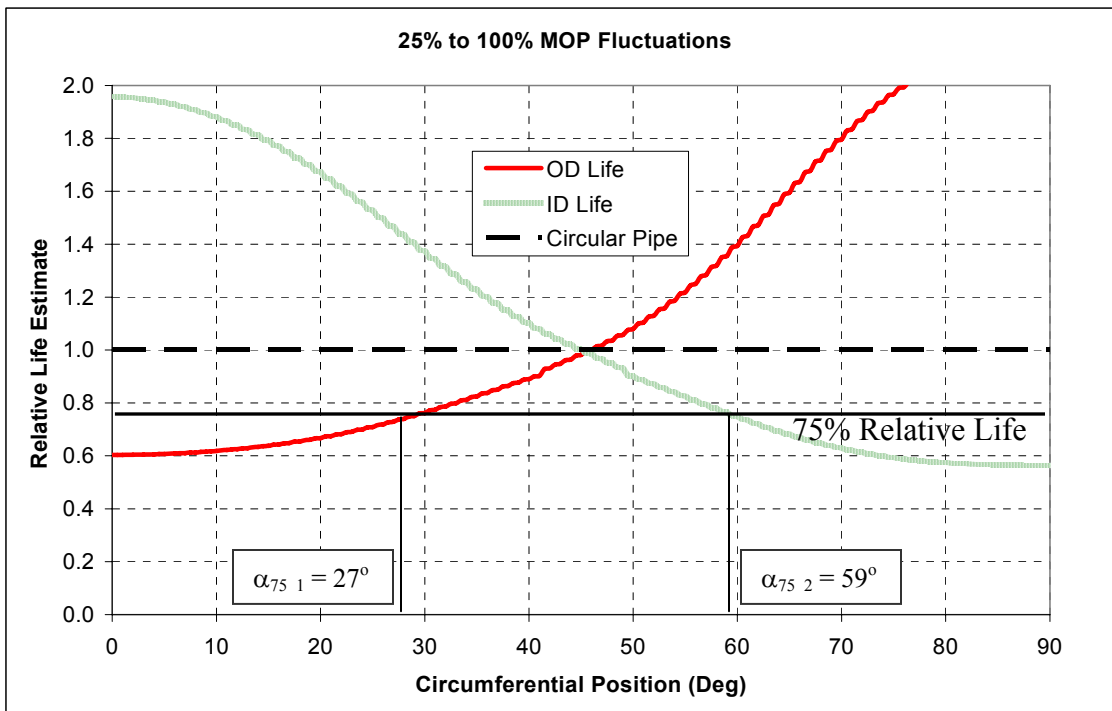


Figure 4.8: Critical Angles

## 4.7 Ovality-Weld Interaction Criteria Development

The criteria was developed as an equation relating the critical half angle,  $\alpha_{crit}$ , to the major geometry and operational input parameters, which will be discussed later in the section.

### 4.7.1 Identification of Scenarios of Interest

Many of the finite element modeling scenarios considered, resulted fatigue life that were very high (capable of supporting in excess of  $1 \times 10^6$  high pressure range load cycles), or the maximum critical angle,  $\alpha_{crit}$ , was equal to zero (i.e. the combination of geometry and operating conditions considered resulted in a minimum relative fatigue life of at least 90% along the entire circumference of the pipe). Therefore, the first stage in developing the ovality-weld interaction criteria was to highlight the scenarios which resulted in non-trivial solutions. These scenarios formed the basis of the regression analysis used to develop the ovality-weld interaction criteria.

The following two criteria were used to highlight the scenarios of interest:

- Scenarios where the estimated fatigue life was less than  $1 \times 10^6$  (fatigue lives greater than  $1 \times 10^6$  were considered non-critical from a failure point of view).
- Scenarios where the maximum critical angle,  $\alpha_{crit}$ , was greater than 0.

Applying the first criterion to the entire post processing results set eliminates all the 75%-100% MOP pressure fluctuation scenarios, which all have fatigue lives greater than 1 million applied load cycles.

In order to address the second criteria, a table of applicable combinations has been assembled. The information, presented in Table 4.2, illustrates all the possible combinations of geometry and operational conditions, independent of the material grade considered. The shaded cells represent scenarios that result in a critical angle,  $\alpha_{crit}$ , of zero, and therefore result in a relative fatigue life of at least 0.90 around the entire circumference of the pipe. These scenarios are not included in the development of the regression equation. Cells that are not shaded represent scenarios where the critical angle is greater than zero. These cells (a total of 544) and the scenarios they represent are used as the basis of the regression analysis discussed in the following section.

### 4.7.2 Regression Analysis

A regression analysis was carried out, for each pressure range considered in the analysis, to develop an equation relating the critical angle,  $\alpha_{crit}$ , to the following three input parameters:

Pipe D/t Ratio: A pipe geometry parameter calculated using the ratio of the nominal pipe outside diameter (D) to the nominal pipe wall thickness (t).

Ovality,  $\omega$  (%): The pipe ovality calculated using the following expression:

$$\omega = \frac{D_{max} - D_{min}}{D_{av}} \times 100$$

where  $D_{max}$  = maximum pipe diameter

$D_{min}$  = minimum pipe diameter

$D_{av}$  = average (nominal) pipe diameter

Relative Fatigue Life (*R.L.*): Expressed as a fraction of the baseline line circular pipe fatigue life, calculated using the ASME design curve [4.1] and applying a stress concentration factor of 3 to account for the potential effects of the weld profile. (e.g. 0.75)

While the pressure range considered for each pipe geometry and material combination was established as a function of MOP, the regression demonstrated that material grade had a relatively small effect on the estimated relative fatigue lives for all the geometry and operational conditions considered, and therefore, the material grade was not considered in the regression analysis.

For the purposes of the regression analysis, it was assumed that a quadratic relationship existed between each of the three input parameters and the critical angle, such that the combined equation had the following form:

$$\alpha_{crit} = \beta \left( \left[ a \left( \frac{D}{t} \right)^2 + b \left( \frac{D}{t} \right) \right] + [c(\omega)^w + d(\omega)] + [e(R.L.)^2 + f(R.L.)] + g \right)$$

where the parameters  $a - g$  represent the constants of the regression equation and  $\beta$  represents a scaling factor (described later).

The regression analysis was carried out using an iterative procedure to minimize the mean squared error between the critical angle based on the finite element results and the critical angle calculated based on the regression equation, as expressed in the equation below:

$$MSE = \sqrt{\frac{\sum_i^n ((\alpha_{crit} \text{ FE Model}) - (\alpha_{crit} \text{ Equation}))^2}{n}}$$

where  $n$  = the total number of models used in the regression analysis (296).

The results of the regression analysis are summarized in Table 4.3 in terms of the regression constants,  $a - I$ , the mean and maximum error associated with the regression equations and the scale factors (discussed below). The agreement between the regression equation and the finite element results is illustrated in Figures 4.9 to 4.11, which compares the predicted critical angle based on the regression equation with the critical angle based on the finite element analysis.

**Table 4.2: Summary of Regression Cases**

	D/t	Relative Life (R.L)											
		37.1	45.4	48.8	67.8	69.7	73.2	85.4	97.5	104.6	128.1	139.5	170.8
Ovality (%)	P.R. (% MOP)												
1	50	90	90	90	90	90	90	90	90	90	90	90	90
		75	75	75	75	75	75	75	75	75	75	75	75
		50	50	50	50	50	50	50	50	50	50	50	50
	75	90	90	90	90	90	90	90	90	90	90	90	90
		75	75	75	75	75	75	75	75	75	75	75	75
		50	50	50	50	50	50	50	50	50	50	50	50
	100	90	90	90	90	90	90	90	90	90	90	90	90
		75	75	75	75	75	75	75	75	75	75	75	75
		50	50	50	50	50	50	50	50	50	50	50	50
2	50	90	90	90	90	90	90	90	90	90	90	90	90
		75	75	75	75	75	75	75	75	75	75	75	75
		50	50	50	50	50	50	50	50	50	50	50	50
	75	90	90	90	90	90	90	90	90	90	90	90	90
		75	75	75	75	75	75	75	75	75	75	75	75
		50	50	50	50	50	50	50	50	50	50	50	50
	100	90	90	90	90	90	90	90	90	90	90	90	90
		75	75	75	75	75	75	75	75	75	75	75	75
		50	50	50	50	50	50	50	50	50	50	50	50
3	50	90	90	90	90	90	90	90	90	90	90	90	90
		75	75	75	75	75	75	75	75	75	75	75	75
		50	50	50	50	50	50	50	50	50	50	50	50
	75	90	90	90	90	90	90	90	90	90	90	90	90
		75	75	75	75	75	75	75	75	75	75	75	75
		50	50	50	50	50	50	50	50	50	50	50	50
	100	90	90	90	90	90	90	90	90	90	90	90	90
		75	75	75	75	75	75	75	75	75	75	75	75
		50	50	50	50	50	50	50	50	50	50	50	50
4	50	90	90	90	90	90	90	90	90	90	90	90	90
		75	75	75	75	75	75	75	75	75	75	75	75
		50	50	50	50	50	50	50	50	50	50	50	50
	75	90	90	90	90	90	90	90	90	90	90	90	90
		75	75	75	75	75	75	75	75	75	75	75	75
		50	50	50	50	50	50	50	50	50	50	50	50
	100	90	90	90	90	90	90	90	90	90	90	90	90
		75	75	75	75	75	75	75	75	75	75	75	75
		50	50	50	50	50	50	50	50	50	50	50	50
5	50	90	90	90	90	90	90	90	90	90	90	90	90
		75	75	75	75	75	75	75	75	75	75	75	75
		50	50	50	50	50	50	50	50	50	50	50	50
	75	90	90	90	90	90	90	90	90	90	90	90	90
		75	75	75	75	75	75	75	75	75	75	75	75
		50	50	50	50	50	50	50	50	50	50	50	50
	100	90	90	90	90	90	90	90	90	90	90	90	90
		75	75	75	75	75	75	75	75	75	75	75	75
		50	50	50	50	50	50	50	50	50	50	50	50
6	50	90	90	90	90	90	90	90	90	90	90	90	90
		75	75	75	75	75	75	75	75	75	75	75	75
		50	50	50	50	50	50	50	50	50	50	50	50
	75	90	90	90	90	90	90	90	90	90	90	90	90
		75	75	75	75	75	75	75	75	75	75	75	75
		50	50	50	50	50	50	50	50	50	50	50	50
	100	90	90	90	90	90	90	90	90	90	90	90	90
		75	75	75	75	75	75	75	75	75	75	75	75
		50	50	50	50	50	50	50	50	50	50	50	50

**Table 4.3: Regression Equation Constants**

Parameter	Pressure Fluctuation Range (% MOP)		
	0% to 100%	25% to 100%	50% to 100%
a	0.0008	-0.0003	-0.001
b	-0.334	-0.180	-0.166
c	-1.266	-0.414	-0.581
d	15.905	6.350	8.631
e	130.904	43.976	41.445
f	-88.533	-18.539	-12.040
g	21.166	18.295	7.814
Scale Factor $\beta$	1.2	1.2	1.3
Mean Error ( $^{\circ}$ )	11	3	4
Maximum Error ( $^{\circ}$ )	40	16.3	17.4

Note that the error statistics for the 0% to 100% MOP pressure range are significantly affected by the overestimation of critical angles greater than  $40^{\circ}$  as illustrated in Figure 4.9.

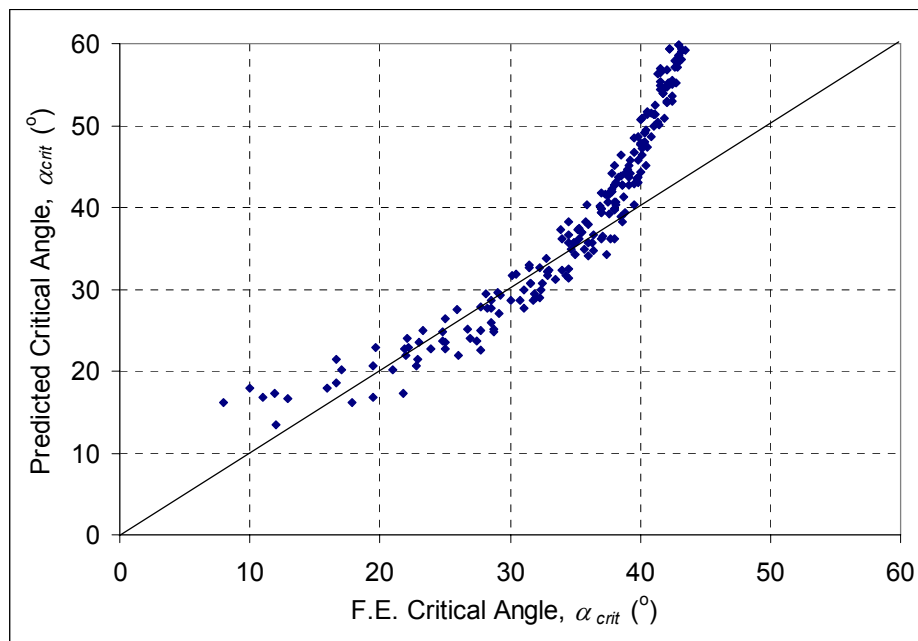


**Figure 4.9: Comparison of Regression Prediction vs. Finite Element Prediction – 0% to 100% MOP Pressure Range**

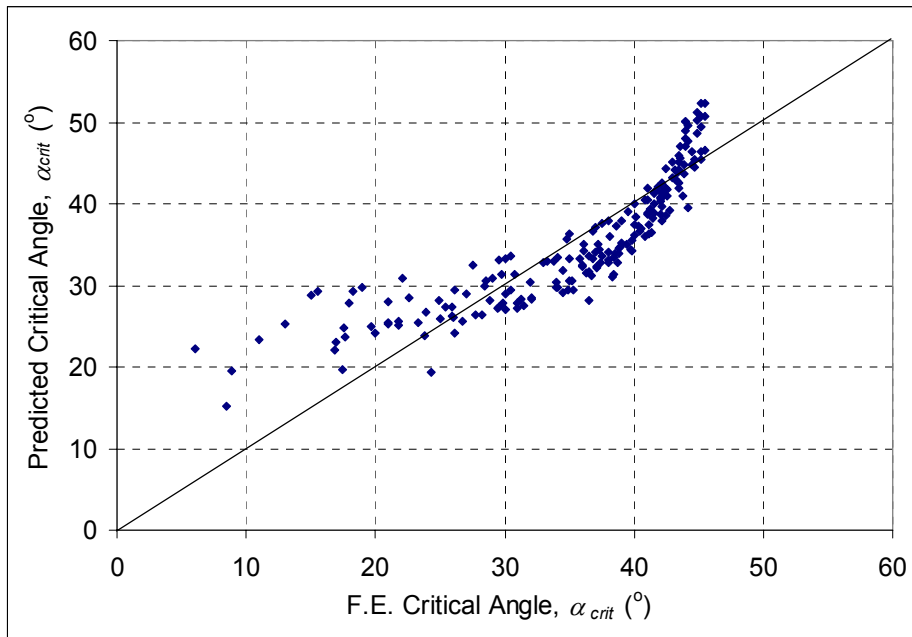


**Figure 4.10: Comparison of Regression Prediction vs. Finite Element Prediction – 25% to 100% MOP Pressure Range**

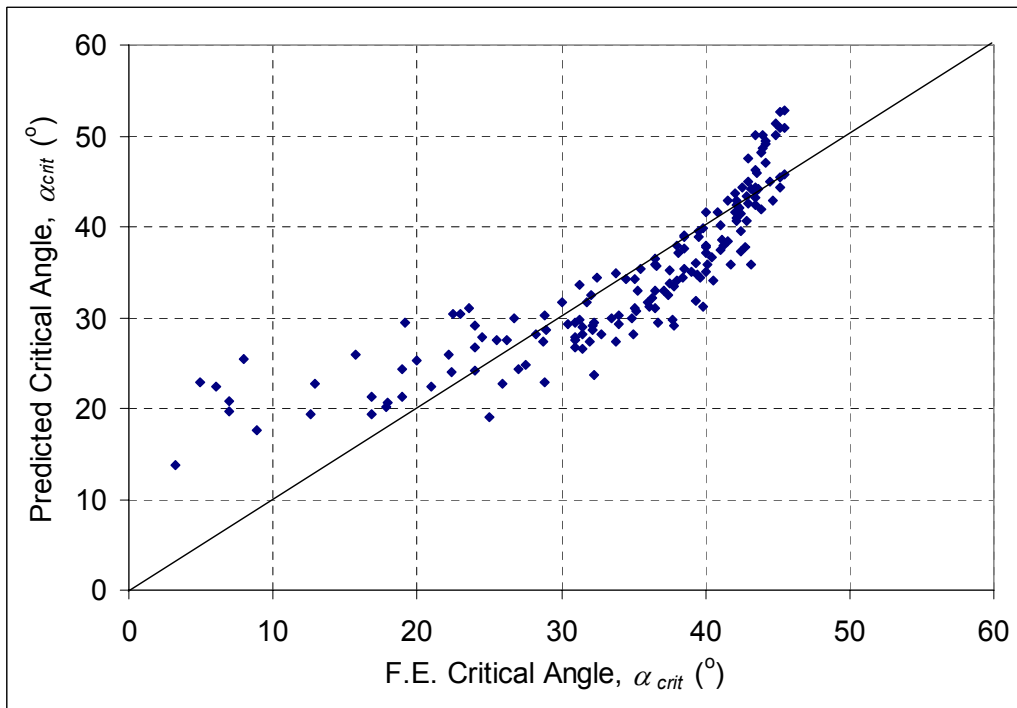


**Figure 4.11: Comparison of Regression Prediction vs. Finite Element Prediction – 50% to 100% MOP Pressure Range**

As can be seen in Figures 4.9 to 4.11, some of the predicted values are un-conservative in that the predicted critical angle is less than the actual critical angle. In order to ensure a more conservative estimate of the critical angle is obtained using the regression equation, an additional scale factor,  $\beta$ , included in the regression equations, which shifts the predicted values and therefore results in a higher predicted critical angle. The effect of including the scale factors is illustrated in Figures 4.12 - 14.

A summary of the mean and maximum errors resulting from the scaled regression equations is presented in Table 4.4

**Table 4.4: Summary of Mean and Maximum Regression Errors**

Regression Equation	Parameter	Pressure Range (% MOP)		
		100%	75%	50%
Baseline	Mean Error (°)	11	3	4
	Maximum Error (°)	40	16.3	17.4
Scaled	Mean Error (°)	20	8	9
	Maximum Error (°)	58	21.3	24.2

It is also noted that both forms of the regression equations predict critical angles greater than 45° for some scenarios. These results are due to the nature of the regression equation and must be viewed as such. However, because these generally occur for scenarios where the critical angle based on the finite element results is very large (> 35°), it is suggested that a result greater than 45° still be taken as an indication of a critical scenario.

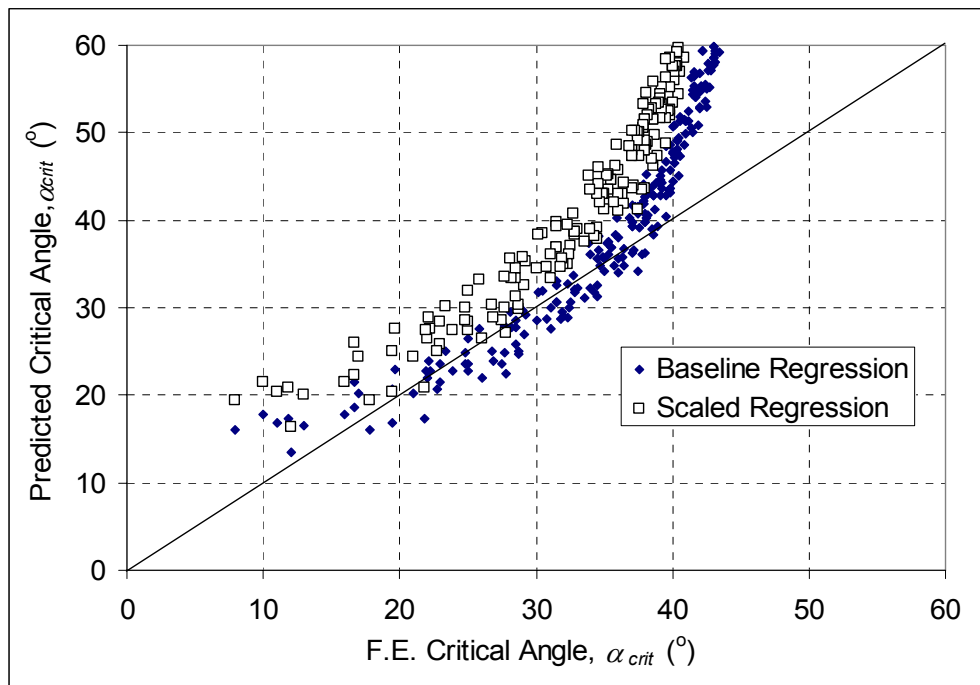


**Figure 4.12: Comparison of Scaled Regression Equation vs. Finite Element Prediction – 0% to 100% MOP Pressure Range**

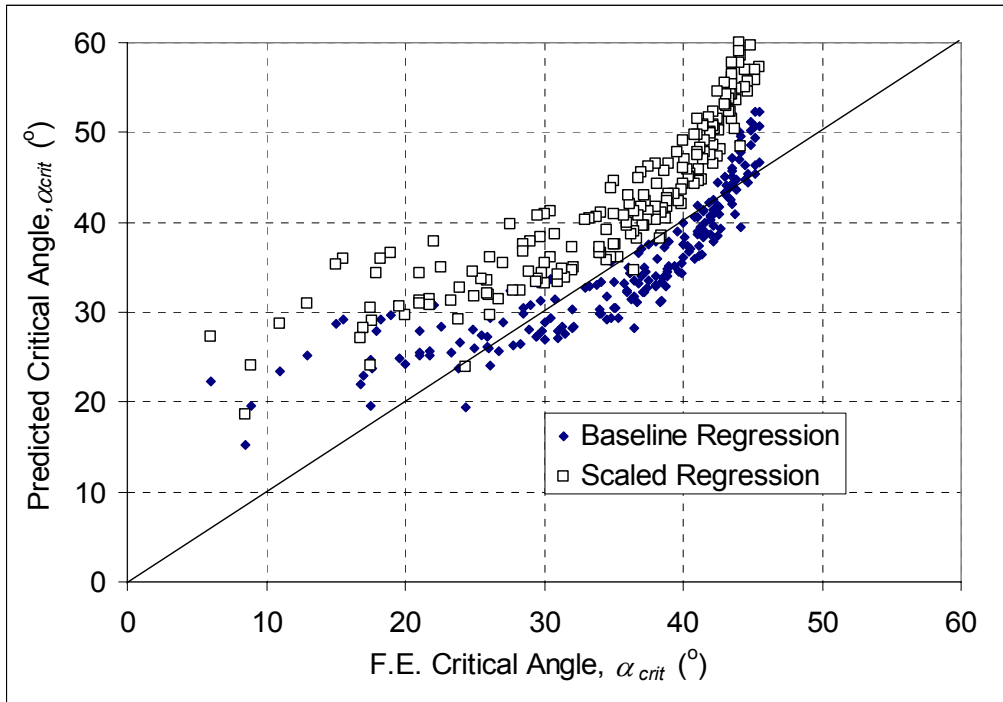


Figure 4.13: Comparison of Scaled Regression Equation vs. Finite Element Prediction – 25% to 100% MOP Pressure Range

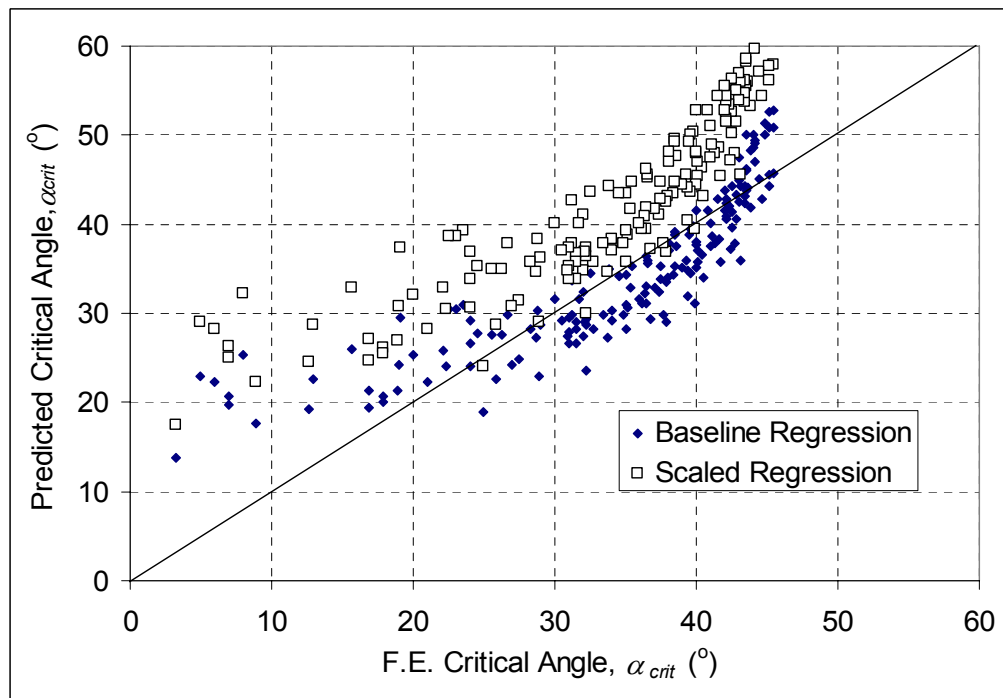


Figure 4.14: Comparison of Scaled Regression Equation vs. Finite Element Prediction – 50% to 100% MOP Pressure Range

#### 4.8 Application of Ovality-Weld Interaction Criteria

The criteria assume that the level of ovality in the un-pressurized state is known through some sort of inspection technique. If not, Figure 4.5 can be used to estimate the zero pressure ovality based on the measured ovality, the internal pressure at the time of the measurement, and the pipe geometry. Using this estimate of the zero pressure ovality ( $\omega$ ), the pipe diameter to thickness ratio ( $D/t$ ), the effective internal pressure fluctuation range ( $P.R.$ ), and the desired relative fatigue life compared to the baseline circular pipe ( $L.R.$ ), an analyst can look up in Table 4.2 whether or not the combination of parameters represents a scenario where the critical angle,  $\alpha_{crit}$ , is zero (represented by a shaded cell). If the cell is not shaded, there is a critical angle associated with the combination of parameters, and either the baseline or the scaled regression equation for the pressure range of interest can be used to estimate the critical angle,  $\alpha_{crit}$ , which represents the area where the long seam weld should not be located.

#### 4.9 Ovality-Weld Interaction Summary

As documented in the previous sections, criteria have been developed to assess the influence of a long seam weld interacting with an ovalized pipe. The criteria provide a means of estimating the critical angle,  $\alpha_{crit}$ , measured from the peak of the major or minor axis of an ovalized pipe, outside of which, a long seam weld must be located in order for the ovality to be considered acceptable for a given pipe geometry, operating conditions and desired relative fatigue life.

The criteria have been developed based on the following assumptions and inputs:

- The interaction criteria was developed based on a long seam weld interaction with an ovalized pipe, however, it may also be used to identify areas in a circumferential girth weld that may deserve additional scrutiny in an ovalized pipe section when the pipe is unearthed in a dig program.
- The criteria are based on the comparison of the fatigue life of a circular pipe with that of an ovalized pipe, where the fatigue life is determined based on the ASME weld design S-N curve [4.1].
- The criteria have developed based on pipe geometries in the range of 324 mm (NPS12) to 610 mm (NPS24) OD with  $D/t$  ratios between 38 and 174.
- The pipe material properties ranged from Grade 359 (X52) to 448 (X65) and the fatigue calculations are limited to materials with UTS values below 552 MPa (80 ksi).
- The criteria consider the following four inputs: pipe  $D/t$  ratio, pipe ovality, the internal pressure fluctuation range, and the desired relative fatigue life ratio.

As with the dent-girth weld interaction criteria, in order to use the ovality-weld interaction criteria, an analysis of the pipeline operating pressure data should be conducted to determine the typical pressure fluctuation regime for the pipeline system. In the absence of this information the 0% to 100% MOP pressure fluctuation equation should be used to ensure a conservative estimate of the critical angle between the ovalized pipe peaks and the long seam weld.

It is acknowledged that the weld geometry and weld material properties have not been incorporated directly into the FE models used to develop these criteria. However, the pipe wall in the models at the allowable weld positions experience very little, if any, plastic deformation or radial deflection, therefore the geometry, stiffening or material property mismatch effects due to the weld would be minimal.

#### **4.10 References**

- 4.1 American Society of Mechanical Engineers, Boiler and Pressure Vessel Code, Section VIII, Division 3, “Alternative Rules for the Construction of High Pressure Vessels.”

## 5. WRINKLE-WELD INTERACTION CRITERIA

As with the dent-weld interaction criteria, the premise behind the wrinkle-weld interaction criteria is based upon the pressure fluctuation response of the wrinkled pipeline predicted by finite element modelling. The interaction criteria, is developed considering the circumferential and longitudinal distances between the wrinkle peak and a location in the pipe that is not affected by the wrinkle feature. The criteria are developed considering the fatigue performance of the damaged pipe segment based on the ASME design S-N curve approach [5.1].

### 5.1 Local Buckling

Many researchers have investigated the local buckling of pipes subjected to pure bending. The investigations have shown that pipe buckling occurs in two different modes: “non-linear collapse” and “bifurcation buckling”. Idealized pipes deform by ovalizing under an applied bending moment. As the deformation increases with increasing moment, it results in a reduced moment carrying capacity, until a limit point is reached where the pipe is no longer capable of resisting increased moment (the point on the moment –curvature plot where the curve has a zero slope as shown in Figure 5.1). This point represents the onset of collapse of the pipe. Bifurcation buckling is characterized by a sudden change in behavior or state (e.g., bifurcation point in a structure’s behavior time history), and can be predicted by an eigenvalue analysis. At the bifurcation point two or more equilibrium paths are possible and deformation can evolve into a pattern that is significantly different from the pre-buckling one.

In the case of perfect structures, both types of behaviors are possible depending on the diameter-to-thickness ratio: for a  $D/t$  less than 35-40, limit point collapse occurs before bifurcation buckling (wrinkling). For larger  $D/t$  ratios, bifurcation buckling occurs earlier and in the plastic range [5.2]. In the case of real world structures, where initial imperfections exist, buckling occurs through non-linear (limit point) collapse.

The behavior of wrinkled pipes is characterized by the moment-curvature relationship. As bending increases, the pipe will, sooner or later, buckle locally and wrinkle. This process takes place when the membrane energy stored in the wall is converted into bending energy. Two typical examples of a moment-curvature relationships are illustrated in Figure 5.1 for wrinkle formation processes with different axial loads applied to the pipe segment. There are various significant points of interest that can be identified in the bending moment-curvature relationship:

- Linear (Elastic) limit
- Onset of buckling
- Limit point (ultimate moment capacity)
- Start of catastrophic capacity reduction
- Softening region

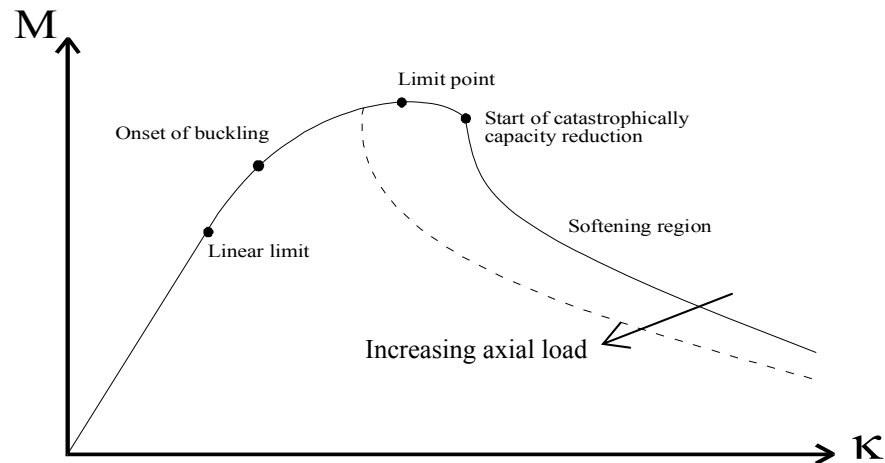


**Figure 5.1: Typical Moment Curvature (M- $\kappa$ ) Relationship for Pipe under Constant Pressure and Axial Force [5.2]**

The onset of buckling is the point where the collapse mode initiates. Following the onset of local buckling, global deformation will continue, but more and more of the applied bending energy will be accumulated in the local buckle. This will continue until the limit point (ultimate moment capacity) is reached, at which point the maximum bending resistance of the pipe is reached and geometrical collapse will occur if the curvature is increased further. Until the point at which the “start of catastrophic capacity reduction” has been reached, the geometric collapse will be gradual and the changes in cross-sectional area small. After this point, material softening sets in and the cross-section will collapse. The limit point and softening portion of the moment (M) curvature ( $\kappa$ ) relationship will shift to the left, for higher axial loads, as illustrated in Figure 5.1.

The moment capacity for metallic pipes is a function of many parameters, the most common being [5.2]:

- Diameter-to-wall thickness ratio;
- Material stress-strain relationship;
- Material imperfections;
- Welds (Longitudinal as well as circumferential);
- Initial out-of-roundness;
- Reduction in wall thickness, e.g., corrosion;
- Cracks (in pipe and/or welding);
- Local stress concentrations, e.g., wall thickness change;
- Additional loads and their amplitudes; and
- Temperature.

### 5.1.1 Bending Moment Capacity

An analytical solution for determining the maximum allowable bending moment of pipes is available [5.2]. The equation accounts for initial out-of-roundness, axial force and internal/external pressure. In order to limit the complexity of the equations the following assumptions apply:

- The pipe is geometrically perfect except for the initial out-of-roundness; and
- The cross-sectional geometry does not change before the ultimate moment is reached.

The interaction between limiting longitudinal and hoop stresses can be described by the following equation.

$$\frac{\sigma_l^2}{\sigma_{ll}^2} - 2\alpha \frac{\sigma_l \sigma_h}{|\sigma_{ll}| |\sigma_{hl}|} + \frac{\sigma_h^2}{\sigma_{hl}^2} = 1$$

The bending moment capacity for local buckling under combined loads can be expressed as:

$$M_{C(\sigma_l, \sigma_h)} = M_p \sqrt{1 - \left(1 - \alpha^2\right) \left(\frac{\sigma_h}{\sigma_{hl}}\right)^2} \cos \left( \frac{\pi}{2} \frac{\frac{\sigma_l}{|\sigma_{ll}|} - \alpha \frac{\sigma_h}{|\sigma_{hl}|}}{\sqrt{1 - \left(1 - \alpha^2\right) \left(\frac{\sigma_h}{\sigma_{hl}}\right)^2}} \right)$$

where:

- $M_c$  = Ultimate bending moment capacity
- $M_p$  = Plastic moment
- $\sigma_h$  = Hoop stress
- $\sigma_{hl}$  = Limit hoop stress for pure pressure
- $\sigma_l$  = Longitudinal stress
- $\sigma_{ll}$  = Limit longitudinal stress for pure longitudinal force

## 5.2 Assumptions Used to Generate the Wrinkle – Weld Interaction Criteria

The wrinkle-weld interaction criteria were developed using a matrix of finite element models to estimate the pipe wall stresses for the fatigue performance estimation. The matrix was assembled to include a range of parameters that could influence the response of wrinkled pipes. The major parameters considered in the development of the criteria included:

- Pipe geometry (D/t)
- Wrinkle Amplitude
- Internal Pressure Fluctuations
- Material Properties

Due to the large number of variables considered in the analysis, it was not deemed practical to consider modeling every possible combination of influential parameters within the scope of this project. Therefore, a matrix was assembled to cover a wide range of scenarios, the results of which could be used to identify trends and generate a wrinkle – weld interaction criteria. The complete numerical modeling matrix used in the analysis is presented in Table 5.1 in Section 5.5. A brief description of the major assumptions/idealizations used in developing the weld interaction criteria is presented in the following subsections.

**Table 5.1: Pipe Wrinkling - Parameter Ranges**

Parameter	Range
Diameter (mm) (in)	508, 762 20, 30
Thickness (mm) (in)	7.14, 9.52 0.281, 0.375
Diameter-thickness ratio	53, 71, 80, 107
Material Grade	359 (X52), 448 (X65)
Wrinkle shapes	Four wrinkles height and length for each specimen as described in Section 5.6
Internal pressure fluctuation (minimum, maximum) MPa	0, MAOP
Circumferential extent of the wrinkle	Greater than 180 degrees of the pipe circumference

### 5.2.1 Pipe Geometry

Two pipe diameters and two wall thickness values were selected for the numerical models to generate D/r ratios ranging from 53 to 171.

### 5.2.2 Material Properties

The same two material grades used for the dent and ovality criteria were also used for the wrinkle criteria, Grade 359 (X52) and Grade 448 (X65). Isotropic material hardening behaviour was used. Flattened strap tensile properties obtained from pipe do not lend themselves well to bilinear stress-strain curve representations, and bilinear curves cannot model the portion of the stress-strain curve just beyond the elastic limit accurately.

### 5.2.3 Wrinkle Amplitude

In general, there are a number of criteria that can be used to describe the geometry of a wrinkled pipe (e.g., ovality, out-of-roundness, length of the wrinkle, height (amplitude) of the wrinkle, the extent of the wrinkle around the circumference etc). The schematic axial profile through the peak of a wrinkled pipe, illustrated in Figure 5.2, presents two simple parameters used to characterize the shape of wrinkled pipe; H, the wrinkle height (amplitude) and ( $L_w$ ) the wrinkle length. The height of the wrinkle is defined based upon the distance between the minimum and maximum radial position of the pipe wall and the length of the wrinkle is defined in terms of the axial distance between the minimum radial position of the pipe wall on either side of the wrinkle feature.

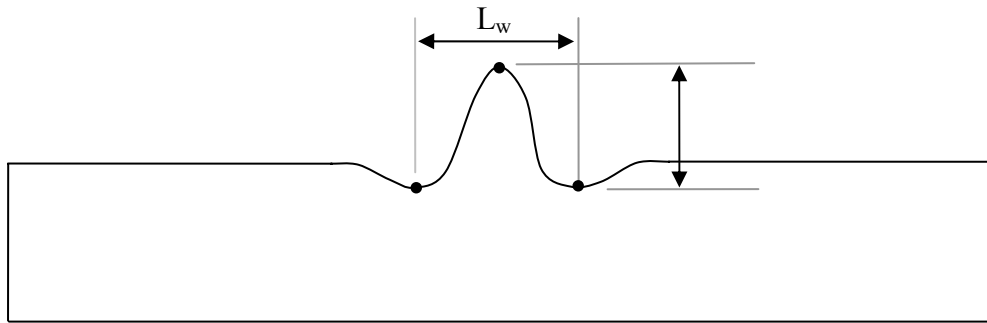


**Figure 5.2: Wrinkle Height and Length**

Several possible parameters were investigated and the wrinkle ratio defined as the ratio of the wrinkle height to wrinkle length appeared to be the most relevant. In order to develop an understanding of the effect of the wrinkle shape aspect ratio on the acceptable relative position of a weld, four wrinkle aspect ratios were considered for each pipe specimen. The amplitudes and lengths are representative of those experienced in service, and were generated by modifying the pipe bending load. Figure 5.3 shows longitudinal pipe wall profiles along a line through the apex of four different wrinkles having different wrinkle amplitude ratios in 508 mm diameter (NPS20) pipe with a 7.14 mm (0.281 inch) wall thickness. Figure 5.4 illustrates transverse section through the apex of four wrinkles with differing amplitude ratios made in 762mm diameter pipe with a 7.14 mm wall thickness.

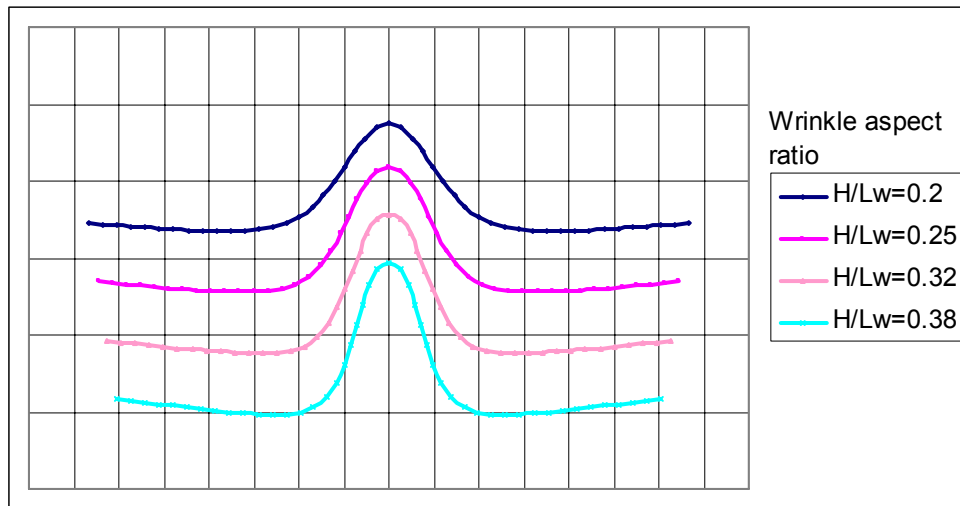


**Figure 5.3: Axial Profile through the Wrinkle Apex for Four Different Wrinkles (D=508 mm, t=7.14 mm, D/t=71)**

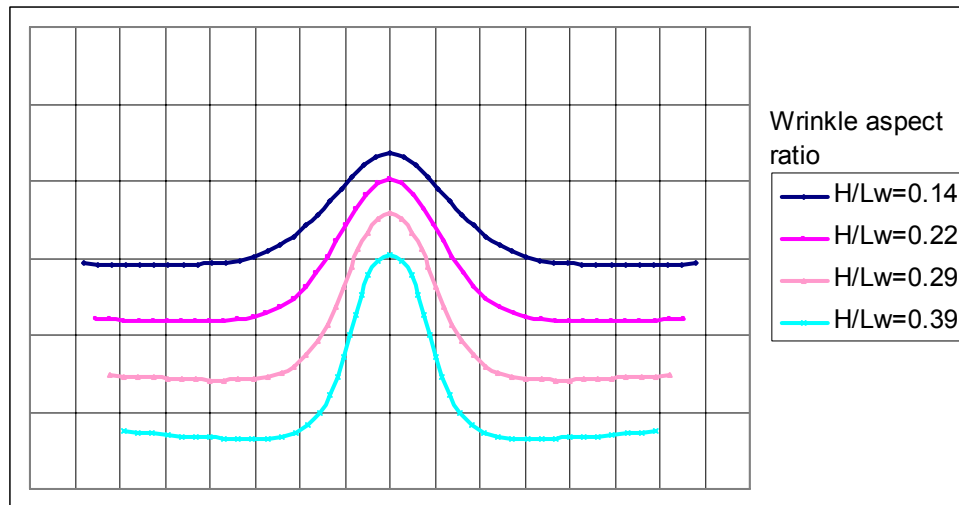


**Figure 5.4: Transverse Profile along the Apex of Four Different Wrinkles (D=762 mm, t=7.14 mm, D/t=107)**

#### 5.2.4 Weld Type and Location

Once again the welds were not explicitly modeled and the variability in weld quality and residual stresses is addressed in the design curve [5.1]. The stress amplification factor of 3 was applied to consider weld geometry effects.

#### 5.2.5 Internal Pressure and Pressure Fluctuations

It is well known and accepted that pipelines operate within different pressure regimes, where the internal operating pressure is a function of a number of variables including product, distance from discharge and suction stations, elevation, etc. As the internal pressure fluctuations have a direct impact on the pipe wall stress fluctuations, and hence fatigue life predictions, it was considered important that the wrinkle-weld interaction criteria account for various pressure fluctuation regimes. Therefore, the numerical modeling matrix includes four internal pressure fluctuation ranges: 75% to 100% MOP, 50% to 100% MOP, 25% to 100% MOP and 0 to 100% MOP.

### 5.3 **Intended Application of the Wrinkle – Weld Interaction Criteria**

Wrinkles are not generally addressed in prescriptive pipeline codes or standards except when specifically dealing with wrinkle bends formed during construction, however, wrinkles can form during service as a result of slope movements. These in-service wrinkles can result in more severe deformation than the wrinkles formed during pipe bending. If a wrinkle detected in service is treated as a wrinkle bend it must be assumed that the formation mechanism is no longer acting so that the pipeline is stable and further gross deformation will not occur. ASME B31.8 [5.4] permits wrinkle bends in pipelines that operate with nominal hoop stresses less than 30% of SMYS unless the pipeline is in sour service. It also states that the long seam weld must be located near the neutral axis in bending and that a pipe bend of more than 1.5 degrees per wrinkle is not permitted on NPS16 or larger pipe. The mandatory requirements of CSA Z662-03 [5.5] state that the design stresses for restrained spans must be less than 0.8 of the critical buckling load and that buckling is not permitted in bends. The non-mandatory annex providing

guidance on limit states design indicates that a stable buckle/wrinkle may be acceptable provided the limit state analysis for the tensile capacity of the pipeline accounts for the effects of wrinkle formation, wrinkle zone softening and section collapse. In order to utilize the wrinkle criteria presented in this study, it should first be determined that the wrinkle is acceptable in accordance with the governing pipeline standard.

The ASME fatigue design curve [5.1] was used to provide a means of characterizing the interaction of a wrinkled pipe based upon an estimation of the pipe fatigue life due to pressure cycling. It interaction criteria should be used in conjunction with the existing standards and practices to assess a wrinkled pipe on a time or cyclic-dependent failure basis assuming that internal pressure fluctuations are the driving force.

#### **5.4 Non-Linear FE Model of Pipeline Buckling**

The objective of this task was to document and demonstrate a finite element model capable of accurately simulating the behavior of girth-welded specimens of line pipe before, during, and after the formation of a wrinkle. Ideally, the resulting FE model would be capable of considering:

- highly nonlinear plastic material behavior;
- internal pressure (static or cyclic);
- axial loads (due to thermal or ground movement);
- flexural loads (due to pipe curvature or ground movement);
- pipe imperfections (ovality , corrosion); and
- residual stresses (from welds or construction).

In order to account for all these effects, the wrinkle formation model was developed using LS-DYNA version 960. LS-DYNA is an explicit FEA code used in highly non-linear and dynamic structural problems. LS-DYNA is widely used in simulating metal forming operations, impacts involving large deformation and highly non-linear material behavior, and scenarios resulting in complex multi-body contact. As the pipe wrinkling process involves high degrees of both structural and material non-linearity, LS-DYNA is well suited to modeling the process.

Appendix D describes the wrinkle formation model development process, including the validation of the model against full-scale trial data and some sensitivity studies demonstrating the effects of material properties and pipe geometry.

In order to achieve a reliable finite element prediction of the wrinkle formation behavior of pipelines, the following factors must be taken into account [5.2]:

- A proper representation of the constitutive law of the pipe material
- A proper representation of boundary conditions
- A proper application of the load sequence
- The ability to address large deformations, large rotations and finite strains
- The ability to model/describe all relevant failure modes.

The following sections discuss each of these aspects of the wrinkle formation model in detail.

### 5.4.1 Finite Element Model Geometry Details

The finite element model used in the parametric study is based on the nonlinear LS-DYNA model developed and demonstrated in Appendix D. The finite element model used in the parametric study differs from that described previously in two primary ways

- In order to reduce computing time, the finite element model used in the parametric study utilizes two planes of symmetry.
- In order to more accurately assess the stresses and strains in the pipe wall, fully integrated 4 noded shell elements have been used in the parametric study finite element model.

The resulting  $\frac{1}{4}$  symmetry finite element model of the pipe is illustrated in Figure 5.5. The elements in the area of the wrinkle peak are 9 mm by 10 mm ensuring an accurate prediction of the stress gradients in the vicinity of the peak. The element size grows larger outside of the wrinkle peak area where the stress gradients are lower. In order to accurately predict the plasticity associated with the wrinkle forming operation, and the subsequent cyclic loads, the shell elements include 9 integration points through the thickness. The fully integrated shell element used in LSDYNA accounts for finite membrane strain and allows for changes in the shell thickness, making it suitable for large strain analysis.

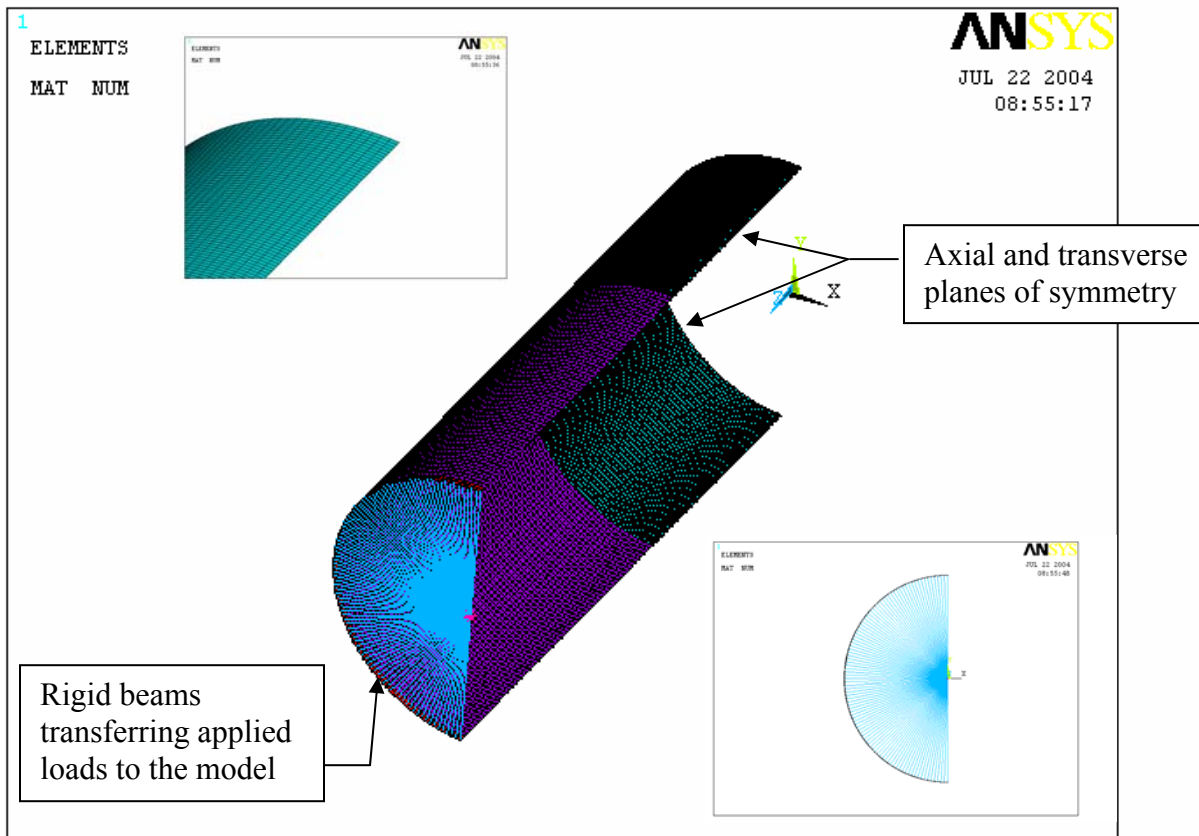


**Figure 5.5: Parametric Study - 1/4 Symmetry Finite Element Model**

Symmetric boundary conditions are applied to the two planes of symmetry, while loads are applied to the central node of the beam elements at the load bearing end of the pipe.

#### 5.4.2 Finite Element Model Material Properties

The true stress-true strain curves developed for X52 and X65 and used for the dent models are used in the parametric study.

#### 5.4.3 Finite Element Model Loading

The applied loads and loading sequence used in the finite element model are based on the actual operational loads experienced by a pipeline in service, including:

- Operational pressure fluctuations;
- Seasonal temperature fluctuations; and
- Annual curvature (wrinkle growth) increases.

In the finite element model, the applied loading sequence includes ten steps, which mimic the actual loading sequence experienced by pipelines in service. The ten steps in the loading sequence are summarized below:

1. Apply the internal operating pressure (MAOP) to the pipe, and apply the total axial load on the pipe wall (due internal pressure and thermal restraint) to the central node at the loaded end of the pipe.
2. Apply an in-plane rotation to the central node at the loaded end of the pipe in order to form the wrinkle.
3. Once the wrinkle has formed, the internal pressure is reduced to zero.
4. Increase the internal pressure to generate SMYS level hoop stresses to simulate a hydrostatic test condition.
5. Internal pressure increased to 100% MOP (assuming MOP generates 72% SMYS level hoop stresses in undeformed pipe)
6. Internal pressure reduced to 90% MOP
7. Internal pressure reduced to 75% MOP
8. Internal pressure reduced to 50% MOP
9. Internal pressure reduced to 25% MOP
10. Internal pressure reduced to zero

The axial load experienced by a pipeline in operation is made up of a combination of thermal restraint effects and Poisson's effect. Due to thermal expansion restraint, temperature changes in the pipeline results in axial loads in the pipeline, ( $F_{th}$ ), according to the following equation [5.3]:

$$F_{th} = - E \alpha \Delta T A_p$$

Where  $E$  is the modulus of elasticity,  $\alpha$  is the coefficient of thermal expansion,  $\Delta T$  is the temperature change and  $A_p$  is the pipe cross-sectional area

For axially restrained pipes with an internal pressure, radial growth of the pipe will result in a longitudinal stress due to Poisson's effect. The pressurization induced axial load, ( $F_p$ ), is calculated using the following equation:

$$F_p = \frac{\nu P D A_p}{2t} = \nu \sigma_h A_p$$

Where  $\nu$  is Poisson's ratio,  $P$  is the internal pressure,  $D$  is the pipe diameter,  $t$  is the pipe wall thickness,  $A_p$  is the pipe cross-sectional area and  $\sigma_h$  is the hoop stress.

With regards to the total axial loads in pipelines, the behavior of buried pipe is generally bound by two idealizations. The first idealization assumes the pipe behaves as an open ended pipe where no longitudinal pressurization loads exist in the pipe wall (other than those due to Poisson's effect). In the second idealization, the longitudinal loads in the pipe wall account for the end-cap effects that may occur in the pipeline. The end-cap effects, (which may be caused by bends in the pipeline, valves etc), are included as an additional longitudinal load in the pipe wall.

For an ideal open-ended pipe, the total longitudinal force on the pipe wall is a combination of the axial thermal load, and the axial load due to Poisson's effect, and is calculated using the following equation:

$$F = \left( \nu \frac{PD}{2t} - E\alpha\Delta T \right) A_p$$

For pipes experiencing end-cap effects, the internal pressure acting on the closed ends results in a longitudinal force on the pipe wall, determined using the following equation:

$$F_{cap} = P \frac{\pi D^2}{4}$$

Therefore the total axial force for a pipe including end cap effects is given by the following equation:

$$F = -\frac{P(\pi D^2)}{4} + \left( \nu \frac{PD}{2t} - E\alpha\Delta T \right) A_p$$

For the purposes of the investigation, the thermal loads are based on a 40°C temperature change (between construction and operational temperature). This thermal loading would be project specific based upon the difference between the temperature at which the pipeline was constructed and the operating temperature. For pipeline projects involving winter construction and or heated liquid operation, this temperature differential is not uncommon. The selected temperature differential in this project is assumed to remain constant, therefore, it will only affect the applied flexural loading magnitude required to achieve a wrinkle of a given shape and the results of this investigation are based upon the high cycle fatigue behavior of wrinkles of given shapes, in the absence of thermal load variation, the selected thermal (axial) load magnitude is not a parameter with a great significance.

For the purposes of the finite element modeling, the pipeline operating pressure is assumed to be equal to the maximum allowable operating pressure (MAOP), where MAOP represents the internal pressure equivalent to a hoop stress that is 72% of the specified minimum yield stress (SMYS). MAOP is calculated using the following formula:

$$MAOP = 0.72 \left( \frac{2t}{SMYS \times D} \right)$$

The applied loads, used in the finite element models, may be calculated using the above equations, and the pipe geometry and material properties summarized previously.

## 5.5 Finite Element Model Matrix

The LS-DYNA finite element model was used to carry out an extensive parametric study to understand and assess the in-service deformation behavior of wrinkled pipe, with the goal of estimating the acceptable distance between a pipeline wrinkle and a girth weld seam. The parameters investigated in this analysis include:

- Pipe geometry – diameter-to-thickness ratio ( $D/t$ );
- Material grade;
- Wrinkle shape, Height-to-length ratio ( $H/L_w$ );
- Wrinkle circumferential extent, defined by the ratio of axial and flexural loading; and
- Internal pressure fluctuations and the resulting cyclic axial loads.

The range of each of the parameters was selected to be representative of current pipeline industry manufacturing and operational practices. The ranges considered in the analysis are summarized in Table 5.1.

## 5.6 Wrinkle/Weld Interaction Criteria

The criteria developed for wrinkles in this project is intended for use with data from in-line inspection technologies capable of determining the three dimensional profile of a wrinkle. Such tools would be required in order to carry out a wrinkle strain analysis in accordance with the ASME B31.8 [5.1] procedures, the same approach used for the dents/weld interaction criteria. The criteria have been developed for symmetrical wrinkle about their crown, along and around the pipeline. Further work will be required to validate the procedures for non-symmetric wrinkles, either along or around the pipeline.

It is noted that the application of the interaction criteria developed in this project may be limited to smaller wrinkles due to limitations in the ability of in-line inspection tools to characterize the shape of larger wrinkles. Larger or deeper wrinkles may have side slopes that are deep enough as to interfere with caliper arms with the passage of the inspection tool causing lift off so that the profile of the wrinkle is not correctly measured. These limitations will have to be reviewed considering the mechanical operation of individual caliper tools.

### 5.6.1 Interaction of Wrinkle and Long Seam Welds

The general approach used to develop the wrinkle/long seam weld interaction criteria is the same as the approach used for dents/long seam welds interaction (Sections 2 and 3). A complete matrix of the 36 finite element models, used in the analysis of open-ended pipes, is presented in Table 5.2. The 36 finite element models consist of four pipe geometries ( $D/t$ 's), two material grades, and four wrinkle amplitudes per model, as outlined in Table 5.1.

In addition to the wrinkle shape characterized by the aspect ratio,  $H/L_w$ , the circumferential extent of a wrinkle is considered to be an important parameter with regards to interaction with a long seam weld. The circumferential extent of the wrinkle of interest in this investigation is defined based upon it having a significant impact on the predicted fatigue life of the weld, as outlined in Section 2.

As illustrated in the schematic cross section in Figure 5.6, the circumferential extent of a wrinkle can be characterized by the enclosed angle ( $2\theta$ ), which may vary from approximately  $45^\circ$  for wrinkles formed predominately through applied moments, to  $360^\circ$  for wrinkles formed by axial loads only.

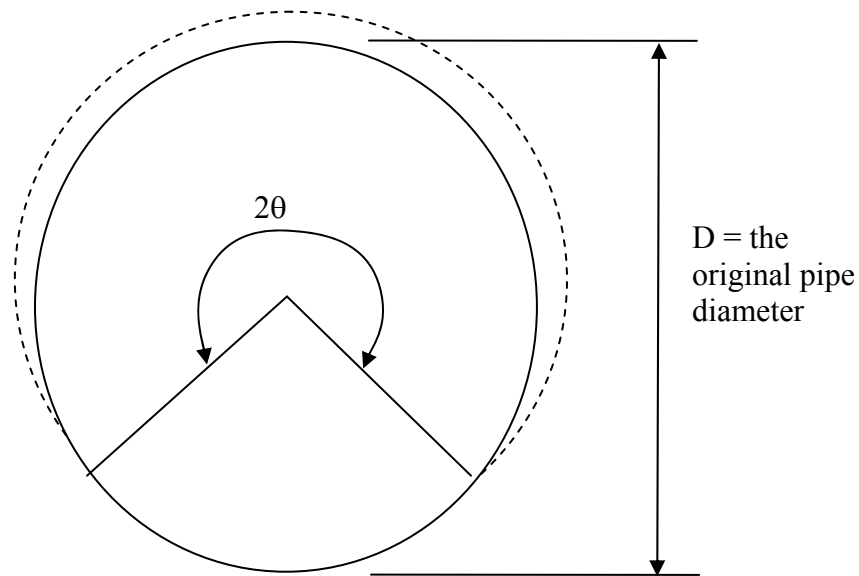


**Figure 5.6: Schematic Transverse Cross-section through the Apex of a Pipe Wrinkle**

The critical enclosed half angle ( $\theta$ ) defining the area having reduced fatigue life that would be an inappropriate location for a long seam weld is estimated for each of the cases summarized in Table 5.2. The half angle is normalized to a non dimensional fraction of 180 degrees and is related to the wrinkle shape characterized by the aspect ratio,  $H/L_w$ .

The results of the investigation are summarized in Figures 5.7 to 5.10 in the form of the normalized critical angle versus the wrinkle shape,  $(H/L_w)$ . Figure 5.7 presents the results for all combinations of pipe geometry, wrinkle amplitude and material grades. As shown in Figures 5.7 to 5.10, the relationship between the normalized critical angle  $(180/\theta)^2$  and the wrinkle-shape ratio  $(H/L_w)$  appears to follow a power law relationship. The normalized critical angle can therefore be expressed in convenient dimensionless form as follows:

$$\left(\frac{180}{\theta}\right)^2 = A \left(\frac{H}{L_w}\right)^B \frac{1}{SF}$$

Where the coefficient  $A=1.4492$ , and the exponent  $B=-0.1049$ , set of constants determined by fitting the finite element results at the critical location for symmetric wrinkle and a given service loading.  $S_f$  is safety factor applied to the result to ensure that in all cases the critical angle is conservatively predicted by the regression equation. It is recommended that the normalized critical angle be calculated using a safety factor of 1.2 to ensure that the estimate of interaction distance is conservative.

As noted above the criteria have been developed for symmetrical wrinkle about their crown, along and around the pipeline and for an applied loading including both axial and flexural loads giving rise to a wrinkle affecting more than half of the pipe circumference. Further work will be required to validate the procedures for unsymmetrical wrinkles, either along or around the pipeline.

Examination of the results in Figures 5.7 to 5.10 indicates that the wrinkle shape, i.e., wrinkle height, wrinkle length and wrinkle aspect ratio ( $H/Lw$ ) play major roles in determining the normalized critical half angle ( $\theta/180$ ) defining unacceptable long seam weld and wrinkle interaction area. Conversely, neither the material grade nor the pressure fluctuation greatly influences the half angle ( $\theta$ ) prediction.

Based on the results, it is evident that increasing  $H/Lw$  ratios result in increasing  $\theta$ , indicating a relationship between wrinkle shape,  $H/Lw$ , and wrinkle propagation around the circumference. More severe wrinkles form with higher aspect ratios, for higher  $H/Lw$ , the long seam weld must be further away from the wrinkle peak than for smaller  $H/Lw$ .

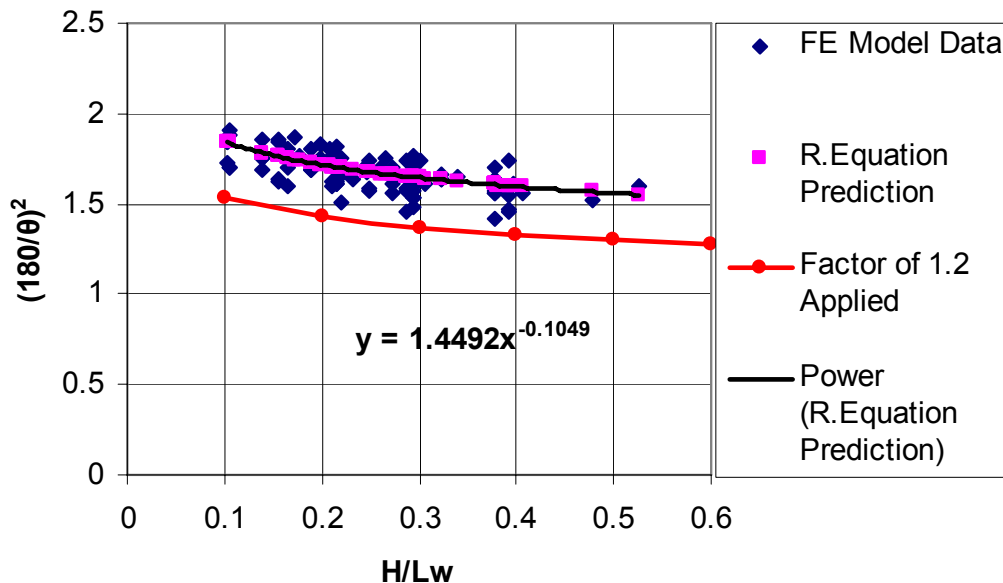


Figure 5.7: Normalized Critical Angle vs. H/Lw

**Table 5.2: Modeling Matrix Used to Estimate Interaction Distances Between Wrinkles and Long Seam Welds**

Model	Yield (Mpa)	UTS (Mpa)	D (mm)	t (mm)	D/t	Amplitude H (mm)	L <sub>w</sub> (mm)	H/L <sub>w</sub>	Half Angle of Life Intersection Point (deg)			
									100%-75%	100%-50%	100%-25%	100%-0%
D20_t281_X52_A8	359	455	508	7.14	71	34.99	175.97	0.20	135.96	136.57	137.87	138.77
D20_t281_X52_A9	359	455	508	7.14	71	40.85	165.61	0.25	137.87	139.07	140.62	141.84
D20_t281_X52_A10	359	455	508	7.14	71	45.25	140.00	0.32	139.79	140.58	142.35	143.67
D20_t281_X52_A11	359	455	508	7.14	71	48.96	129.66	0.38	141.70	140.72	143.15	144.78
D20_t375_X52_A9	359	455	508	9.53	53	25.84	248.10	0.10	130.21	131.11	132.05	132.74
D20_t375_X52_A10	359	455	508	9.53	53	34.44	222.75	0.15	132.13	132.52	133.40	133.96
D20_t375_X52_A11	359	455	508	9.53	53	41.44	196.88	0.21	135.96	135.69	135.36	135.73
D20_t375_X52_A12	359	455	508	9.53	53	46.60	187.39	0.25	137.87	136.28	136.42	136.59
D30_t281_X52_A4	359	455	762	7.14	107	36.24	261.68	0.14	135.96	135.85	136.82	138.44
D30_t281_X52_A5	359	455	762	7.14	107	46.32	215.25	0.22	141.70	141.26	142.13	143.85
D30_t281_X52_A6	359	455	762	7.14	107	53.95	183.76	0.29	145.53	145.48	146.37	147.88
D30_t281_X52_A7	359	455	762	7.14	107	59.79	152.34	0.39	149.36	148.30	149.41	151.08
D30_t375_X52_A5	359	455	762	9.53	80	32.26	312.40	0.10	132.13	132.42	133.03	133.80
D30_t375_X52_A6	359	455	762	9.53	80	46.10	280.85	0.16	137.87	136.66	137.53	138.90
D30_t375_X52_A7	359	455	762	9.53	80	55.26	250.34	0.22	139.79	139.83	140.43	141.58
D30_t375_X52_A8	359	455	762	9.53	80	62.60	219.02	0.29	143.62	143.00	143.45	144.16
D20_t281_X65_A9	448	531	508	7.14	71	42.62	163.34	0.26	138.15	138.28	138.68	139.32
D20_t281_X65_A10	448	531	508	7.14	71	46.83	137.79	0.34	139.95	140.14	140.47	140.71
D20_t281_X65_A11	448	531	508	7.14	71	50.49	127.24	0.40	141.67	141.48	141.69	141.86
D20_t281_X65_A12	448	531	508	7.14	71	53.38	101.55	0.53	142.40	143.21	143.37	143.51
D20_t375_X65_A10	448	531	508	9.53	53	37.89	219.20	0.17	131.87	132.09	132.90	133.96
D20_t375_X65_A11	448	531	508	9.53	53	43.76	209.93	0.21	133.84	133.61	134.08	134.74
D20_t375_X65_A12	448	531	508	9.53	53	48.99	184.32	0.27	135.85	135.55	135.84	136.27
D20_t375_X65_A13	448	531	508	9.53	53	52.78	175.49	0.30	136.36	136.43	136.66	137.04
D30_t281_X65_A5	448	531	762	7.14	107	48.38	228.61	0.21	137.91	138.65	139.95	142.01
D30_t281_X65_A6	448	531	762	7.14	107	55.46	181.89	0.30	141.62	141.97	143.16	145.30
D30_t281_X65_A7	448	531	762	7.14	107	61.01	150.45	0.41	143.86	145.19	146.00	147.72
D30_t281_X65_A8	448	531	762	7.14	107	64.98	136.06	0.48	145.79	147.18	147.91	149.55
D30_t375_X65_A6	448	531	762	9.53	80	49.01	277.95	0.18	135.34	135.58	136.41	137.76
D30_t375_X65_A7	448	531	762	9.53	80	57.56	247.71	0.23	140.76	140.00	140.00	140.44
D30_t375_X65_A8	448	531	762	9.53	80	64.73	216.29	0.30	140.35	140.35	141.27	142.49
D30_t375_X65_A9	448	531	762	9.53	80	70.33	185.08	0.38	143.40	142.07	143.23	144.04
D20_t281_X52_A8_I	359	455	508	7.14	71	31.05	165.38	0.19	137.87	137.21	138.06	138.51
D20_t281_X52_A9_I	359	455	508	7.14	71	37.87	138.64	0.27	137.87	139.71	141.16	141.72
D20_t281_X52_A10	359	455	508	7.14	71	39.64	134.97	0.29	137.87	139.15	141.26	142.11
D20_t281_X52_A11	359	455	508	7.14	71	45.84	121.12	0.38	137.87	141.10	143.28	144.30

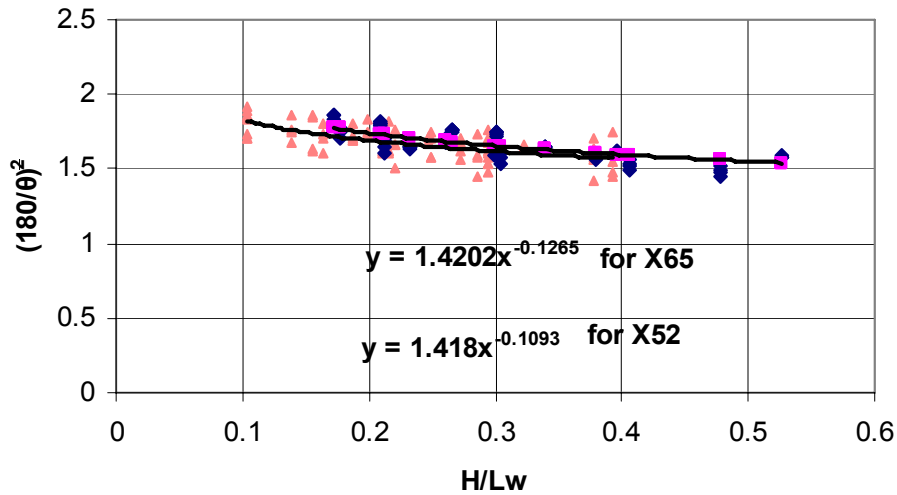


Figure 5.8: Normalized Critical Angle vs. H/Lw: Effect of Material Grade

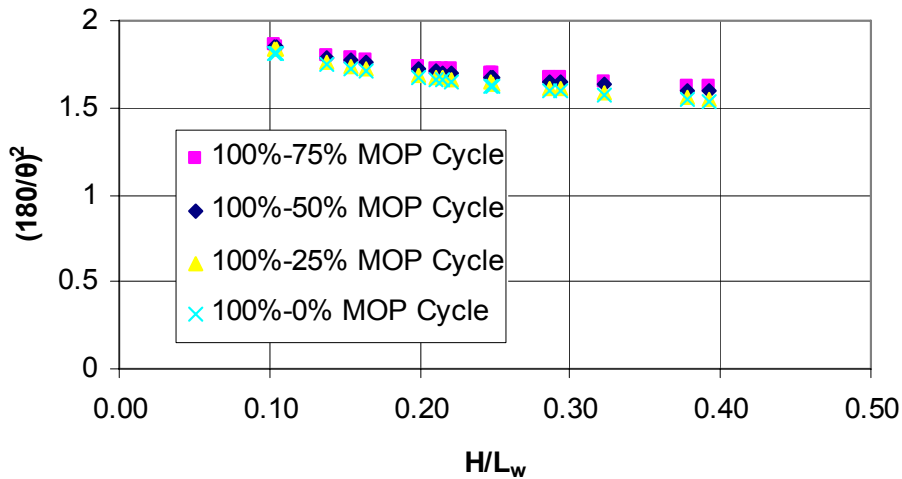


Figure 5.9: Normalized Critical angle vs. H/Lw: Effect of pressure fluctuation -X52

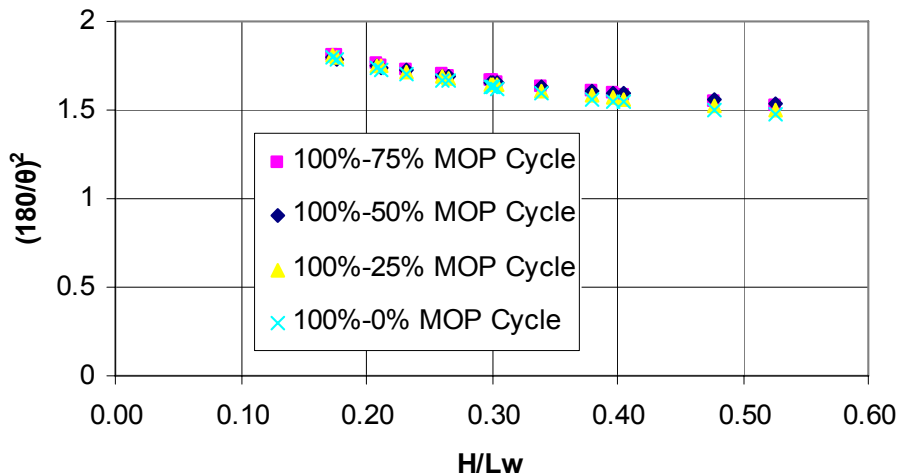
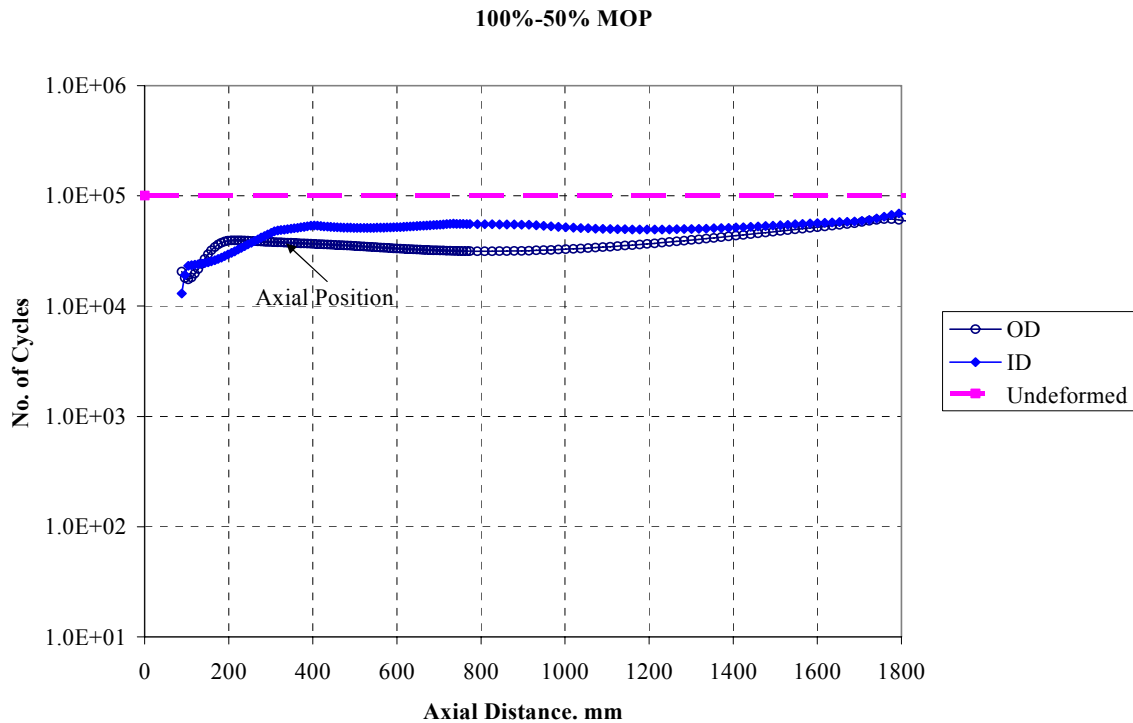


Figure 5.10: Normalized Critical Angle vs. H/Lw: Effect of Pressure Fluctuation -X65

### 5.6.2 Interaction of Wrinkles with Girth Welds

The general approach used to develop the wrinkle girth weld interaction criteria is similar to the approach used for dents/girth welds interaction. A complete matrix of the 32 finite element models, used in the analysis of open-ended pipes, is presented in Table 5.3. The finite element models consist of four pipe geometries ( $D/t$ 's), two material grades, and four wrinkle amplitudes per model.

The development of girth weld interaction criteria was not as straight forward as long seam weld. As evident in Figure 5.11 and 5.12, in some instances the number of design cycles for the applied loading in the wrinkled pipe never approaches the design number of cycles for the same pressure fluctuation in undeformed pipe segment. This difference is due to the inevitable ring deflection (ovality) that forms during the initial stage of wrinkle forming. When the pipe is subjected to axial load and bending, the pipe cross section anticipates ring deflection, part of this deflection is an artifact of the model boundary conditions. A correction was applied to the FE model life prediction. The location where the OD and ID life prediction curves slope approach zero indicates the boundary between the areas in which a weld would be acceptable or unacceptable based upon on its affect on the pipe segment fatigue life. Figures 5.11 and 5.12 illustrate the results of the process used to identify this boundary point.



**Figure 5.11: Fatigue Life Estimate for Model D20\_t281\_x52\_A8 at Various Locations along an Axial Section through the Wrinkle Apex**

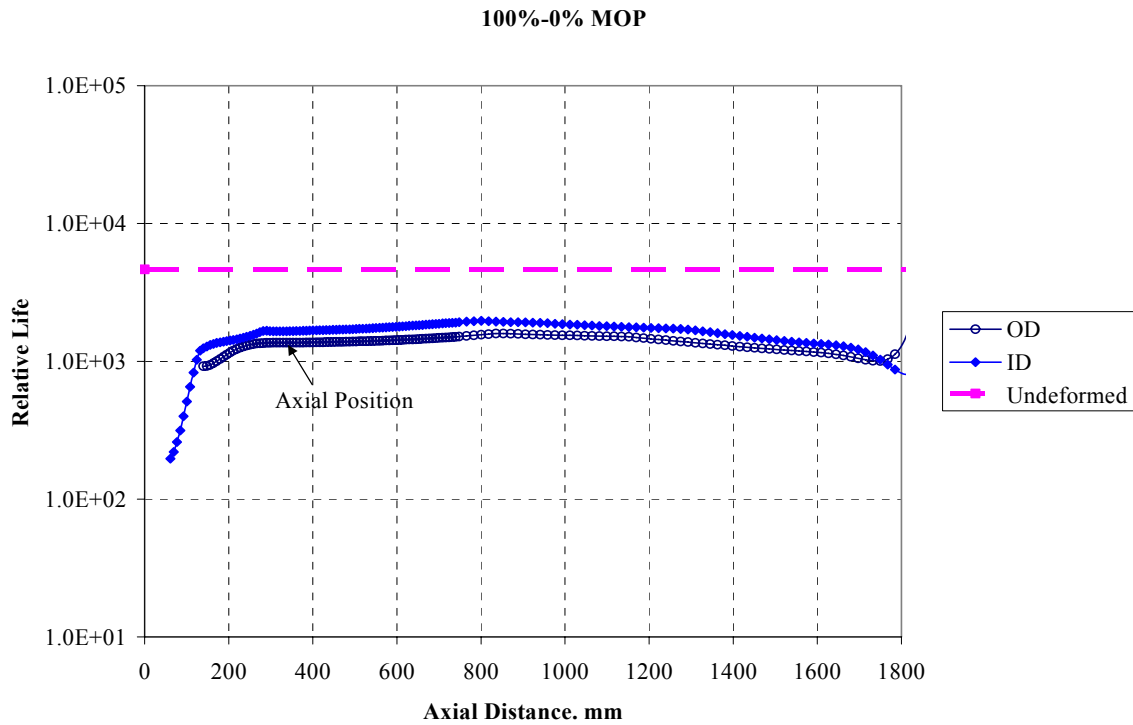


**Figure 5.12: Life estimate for model D30\_t375\_X65\_A9 at Various Locations along an Axial Section through the Wrinkle Apex**

The critical distance ( $L$ ) between a girth weld seam and a wrinkle peak, for cases summarized in Table 5.3, is normalized with respect to the wrinkle aspect ratio,  $H/L_w$ . The critical distance is taken to be the axial distance between the peak of the wrinkle and the point along the axis of the pipe at which the OD and ID fatigue life prediction due to the pressure fluctuation meets the applicable life criteria or stabilizes to a value no longer influenced by the wrinkle feature.

The results of the investigation are summarized in Figures 5.13 to 5.16 in the form of the normalized critical distance versus the pipe geometry ( $D$ ). Examination of the results in Figures 5.13 to 5.16 indicates that the proposed criterion can be applied to all material types and pressure fluctuation ranges in determining the normalized critical distance ( $L/D$ ) between a girth weld and a wrinkle peak.

**Table 5.3: Summary of FE Results Used to Estimate Interaction Distances between Wrinkles and Girth Welds Seam**

Model	Yield (Mpa)	UTS (Mpa)	D (mm)	T (mm)	D/t	Amplitude H (mm)	L <sub>w</sub> (mm)	H/L <sub>w</sub>	Axial Position of Life Intersection (mm)			
									100%-75%	100%-50%	100%-25%	100%-0%
D20_t281_X52_A8	359	455	508	7.14	71	34.99	175.97	0.20	229.90	261.39	300.75	348.00
D20_t281_X52_A9	359	455	508	7.14	71	40.85	165.61	0.25	201.05	224.66	271.86	326.94
D20_t281_X52_A10	359	455	508	7.14	71	45.25	140.00	0.32	188.15	188.15	227.47	298.21
D20_t281_X52_A11	359	455	508	7.14	71	48.96	129.66	0.38	222.18	222.18	222.18	222.18
D20_t375_X52_A9	359	455	508	9.53	53	25.84	248.10	0.10	257.05	296.10	335.14	405.48
D20_t375_X52_A10	359	455	508	9.53	53	34.44	222.75	0.15	259.95	267.75	283.36	322.38
D20_t375_X52_A11	359	455	508	9.53	53	41.44	196.88	0.21	207.90	246.94	262.54	278.13
D20_t375_X52_A12	359	455	508	9.53	53	46.60	187.39	0.25	234.28	242.08	257.67	288.84
D30_t281_X52_A4	359	455	762	7.14	107	36.24	261.68	0.14	321.25	368.81	448.10	582.95
D30_t281_X52_A5	359	455	762	7.14	107	46.32	215.25	0.22	266.28	290.05	337.59	393.06
D30_t281_X52_A6	359	455	762	7.14	107	53.95	183.76	0.29	282.17	353.46	377.22	416.84
D30_t281_X52_A7	359	455	762	7.14	107	59.79	152.34	0.39	242.64	258.47	274.31	282.23
D30_t375_X52_A5	359	455	762	9.53	80	32.26	312.40	0.10	416.74	487.73	535.09	700.90
D30_t375_X52_A6	359	455	762	9.53	80	46.10	280.85	0.16	306.29	400.93	471.91	566.62
D30_t375_X52_A7	359	455	762	9.53	80	55.26	250.34	0.22	251.55	298.89	354.07	464.44
D30_t375_X52_A8	359	455	762	9.53	80	62.60	219.02	0.29	243.65	314.66	369.84	464.44
D20_t281_X65_A9	448	531	508	7.14	71	42.62	163.34	0.26	200.11	208.00	255.29	286.80
D20_t281_X65_A10	448	531	508	7.14	71	46.83	137.79	0.34	210.89	234.51	242.38	266.00
D20_t281_X65_A11	448	531	508	7.14	71	50.49	127.24	0.40	221.27	229.14	237.01	244.88
D20_t281_X65_A12	448	531	508	7.14	71	53.38	101.55	0.53	216.11	216.11	216.11	216.11
D20_t375_X65_A10	448	531	508	9.53	53	37.89	219.20	0.17	227.20	258.52	274.17	282.00
D20_t375_X65_A11	448	531	508	9.53	53	43.76	209.93	0.21	222.53	246.00	261.64	277.28
D20_t375_X65_A12	448	531	508	9.53	53	48.99	184.32	0.27	233.07	240.89	248.70	272.14
D20_t375_X65_A13	448	531	508	9.53	53	52.78	175.49	0.30	212.89	220.69	244.10	267.50
D30_t281_X65_A5	448	531	762	7.14	107	48.38	228.61	0.21	289.01	352.47	352.47	376.27
D30_t281_X65_A6	448	531	762	7.14	107	55.46	181.89	0.30	297.31	305.24	392.48	392.48
D30_t281_X65_A7	448	531	762	7.14	107	61.01	150.45	0.41	265.59	273.52	281.45	289.38
D30_t281_X65_A8	448	531	762	7.14	107	64.98	136.06	0.48	290.01	305.85	345.45	392.99
D30_t375_X65_A6	448	531	762	9.53	80	49.01	277.95	0.18	273.51	336.73	415.71	478.90
D30_t375_X65_A7	448	531	762	9.53	80	57.56	247.71	0.23	258.33	297.83	337.31	439.93
D30_t375_X65_A8	448	531	762	9.53	80	64.73	216.29	0.30	321.52	329.42	337.31	345.20
D30_t375_X65_A9	448	531	762	9.53	80	70.33	185.08	0.38	297.95	305.84	321.62	329.51

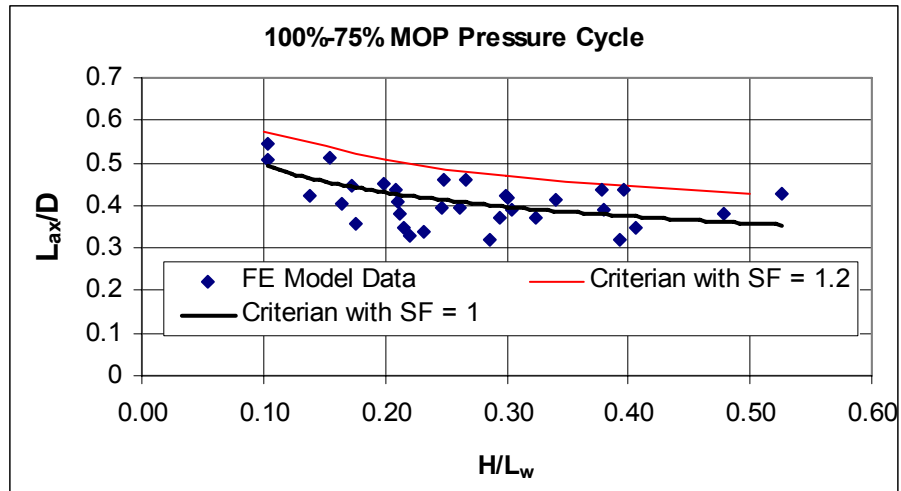


**Figure 5.13: Wrinkle Girth Weld Interaction Criteria Performance for 100% to 75% MOP Pressure Fluctuations**

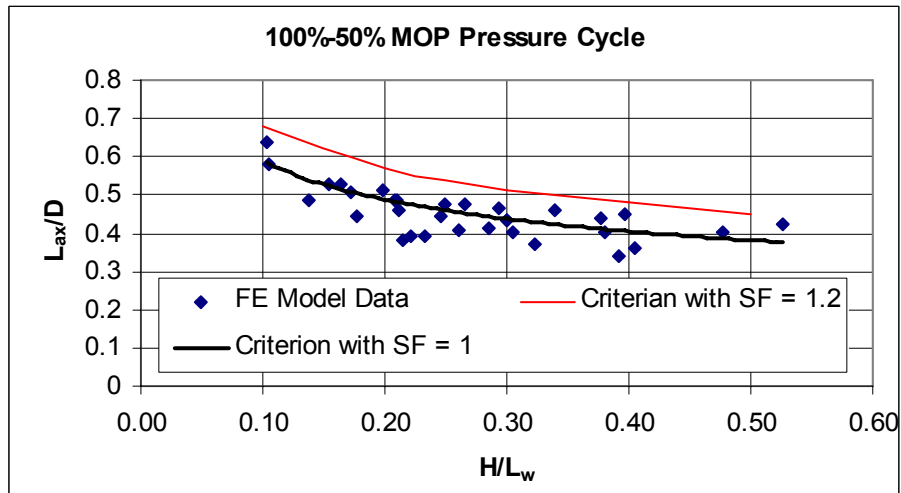


**Figure 5.14: Wrinkle Girth Weld Interaction Criteria Performance for 100% to 50% MOP Pressure Fluctuations**

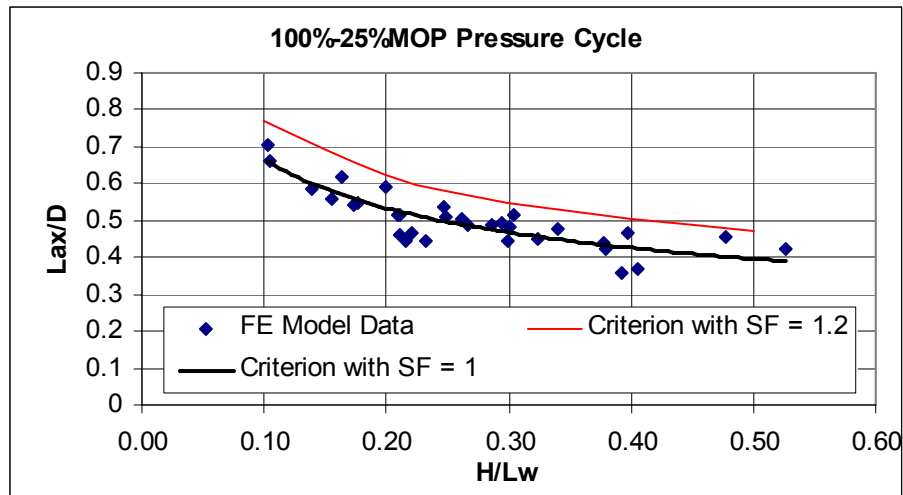


**Figure 5.15: Wrinkle Girth Weld Interaction Criteria Performance for 100% to 25% MOP Pressure Fluctuations**

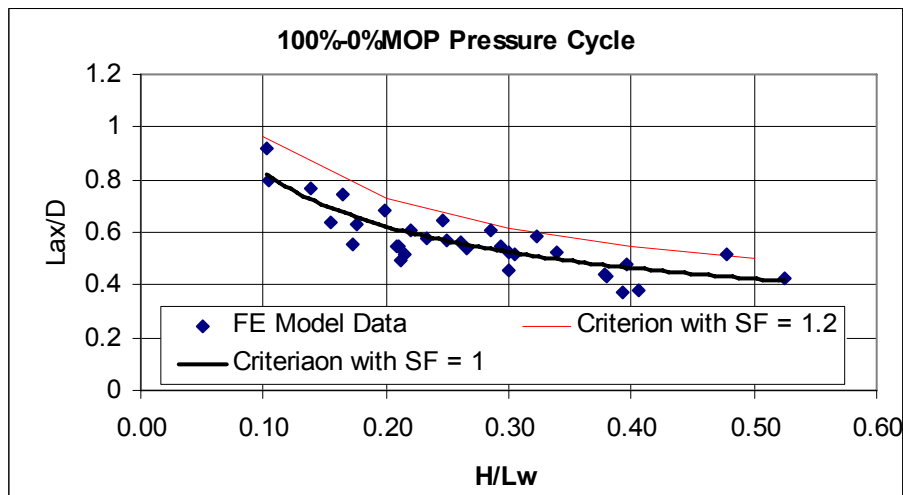


**Figure 5.16: Wrinkle Girth Weld Interaction Criteria Performance for 100% to 0% MOP Pressure Fluctuations**

Based on the results it is evident that increasing  $H/Lw$  ratios result in decreasing  $L/D$ , indicating that for smaller  $H/Lw$ , the girth weld seam must be further away from the wrinkle peak than in larger  $H/Lw$ . It is worth noting that for the cases considered in the analysis, the maximum normalized distance ( $L/D$ ) is approximately 0.9, indicating that girth weld seams that are more than 90% of the pipe diameter away from the wrinkle peak, are no longer adversely affected by the wrinkle. It should be noted that residual pipe ovality away from the wrinkle peak may need to be considered in parallel with the wrinkle assessment to identify the acceptability of the weld interaction.

As shown in Figure 5.13 to 5.16, the relationship between the normalized critical distance ( $L/D$ ) and the wrinkle shape ratio ( $H/L_w$ ) appears to follow a power law relationship. Therefore, the normalized critical distance in the axial direction can be expressed in convenient dimensionless form as follows:

$$\frac{L_{ax}}{D} = A \left( \frac{H}{L_w} \right)^B \left( \frac{552}{UTS} \right)^{0.0625} S_f$$

where:  $A=0.312$

$$B = -0.2922 * R - 0.1044$$

$R$  is the stress ratio      $R = 0.25$  for the 75% to 100% MOP pressure fluctuation range  
                                     $R = 0.50$  for the 50% to 100% MOP pressure fluctuation range  
                                     $R = 0.75$  for the 25% to 100% MOP pressure fluctuation range  
                                     $R = 1.0$  for the 0% to 100% MOP pressure fluctuation range

$S_f$  is the safety factor included in the criterion (1.2)

$UTS$  is the material minimum specified UTS in MPa

$H/L_w$  is the wrinkle shape factor

Where the coefficient  $A$ , and the exponent  $B$ , set of constants determined by fitting the finite element results at the critical location for symmetric wrinkle and a given service loading.  $S_f$  is a safety factor used to ensure that the normalized critical distances are conservatively predicted by the regression equation. It is recommended that the normalized critical distance ( $L/D$ ) be calculated using a safety factor of 1.2 to ensure that the estimate of interaction distance is conservative. The stress or pressure ratio  $R$  is included in the regression to consider the effect of the applied loading range. Figures 5.13 to 5.16 illustrate the agreement of the regressed interaction criterion with the FEA based analysis results including a safety factor of 1 and 1.2.

To apply the above interaction criteria the operating pressure spectrum for the pipeline needs to be characterized using a cycle counting algorithm [5.6] (rainflow counting algorithm is recommended). The pressure spectrum used should be representative of the operation of the pipeline system over its entire service life assuming that the wrinkle has been present for the entire time. With the completion of this characterization the pressure range data for the regression equation is defined based upon the pressure ranges that are typically observed. IT is suggested that the pressure range that is only exceeded 20% of the time be used (the 80<sup>th</sup> percentile).

## 5.7 Wrinkle-Weld Interaction Summary

As documented in the previous sections, criteria have been developed to assess the significance of a long seam and girth weld interaction with wrinkles in a pipeline segment. The criteria provide a means of estimating the critical half circumferential angle ( $\theta$ ) and axial distance ( $L_{ax}$ ) from the wrinkle peak that bound the circumferential and axial zones in which a weld would have a significantly reduced fatigue life for a range of materials, geometries and operating conditions.

The criteria have been developed based on the following assumptions and inputs:

- The interaction criteria were developed for wrinkles developed due to a combination of axial and bending loads and thus relate to a range of wrinkle shapes that are likely to exist in service.
- The wrinkle criteria are developed assuming that the wrinkle shape is stable. If the wrinkle exists in a zone for which active soil movement is a concern that will alter the amplitude or shape of the wrinkle then a more detailed treatment of the wrinkle integrity is required.
- The criteria are based on the comparison of the wrinkled pipe segment fatigue life with that of the ovalized pipe at a distance from the wrinkle, where the fatigue life is determined based on the ASME weld design S-N curve [5.1].
- The criteria have been developed based on pipe geometries in the range of 508 mm (NPS20) to 762 mm (NPS30) OD with D/t ratios between 53 and 107.
- The pipe material properties ranged from Grade 359 (X52) to 448 (X65) and the fatigue calculations are limited to materials with UTS values below 552 MPa (80 ksi).
- No consideration is given to support that might be provided by the soil surrounding the wrinkled pipe segment.
- The criteria consider the following four inputs: pipe diameter, pipe wrinkle amplitude, and the internal pressure fluctuation range.

As with the dent-girth weld and ovality interaction criteria, in order to use the wrinkle-weld interaction criteria, an analysis of the pipeline operating pressure data should be conducted to determine the typical pressure fluctuation regime for the pipeline system. In the absence of this information the 0% to 100% MOP pressure fluctuation equation should be used to ensure a conservative estimate of the critical angle between the wrinkled pipe peaks and welds.

It is acknowledged that the weld geometry and weld material properties have not been incorporated directly into the FE models used to develop these criteria. However, the pipe wall in the models at the allowable weld positions experience very little, if any, plastic deformation or radial deflection, therefore the geometry, stiffening or material property mismatch effects due to the weld would be minimal.

## **5.8 References**

- 5.1 American Society of Mechanical Engineers, Boiler and Pressure Vessel Code, Section VIII, Division 3, "Alternative Rules for the Construction of High Pressure Vessels."
- 5.2 Hauch, S., & Y. Bai, "Use of finite Element analysis for local Buckling design of Pipelines" OMAE'99.
- 5.3 Palmer, A., "Are we ready to construct submarine pipeline in the Artic", OTC, 2000.
- 5.4 ASME B31.8-2003, "Gas Transmission and Distribution Piping Systems", ASME.
- 5.5 CSA Z662-03, "Oil and Gas Pipeline Systems", CSA.
- 5.6 ASTM Standard E 1049, "Standard Practices for Cycle Counting in Fatigue Analysis", 1985, Reapproved 1997.

## 6. CONCLUSIONS

Within the context of this project, mechanical damage has been defined as any mechanism that results in deformation or metallurgical damage to a pipe wall as a result of third party activities, mishandling during construction, pipeline bedding material consolidation, or ground movement. Specifically, the project has focused on three forms of mechanical damage and the potential for interaction with girth welds or long seam welds that may negatively impact the long term integrity of a pipeline with a reduction in fatigue performance when subjected to internal pressure fluctuations. The three forms of mechanical damage investigated were; restrained rock dents that occur during initial construction, pipe ovality, and wrinkles.

It is recognized that the results are not all-encompassing; however, it is a step forward. Currently, pipeline codes, primarily in the case of dents, classify dents that interact with a weld as repairable defects, however, there is no definition provided to describe the conditions which govern interaction. This leads to interpretations based upon operator experience and the results can vary significantly from operator to operator. This project was undertaken to demonstrate that for the three mechanical damage features listed above, a consistent analytical process could be used to define the distance which governs the interaction with weld seams.

The criteria presented in this report cannot be used to determine the remaining life of a mechanical damage feature that is interacting with a weld seam. It is only intended to provide a consistent approach to assess interaction. In terms of evaluating whether a defect is repairable, the guidance presented in existing codes or standards should be used unless other information is available. For example, the CSA code bases repair requirements on dent depth, while the ASME code for gas pipelines provides a means of estimating the allowable strain for a dent. Once the interaction between a weld and dent is established, the appropriate code clause may be used to determine if a repair is required.

The interaction criteria between weld seams and each of the three forms of mechanical damage were developed using similar procedures. A matrix of numerical models was used to characterize pipe wall stress fluctuations resulting from internal pressure fluctuations to estimate the fatigue performance of a deformed pipe segment using the ASME Boiler and Pressure Vessel code fatigue design curve for low carbon steel weldments. The resulting fatigue life estimates were then compared back to the life estimate that would result from a flawless pipe segment to determine the distance from the centre of the feature, in both the axial and circumferential orientations, that a weld seam could be located without reducing the fatigue performance of the pipe. After this data was gathered for the matrix of numerical models, regression analyses were carried out to generate equations that predict interaction distances between the mechanical damage features and either the longitudinal or girth welds.

There are a number of parameters which can influence a fatigue life prediction for a weldment including the weld geometry, weld and base metal material properties, residual stresses and the presence of weld imperfections. Explicitly including such parameters in the numerical models would have been an insurmountable task. Instead, the ASME design curve accounts for many of these factors given that it is a lower bound fit to fatigue data from a large variety of welds having a range of material properties, residual stress states and initial imperfections. To address potential weld geometry effects a stress concentration factor of 3 was applied to the stress fluctuations obtained from the numerical models.

The ASME design curve is limited to base materials with a maximum ultimate tensile strength of 550 MPa (80 ksi), therefore the maximum material grade that could be included in the present analysis was Grade 448 (X65).

The operating pressure regime of pipelines can vary. Gas transmission pipelines may operate with high mean pressurization levels and low pressure fluctuation ranges, while liquid transmission pipelines usually operate with lower mean pressures and larger pressure fluctuations. The nonlinearities associated with mechanical damage features (both geometric and material related) can result in nonlinear relationships between internal pressure and pipe wall stress fluctuations. Therefore, for the three damage mechanisms, the criteria were developed to incorporate four operating pressure fluctuation ranges based upon the nominal maximum operating pressure (assuming MOP equates to hoop stresses of 72% of SMYS in undeformed pipe):

- 75% to 100% MOP
- 50% to 100% MOP
- 25% to 100% MOP
- 0% to 100% MOP

Prior to applying any of the criteria, an evaluation of the typical operation of the pipeline should be conducted first to determine which of the four pressure fluctuation ranges above most apply. Based upon this information the most appropriate input parameters and equations can be selected.

Example 1: A steadily operating gas pipeline has a mean stress of 85% MOP and typical pressure cycle R-ratios (ratio of minimum to maximum pressure) of 0.9 generating typical pressure cycles from 80% to 90% MOP. This pipeline would be classified using the 75% to 100% MOP pressure fluctuation range.

Example 2: A liquid petroleum pipeline has a mean stress of 50% MOP and typical pressure cycle R-ratios of 0.5 generating typical pressure cycles from 33% to 67% MOP. This pipeline would be classified using the 25% to 100% MOP pressure fluctuation range.

If the pressure data is not available to characterize the typical pipeline operation then it would be conservative to assume that the pipeline typically operates in the 0% to 100% MOP range.

## **6.1 Dent-Weld Interaction Criteria**

The dent-weld interaction criterion is applicable to rock dents resulting from initial construction damage. Details of several sensitivity studies conducted to evaluate the numerical modeling results generated from a range in input parameters are provided in Section 3 and Appendices A, B and C.

Twenty-one numerical models were used to develop the criteria incorporating a range of input parameters:

- Pipe diameter: 324 mm and 610 mm (NPS12 and NPS24);
- Pipe wall thickness: 4.78 mm, 7.14 mm, 8.74 mm (0.188 inches, 0.281 inches, 0.344 inches);

- D/t ratios: 37, 45, 68, 70, 96;
- Indenter diameters: 24.5 mm, 50.8 mm, 101.2 mm (1.0 inches, 2 inches, 4 inches);
- Indentation depths: 3% and 6% of the diameter; and
- Material grades: 359 and 448 (X52 and X65).

The interaction of dents with long seam welds occurred within the region of inward radial deflection as defined in Figure 6.1 (Figure 3.9 reproduced in this Section). Outside of this region, there was no reduction in fatigue life when compared to an undented pipe segment.

The criteria necessary to determine girth weld interaction required the definition of parameters describing the pipe and dent geometry and material properties:

**Ultimate Strength Ratio:** A material property parameter calculated using the ratio of the pipe material ultimate tensile strength (in practical terms the specified minimum ultimate strength) and the 552 MPa (80 ksi) maximum value applicable for materials evaluated using the ASME design fatigue curve.

**Pipe D/t Ratio:** A pipe geometry parameter calculated using the ratio of the nominal pipe outside diameter (D) to the nominal pipe wall thickness (t).

**Dent Depth (%):** A dent geometry parameter defined as the dent depth as a percentage of the pipe's nominal outside diameter (d).

**Dent Depth to Length Ratio:** A dent geometry parameter defined as the depth of the dent (d) in mm divided by the square root of the length of the dent shoulder in mm (L).

**Axial Dent Sharpness:** A dent geometry parameter defined as the distance from the dent peak to the location of the half peak height (l) divided by the square root of length of the dent shoulder (L).

While there would be some influence of material properties on the dent formation process and resulting residual stresses and strains one of the biggest influences of the material properties is the increase in stress fluctuations associated with the pressure fluctuation ranges.

Based upon a regression analysis, the axial interaction distance (in mm) is defined using Equation 6.1 and Table 6.1 (Equation 3.2 and the coefficients list in Table 3.5 both reproduced in this Section).

$$I_{axial} = 1.2 \left[ A_{SR}(SR)^2 + B_{SR}(SR) + C_{SR} \right] + \left[ A_{D/t} \left( \frac{D}{t} \right)^2 + B_{D/t} \left( \frac{D}{t} \right) + C_{D/t} \right] + \left[ A_d(d)^2 + B_d(d) + C_d \right] + \left[ A_{d/\sqrt{L}} \left( \frac{d}{\sqrt{L}} \right)^2 + B_{d/\sqrt{L}} \left( \frac{d}{\sqrt{L}} \right) + C_{d/\sqrt{L}} \right] + \left[ A_{l/\sqrt{L}} \left( \frac{l}{\sqrt{L}} \right)^2 + B_{l/\sqrt{L}} \left( \frac{l}{\sqrt{L}} \right) + C_{l/\sqrt{L}} \right] \quad \text{Eqn. 6.1}$$

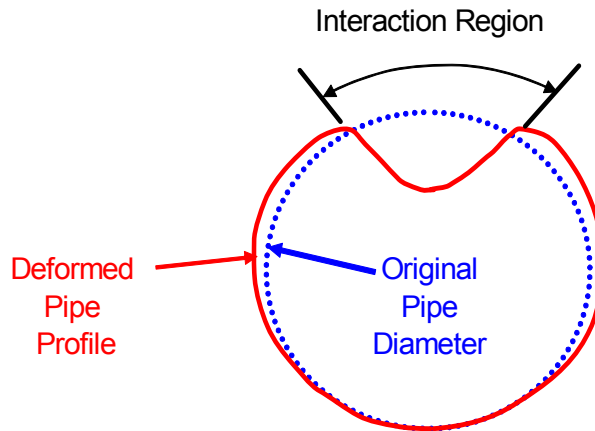


**Figure 6.1: Illustration of the Region on a Dented Pipe Segment where a Symmetrical Dent and Long Seam Weld would Interact to Reduce the Fatigue Life of the Pipe Segment**

**Table 6.1: Details of Regression Equations to Estimate Maximum Dent-Girth Weld Interaction Distances**

Pressure Range (% MOP)	Regression Equation Coefficients						Mean Error (mm)	Max Error (%)	Min Error (%)
	Coeff	SR	D/t	d	d/√L	l/√L			
75 – 100	A	415.82	0.02	66.46	265.25	-406.98	22	15	-11
	B	336.06	-4.56	-698.62	-350.33	1689.98			
	C	233.33	233.33	233.33	233.33	233.33			
50 – 100	A	87.16	-0.02	-157.18	-299.73	-7435.48	31	19	-12
	B	-252.71	2.23	1180.18	776.62	8277.58			
	C	-682.75	-682.75	-682.75	-682.75	-682.75			
25 – 100	A	183.85	-0.03	-167.01	-274.63	-8206.91	28	16	-9
	B	-225.83	4.11	1218.56	737.45	9402.45			
	C	-743.21	-743.21	-743.21	-743.21	-743.21			
0 – 100	A	-16.15	0.05	43.98	470.19	-7448.47	18	8	-4
	B	115.58	-10.07	-811.53	-600.68	10166.21			
	C	265.54	265.54	265.54	265.54	265.54			

### 6.2 Ovality-Weld Interaction Criteria

The ovality interaction criteria was developed to determine the position, with respect to the major and minor axes of the ovalized cross-section, where a long seam weld could be located to minimize the reduction in the fatigue capacity of the pipe section. Unlike the case of a dented pipe, the deformation associated with ovalization restricts the region where the ovalized pipe has the same fatigue performance as a perfectly round pipe to an impractically small percentage of the total cross-section. The criteria was therefore established to define regions where the fatigue performance is 90%, 75% or 50% of a round pipe and it becomes the choice of the stakeholders or perhaps regulators to select the level of performance that is most appropriate.

It was observed that the amount of ovality was directly proportional to the internal pressure and the application of the criteria at the present time assumes that the pipe shape with no internal pressure is attainable. For example for a 324 mm (NPS12) diameter pipe, with a wall thickness of 4.78 mm (0.188 inches) which is ovalized to 10% with no internal pressure, the ovality at MOP reduced to 0.3%.

A matrix of 144 numerical models was used to generate the interaction criteria, consisting of the following parameters:

- Pipe diameter: 324 mm and 1219 mm (NPS12 and NPS48)
- Pipe wall thickness: 4.78 mm to 12.5 mm (0.188 inches, 0.500 inches)
- D/t ratios: 37.1 to 170.8
- Ovality levels: 1%, 2%, 4%, 6%
- Material grades: 359 and 448 (X52 and X65)

After the initial hydrostatic test the pipe wall fluctuations occurred in the linear-elastic regime. Only small amounts of pipe wall plastic deformation were observed during the re-rounding process at hydrostatic test pressure levels. Therefore, a detail sensitivity analysis to input parameters and numerical modeling factors was not required.

Based on a regression analysis, the critical angle,  $\alpha_{crit}$ , measured from the peaks of the ovalized pipe is calculated using the following equation:

$$\alpha_{crit} = \beta \left( \left[ a \left( \frac{D}{t} \right)^2 + b \left( \frac{D}{t} \right) \right] + [c(\omega)^w + d(\omega)] + [e(R.L.)^2 + f(R.L.)] + g \right)$$

where the regression coefficients are summarized in Table 6.2. R.L. is the target fraction of fatigue life of the ovalized pipe relative to a circular pipe including the effects of the weld stress concentration. Since ovality will always reduce the fatigue life of a pipe segment in the presence of fluctuating pressures, this parameter can be set by the user or regulator to define the life reduction that would be acceptable. There is no appreciable reduction in fatigue life for pressure fluctuations from 75% to 100% MOP.

**Table 6.2: Regression Equation Constants**

Parameter	Pressure Range (% MOP)		
	0% to 100%	25% to 100%	50% to 100%
<b>a</b>	<b>0.0008</b>	<b>-0.0003</b>	<b>-0.001</b>
<b>b</b>	<b>-0.334</b>	<b>-0.180</b>	<b>-0.166</b>
<b>c</b>	<b>-1.266</b>	<b>-0.414</b>	<b>-0.581</b>
<b>d</b>	<b>15.905</b>	<b>6.350</b>	<b>8.631</b>
<b>e</b>	<b>130.904</b>	<b>43.976</b>	<b>41.445</b>
<b>f</b>	<b>-88.533</b>	<b>-18.539</b>	<b>-12.040</b>
<b>g</b>	<b>21.166</b>	<b>18.295</b>	<b>7.814</b>
<b>Scale Factor <math>\beta</math></b>	<b>1.2</b>	<b>1.2</b>	<b>1.3</b>

### 6.3 Wrinkle-Weld Interaction Criteria

Criteria were developed to determine acceptable positions of girth welds and long seam welds with respect to the crest of a single peaked wrinkle formed as a result of a combined axial load and bending moment. A matrix of finite element models was generated using the following input parameters:

- Pipe diameter: 508 mm and 762 mm (NPS20 and NPS30)
- Pipe wall thickness: 7.14 mm and 9.52 mm (0.281 inches, 0.0.375 inches)
- D/t ratios: 53,71 80,107
- Wrinkle amplitudes: 31 mm to 70 mm (1.22 inches to 2.76 inches)
- Circumferential extent of wrinkle: Greater than 180°
- Material grades: 359 and 448 (X52 and X65)

In the simulation of wrinkle features the wrinkle geometry was characterized based upon the wrinkle height and length. Figure 6.2 illustrates the characterization of a wrinkle’s length and height and is reproduced here.

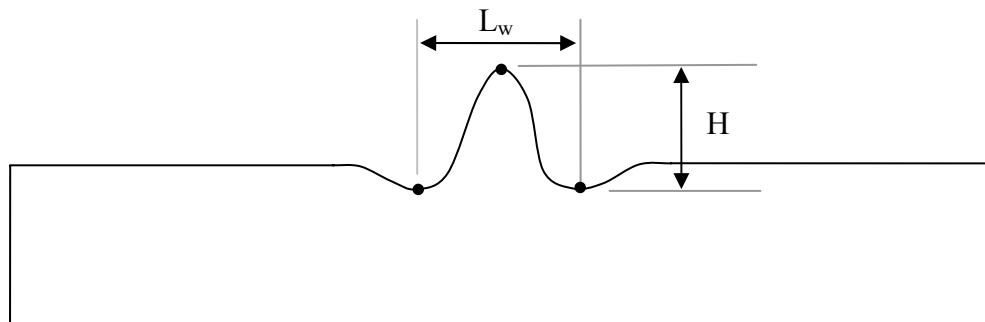


**Figure 6.2: Wrinkle Height and Length**

The interaction of dents with wrinkles occurs within the region of outward and minor inward radial deflection. This region will undergo significant cyclic deformation due to pressure fluctuations. Outside of this region, there are significantly reduced stress fluctuations and while the pipe may remain ovalized the effect of the wrinkle is no longer evident. The criteria developed identify the bound on this region to permit the significance of the interaction of welds with wrinkle features. The criteria for girth and long seam weld interaction require the definition of parameters related to pipe geometry, material, wrinkle amplitude and operational pressure fluctuations:

- Ultimate Strength Ratio: A material property parameter calculated using the ratio of the pipe material ultimate tensile strength (in practical terms the specified minimum ultimate strength) and the 552 MPa (80 ksi) maximum value applicable for materials evaluated using the ASME design fatigue curve.
- Pipe Diameter: A pipe outside diameter (D) used to normalize the axial interaction distance.

**Wrinkle Shape Ratio:** This parameter describes the wrinkle shape in terms of the ratio of height to length ( $H/L_w$ ) as defined in Figure 6.2.

While there would be some influence of material properties on the wrinkle formation and growth process and resulting residual stresses and strains one of the biggest influences of the material properties is the increase in stress fluctuations associated with the pressure fluctuation ranges. The importance of pressure fluctuations is based upon the assumption that ground movement or thermal load fluctuations, which are also significant, are not frequently applied to the pipe segment. This conclusion is for stable wrinkles (i.e., wrinkles at which the applied loading is not high enough to cause permanent changes in the wrinkle shape. No significant thermal or soil load fluctuations).

Based upon a regression analysis, the axial distance from the wrinkle crest (in mm) identifying weld interaction was defined as:

**Wrinkle – Weld Interaction = Axial Position of Girth Welds**

$$\frac{L_{ax}}{D} = A \left( \frac{H}{L_w} \right)^B \left( \frac{552}{UTS} \right)^{0.0625} S_f$$

where:  $A=0.312$

$$B = -0.2922 * R - 0.1044$$

R is the stress ratio

- R = 0.25 for the 75% to 100% MOP pressure fluctuation range
- R = 0.50 for the 50% to 100% MOP pressure fluctuation range
- R = 0.75 for the 25% to 100% MOP pressure fluctuation range
- R = 1.0 for the 0% to 100% MOP pressure fluctuation range

SF is the safety factor included in the criterion (1.2)

UTS is the material minimum specified UTS in MPa

$H/L_w$  is the wrinkle shape factor

To apply the above interaction criteria the operating pressure spectrum for the pipeline needs to be characterized using a cycle counting algorithm (rainflow counting algorithm is recommended). The pressure spectrum used should be representative of the operation of the pipeline system over its entire service life assuming that the wrinkle has been present for the entire time. With the completion of this characterization the pressure range data for the regression equation is defined based upon the pressure ranges that are typically observed. It is suggested that the pressure range that is only exceeded 20% of the time be used (the 80<sup>th</sup> percentile).

Based upon a regression analysis, the circumferential angle from the wrinkle crest (in degrees) identifying weld interaction was defined as:

**Wrinkle – Weld Interaction = Circumferential Position Long Seam Weld**

$$\left(\frac{180}{\theta}\right)^2 = A \left(\frac{H}{L_w}\right)^B \frac{1}{SF}$$

where:      A = 1.4492      and      B = -0.1049  
                  $\theta$  is the angular position in degrees  
                 SF is the safety factor included in the criterion (1.2)  
                  $H/L_w$  is the wrinkle shape factor

## 7. RECOMMENDATIONS

After a thorough review of these results by the stakeholders (both pipeline operators and regulators) additional recommendations may arise for the continuation and improvement of the criteria developed under the scope of this project. BMT acknowledges that the results may not be applicable to every scenario faced by pipeline operators and presents the following recommendations for further study:

### 7.1 Dent-Weld Criteria Recommendations

- The model matrix could be expanded to include larger diameter and thicker walled pipe to ensure that the equations are applicable to the full range of seam welded pipe geometry combinations.
- The criteria are applicable to construction related rock dents. Further research could be carried out to examine the applicability to unrestrained dents resulting from third party contact. However, this would not be a trivial task due to the number of additional parameters that would have to be considered (initial indentation depth, the presence of gouges, etc.).
- The ASME design curve for carbon steel welds restricts the maximum ultimate tensile strength to 551 MPa (80 ksi). The use of other fatigue design curves could be investigated to ensure that the criteria can be applied to higher strength pipe steel.
- More sophisticated material models could be examined to evaluate their effect on the criteria.

### 7.2 Ovality-Weld Criteria Recommendations

- The influence of internal pressure on the measured ovality could be explored more thoroughly in order to accurately predict the zero pressure ovality used in developing the interaction criteria. Currently a conservative estimate based on the results of the finite element analysis has been proposed.
- The model matrix could be expanded to include more material grades and more accurate material models, in order to further develop and understanding of the effects material grade have on both residual ovality and estimated fatigue life of ovalized pipelines.
- Currently the criteria assume that the pipe receives no support from the surrounding soil. Further development could focus on accounting for the restraint provided by the surrounding soil that would contribute to reducing the deformation and hence stress fluctuations associated with an ovalized pipe.

### 7.3 Wrinkle-Weld Criteria Recommendations

- The model matrix could be expanded to include a larger range of pipe diameter and thickness combinations to ensure that the equations are applicable to the full range of seam welded pipe geometry combinations.

- The criteria are applicable to stable wrinkles formed with a range of axial and flexural load combinations. A wider range of load combinations and the effect of wrinkle growth could be considered however this would be a large undertaking.
- The ASME design curve for carbon steel welds restricts the maximum ultimate tensile strength to 551 MPa (80 ksi). The use of other fatigue design curves could be investigated to ensure that the criteria can be applied to higher strength pipe steel.
- The effect of soil restraint on in service wrinkle formation could also be considered to reduce the conservatism of the results.



**APPENDIX A**  
**FE MODEL SENSITIVITY STUDIES FOR DENTED PIPE**

## A.1 INTRODUCTION

This Appendix provides details of the FE model sensitivity studies carried out by BMT Fleet Technology Limited to generate consistent pipe wall stress data in the region surrounding a dent created by a blunt indenter. All FE modeling has been completed using ANSYS Structural Version 8.1 and the sensitivity analysis is based upon data extracted from API 1156 study, “Effects of Smooth and Rock Dents on Liquid Petroleum Pipelines” [A.1, A.2].

Several assumptions were necessary due to the lack of information provided in the full scale test program documents (both the API study [A.1, A.2] and others). These assumptions included:

- Pipe material model; and
- Exact pipe geometry and support conditions used in full scale test programs

Because of the lack of information generated and/or provided in the reports documenting full scale test programs conducted by other researchers it was not possible to fully validate stress and strain predictions generated by the BMT modeling process. The sensitivity analysis has been completed to identify the effects of input parameter assumptions on the resulting stress state in the region of a dent on a relative basis. None of the stress results presented in this document should be considered exact values especially in the most highly deformed regions of the pipe.

FE model solutions are sensitive to a variety of modeling parameters, such as:

- Element type, size and shape;
- Element properties and solution options;
- Applied boundary conditions used to simulate actual structural restraints; and
- Nonlinear solver options.

Provided in this Appendix is a summary of the results of the most prominent FE modeling iterations designed to evaluate the effects of various assumptions required to model the indentation of line pipe material based upon the limited input data available. The dent model has developed through research projects over a period of several years and is considered proprietary so not all of the work related to the design of the modeling process is included in this document. Instead, the majority of the most influential assumptions and modeling parameters are discussed to illustrate the scope of work completed to date and the potential variability in the model output.

## A.2 API 1156 FULL SCALE DENT TESTS

The primary FE model used in this sensitivity study was designed to simulate API 1156 full scale test UD12A-3 [A.1]. Details provided in the API 1156 report [A.1] for this dent are given below:

- Pipe OD = 323.85 mm (NPS 12);
- Pipe WT = 4.85 mm (0.190 inches);
- Pipe 0.5% Yield Strength = 371.5 MPa (53.8 ksi);
- Pipe UTS = 529.5 MPa (76.7 ksi);
- Initial dent depth 12% of OD;
- Indenter – Spherical, 219.08 mm diameter (8.625 inches);
- Dent unrestrained (indenter removed after initial indentation);
- Pipe indented to 12% of the OD with no internal pressure;

- Indenter removed with no internal pressure (re-rounded depth measured 3.8%);
- Pressure increased to 6452 kPa (936 psi) (65% SMYS);
- Pressure decreased to 0 kPa (0 psi) (depth measured );
- Subjected to 24,463 cycles between 7612 kPa (1104 psi) (72% SMYS) and 3792 kPa (550 psi) (36% SMYS);
- Subjected to 31,045 cycles between 8274 kPa (1200 psi) (78% SMYS) and 689 kPa (100 psi) (6.5% SMYS) when a leak occurred;
- Leak was from a 50 mm (2 inch) long crack in the axial shoulder of the dent that initiated on the OD surface; and
- The dent depth was measured after the final depressurization of the pipe (2.5%).

Two additional API 1156 [A.1, A.2] dent tests have been included in the sensitivity study to a lesser degree to ensure that the major modeling assumptions used for the UD12A-3 model are applicable to a wider range of dent geometries. Details of the additional dent tests are provided below.

Test UD18A'-28 [A.1]:

- Pipe OD = 323.85 mm (NPS 12);
- Pipe WT = 4.75 mm (0.187 inches);
- Pipe 0.5% Yield Strength = 379.0 MPa (54.9 ksi);
- Pipe UTS = 538.5 MPa (78.0 ksi);
- Initial dent depth 18% of OD;
- Indenter – Spherical, 219.08 mm diameter (8.625 inches);
- Dent unrestrained (indenter removed after initial indentation);
- Pipe indented to 18% of the OD with no internal pressure;
- Indenter removed with no internal pressure (rebounded depth measured 11.3%);
- Subjected to 24,416 cycles between 7612 kPa (1104 psi) (72% SMYS) and 3792 kPa (550 psi) (36% SMYS);
- Subjected to 4,790 cycles between 8274 kPa (1200 psi) (78% SMYS) and 689 kPa (100 psi) (6.5% SMYS) when a leak occurred;
- Leak was from a 58.5 mm (2.3 inch) long crack at the center of the dent that initiated on the OD surface; and
- The dent depth was measured after the final depressurization of the pipe (0.8%).

Test UD6A''-68SR [A.2]:

- Pipe OD = 323.85 mm (NPS 12);
- Pipe WT = 4.93 mm (0.194 inches);
- Pipe 0.5% Yield Strength = 365.9 MPa (53.0 ksi);
- Pipe UTS = 538.5 MPa (78.0 ksi);
- Initial dent depth 6% of OD;
- Indenter – Double dent, two spherical indenters, each 114.3 mm diameter (4.5 inches), 2.25 inches between peaks;
- Dent unrestrained (indenter removed after initial indentation);
- Pipe indented to 6% of the OD with no internal pressure;
- Indenter removed with no internal pressure (rebounded depth measured 2.4%);
- Subjected to 9,802 cycles between 8274 kPa (1200 psi) (78% SMYS) and 689 kPa (100 psi) (6.5% SMYS) when a leak occurred;
- Leak was from a 89 mm (3.5 inch) long crack at the center of the dent that initiated on the OD surface; and
- The dent depth was measured after the final depressurization of the pipe (1.2%).

### **A.3 LIMITATIONS IN REPORTED FULL SCALE TEST DATA**

There are several deficiencies in the reporting of parameters in the API 1156 reports [A.1, A.2] which necessitate the use of assumptions in the numerical modeling trials that impact the accuracy of the FE model solutions.

Test Specimen and Apparatus Geometry:

The length of the pipe segment used in the test was not explicitly stated in the report. Based upon photographs it appeared as though the length of the segments was about 10 times the pipe OD (excluding the hemispherical end caps on each end) so this value was assumed for the FE models. The length of the pipe and associated boundary conditions can influence the stress and strain state in the dent region, particularly in the axial direction.

The pipe was indented using a hydraulic ram. To prevent vertical displacement and over constraining the pipe in the circumferential orientation the pipe was supported in a saddle under the ram. The radius of curvature and the length of the saddle were not reported, but these parameters can influence the dent geometry and pipe wall deformation.

Material Property Data:

The 0.5% offset yield strength and the ultimate tensile strength were obtained from transverse orientation flattened strap specimens. No other material property information relevant to numerical modeling of the pipe behavior was reported and this limited data is insufficient to properly characterize the three dimensional, highly nonlinear and cyclic stress-strain response of the pipe material.

Neither stress-strain curves nor the strain corresponding with the pipe material UTS are provided for the flattened strap specimens in the API Report [A.1]. This makes it difficult to accurately model the work hardening behavior of the pipe material. While flattened strap material property data is sufficient to confirm the grade of pipe material, this data does not truly represent the mechanical properties of a pipe in-service. The flattening process will affect the yield strength and ductility of the material. Glover and Rothwell [A.3] report a decrease of around 10%-12% in the yield strength measured from transverse orientation flattened strap specimens compared to machined round specimens or ring expansion tests for high strength pipeline steels. They also indicate [A.3] that the yield strength and ultimate strength in the hoop direction were about 20% and 5% higher, respectively, than in the longitudinal direction. In order to properly model the nonlinear three dimensional behavior of a pipe segment, both during and post indentation, the mechanical properties must be determined in both the axial and transverse orientations. Flattened strap tensile test results alone are not sufficient to characterize the transverse orientation properties. Ring expansion testing or the testing of sub-sized machined round or flat specimens is also required.

In order to properly model the cyclic behavior of the pipe, cyclic stress-strain curves are required to account for cyclic hardening or softening of the material and shakedown effects. This data is not available for the material used in the API test program.

#### A.4 NUMERICAL MODEL GENERATION

Keeping in mind the limitations discussed in Section A.3, numerical models have been generated in ANSYS 8.1 to simulate the full scale testing presented in the API 1156 [A.1, A.2] reports. The basics of the numerical model generation are presented in this section and results of the sensitivity studies will be presented in detail later in this section.

##### Model Geometry and Restraint Conditions

A  $\frac{1}{4}$  symmetry model was used to reduce the computation requirements. The primary model used to simulate test UD12A-3 in the sensitivity study excluded the support saddle to reduce the number of degrees of freedom and solution time. The model had the boundary conditions shown in Figure A.1 and, instead of a saddle, vertical restraints were applied along the bottom edge of the pipe. Based upon photographs from the API 1156 report [A.1] the length of the saddle was estimated to be 900 mm so the model was restrained vertically along nodes at the pipe centerline for a distance of 450 mm starting  $180^\circ$  from the center of the dent.

Symmetry boundary conditions were applied to the nodes along the axial and transverse plains of symmetry and the node on the bottom of the pipe at the intersection of the plains of symmetry was restrained in all directions to provide numerical stability. Finally, a vertical displacement was applied to the pilot node of the spherical element used to indent the pipe to the appropriate depth. The spherical indenter was centered at the intersection of the planes of symmetry.

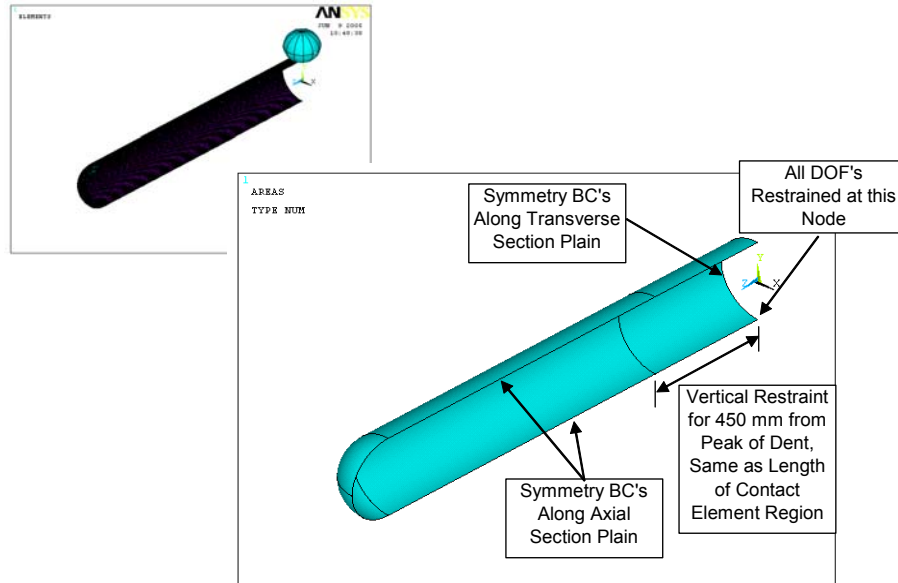


**Figure A.1: 1/4 Symmetry Model and Boundary Conditions (Applied to Nodes) used to Simulate UD12A-3 without the Saddle**

A second model geometry incorporating the saddle was included in the sensitivity study with the boundary conditions shown in Figure A.2. The radius of curvature of the saddle was estimated to be 1.5 times the radius of the pipe. Due to the increased solution times associated with this model and the results presented later, the use of this model was limited.

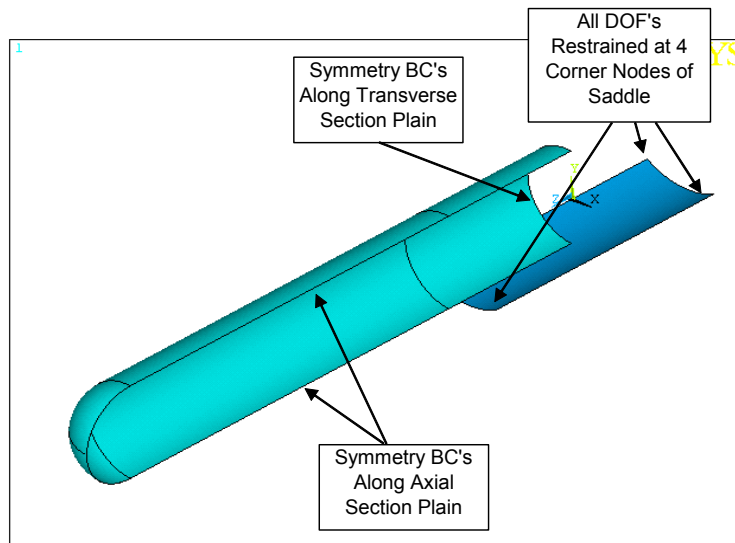


**Figure A.2: 1/4 Symmetry Model and Boundary Conditions (Applied to Nodes) used to Simulate UD12A-3 with the Saddle (Indenter not Shown)**

The geometry and boundary conditions used to model test UD18A'-28 were identical to those in the UD12A-3 model. In order to generate the double dent profile for UD6A-68SR, the spherical indenter was offset axially by a distance of 31.75 mm from the intersection of the symmetry planes to simulate the 57.15 mm peak-to-peak spacing of the double dome indenter. Neither of these models was simulated using a saddle.

### Element Selection and Meshing Details

The ANSYS help files [A.4] indicate that first-order elements with reduced integration are the most accurate for bending dominated problems. Four-noded SHELL181 elements were used to mesh the pipe in the FE models. These elements support large strain/large displacement applications and provide several other options which make them attractive for the dent modeling process, including:

- Generation of specialized element meshes can be more easily managed with 4-noded elements than with the higher order 8-noded elements (i.e., SHELL93). The mid-side nodes can make mesh generation more complex.
- Some past applications of the dent model have used prescribed nodal displacements to form a dent which becomes easier to implement when 4-noded elements are used.
- SHELL181 elements can be defined using layers and the thicknesses of the elements can be modified so that local wall thickness reductions isolated to the OD or the ID surfaces are possible for applications of the dent model combined with metal loss.

With the exception of the end cap, the entire pipe was meshed using elements with a 1:1 aspect ratio. SHELL181 element edge lengths of 5 mm and 10 mm have been investigated. From a practical viewpoint using smaller elements would result in increased demands on the computer processing power and significant increases in solution times. One UD12A-3 model was run using 8-noded SHELL93 elements with 5 mm element edge lengths and 1:1 aspect ratios to evaluate the effects of the higher order elements and decreased node spacing.

The corner nodes of the elements were defined at the mid-thickness of the pipe wall and the element real constants set was used to set the pipe wall thickness. Element coordinate systems were rotated so that the X-direction represented the hoop direction, the Y-direction represented the axial direction and the Z-direction represented the radial direction.

The pipe was indented using a contact element pair. The indenter was modeled using a rigid spherical TARGE170 element generated using the TSHAP command, while CONTA173 elements were overlaid on the pipe body mesh on the top half of the pipe for an axial distance of 450 mm. The results of the convergence study used to select appropriate contact element stiffness parameters and contact assumptions are discussed in Section A.5.

A second contact element pair was used in the model containing the saddle. The saddle was meshed with rigid TARGE170 elements with 10 mm edge lengths and 1:1 aspect ratios. The CONTA173 elements were overlaid on the pipe body mesh on the bottom half of the pipe extending 10 mm past the edge of the saddle. Contact modeling parameters were assigned to these elements to ensure that any penetration of the saddle elements into the pipe wall was negligible.

### Pipe Material Mechanical Properties

As previously discussed, the API 1156 Reports [A.1, A.2] only supplied the 0.5% yield strength and the ultimate tensile strength from flattened strap transverse orientation tensile specimens so several assumptions had to be made to generate a material property curve for the nonlinear analysis. A tri-linear model was used to approximate the stress-strain behaviour of a typical pipe material, which for the base scenario was assumed to be isotropic. The assumptions are outlined below for the UD12A-3 model and the resulting stress-strain curve is shown in Figure A.3 after conversion to true stress and true strain.

- Elastic modulus = 207 GPa (30,000 ksi), Poisson’s ratio = 0.3;
- First point: engineering strain = 0.0015, engineering stress = 311 MPa (45.1 ksi) (using elastic modulus);
- Second point: engineering strain = 0.005, engineering stress 372 = MPa (54.0 ksi) (reported yield strength); and
- Third point: engineering strain = 0.010, engineering stress = 530 MPa (76.9 ksi) (assumed that UTS occurs at 10% strain)

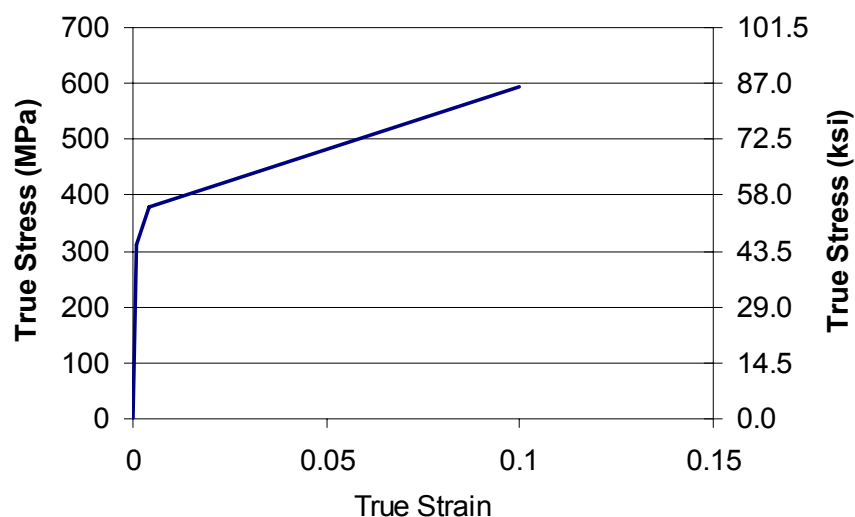


**Figure A.3: True Stress – True Strain Behavior Assumed for the UD12A-3 Models**

### A.5 SENSITIVITY STUDIES

Pipe wall strains were not measured during the course of the API 1156 [A.1] testing program therefore it is impossible to validate the accuracy of the FE models via direct comparisons of pipe wall strains. The solutions generated from the various models used in the sensitivity study were evaluated using the following criteria:

- Comparison of dent depths at various stages in the FE modeling process to those reported for the full scale tests.
- Convergence of axial and hoop direction stress solutions from the FE models.

The comparisons of stress results discussed in this document will be presented in terms of the OD surface stresses and presented for individual nodes or the mean error for the node set typically boxed by the region 50 mm axially and 50 mm circumferentially from the dent peak as illustrated in Figure A.4. The mean error is defined as:

$$\text{Mean Error} = \sqrt{\frac{\text{Sum of Squared Errors for Each Node}}{\text{No. of Nodes}}}$$

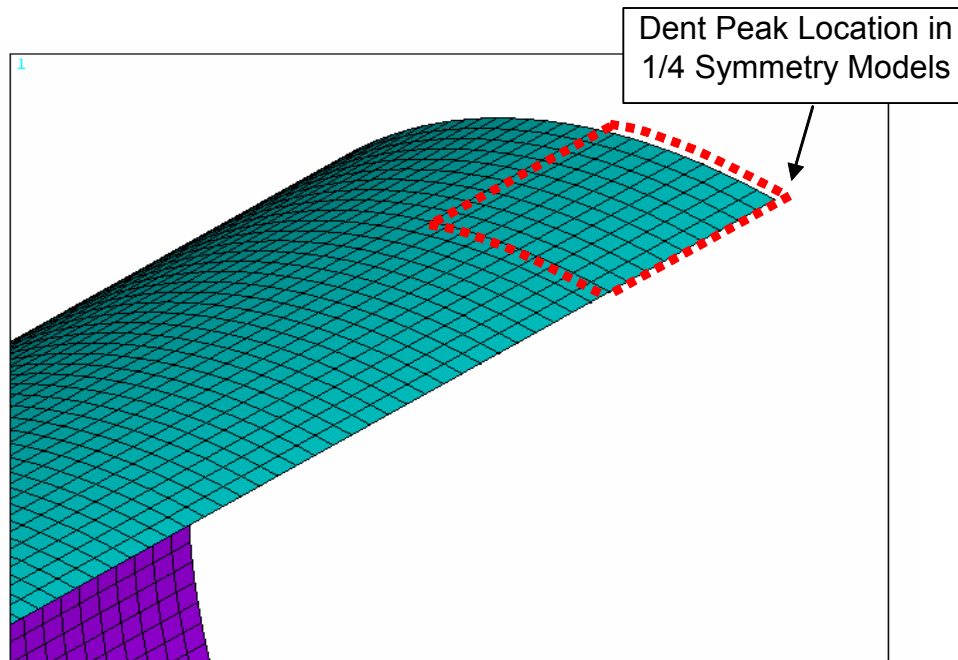


**Figure A.4: Node Set used for Mean Error Calculation in Sensitivity Studies**

#### Material Model Hardening Rules

The two most basic material hardening rules used in numerical modeling are isotropic hardening and kinematic hardening. These hardening rules are described pictorially in Figure A.5. For isotropic hardening the yield surface is assumed to expand uniformly with increasing plasticity. This rule is only valid for monotonically increasing loads. If load reversals exist then this hardening rule can generate errors in the magnitudes of stress and strain resulting from the reversal because yielding will be delayed under reversed loading conditions. The kinematic hardening rule assumes that the yield surface translates, but maintains the same size. Therefore, when load reversals are experienced, yielding will occur when the magnitude of the reversal exceeds a maximum value of 2 times the original yield strength of the material. This hardening rule is more accurate for cyclic loading, but can generate errors in large strain applications. More complex material models exist, but will not be discussed in detail in this report since the API test program [A.1, A.2] did not provide sufficient material property data to consider these advanced hardening rules.

An early evaluation of the effect of material properties and hardening rules was undertaken by BMT to simulate test UD18A'-28 and the results were compared in terms of the pipe wall rebound after indentation, elastic rebound with no internal pressure and the final dent shape following simulation of the pressure fluctuations used in the full scale test. The following cases were considered:

- Case 1: Multi-linear isotropic (MISO) using a stress-strain curve similar to Figure A.3.
- Case 2: Multi-linear isotropic (MISO) with the stress at 0.5% strain increased by 10% above the value in the API Report [A.1].
- Case 3: Multi-linear kinematic (KINH) using a stress-strain curve similar to Figure A.3.
- Case 4: Multi-linear kinematic (KINH) with the stress at 0.5% strain increased by 10% above the value in the API Report [A.1].
- Case 5: Hill & multi-linear kinematic (Hill + KINH) with the stress at 0.5% strain increased by 10% above the value in the API Report [A.1] in the transverse orientation and equal to the value in the API Report in the longitudinal orientation.

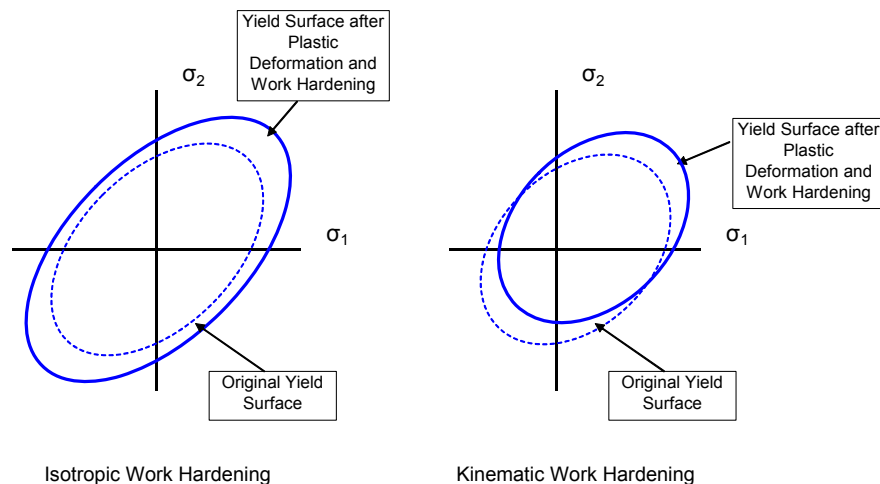


**Figure A.5: Yield Surfaces Resulting from Plastic Deformation and Work Hardening using Isotropic and Kinematic Work Hardening Assumptions**

Cases 1 and 3 were selected to compare the impact of the different hardening rules when using the flattened strap tensile properties of the pipe material. Cases 2, 4 and 5 used modifications to the flattened strap data based upon the observations reported by Glover and Rothwell [3] in their comparison of flattened strap tensile results to ring expansion and machined round tensile data. By themselves, the KINH and MISO models assume the materials are isotropic (i.e., the same in all orientations). The addition of the Hill plasticity model in Case 5 permits material anisotropy.

The results are summarized in Table A.1. There was very little difference in the predicted dent depth after elastic rebound following the removal of the indenter in all cases. After pressure cycling, the kinematic hardening assumptions provided the best estimate of the final dent depth. Further study in this area is warranted; however, more detailed materials characterization work would have been required to properly evaluate the anisotropy of the material properties and to include the material's cyclic stress-strain response in the numerical modeling. Given the limited information available in the API 1156 Report [A.1], the kinematic hardening model was used for all remaining sensitivity studies, but it is noted that kinematic hardening alone cannot account for cyclic softening which likely explains the over prediction of the final dent depth in Cases 3 and 5.

**Table A.1: Re-Rounding Behavior in UD18A'-28 Dent Models using Different Hardening Rules in ANSYS**

Loading Scenario	Dent Depth (%)					
	Full Scale Test [1]	Case 1 (MISO)	Case 2 (Mod. MISO)	Case 3 (KINH)	Case 4 (Mod. KINH)	Case 5 (Hill + KINH)
Initial Depth	18.0	18.1	18.1	18.1	18.1	18.1
Rebound No Pressure	11.3	12.4	12.1	12.2	12.4	12.4
Final Depth	0.8	4.6	5.0	2.4	3.0	2.7

### Contact Element Assumptions

Contact element assumptions were studied in detail for the TARGE170 and CONTA173 element pair used to indent the pipe in the UD12A-3 model. The primary contact parameters considered were:

- Contact element stiffness, FKN;
- Contact penetration tolerance, FTOLN; and
- Friction assumption

All of the models described in this sub-section used a mesh in the pipe body comprised of 1:1 aspect ratio SHELL181 elements with a 5 mm edge length. The initial indentation depth, initial elastic rebound with zero pressure and final dent depth after pressure cycling varied by less than 1% of the pipe OD for a wide range of the contact element parameters studied, however, the resulting stress distribution in the dent region varied considerably. Sensitivity studies were conducted to ensure that convergence of the stress solution could be achieved.

Contact stiffness, FKN, values normally range between 0.01 and 10 with the default set at 1.0. The ANSYS help file [A.4] recommends a value between 0.01 and 0.1 for bending dominated problems, but also notes that when the underlying element can deform plastically the value of FKN specified is automatically reduced by a factor of 100. FKN was varied and the OD surface hoop stresses in the contact region were examined for every model. Figure A.6 illustrates the

variability in OD surface hoops stresses when FKN is varied even though very similar dent profiles were observed with each solution (Figure A.7). Node 1 was located at the intersection of the symmetry planes under the indenter, while nodes 283 and 372 are located along the axial centerline of the pipe in the deformed region.

After an appropriate FKN value was selected to achieve a converged stress solution in the dent region, the impact of varying the penetration tolerance, FTOLN, was examined in a second convergence study. The FTOLN value sets the limits of allowable penetration of the target element. It is often expressed as a multiple of the thickness of the element underlying the contact element and has a default value of 0.1 [A.4]. Figure 3.8 illustrates the dependence of the OD surface hoop stress solution in the dent region on the FTOLN value. The stress results were scrutinized considering both stress convergence and ANSYS and possible excessive penetration when selecting an appropriate FTOLN value.

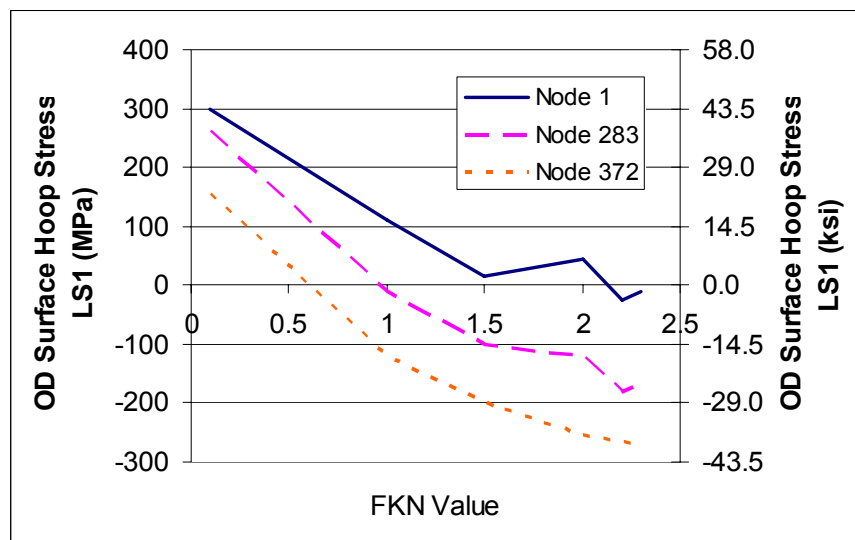


**Figure A.6: Variations in the OD Surface Hoop Stress Predictions for UD12A-3 with Increasing FKN**

Less detailed sensitivity studies were conducted to simulate full scale tests UD18A'-28 and UD6A''-68SR to confirm that the FKN and FTOLN values would generate consistent stress results for a variety of dent depths and dent shapes.

ANSYS provides contact element options which permit the program to update stiffness parameters during the solution depending upon the deformation experienced by the elements. These options were examined throughout the course of the sensitivity studies and it was determined that these model solutions were not influenced significantly if these options were incorporated into the models.

The coefficient of friction between the indenter and the pipe used in the full scale tests was not measured, however, friction between the two surfaces could have an impact on the strains (and stresses) generated in the pipe during indentation. This was examined using two models for

UD12A-3 with one model assuming that friction effects were negligible (coefficient of friction = 0) and the second assuming perfectly rough friction (coefficient of friction is infinite, sliding not possible). As illustrated in Figure A.9, significantly different stress magnitudes can be observed in the dent region depending upon the friction assumption used. Node 4 is located along the circumferential symmetry plane approximately 10 mm from the peak of the dent. The mean error between the zero friction and infinite friction model hoop stress values for the node set defined in Figure A.4 was 30 MPa (4.4 ksi) with the hoop stresses ranging from -525 MPa (-76.1 ksi) to 200 MPa (29.0 ksi). Similarly for the axial stresses, the mean error was 43 MPa with stresses ranging from -412 MPa (-59.8 ksi) to 302 MPa (43.8 ksi). Outside of the immediate indenter contact region the stresses were virtually identical. The remainder of the sensitivity studies discussed in this report use the zero friction assumption.

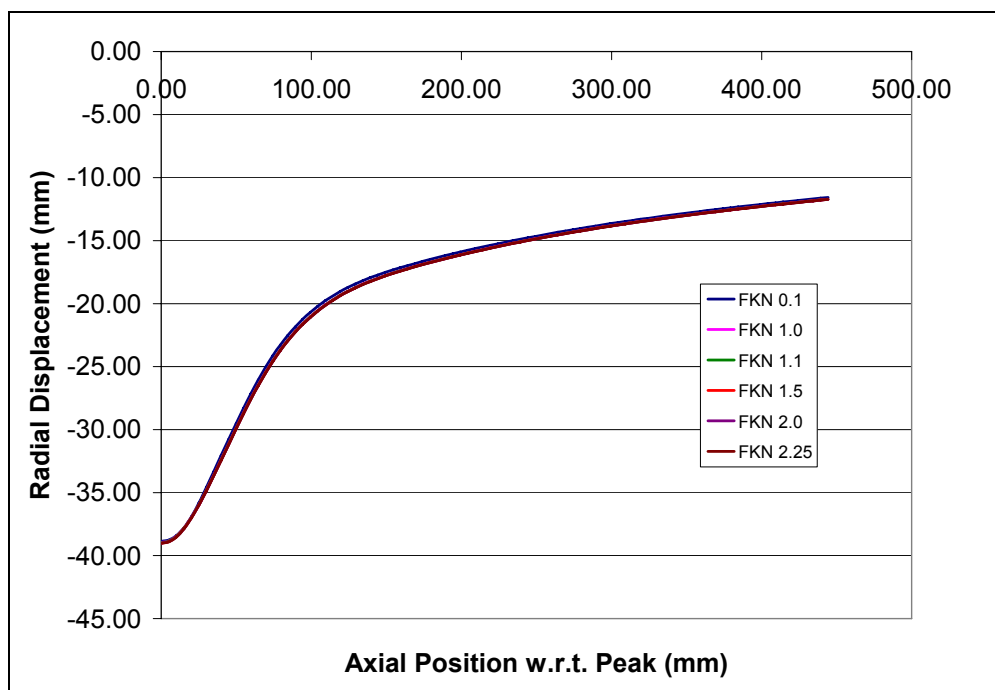


**Figure A.7: Dent Profiles Observed after Indentation in the UD12A-3 Models with Changes to FKN**

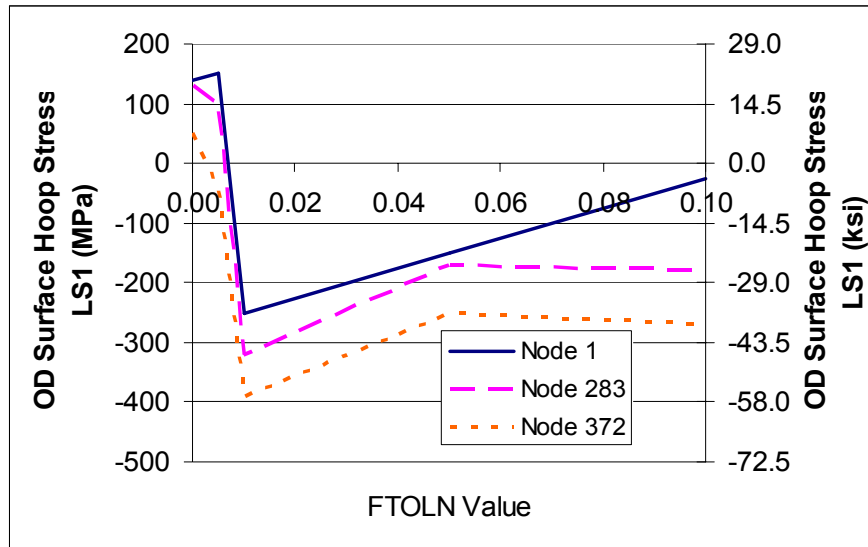


**Figure A.8: Variations in the OD Surface Hoop Stress Predictions for UD12A-3 for Different FTOLN Values**

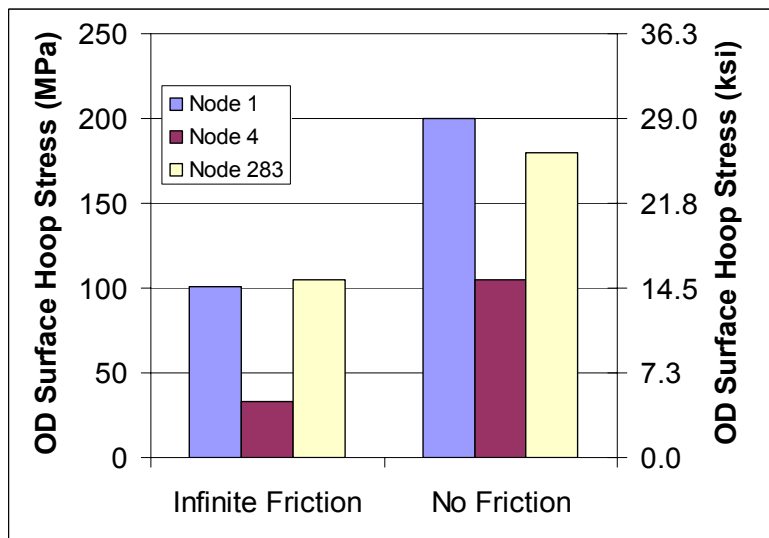


**Figure A.9: OD Surface Stress Solution for UD12A-3 Models Following Indentation with Different Contact Element Friction Assumptions**

## Model Restraint

The FE model stress results were sensitive to the boundary conditions used to simulate the restraint conditions during pipe indentation. There were no dimensions provided in the API 1156 reports [A.1, A.2] for the support saddle so the dimensions were estimated from photographs. In addition, inclusion of the support saddle and the required contact element pair greatly increased the solution time of the modelling process. Sensitivity studies were conducted to evaluate:

- The impact of replacing the saddle with vertical restraints applied along the bottom edge of the pipe model.
- The sensitivity of the stress results to the length of the pipe restrained vertically along the bottom edge.

Several models were used:

- Standard UD12A-3 model with vertical restraints applied for a distance of 450 mm from the peak (Figure A.1).
- UD12A-3 model with the vertical restraints replaced by a rigid saddle (Figure A.2).
- UD12A-3 model with vertical restraints applied for a distance of 300 mm from the peak.
- UD12A-3 model with vertical restraints applied for a distance of 900 mm from the peak.

The dent depths for the various models used in this study are compared to the full scale test results in Table A.2 for initial indentation and rebound at zero pressure. All of the FE models over predicted the dent depth after elastic rebounding. Some of this error was expected given the limited material property data available. The 900 mm vertical restraint model generated the most significant over estimate. There was a slight difference between the 450 mm vertical restraint model and the 450 mm saddle model (0.2%) which had a similar dent depth estimate to the 300 mm vertical restraint model. These results indicate a dependency on the restraint condition, but the sensitivity of the restraint condition lessened as the restrained region was shortened.

**Table A.2: Comparison of Dent Depths during Indentation and Re-rounding of UD12A-3 Models used to Evaluate Pipe Restraint Conditions**

Loading Scenario	Dent Depth				
	Full Scale Test [1] (%OD)	450 mm Vertical Restraints (%OD)	300 mm Vertical Restraints (%OD)	900 mm Vertical Restraints (%OD)	450 mm Saddle (%OD)
<b>Initial Indentation</b>	12.0	12.1	12.1	12.1	12.1
<b>Rebound No Internal Pressure</b>	6.8	7.5	7.3	7.9	7.3

Table A.3 summarizes the model results in terms of the mean error in OD surface hoop stress for the node set defined in Figure A.4 compared to the model with the nodes along the bottom of the pipe vertically restrained for 450 mm (the mean errors for the axial stresses were similar). The stress ranges for the node sets are also provided. The stress solutions for the 450 mm vertical restraint model and the saddle model were virtually identical indicating that the vertical restraints could be used in place of the saddle. However, there was an obvious sensitivity of the models to length of the restrained region along the bottom of the pipe.

**Table A.3: Comparison of OD Surface Hoop Stress Results for UD12A-3 Models using Different Vertical Restraint Conditions**

Hoop Stress Comparison Parameter for Node Set	450 mm Vertical Restraints	300 mm Vertical Restraints	900 mm Vertical Restraints	450 mm Saddle
Mean Error (MPa)	N/A	14	21	2
Stress Range (MPa)	-525 to 200	-525 to 190	-425 to 213	-525 to 200

#### Model Length

The pipe length used in the validation models was assumed to be 10 times the pipe OD (10D) excluding the hemispherical end caps (length of  $\frac{1}{4}$  symmetry model is 5D). The sensitivity of the dent region stresses to pipe length was evaluated using a second UD12A-3 model which simulated a total length of 8D. The initial dent depth and the rebounded depth at zero internal pressure for the shorter pipe model were virtually identical to the standard 10D model. Table A.4 provides a summary of the dent region OD surface stresses for the node set defined in Figure A.4 for both models. Within this range of pipe lengths the differences appear to be negligible. It is noted, however, that for an infinitely long pipe with no end caps, representing an in-service pipeline, this trend will likely not hold true unless the axial restraint conditions of the pipe are carefully considered.

**Table A.4: Comparison of OD Surface Stress Results for 10D and 8D Pipe Length Models of UD12A-3**

Stress Comparison Parameter for Node Set	10D Pipe Length Model		8D Pipe Length Model	
	Axial	Hoop	Axial	Hoop
Mean Error (MPa)	N/A	N/A	7	5
Stress Range (MPa)	-412 to 312	-525 to 200	-416 to 298	-525 to 198

### Element Size

An element size convergence study was conducted using SHELL181 elements down to a 5 mm by 5 mm square for the pipe body mesh of UD12A-3. To consider the impact of using higher order elements (or smaller 4-noded elements) an additional model was run using quadratic shell elements (SHELL93) with 5 mm edge lengths. The solution time for the SHELL93 model required approximately 7 times the computational time as the SHELL181 model. This may be improved upon by modifying the element mesh outside of the contact region.

As evident from the stress results presented in Table A.5 for the node set extracted from the region measuring 30 mm in the axial orientation and 100 mm circumferentially from the dent peak, convergence in the stress solution was not achieved when changing the SHELL181 element edge lengths from 10 mm to 5 mm. The mean errors are smaller between the 5 mm SHELL181 elements and the 5 mm SHELL93 elements suggesting that the stress solution is converging as the node spacing decreases. It is also possible that some of the difference between the SHELL181 and SHELL93 elements is due to the element formulations.

The initial and rebounded dent depths in the element size sensitivity study models varied by less than 0.1% of the pipe OD and there was minimal variation in the axial and circumferential dent profiles.

**Table A.5: Comparison of OD Surface Stress Results for UD12A-3 Models used in the Element Size Study (Node set 30 mm axially by 100 mm circumferentially)**

Stress Comparison Parameter for Node Set	5 mm 1:1 Aspect Ratio SHELL181 Elements		10 mm 1:1 Aspect Ratio SHELL181 Elements		5 mm 1:1 Aspect Ratio SHELL93 Elements	
	Axial	Hoop	Axial	Hoop	Axial	Hoop
Mean Error (MPa)	N/A	N/A	21	35	16	21
Stress Range (MPa)	-428 to 302	-441 to 200	-418 to 268	-447 to 198	-454 to 285	-505 to 410

The difference in the stress solutions for all of the element sensitivity models decreases significantly outside of the immediate contact and highest deformation regions. For instance, when comparing the stress results for nodes located beyond a distance of 30 mm axially from the peak for the SHELL181 and SHELL93 models the mean error in the axial stress components is about 3 MPa (0.4 ksi) and in the hoop stress component it is about 2 MPa (0.3 ksi).

### Discussion of Sensitivity Study Results

The sensitivity study conducted to evaluate the dent modeling process has illustrated that the non-linear solution is sensitive to a variety of modeling assumptions and ANSYS options including:

- Material property data and work hardening model
- Contact element parameters
- Model restraint conditions
- Element mesh

The region experiencing the most sensitivity to input parameters is the region of the highest deformation closest to the indenter contact point. When evaluating the dent interaction with a weld seam this would, in essence, correspond with the indenter very close to the weld seam and the weld seam region experiencing significant plastic deformation. The premise behind the proposed dent-weld interaction criteria is to define the distance from maximum deformation to a location where the weld region would experience predominantly an elastic load response to internal pressure changes similar to an undeformed pipe. At this distance from the dent peak the sensitivity of the FE model solution results to parameters like those listed above were greatly reduced based upon the observations from the sensitivity study.

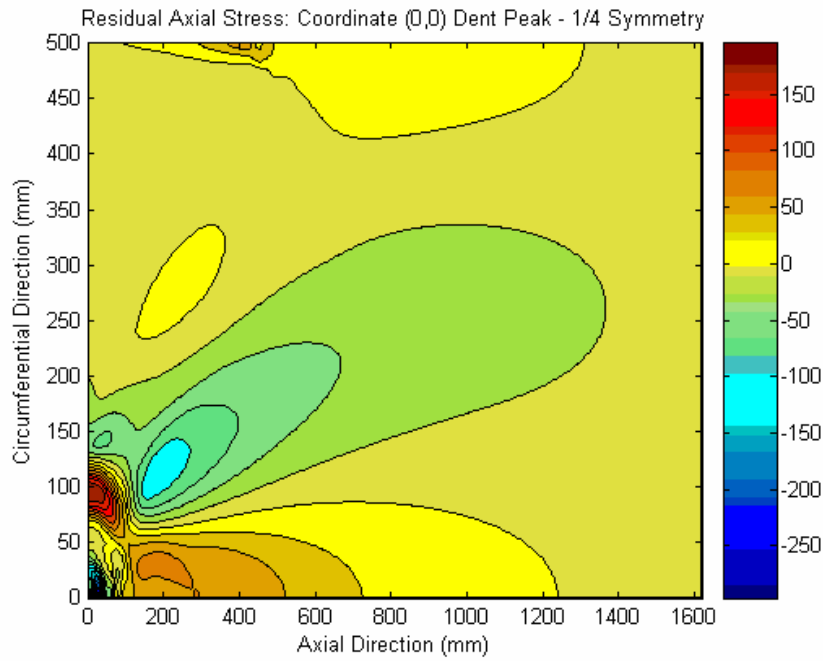
It is acknowledged that the rebound behaviour exhibited by the dent models does not provide an exact match to the full scale test program results. However, this is likely due in large part to the lack of material property information applicable to large scale deformation of the pipe wall and cyclic pressure loading. This type of information would not be readily available for any in-service pipeline and will have to be accepted at the present time as a source of variability in the modeling results.

## **A.6 REFERENCES**

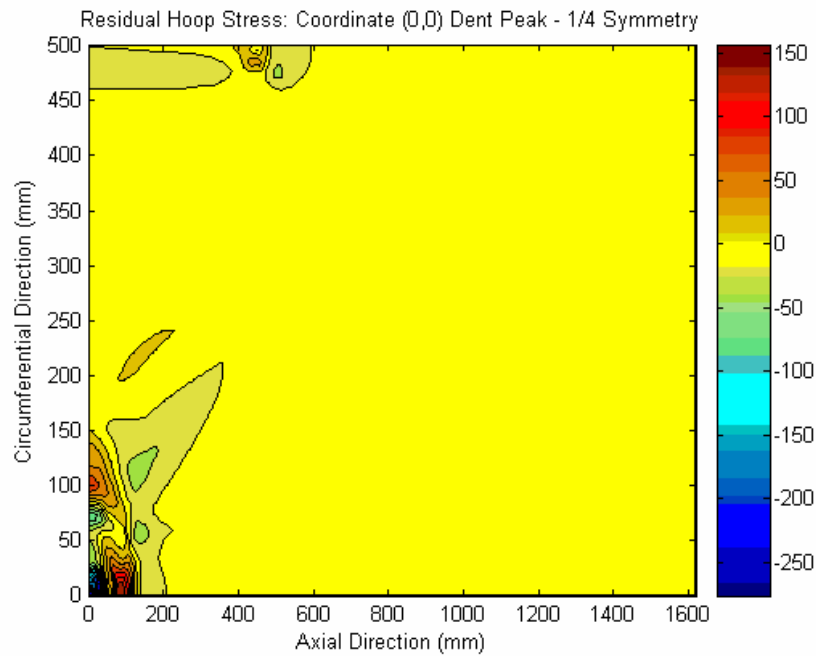
- A.1 API Publication 1156, “Effects of Smooth and Rock Dents on Liquid Petroleum Pipelines”, First Edition, November, 1997.
- A.2 API Publication 1156 – Addendum, “Effects of Smooth and Rock Dents on Liquid Petroleum Pipelines (Phase II)”, October, 1999.
- A.3 Glover, A. & B. Rothwell, “Yield Strength and Plasticity of High Strength Pipelines”, Pipeline Technology Conference, Ostend, Belgium, 9-13 May, 2004, Vol. 1, pp.65-79.
- A.4 ANSYS Version 8.1 Help File.



**APPENDIX B**  
**PLOTS OF RESIDUAL STRESS FIELDS**  
**FOLLOWING DENT RE-ROUNDING FOR**  
**DIFFERENT PIPE MODEL ELEMENT SIZES**

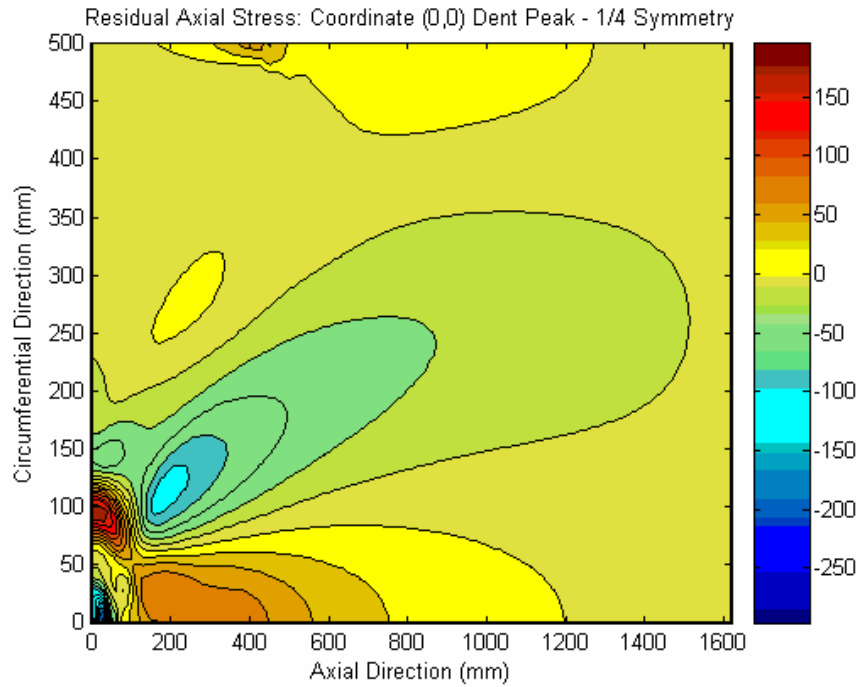


(a)

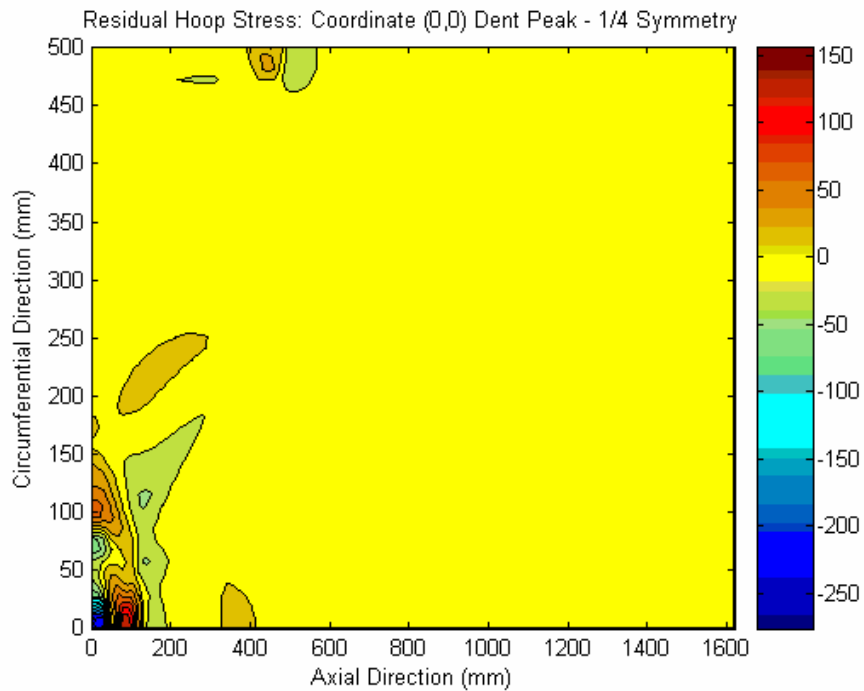


(b)

**Figure B.1: Residual (a) Axial and (b) Hoop Pipe Wall Stresses from the 5 mm SHELL181 Model (units of MPa)**

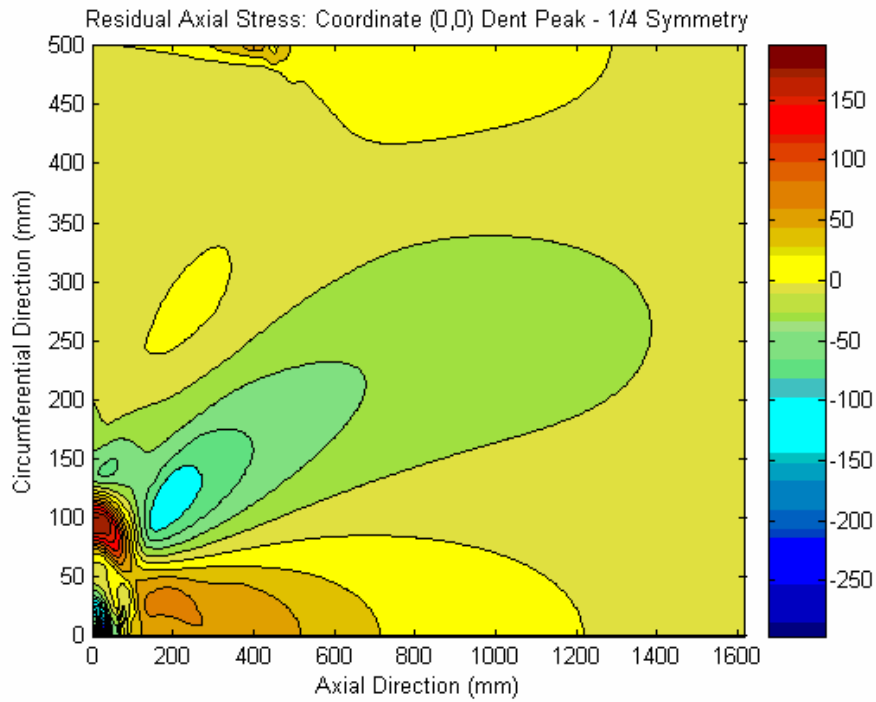


(a)

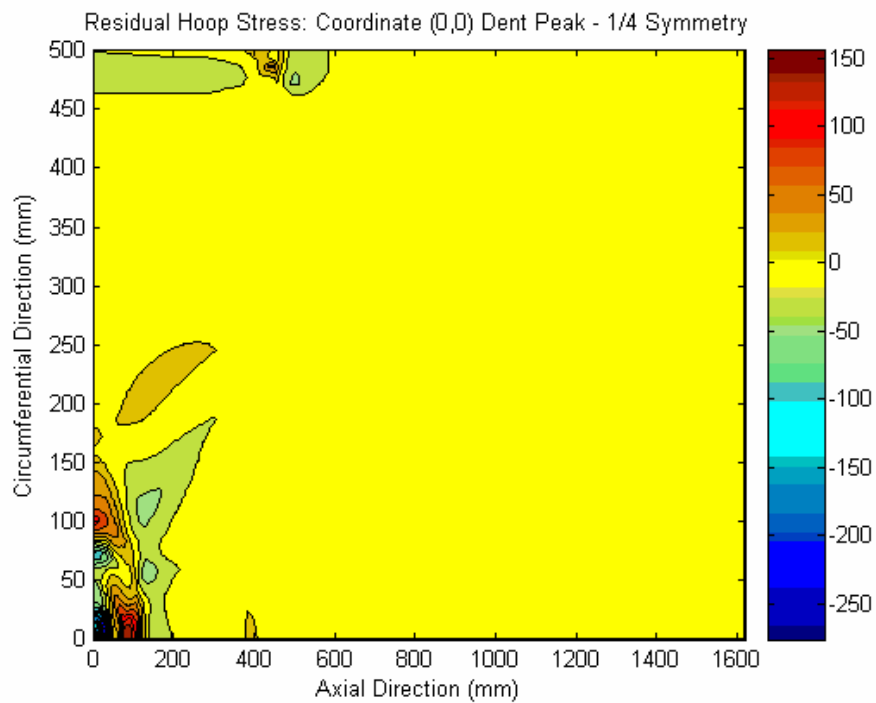


(b)

**Figure B.2: Residual (a) Axial and (b) Hoop Pipe Wall Stresses from the 10 mm SHELL181 Model (units of MPa)**



(a)

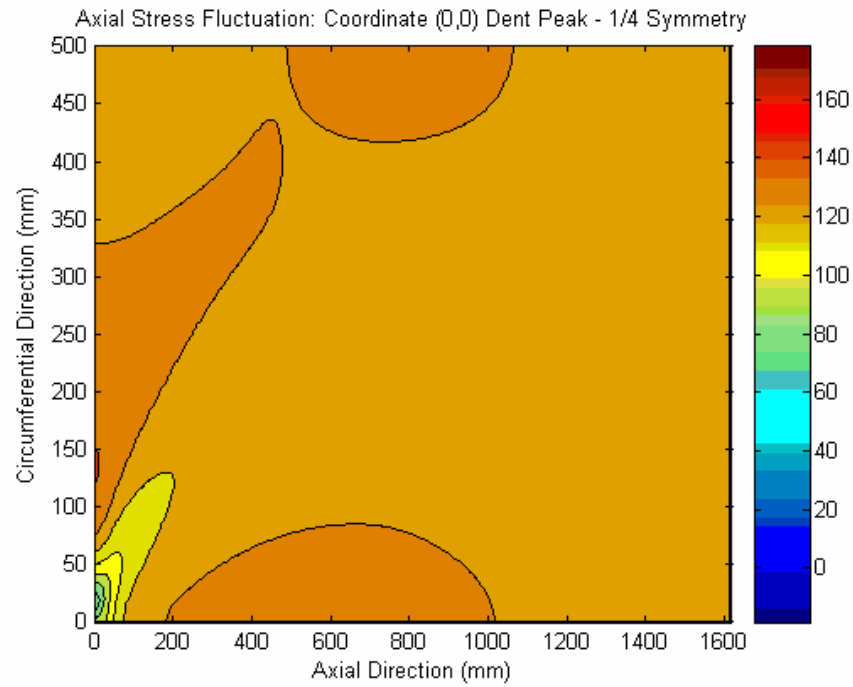


(b)

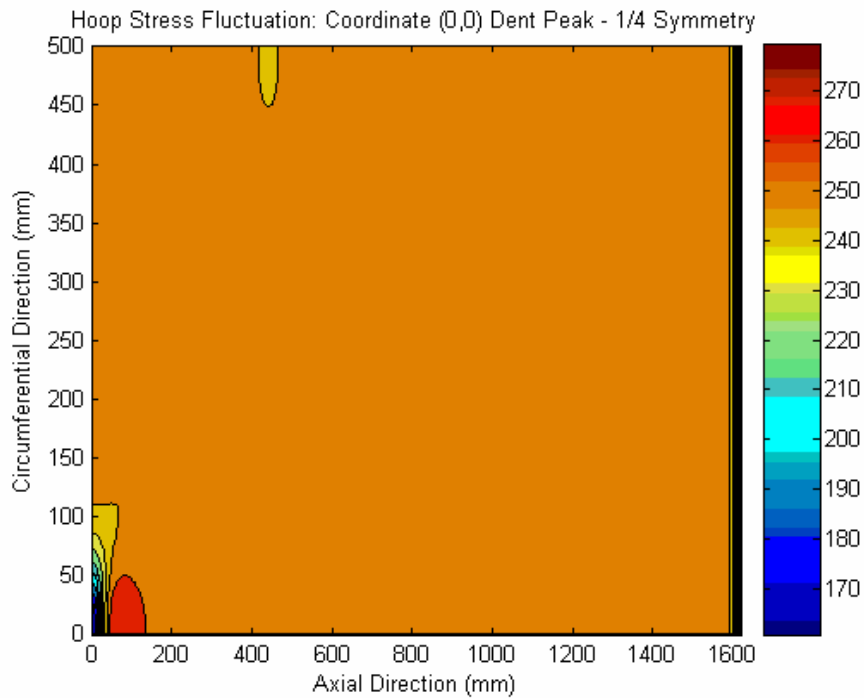
**Figure B.3: Residual (a) Axial and (b) Hoop Pipe Wall Stresses from the 5 mm SHELL93 Model (units of MPa)**



**APPENDIX C**  
**RESULTS OF SENSITIVITY STUDY**  
**TO EVALUATE BOUNDARY CONDITIONS**  
**EFFECTS ON STRESS FLUCTUATIONS**  
**IN PIPE WITH RESTRAINED DENTS**

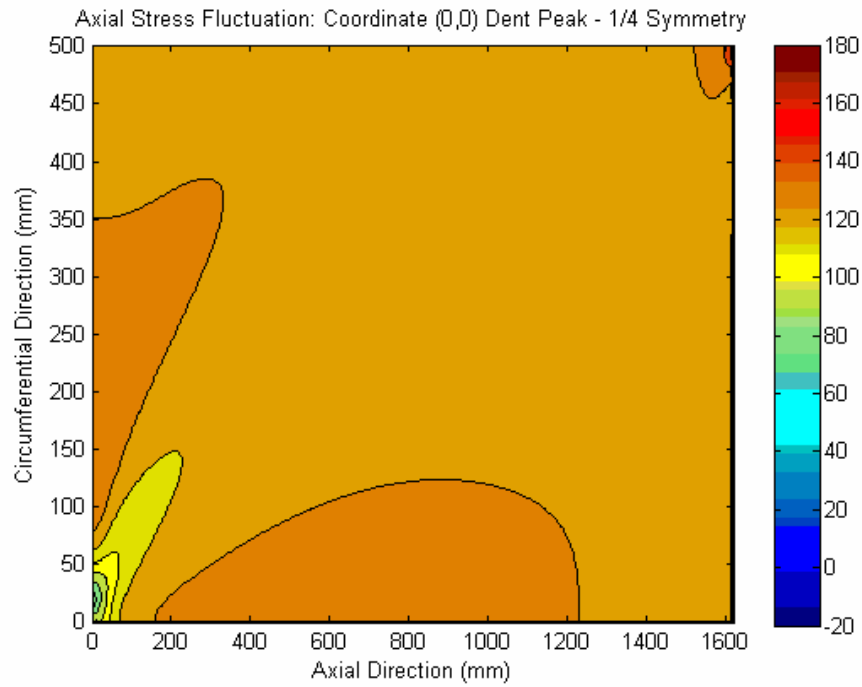


(a)

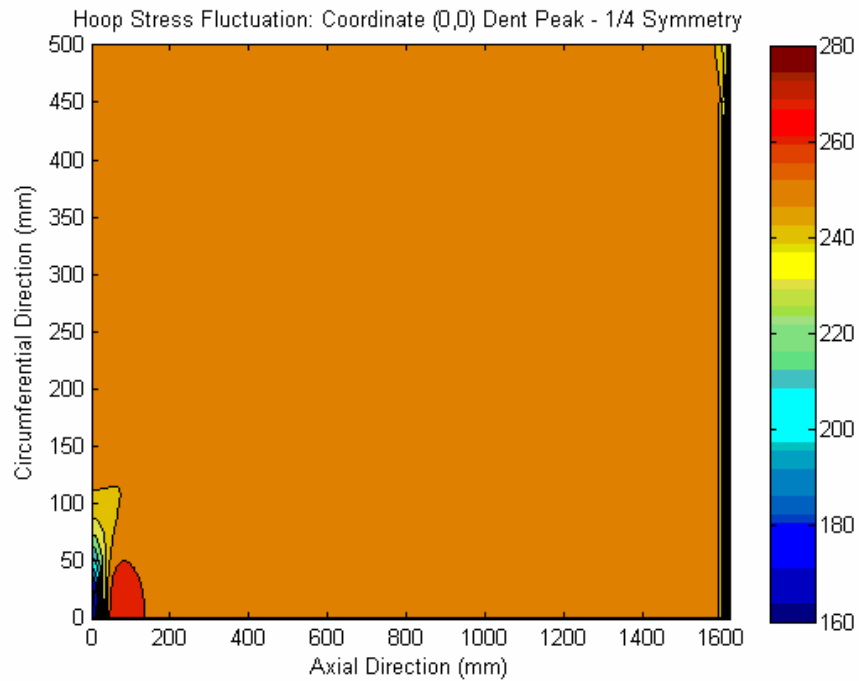


(b)

**Figure C.1: (a) Axial and (b) Hoop Stress Fluctuations for 72% of SMYS Pressure Fluctuation from Model RD12\_ec (units of MPa)**

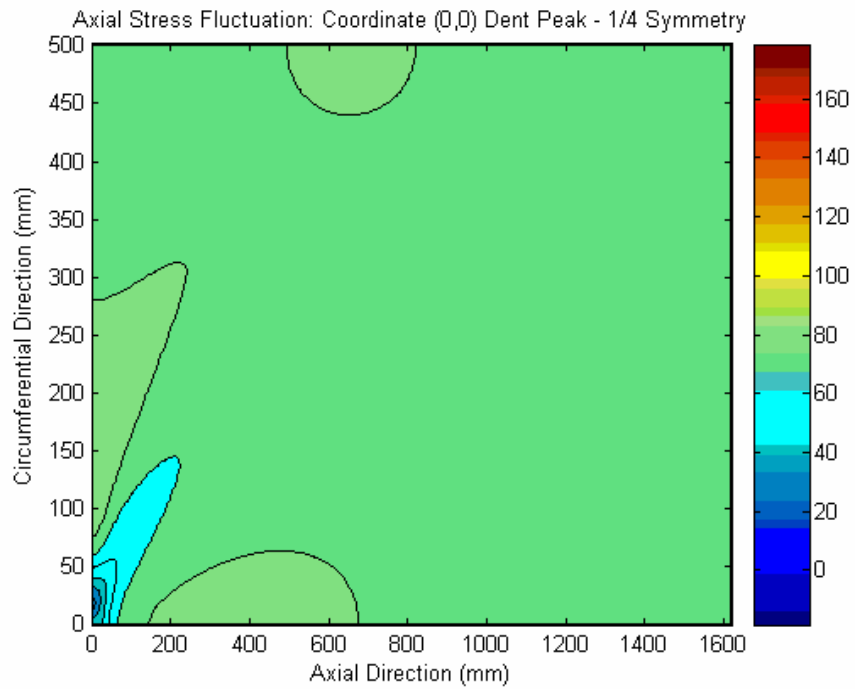


(a)

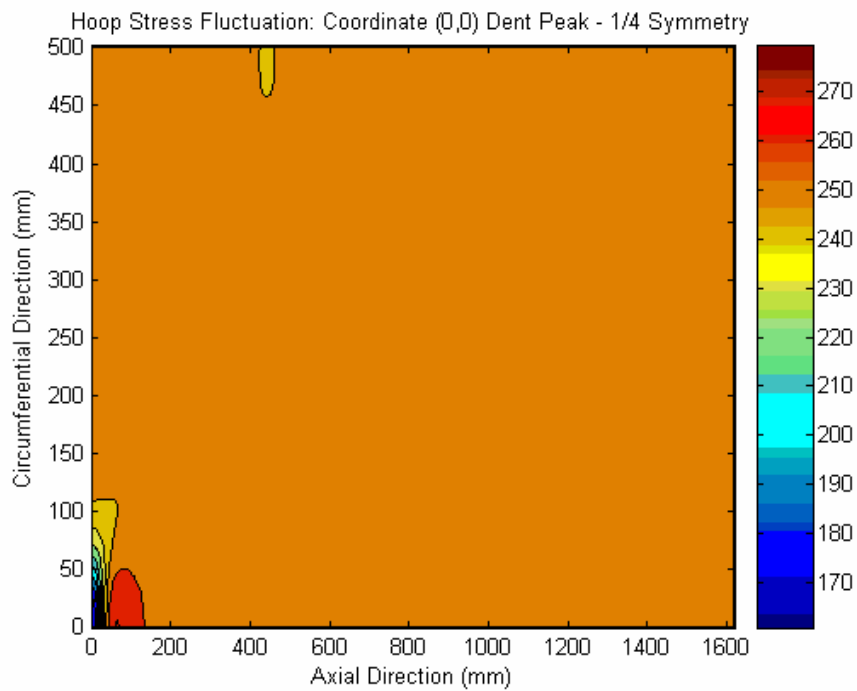


(b)

**Figure C.2: (a) Axial and (b) Hoop Stress Fluctuations for 72% of SMYS Pressure Fluctuation from Model RD12\_ec\_1 (units of MPa)**

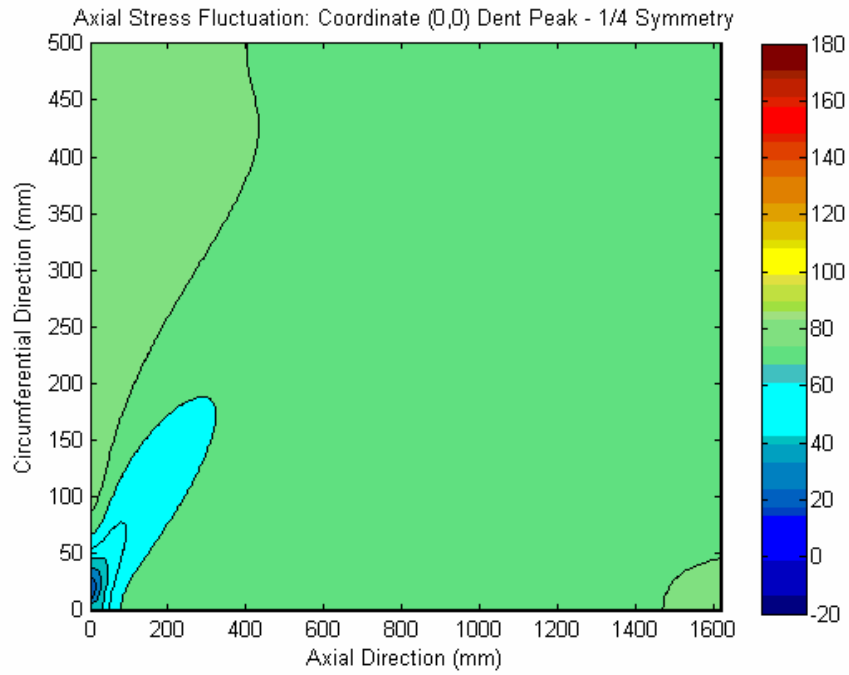


(a)

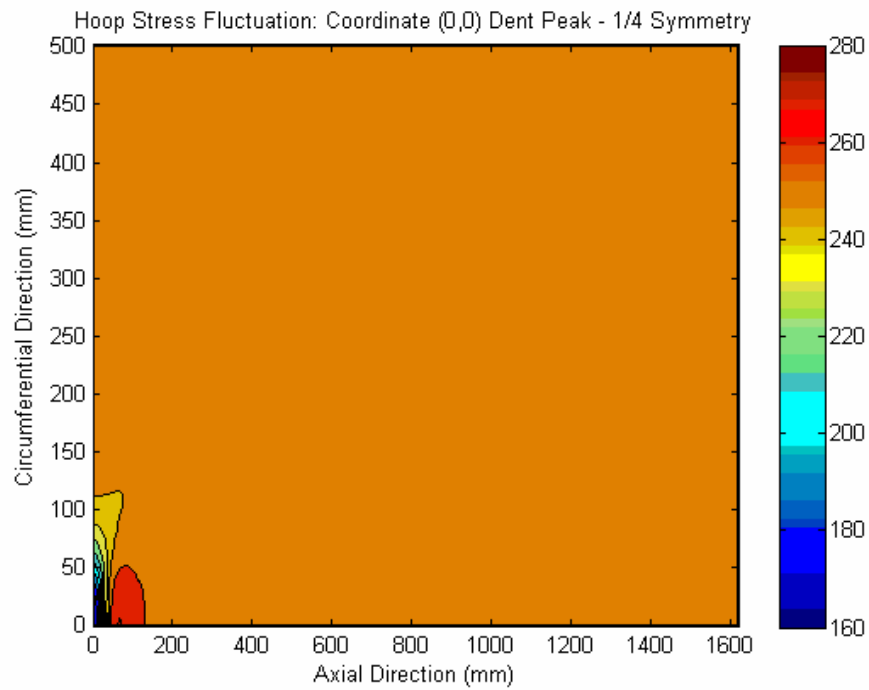


(b)

**Figure C.3: (a) Axial and (b) Hoop Stress Fluctuations for 72% of SMYS Pressure Fluctuation from Model RD12\_ncr (units of MPa)**



(a)



(b)

**Figure C.4: (a) Axial and (b) Hoop Stress Fluctuations for 72% of SMYS Pressure Fluctuation from Model RD12\_ncr\_a (units of MPa)**



**APPENDIX D**  
**PIPELINE WRINKLE FE MODEL VALIDATION**  
**AND SENSITIVITY STUDIES**

### D.1 WRINKLE FINITE ELEMENT MODEL

A cross-section of the general finite element model used in developing the wrinkle formation model, including weld seams, is shown in Figure D.1. The length of pipe modeled is generally taken to be six times the pipe diameter in order to ensure that the model is capable of capturing all possible collapse modes. The model uses 10 mm, 4 noded, reduced integration shell elements to model the entire pipe length. The shell elements account for finite membrane strain and allow for changes in shell thickness, making it suitable for large strain analysis.

In the model, the girth weld seam is modeled using general weld metal material properties gathered from past experience.

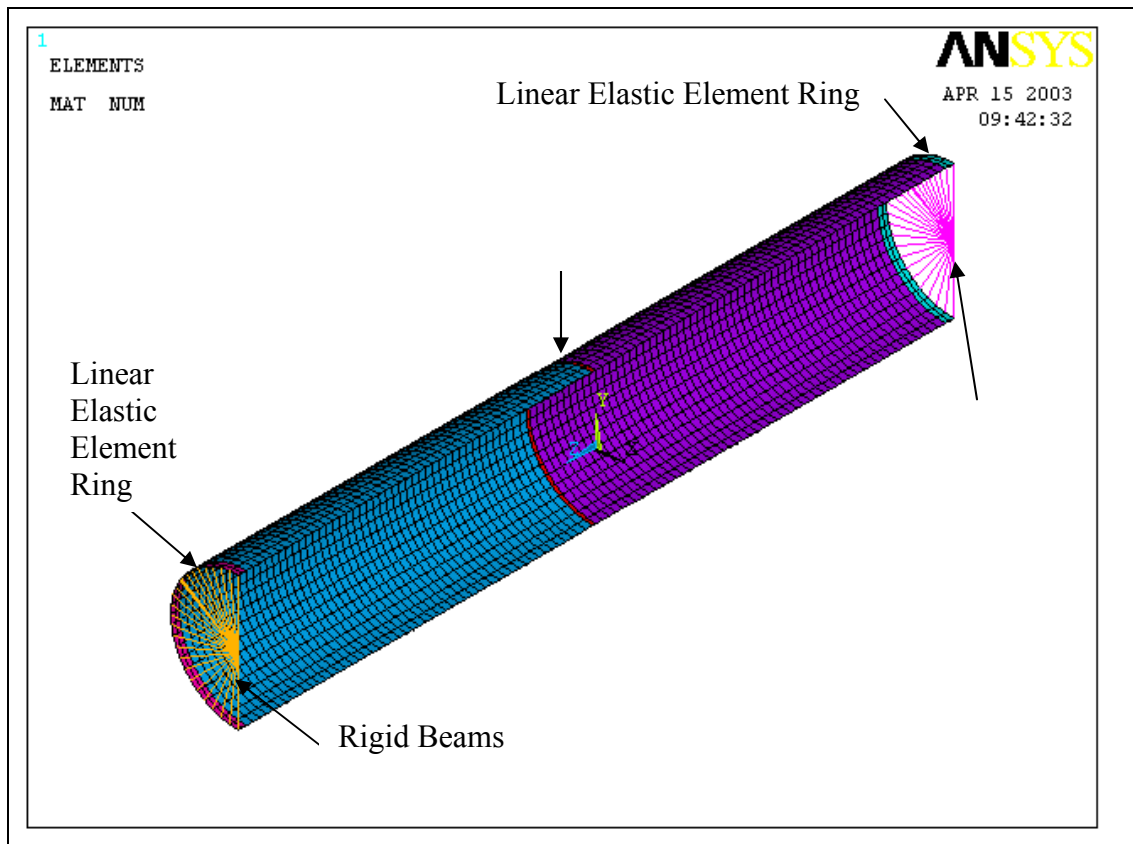


**Figure D.1: LS-DYNA Finite Element Model**

The ends of the pipe are modeled using a “spider” of rigid linear beam elements between a node at the axial centre line of the pipe and the nodes around the pipe circumference. The central node and rigid beam elements are used to evenly distribute the applied loads to the pipe ends. In order to limit local buckling and excessive plasticity at the ends of the pipe (due to the presence of the rigid beams) the last row of elements at either end of the pipe are modeled using linear elastic material properties.

A thorough examination of the mesh size has been carried out [D.1], in which it was concluded that the buckling half wavelength  $\lambda$  must be captured by at least 4 second order shell elements in the longitudinal direction, while in the circumferential direction a second element order element should not subtend an angle more than  $15^\circ$  (12 elements on the half circumference).

Furthermore, the ratio between the two dimensions must not exceed 2 or 3 [D.2]. In the LS-DYNA model, an element size of 10 mm was used, which accurately captures both the moment-curvature response and the general wrinkle shape.

### D.1.1 Material Model

Due to the large displacements and large strains associated with wrinkle formation, the material model used in the finite element analysis plays a significant role. In the post-buckling phase, strain levels between 10% and 20% are common and the material definition must therefore be capable of accurately modeling the material response at these strain levels.

In order to ensure adequate material modeling over the required range, a Ramberg - Osgood [D.3] material model is used to represent the stress-strain curve of the pipe material. The Ramberg-Osgood material model is described using the following equation:

$$\varepsilon(\sigma) = \frac{\sigma}{E} \left[ 1 + \frac{3}{7} \left( \frac{\sigma}{\sigma_R} \right)^{n-1} \right]$$

Where  $\varepsilon$  is the true strain,  $\sigma$  is the uniaxial tensile stress,  $E$  is the initial Young's modulus, and  $n$  and  $\sigma_R$  are Ramberg-Osgood parameters.

The Ramberg-Osgood model requires that the Young's Modulus and at least two points on the stress-strain curve be known [D.4]. The two points can be any where along the curve, and are generally represented by the specified minimum yield strength (SMYS), which is assumed to occur at a strain of 0.5%, and the ultimate tensile strength (UTS), which is assumed to occur at a strain of 12%.

Example true stress- true strain curves are presented for X52 and X70 in Figure D.2. The two points used in conjunction with the Ramberg-Osgood model to create the curves are summarized in Table D.1.

**Table D.1: X52 and X70 Material Properties**

Mat.	Point	Engineering Stress (MPa)	Engineering Strain (%)
X52	1	359	0.5
	2	455	12
X70	1	482	0.5
	2	565	12

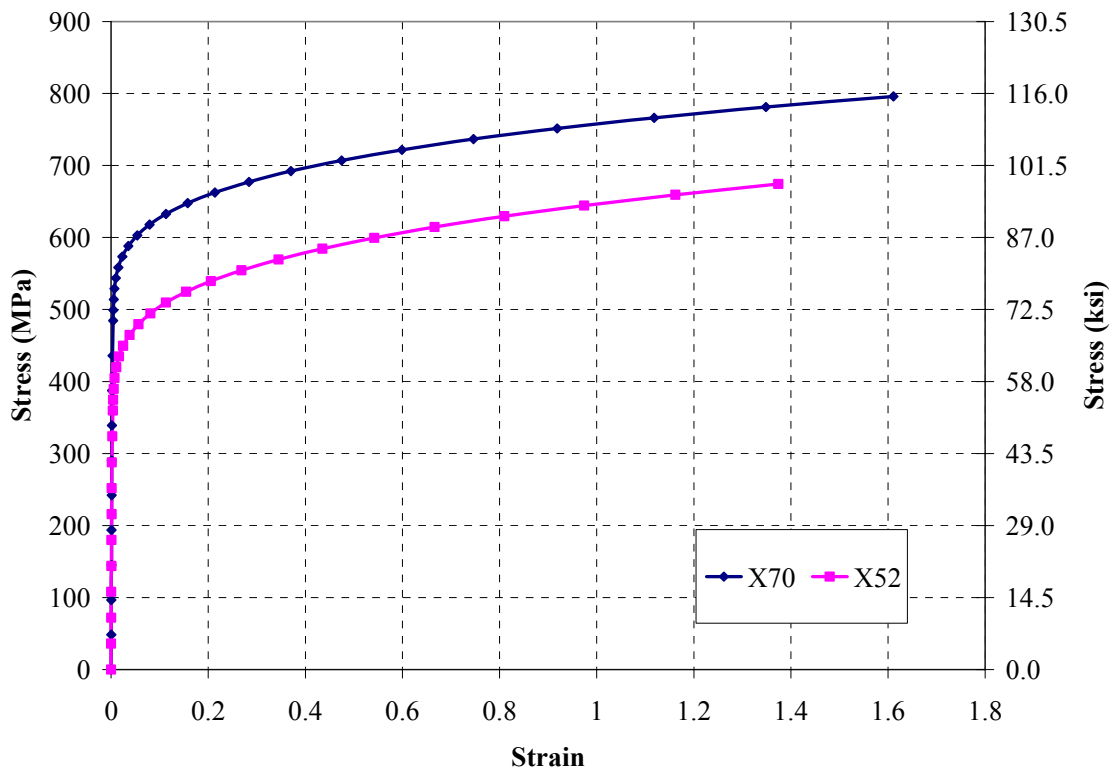


**Figure D.2: True Stress - True Strain Curves – X52 and X70**

D.1.2 Boundary Conditions and Load Sequence

The boundary conditions used in the wrinkle formation model are dependent on the number of symmetry planes assumed in the model. For some scenarios, the use of a quarter symmetry model is acceptable and results in two planes of symmetry, to which symmetry boundary conditions must be applied. In addition the central node at one end of the pipe is held rigid in all six degrees of freedom. For a full pipe model, where no planes of symmetry exist, only the rigid boundary condition at the end of the pipe is applied.

The loads applied to the model must reflect the actual loading conditions and sequence. Therefore, in general, internal pressure loading and axial loads (due to thermal expansion/contraction or soil movements) are applied as they generally represent actual operating conditions. With these loads held constant, an out of plane rotation is applied to the central node of the free end of the pipe in order to form the wrinkle/buckle. A slight imperfection is included in the model in order to initiate the wrinkle/buckle at the desired location. Many forms of imperfection can be used to initiate the wrinkle/buckle, including reducing element thickness, applying local radial loads or pressures, or changing the pipe geometry. In the BMT FTL model, the imperfection is in the form of a slight ovality of the pipe (0.3% - 0.6% of the wall thickness) at the longitudinal centerline of the pipe.

## D.2 VALIDATION EXAMPLES

Validation of the LS-DYNA finite element model is carried out using a variety of sources including full-scale experimental data, alternative finite element analyses and previously developed analytical models.

The full-scale experimental data used to validate the finite element model is taken from [D.5], in which full size pipe specimens were subjected to constant axial force, constant internal pressure and monotonically increasing curvature. The test specimens all contained girth welds at the mid-span. The curvature was increased until large amplitude wrinkles formed in the pipe specimen. In the experimental program all pressurized specimens developed bulging wrinkles while unpressurized specimens developed diamond pattern buckles. Local buckling was defined as the point at which load carrying capacity is reduced (the softening point). For bulging type wrinkles, occurring in pressurized specimens, the wrinkle was close to the girth-weld seam, but did not contain it. For diamond buckles, occurring in unpressurized specimens, the buckles often straddled the weld seam [D.6]. Of the seven tests performed, four are presented as sample validation cases for the BMT FTL finite element model.

Details of the four full-scale specimens presented for the model validation are in Table D.2. Note that the specimen designations in Table D.2, namely, UGA12W, HGA12W, and DGA12W refer to specimens that are un-pressurized, half pressurized (0.36 SMYS) and fully pressurized (0.72 SMYS), respectively.

**Table D.2: FE Model Validation – Full Scale Specimen Data**

Test Description	UGA12W	HGA12W	DGA12W	UGA20W
Outer Diameter (mm)	324	324	324	508
Wall thickness (mm)	6.35	6.35	6.35	7.9
Material	X52 (358 MPa)	X52 (358 MPa)	X52 (358 MPa)	X56 (386 MPa)
Internal Pressure (MPa)	0	5.16	10.33	0
Initial Axial Force (KN)	644	407	170	1311

The material models for X52 and X56, used in the validation examples are shown in Figure D.3. The true stress- true strain curves are derived from the specified minimum material properties summarized in Table D.3.

**Table D.3: X52 and X56 Material Properties**

Mat.	Point	Engineering Stress (MPa (ksi))	Engineering Strain (%)
X52	1	359 (52)	0.5
	2	455 (65)	12
X56	1	386 (56)	0.5
	2	489 (70)	12

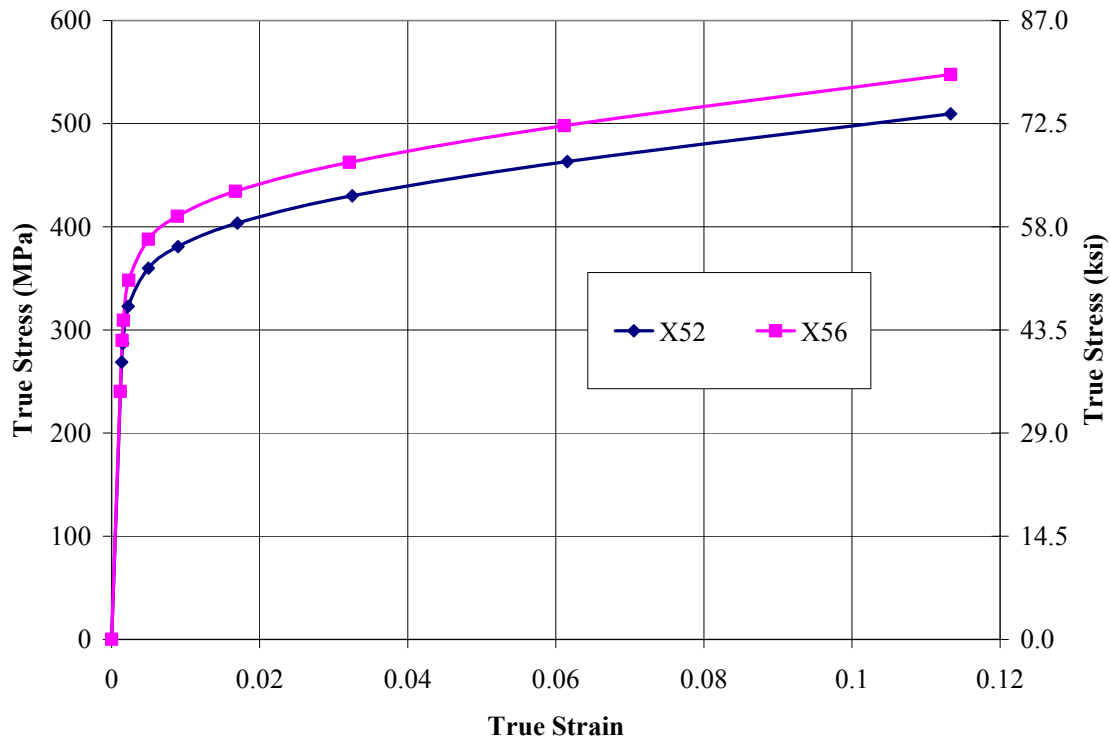


**Figure D.3: True Stress – True Strain Curves – X52 and X56 Materials**

### D.2.1 Validation of LS-DYNA Finite Element Model

Currently available experimental data is limited to moment vs. curvature results, and to the general shape of the buckle or wrinkle formed during the experiment. Detailed experimental data regarding the amplitude and wavelength of the wrinkle or the stresses and strains in the wrinkle is not currently available. Therefore, the validation of the LS-DYNA finite element model is carried out by comparing the results of the simulations to the experimental results in terms of the moment-curvature relationship and the buckling mode shape.

Results are presented in Figures D.2 to D.6 in terms of the global moment (defined as the average of the two end moments applied to the full scale specimen) vs. global curvature (defined as the sum of the end rotations divided by the total pipe length) and the predicted and observed wrinkle geometry.

Figure D.4 illustrates the global moment versus global curvature for the unpressurized X52 specimen (UGA12W). The results indicate that the BMT FTL LS-DYNA model agrees reasonably well with both the experimental results [D.5], and with the calibrated ABAQUS model [D.6]. There is also good agreement between the predicted and observed buckling shapes as illustrated in Figure D.5. The diamond shape buckle observed in both the experimental results and the model results is a typical deformation pattern observed in unpressurized pipes.

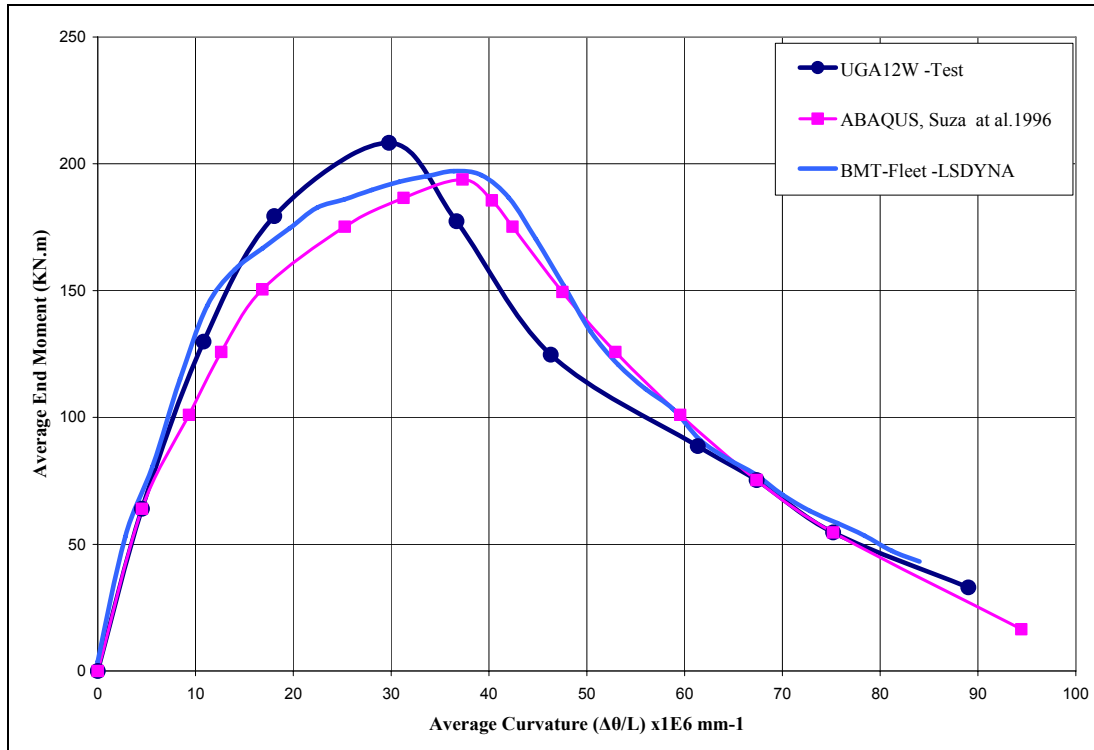


Figure D.4: End Moment vs. Curvature – Unpressurized Pipe (UGA12W)

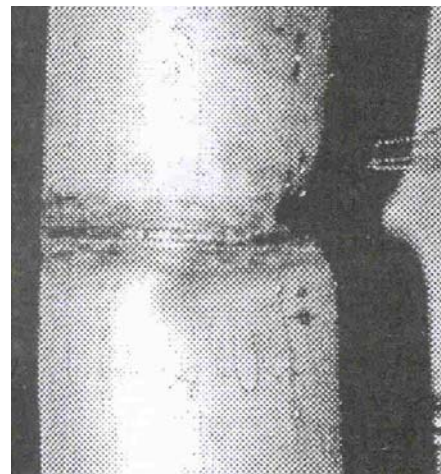
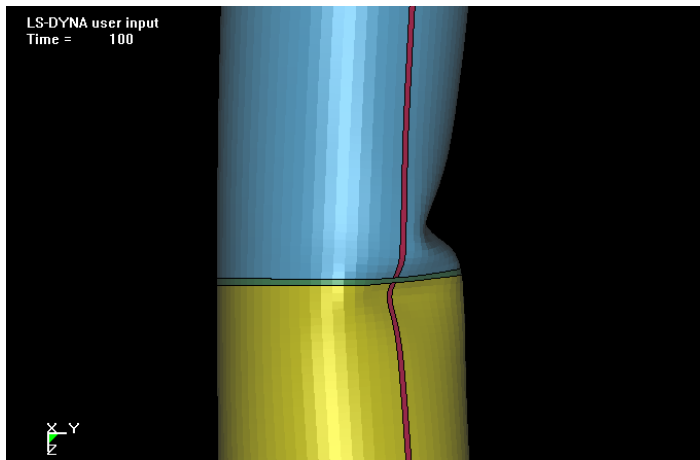
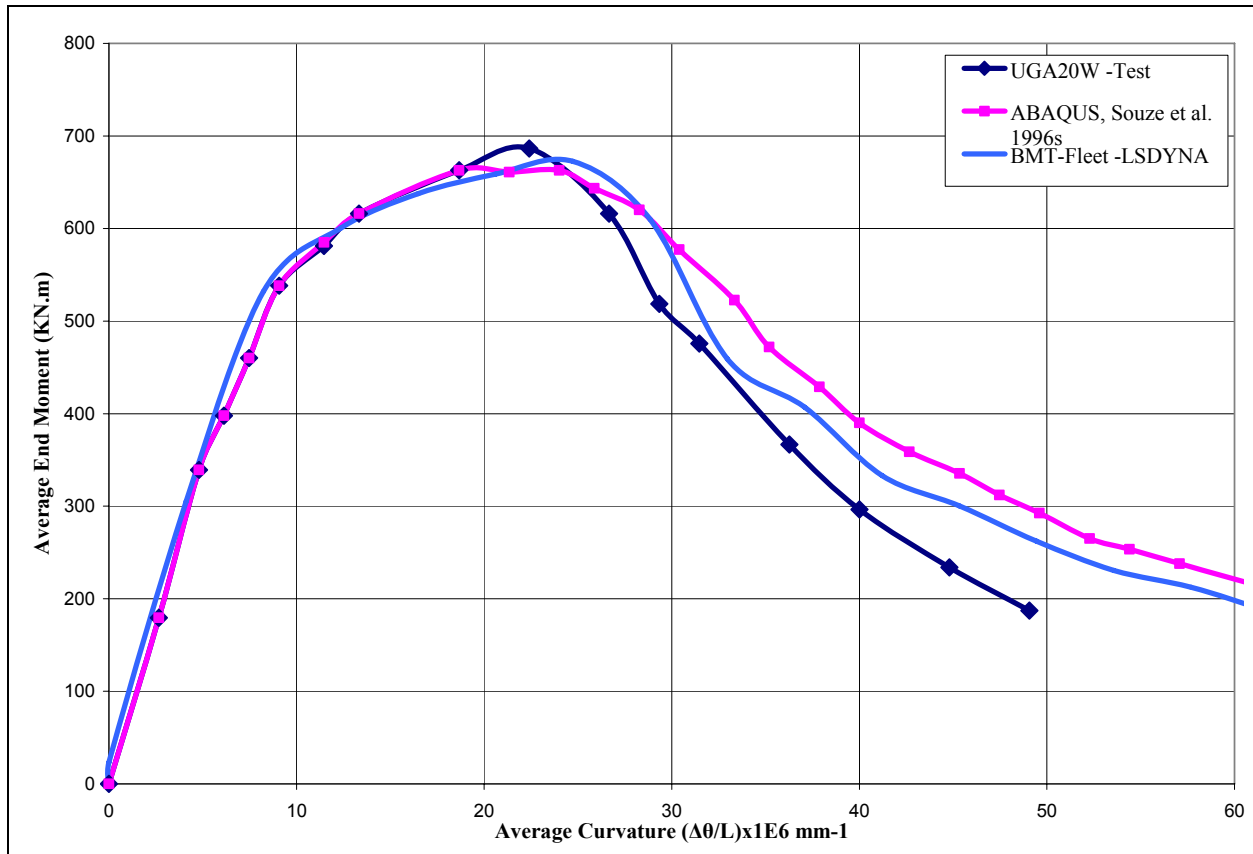


Figure D.5: Comparison of Predicted and Observed Wrinkle Geometry – (UGA12W)

Similar results are presented for the larger unpressurized X56 pipe (UGA20W) in Figure D.6. Once again there is good agreement between the BMT FTL LS-DYNA model, the experimental results and the calibrated ABAQUS model.



**Figure D.6: End Moment vs. Curvature – Unpressurized Pipe (UGA20W)**

Results for the fully pressurized X52 pipe (DGA12W) are presented in Figures D.7 and D.8. Although the moment versus curvature results do not correlate as well as for the unpressurized specimens, the correlations are still considered adequate. As is evident in Figure D.8, both the experimental specimen and the model exhibit bulging type wrinkles, which are typical for pipes with sufficient internal pressure.

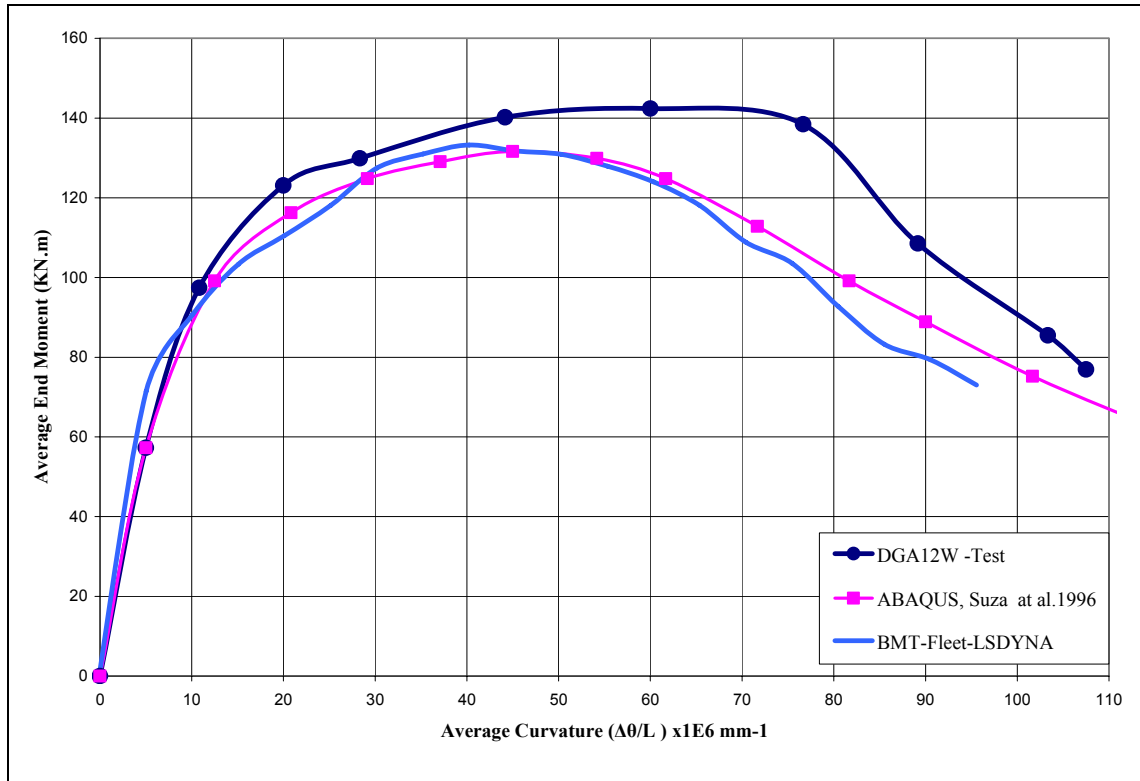


Figure D.7: End Moment vs. Curvature – Fully Pressurized Pipe (DGA12W)

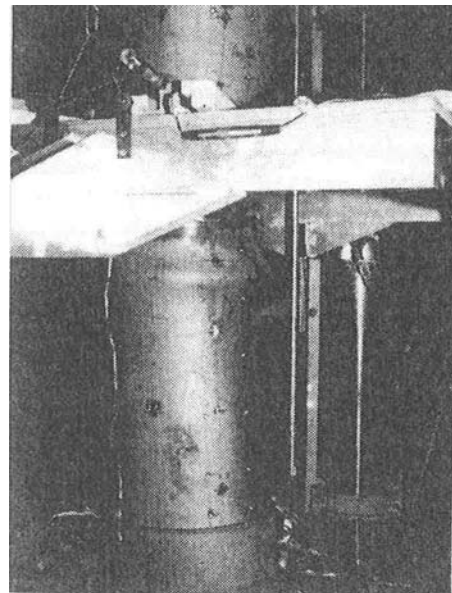
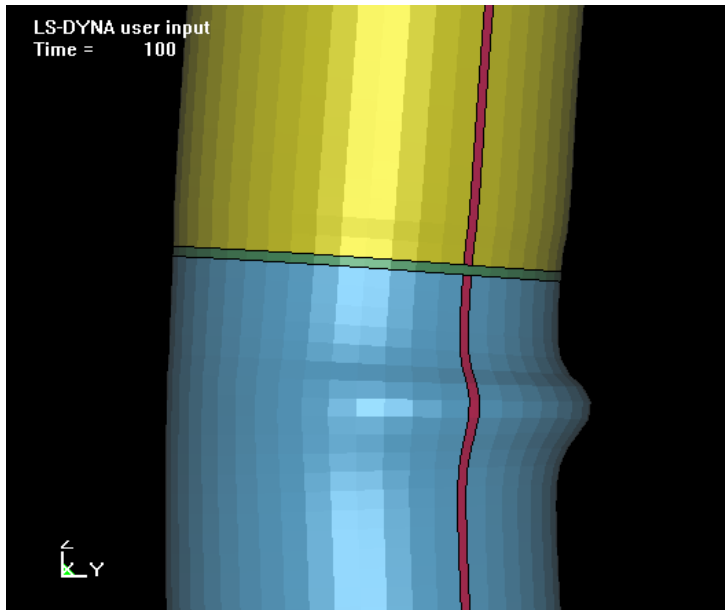
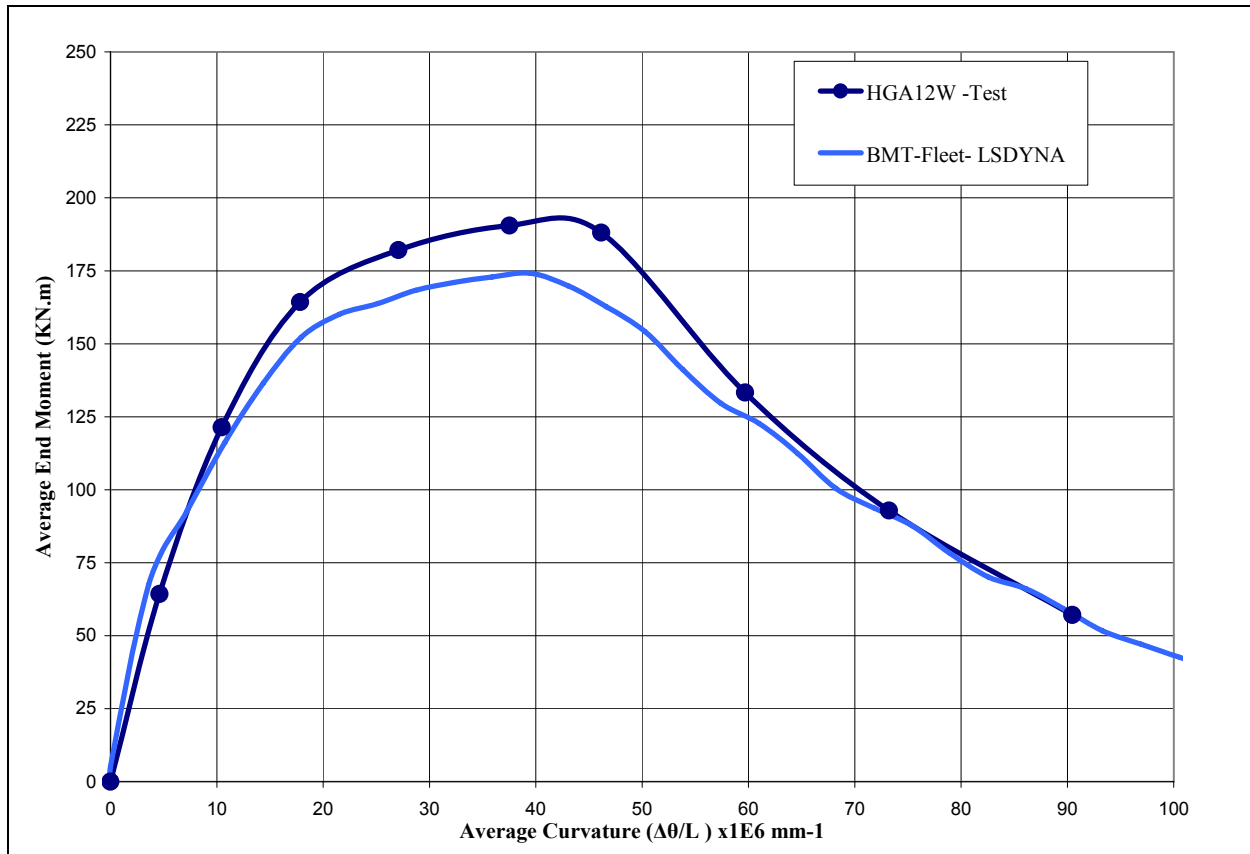


Figure D.8: Comparison of Predicted and Observed Wrinkle Geometry – (DGA12W)

The moment-curvature results for the half pressurized pipe (HGA12W) are presented in Figure D.9. As with the fully pressurized results, although the results do not correlate as well as for the un-pressurized specimens, the results are considered reasonable.



**Figure D.9: Moment vs. Curvature - Half Pressurized Pipe (HGA12W)**

### D.3 DISCUSSION OF VALIDATION RESULTS

As illustrated in the previous section, the results of the BMT FTL LS-DYNA model agrees well with both the experimental results [D.5] and the calibrated ABAQUS model [D.6], in terms of both the global moment versus curvature behavior and the global wrinkle geometry.

The BMT FTL results have been generated using generic material stress-strain curves that were created based on the minimum specified material properties (SMYS and UTS). Better agreement between the experimental results and the BMT FTL model could possibly be achieved with the use of more accurate material properties based on tensile test data. In addition, the wrinkles/buckles formed in the experimental specimens generally will form at some imperfection in the specimen. The BMT FTL model assumes a minor initial imperfection in order to initiate the wrinkle/buckle. A more accurate description of the experimental specimen geometry, particularly any imperfections which may initiate a wrinkle or buckle will also result in improved predictions.

As mentioned previously, the currently available experimental data is limited to the general global moment-curvature behavior, and the global wrinkle deformation behavior. Ideally, more detailed experimental results, including deformed shape measurements and measured strains in the wrinkle/buckle, would allow for a more detailed validation of the BMT FTL model. Should more detailed experimental results be made available, further validation and refinement of the BMT FTL model will be carried out at that time.

General sensitivity studies have been conducted in order to understand the affect variations in the model inputs have on the results of the finite element model. The studies provide an indication as to how sensitive the model results (i.e., wrinkle amplitude and wavelength, peak strain, moment-curvature response) are to the modeling inputs such as the mesh size, the assumed imperfection and the shape of the stress-strain curve. The sensitivity studies indicate that, although the wrinkle dimensions and the detailed stress and strain distribution within the wrinkle can be sensitive to some inputs, the general behavior (e.g., moment-curvature, general shape, far field stress-strain distribution) are not sensitive to small variations in the model inputs. As will be discussed further in the report, the wrinkle/weld interaction criteria developed using the finite element model is concerned primarily with the stress and strains some distance away from the wrinkle, and thus is not considered to be affected greatly by possible variations in input parameters.

## **D.4 DEMONSTRATION OF FINITE ELEMENT MODEL**

### **D.4.1 Strength Capacity of Pipes Subjected to Combined Loads**

The following section presents a demonstration of the use of the BMT FTL LS-DYNA finite element model, in which the model is used to predict the strength capacity of pressurized pipes. Included in the demonstration is an investigation into the effects of pipe geometry and material properties on the strength capacity of pressurized pipes. A further validation of the BMT FTL model is carried out by comparing the results of the finite element analyses with the bending moment capacity predicted based on the relationship discussed in Section 5.1.1.

#### D.4.2 Effect of Pipe Geometry

In order to develop an understanding of the effects of pipe geometry on the moment capacity of pipes subjected to combined loads, the analysis considered a wide range of pipe diameters with varying D/t ratios. The pipe geometries included in the analysis are summarized in Table D.4. The X52 true stress- true strain curve presented in Figure D.3 are used for all the pipe geometries considered.

**Table D.4: Summary of Pipe Geometries**

OD		Wall thickness		D/t	$\sigma_y$ (MPa (ksi))
(inch)	(mm)	(inch)	(mm)		
20	508	0.281	7.14	71	358 (52)
20	508	0.375	9.53	53	358 (52)
20	508	0.281	7.14	71	482 (70)
20	508	0.375	9.53	53	482 (70)
30	762	0.281	7.14	107	358 (52)
30	762	0.375	9.53	80	358 (52)
30	762	0.281	7.14	107	482 (70)
30	762	0.375	9.53	80	482 (70)
42	1066.8	0.281	7.14	149	358 (52)
42	1066.8	0.375	9.53	112	358 (52)
42	1066.8	0.281	7.14	149	482 (70)
42	1066.8	0.375	9.53	112	482 (70)

The effect of pipe geometry on the bending moment capacity of pipes is illustrated in the moment-curvature plots presented in Figures D.10 to D.12. The results illustrate that with decreasing D/t ratio, there is a corresponding increase in the peak moment capacity. Similarly, an increase in global curvature at the bifurcation point (indicating an increase the critical buckling strain) is evident with decreasing D/t ratio.

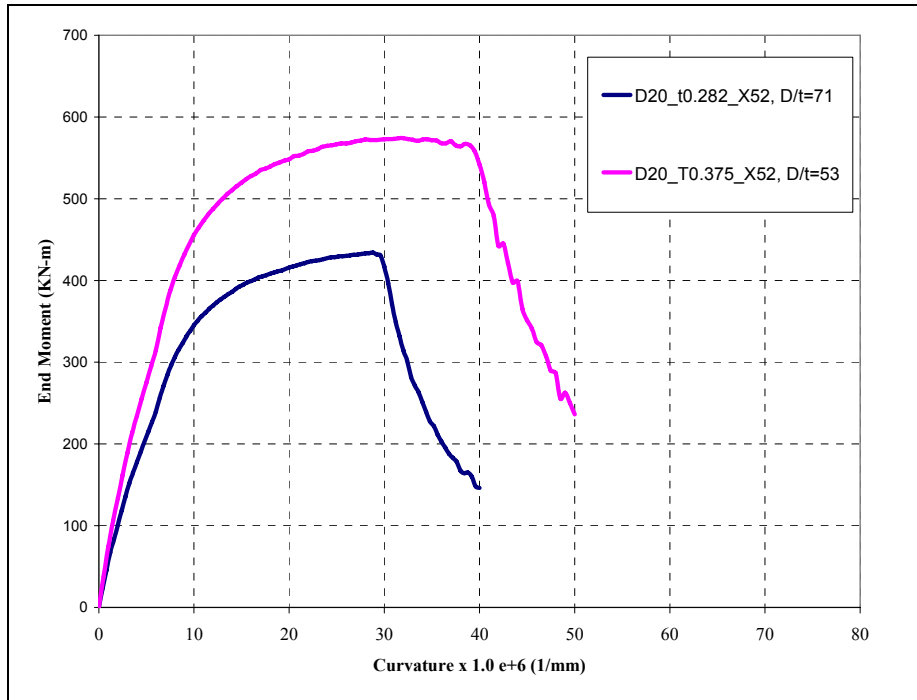


**Figure D.10: Moment - Curvature Response - X52 - D/t = 53 and 71**

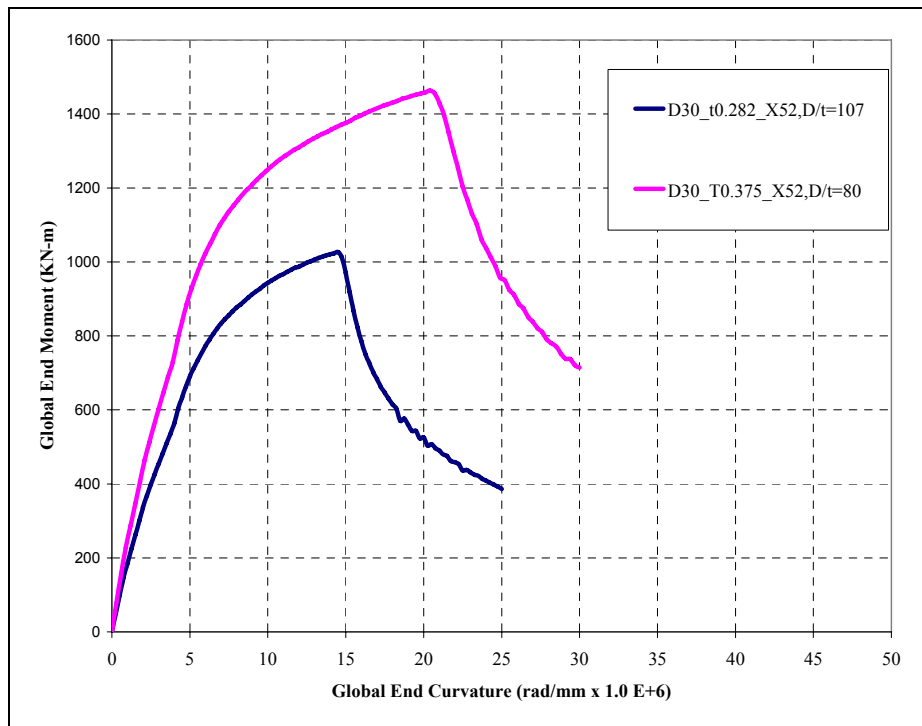


**Figure D.11: Moment - Curvature Response - X52 - D/t = 81 and 107**

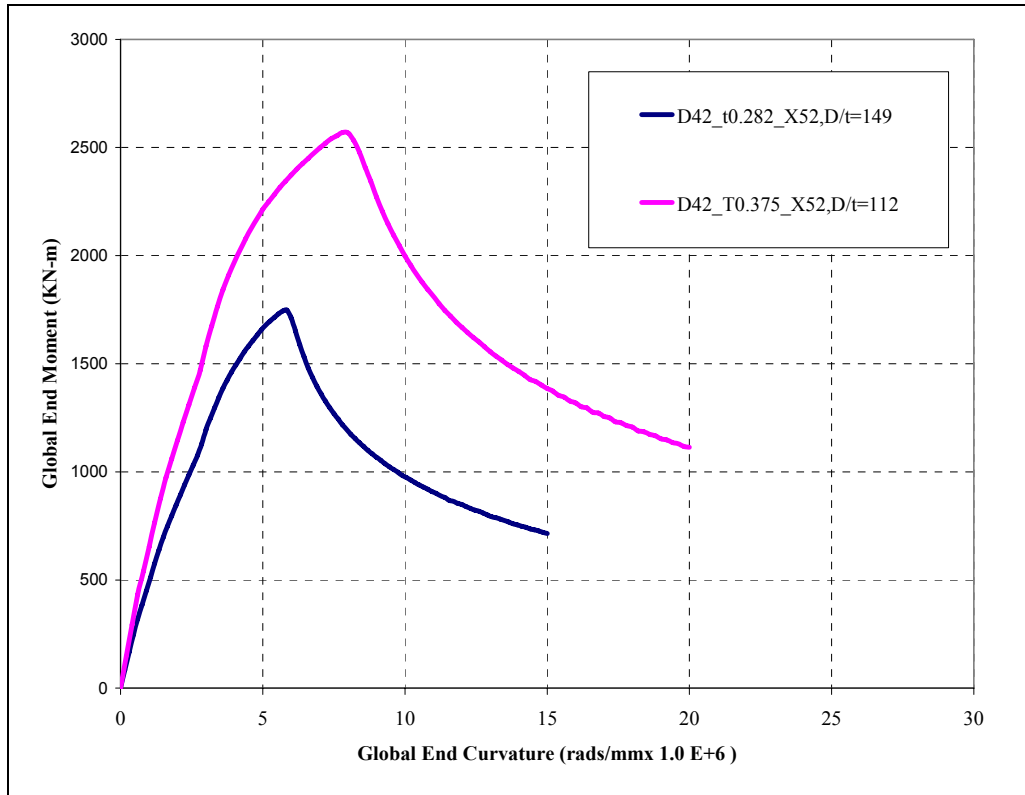
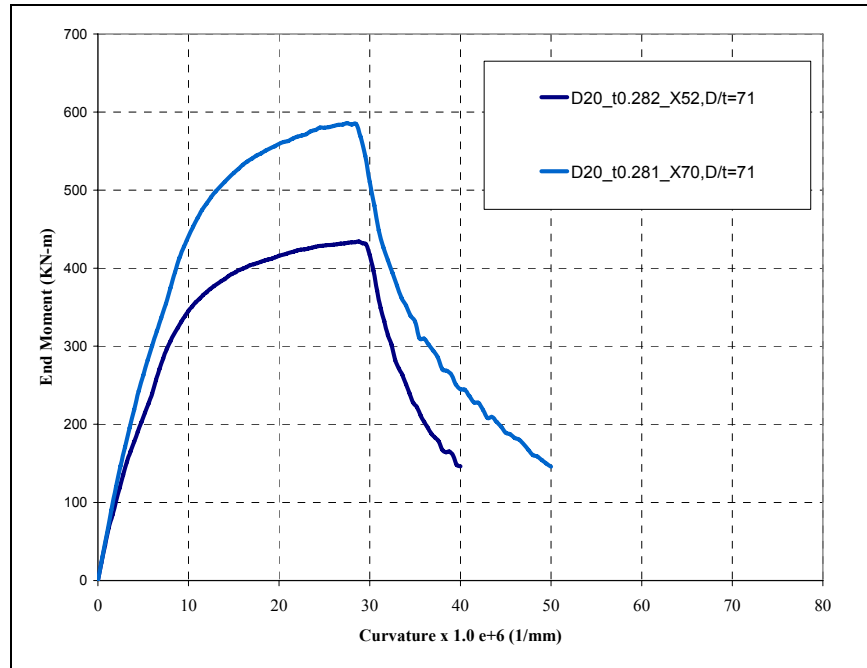


Figure D.12: Moment - Curvature Response - X52 - D/t = 112 and 149

### D.4.3 Effect of Pipe Material Properties

The effect of pipe material grade on the moment-curvature response is demonstrated using two different material grades, X52 and X70. The true stress – true strain curves for the two materials are illustrated in Figure D.3.

The results of the investigation are presented in Figures D.13 to D.15. The figures show the moment-curvature response for three values of D/t, 71, 107 and 112. The results indicate that with increasing material grade, there is a corresponding increase in peak moment capacity of the pipe. Conversely, with increasing material grade, there is a slight reduction in the global curvature at the bifurcation point indicating a reduction in the critical buckling strain.



**Figure D.13: Moment-Curvature Response – X52 and X70 - D/t=71**

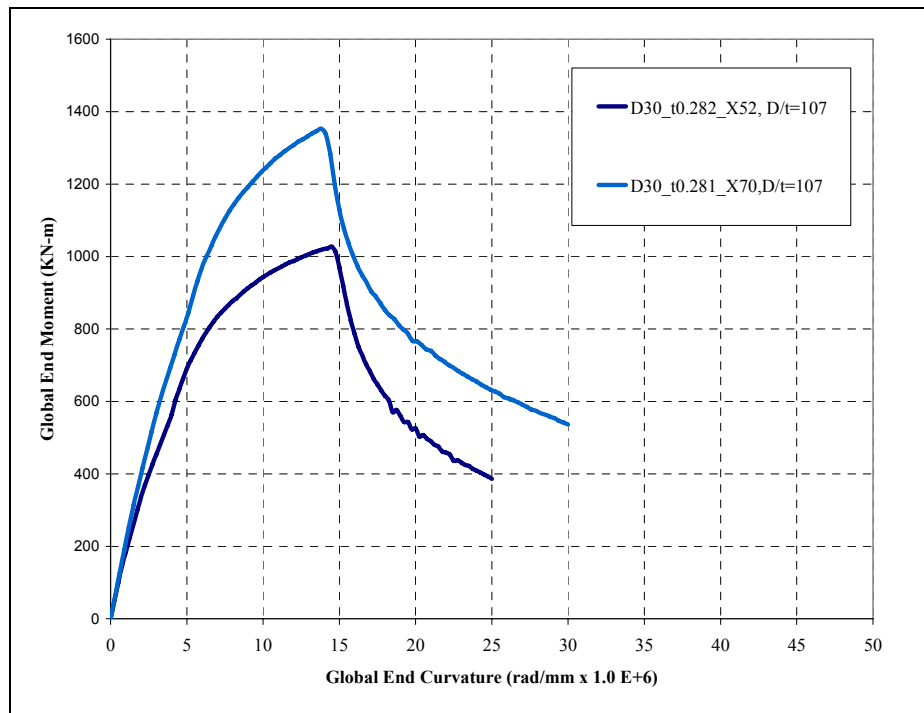


**Figure D.14: Moment-Curvature Response – X52 and X70 - D/t=107**

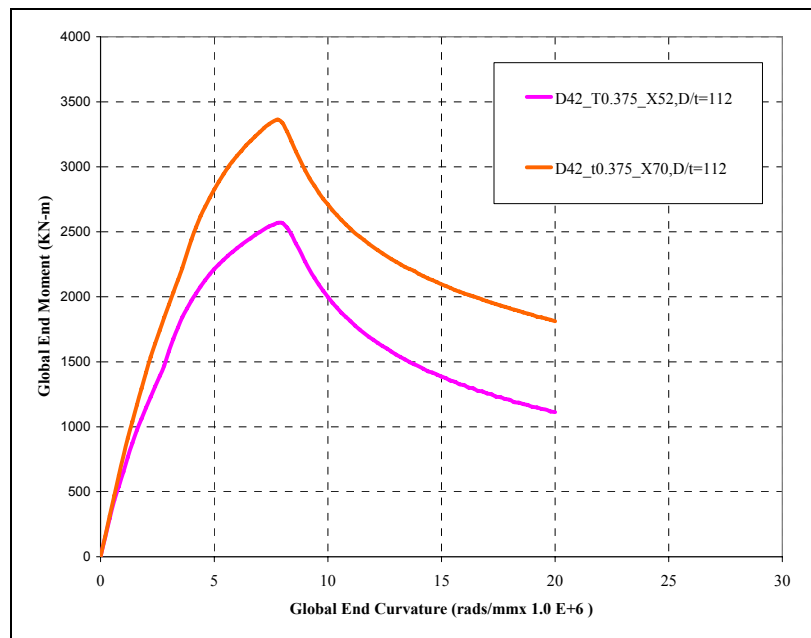


**Figure D.15: Moment-Curvature Response – X52 and X70 - D/t=112**

A comparison of the finite element model peak moment and the peak moment predicted using the analytical model described in Section 5.1.1 is presented in Table D.5. The agreement between the analytical expression and the FE prediction is very good for the entire range of geometries and material grades considered.

**Table D.5: Comparison - FE Predictions and Analytical – Peak Moment Capacity**

OD		Wall thickness		D/t	Mat.	$\sigma_y$ (MPa)	FEM Peak Moment (kN-m)	Analytical Peak Moment (kN-m)	FEM-to Analytical Ratio
(inch)	(mm)	(inch)	(mm)						
20	508	0.281	7.14	71	X52	358	434.3	442.0	0.98
20	508	0.375	9.53	53	X52	358	574.2	592.0	0.97
20	508	0.281	7.14	71	X70	482	585.8	575.9	1.02
20	508	0.375	9.53	53	X70	482	779.8	761.2	1.02
30	762	0.281	7.14	107	X52	358	1026.7	1020.1	1.01
30	762	0.375	9.53	80	X52	358	1463.0	1350.0	1.08
30	762	0.281	7.14	107	X70	482	1352.4	1308.8	1.03
30	762	0.375	9.53	80	X70	482	1930.9	1733.5	1.11
42	1067	0.281	7.14	149	X52	358	1747.6	2007.0	0.87
42	1067	0.375	9.53	112	X52	358	2569.6	2667.0	0.96
42	1067	0.281	7.14	149	X70	482	2304.8	2578.0	0.89
42	1067	0.375	9.53	112	X70	482	3362.6	3262.0	1.03

## D.5 REFERENCES

- D.1 Bruschi, R., Monti, P., Bolzoni, G. & R. Tagliaferri, "Finite Element Methods as Numerical Laboratory for Analysing Pipeline Response under Internal Pressure, Axial Load, Bending", Proceedings of OMAE'95.
- D.2 Batterman S.C., 'Plastic Buckling of Axially Compressed Cylindrical Shells," AIAA Journal, Vol3., N02, Jan 1965.
- D.3 Ramberg-Osgood 1943.
- D.4 Hauch, S., & Y. Bai, "Use of finite Element analysis for local Buckling design of Pipelines" OMAE'99.
- D.5 Yoosef-Gjhosdi, N., Kulak, G.L., and Murray, D.W. (1995). Some Test Results for Wrinkling of Girth-Welded Line Pipe. Proc. Of the 14<sup>th</sup> Inter.. Con. On OMAE, Vol. V- Pipeline Technology, ASME, Copenhagen, pp. 379-388.
- D.6 Souza, L.T, and Murray, D.W., 1996. "Analysis for Wrinkling Behaviour of Girth-Welded Line Pipe", International Pipeline Conference, Vol. 2, American Society of Mechanical Engineers, Calgary, Alberta. June. PP.835-844.



**APPENDIX E**  
**PIPE SOIL INTERACTION**

## **E.1 INTRODUCTION**

Wrinkle, dent and ovalization interaction criteria developed in the main body of this report describe the behavior of the damaged pipe segments in air subjected to combined pressure fluctuations and external loading. It is noted that the soil surrounding an ovalized, dented, wrinkled or wrinkle-bend pipeline segment can affect the in-service response of the pipeline segment. The conclusions developed in this project related to mechanical damage interaction with welds conservatively neglected the restraint offered by the soil in assessing the response of damaged pipe segments in air.

This task was proposed to demonstrate, in a preliminary fashion, the potential effects of neglecting soil restraint in considering the behavior of damaged pipeline segments and how this effect may be considered in future. This demonstration task compared the response of the pipeline with and without soil restraint for three soil types. This investigation was not expected to result in a comprehensive understanding of the effect of soil restraint; however, it was intended to provide a reasonable bound on the potential effects of soil restraint for consideration in either damage assessment or in the direction of future research.

The sample applications used in this task focus on the assessment of wrinkled pipe segments confined in soils and air that provide different levels of pipe restraint to demonstrate the differences in pipe behavior that could develop with the consideration of soil restraint.

## **E.2 FINITE ELEMENT MODELING**

In order to develop a complete finite element prediction of pipe soil interaction and wrinkle formation behavior in pipelines, the following issues must be considered:

- the constitutive law of the soil material,
- the constitutive law of the pipe material,
- the form and sequence of the pipe and soil loading,
- the ability to address large deformation, large rotation and finite strains in the model,
- The ability of the model to account for the nonlinear behavior of soil materials and the relative slip separation at pipe/soil interface, and
- the ability of the model to describe all relevant failure modes.

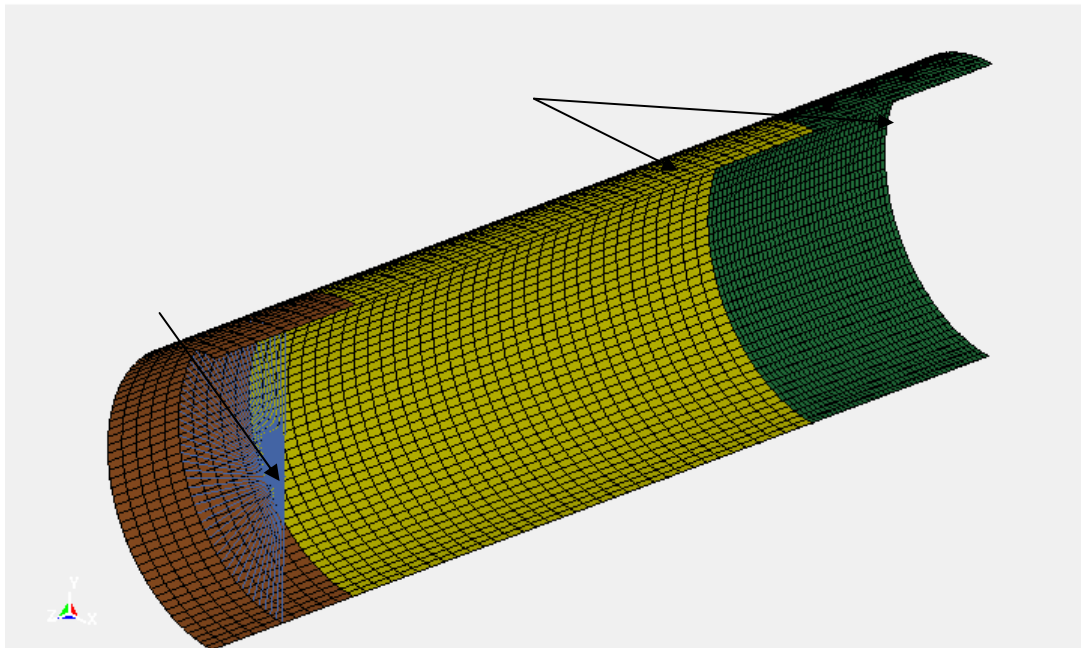
The following sections discuss each of these aspects of the pipe-soil interaction process and how they apply in the wrinkle formation and loading simulation in detail.

### E.3 FINITE ELEMENT MODEL DETAILS

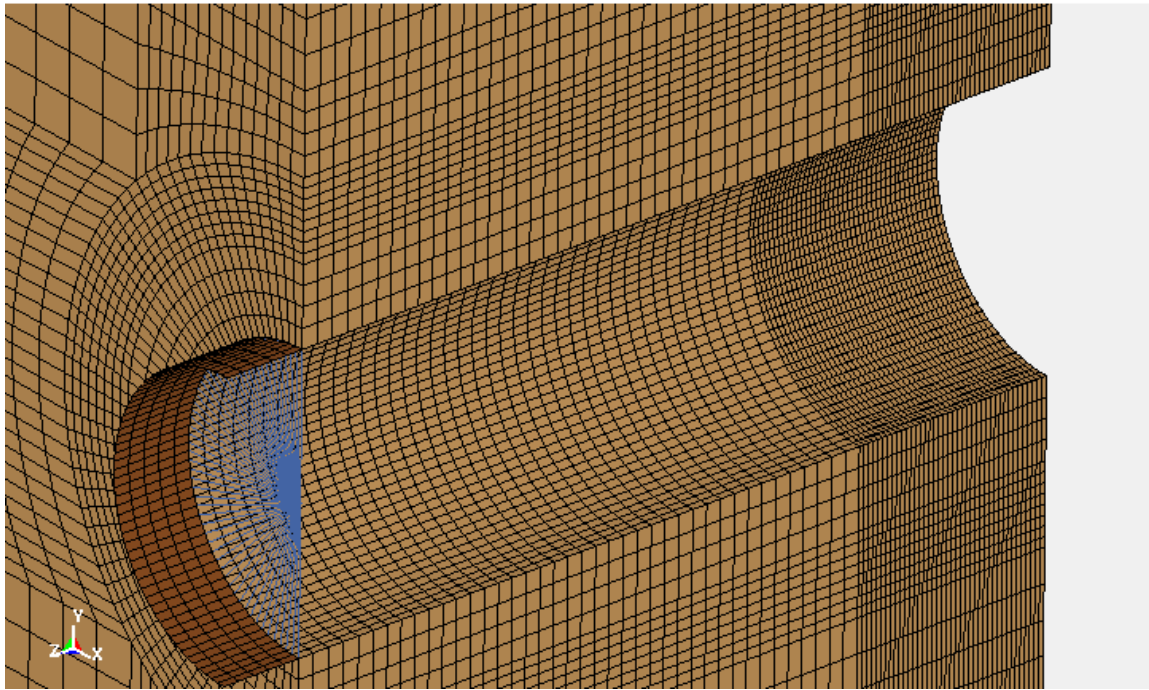
To better understand the local implications of the pipe soil interaction sample models were developed to illustrate the simulation process. The model that was developed and used in this task was an LS Dyna shell element finite element model considering the restraint of the surrounding soil. A cross-section of the shell pipe model used in developing the wrinkle formation is presented in Figure E.1. Due to the symmetry only quarter of the pipe was modeled, the half length of the model is 2000 mm, the model uses 12.5 mm, 4 noded, reduced integration shell elements. The shell model account for finite membrane strains and allow for changes in shell thickness, making it suitable for large strain analysis.

The end of the pipe is modeled using a “spider” of rigid beams elements between a node at the axial center line of the pipe and the nodes around the pipe circumference. The central node and rigid beams are used eventually to distribute the applied loads to the pipe ends. In order to limit local buckling and excessive plasticity at the ends of the pipe the last row of elements at the end of pipe is modeled using linear elastic material properties. The outer diameter of the pipe used in the sample applications is 711 mm (28 in), the wall thickness is 9.4 mm and the pipe diameter over wall thickness ratio is 72.

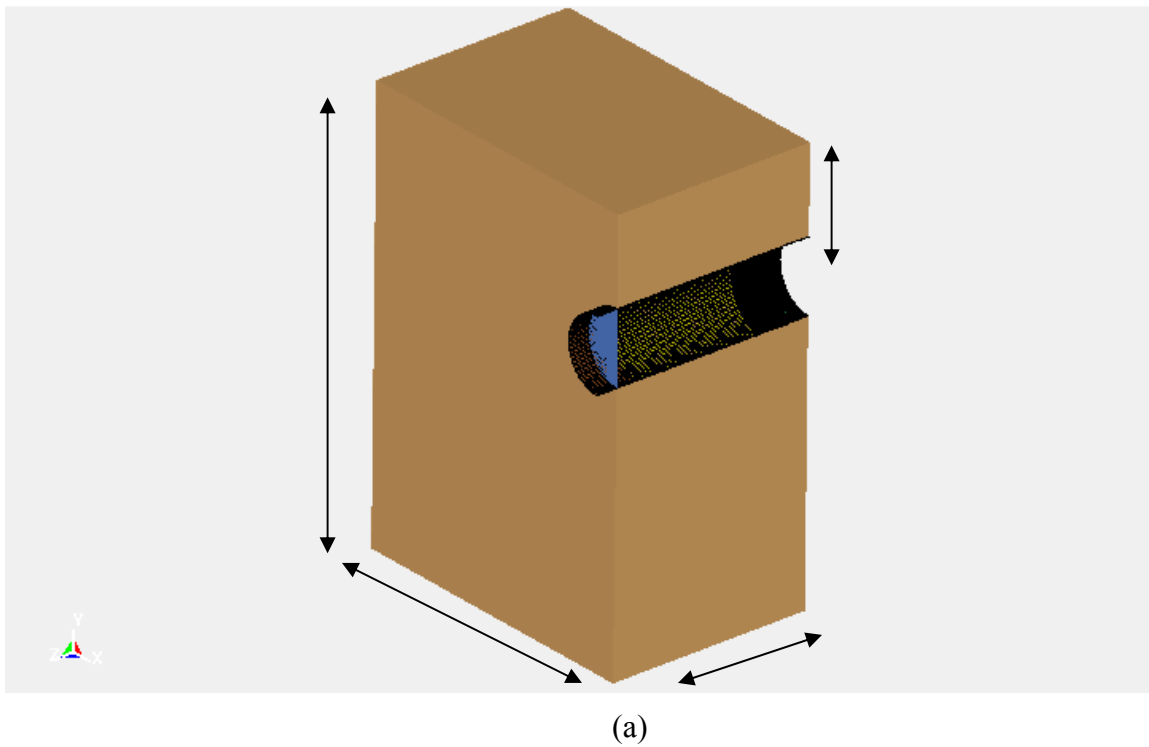
A finite element model using fully 3D continuum representation of the soil and accounting for the nonlinear behavior of the soil materials is shown in Figure E.2. The dimensions of the model are presented in Figure E.3 (a) and the boundary conditions are presented in Figure E.3 (b).

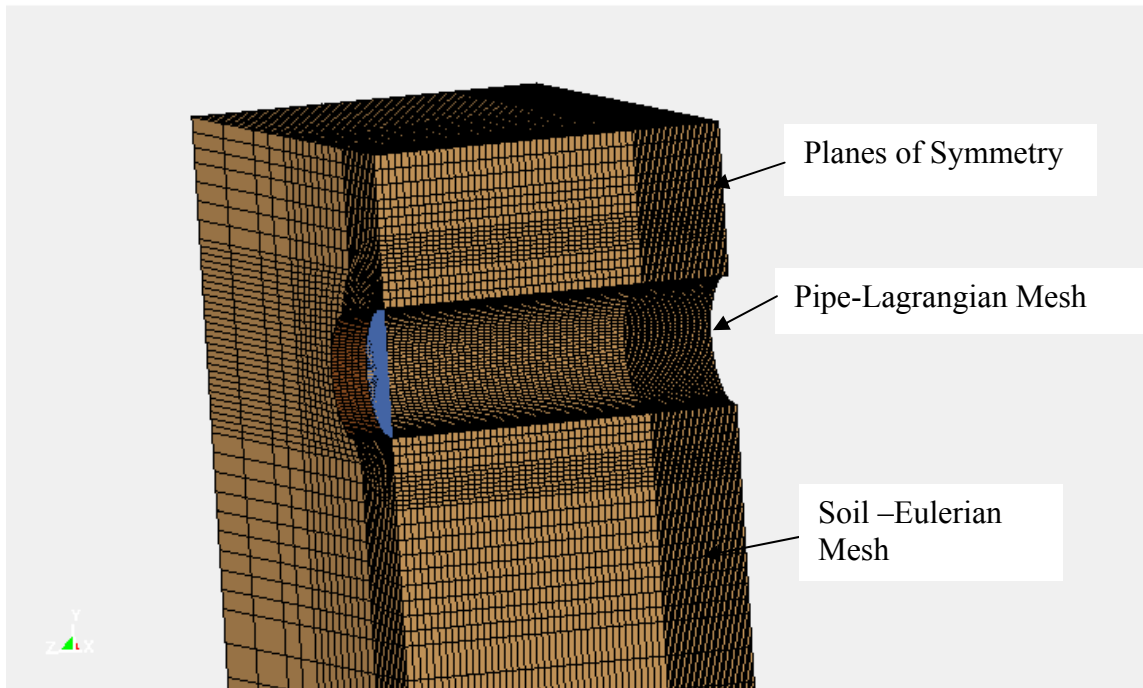


**Figure E.1 A Quarter Symmetry Finite Element Model- Pipe Meshing**



**Figure E.1 LS-DYNA Finite Element Model: Soil and Pipe Meshing**





(b)

**Figure E.2 Finite Element Model: Boundary Condition**

### E.3.1 ALE Pipe Soil Interaction Model

Soil pipe interaction modeling requires a numerical modeling software with large deformation capabilities; this requirement is difficult to meet for Lagrangian-based codes. LS-DYNA offers the possibility of using the Eulerian capabilities for modeling materials that undergo large deformations. The multi-material Eulerian formulation is an approach that allows multiple materials to exist within each solid element and let the material flow from one element to another. The Lagrangian coupling allows structural element to be placed within the Eulerian mesh. Interaction between the Eulerian elements (i.e., fluid, soil) and structural elements Lagrangian (i.e., pipe) is handled by contact algorithms.

The work presented on this section has focused on the use of the existing LS-DYNA wrinkle model as a baseline and concerned with investigating both soil constitutive model and the use of the LS-DYNA multi-material Eulerian technique.

### E.3.2 Pipe and Soil Material

Soil materials can have pronounced non-linear behaviors and correct numerical simulation of their load-deformation behavior requires sophisticated constitutive models. In this study, two constitutive models available within the LS-DYNA framework were used:

- Soil-and Foam Model, and
- Cap Model.

### E.3.2.1 Soil and Foam Model

One of the classical geomaterial models is that attributed to Drucker and Prager (1952) and has the stress invariant for

$$\sqrt{J_2} = \alpha J_1 + k = 3\alpha P + k$$

In which  $\alpha$  and  $k$  are material constants related to frictional and cohesion of the material, respectively.

The Soil and Foam Model is the most basic of the geomaterial models available in LS-DYNA. It is also the oldest and therefore has had a considerable amount of user experience, and feedback and is thus quite robust [1]. The Soil and Foam model has a mean stress (pressure) dependent strength, typical geomaterials, of the form:

$$J_2 = a_0 + a_1 P + a_2 P^2$$

Where  $p$  is the mean stress and coefficients,  $a_0$ ,  $a_1$ , and  $a_2$ , are determined by calibrating (fitting) the model to tri-axial compression data.

The Soil and Foam Model will be identical to the Drucker-Prager Model with the following parameters:

$$a_2 = 9\alpha^2$$

$$a_1 = 6\alpha k$$

$$a_0 = k^2$$

The Soil and Foam Model request the volume strains be in form of the natural log of the relative volume, which is negative in compression. The other input parameters required for the Soil and Foam Model are:

- Elastic Shear Modulus,  $G$
- Bulk Unloading Modulus,  $K$
- Pressure Cutoff for Tensile Failure

### E.3.2.2 Cap Model

A challenging problem in computational geomechanics is the development of constitutive stress-strain models for soil that provide adequate physical representation of the observed mechanical behaviors. Elasto-plastic soils models are a class of materials model that can account for hardening and softening behavior of soil materials. A series of the limitations of the published finite element software mainly related to a constitutive modeling have been identified. A commonly used model is an inviscid, two-invariant geologic Cap Model. In general, a Cap Model falls within the framework of the classical incremental theory of plasticity and is based on a loading function which serves as both a yield surface and plastic potential. The name cap model derives from the shape of the elliptical yield surface which looks like “caps”. The loading function for the Cap Model shown in Figure E.4 consists of two envelopes, fixed and moving yield surfaces.

### E.3.2.2.1 Fixed Yield Surface

The fixed yield surface, which can be considered to be an ultimate yield surface, is expressed as:

$$f_1(J_1, \sqrt{J_{2D}}) = 0$$

In the initial Cap Model, DiMaggio and Sandler, the fixed surface was assumed to be composed of an initial portion of the Drucker-Prager envelope joined smoothly to the subsequent von Mises surface (Figure 8.4), [2].

The expression of  $f_1$  adopted By DiMaggio and Sandler is given by

$$f_1 = \sqrt{J_{2D}} + \gamma e^{-\beta J_1} - \alpha = 0$$

Where  $\alpha$ ,  $\beta$  and  $\gamma$  are material parameters.

The Simo et al. model implemented in LS-DYNA, referred to now as the Geological Cap Mode, uses a similar form with additional term

$$f_1 = \sqrt{J_{2D}} + \gamma e^{-\beta J_1} - \alpha - \theta J_1 = 0$$

The additional term,  $\theta J_1$ , is convenient for fitting shear failure data that has a fairly linear representation in stress space, recall Drucker-Prager Model form

$$\sqrt{J_{2D}} = \alpha J_1 + k$$

### E.3.2.2.2 Yield Caps

The yield surfaces are expressed as:

$$f_c(J_1, \sqrt{J_{2D}}, k) = 0$$

Where  $k$  defines the deformation history, and usually taken as the volumetric plastic strain.

DiMaggio and Sandler adopted an elliptical cap for representing yield surfaces

$$f_c = R^2 J_{2D} + (J_1 - C)^2 = R^2 b^2$$

Where  $Rb = (X - C)$ ,  $R$  provides the shape (ellipticity) of the cap surface,  $X$  is the value of  $J_1$  at the intersection of the cap with  $J_1$ -axis,  $C$  the value of  $J_1$  at the center of the ellipse, and  $b$  is the value of  $\sqrt{J_{2D}}$  when  $J_1 = C$ . The value of  $X$ , which is the hardening parameters, depends on the plastic volumetric strain  $\varepsilon_v^p$ .

$$X = -\frac{1}{D} \text{Ln} \left( 1 - \frac{\varepsilon_v^p}{W} \right) + Z$$

Where  $D$ ,  $Z$ , and  $W$  are material parameters

The movement of the cap is controlled by the increase or decreases in the volumetric strain through the hardening parameter  $X$ : thus the dilation/compaction properties of soils may be represented.

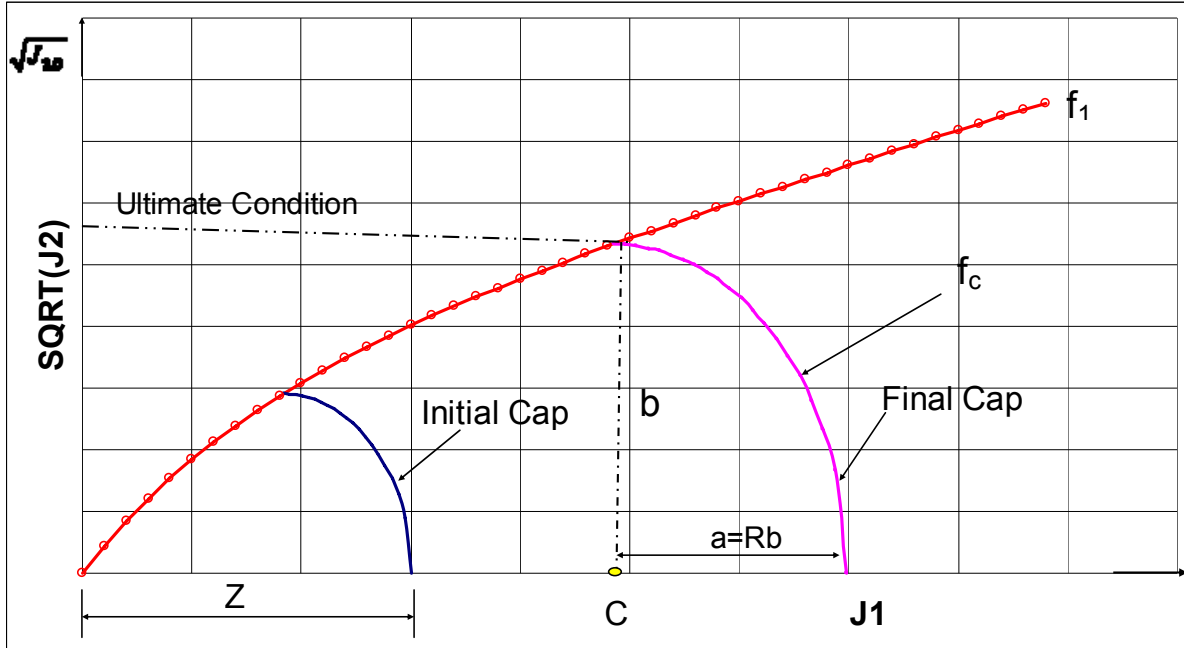


**Figure E.3: Yield Surface for Cap Model**

#### E.3.2.2.3 Cap Model Example

The behavior of conventional triaxial specimen is analyzed using the cap model. The following soil parameters, reported in [2] were used:

- $\alpha = 5.6 \text{ psi (38.58 kPa)}$
- $\gamma = \text{psi (38.58 kPa)}$
- $\theta = 0.11$
- $\beta = 0.062 \text{ (psi)}^{-1} [0.009 \text{ (kPa)}^{-1}]$
- $R = 2$
- $D = 0.05 \text{ (psi)}^{-1} [0.00725 \text{ (kPa)}^{-1}]$
- $W = 0.18$
- $G = 1480 \text{ (psi) [10.2 MPa]}$
- $P_0 = 10 \text{ psi [68.90 MPa]}$

During loading the cap surface expands until an ultimate state is reached, Figure E.4. Figure E.5 illustrates the soil behavior under cycling loading; the sample was loaded, unloaded and reloaded along the path OABACDCEFEFGHGI.

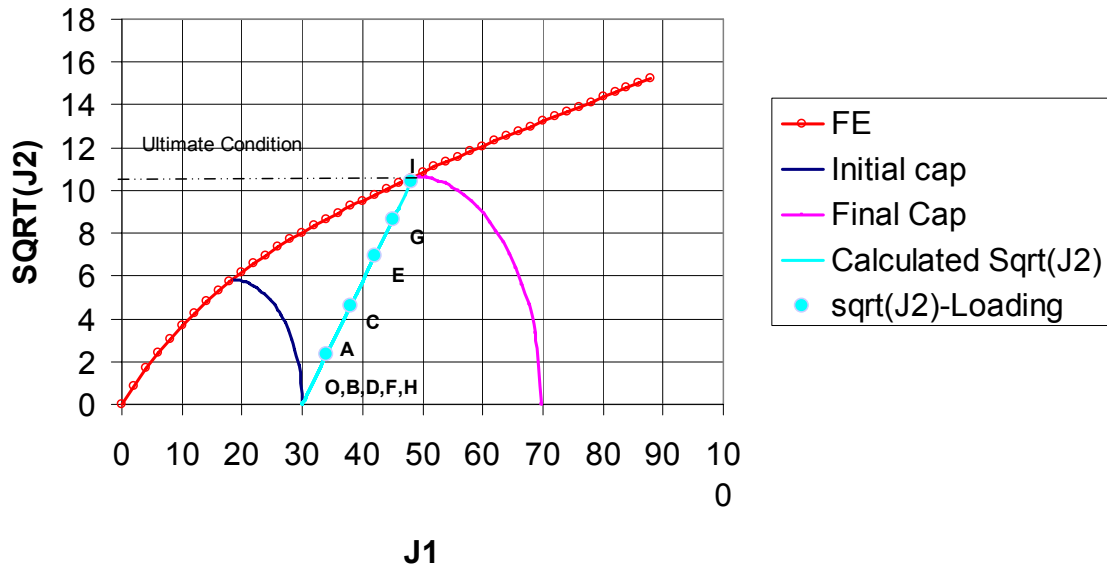


Figure E.4: Generalized Behavior of Soil using the Cap Model

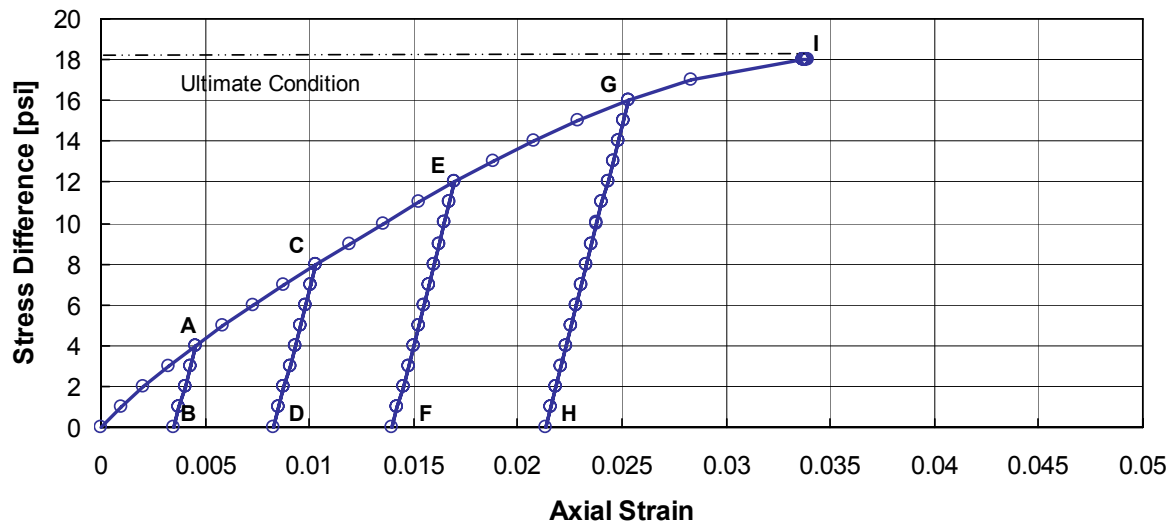


Figure E.5: Triaxial Test Behavior from Cap Model

## E.4 NUMERICAL MODEL MATRIX

The FE model matrix was comprised of four runs and designed to compare the pipe behavior loaded in air and in soil. The matrix is summarized in Table E.1

**Table E.1: Numerical Model Matrix:**

Model	Soil Constitutive Model	Soil Constitutive Model Parameters	
In air	-	-	-
Soil1	Soil and Foam Model	$J_2 = a_0 + a_1P + a_2P^2$	<ul style="list-style-type: none"> <li>• <math>a_0=0</math></li> <li>• <math>a_1=0</math></li> <li>• <math>a_2=0.602</math></li> <li>• <math>G=34.5</math> MPa</li> <li>• <math>K=20.9</math> MPa</li> <li>• Density= 1890 Kg/m<sup>3</sup></li> </ul>
Soil2	Soil and Foam Model	$J_2 = a_0 + a_1P + a_2P^2$	<ul style="list-style-type: none"> <li>• <math>a_0=0</math></li> <li>• <math>a_1=0</math></li> <li>• <math>a_2=0.602</math></li> <li>• <math>G=12.5</math> MPa</li> <li>• <math>K=20.9</math> MPa</li> <li>• Density= 1890 Kg/m<sup>3</sup></li> </ul>
Soil3	Cap Model	$f_1 = \sqrt{J_{2D}} + \gamma e^{-\beta J_1} - \alpha - \theta J_1 = 0$ $f_c = R^2 J_{2D} + (J_1 - C)^2 = R^2 b^2$ $X = -\frac{1}{D} \text{Ln} \left( 1 - \frac{\varepsilon_v^p}{W} \right) + Z$	<ul style="list-style-type: none"> <li>• <math>\alpha= 500</math> Pa</li> <li>• <math>\gamma= 0</math> Pa</li> <li>• <math>\theta=0.2</math></li> <li>• <math>\beta=0.0</math> (pa)<sup>-1</sup></li> <li>• <math>R=4</math></li> <li>• <math>D=1.26E-6</math> (pa)<sup>-1</sup>]</li> <li>• <math>W=0.06</math></li> <li>• <math>G=1</math> MPa</li> <li>• <math>K=10</math> MPa</li> <li>• Density =1400 Kg/m<sup>3</sup></li> </ul>

### E.4.1 Analyses Procedure

The applied loads and loading sequence used in the finite element model are based on the actual operational loads experienced by a pipeline in service, including:

- Operational pressure fluctuations;
- Seasonal temperature fluctuations; and
- Annual curvature (wrinkle growth) increases.

In the finite element model, the applied loading sequence includes five steps, which mimic the actual loading sequence experienced by pipelines in service. The five steps in the loading sequence are summarized below:

1. First a geostatic step is performed to establish the initial stress state in soil before pipe loading was developed by applying the gravity to the whole model.
2. Apply the internal operating pressure (MAOP) to the pipe, and apply the total axial load on the pipe wall (due internal pressure and thermal restraint) to the central node at the loaded end of the pipe.
3. Apply an in-plane rotation to the central node at the loaded end of the pipe in order to form the wrinkle.
4. Once the wrinkle has formed, the internal pressure reduced to 75% MOP.
5. Internal pressure reduced to 50% MOP

Load step one applies only for pipe loaded in soil and the loading steps 2, 3, 4, and 5 are similar for both pipe in air and pipe in soil.

The axial load experienced by a pipeline in operation is made up of a combination of thermal restraint effects and Poisson's effect.

Due to thermal expansion restraint, temperature changes in the pipeline results in axial loads in the pipeline, ( $F_{th}$ ), according to the following equation [14]:

$$F_{th} = - E \alpha \Delta T A_p$$

Where  $E$  is the modulus of elasticity,  $\alpha$  is the coefficient of thermal expansion,  $\Delta T$  is the temperature change and  $A_p$  is the pipe cross-sectional area.

For axially restrained pipes with an internal pressure, radial growth of the pipe will result in a longitudinal stress due to Poisson's effect. The pressurization induced axial load, ( $F_p$ ), is calculated using the following equation:

$$F_p = \frac{\nu P D A_p}{2t} = \nu \sigma_h A_p$$

Where  $\nu$  is Poisson's ratio,  $P$  is the internal pressure,  $D$  is the pipe diameter,  $t$  is the pipe wall thickness,  $A_p$  is the pipe cross-sectional area and  $\sigma_h$  is the hoop stress.

With regards to the total axial loads in pipelines, the behavior of buried pipe is generally bound by two idealizations. The first idealization assumes the pipe behaves as an open ended pipe where no longitudinal pressurization loads exist in the pipe wall (other than those due to Poisson's effect). In the second idealization, the longitudinal loads in the pipe wall account for the end-cap effects that may occur in the pipeline. The end-cap effects, (which may be caused by bends in the pipeline, valves etc), are included as an additional longitudinal load in the pipe wall.

For an ideal open ended pipe, the total longitudinal force on the pipe wall is a combination of the axial thermal load, and the axial load due to Poisson's effect, and is calculated using the following equation:

$$F = \left( \nu \frac{PD}{2t} - E \alpha \Delta T \right) A_p$$

For the purposes of the investigation, the thermal loads are based on a 40°C temperature change (between construction and operational temperature).

For the purposes of the finite element modeling, the pipeline operating pressure is assumed to be equal to the maximum allowable operating pressure (MAOP), where MAOP represents the internal pressure equivalent to a hoop stress that is 72% of the specified minimum yield stress (SMYS). MAOP is calculated using the following formula:

$$MAOP = 0.72 \left( \frac{2t}{SMYS \times D} \right)$$

## E.5 RESULTS

Load step 4 and 5 were used to determine the wrinkle interaction with the girth weld and long seam welds in the development of interaction criteria. These load steps are used here to illustrate the effect of the soil on the behavior of the wrinkled pipe segment considering pressure cycle combinations:

- 75% to 100% MOP
- 50% to 100% MOP

The general approach used to determine the wrinkle/long seam and girth weld interaction is similar to the approach used for the wrinkle/long seam and girth weld interaction for pipe loaded in air.

The wrinkle height and length of the wrinkled pipe at the end of post buckling analysis for analyzed cases are shown in Figure E.6. It can be observed that due to the external soil pressure the wrinkle amplitude (H) increase and the wrinkle length ( $L_w$ ) decrease for the pipe loaded in soil compare to the pipe loaded in air, the results are presented in Table E.2. This result illustrates the restraint offered by the soil that will concentrate wrinkle growth rather than letting the pipe ovalize more generally and the wrinkle form into a broader feature.

**Table E.2: Wrinkle –Girth Weld and Long Seam Interaction Distances**

Model	Amplitude	$L_w$	H/ $L_w$	Axial Position (mm)		Critical Half Angle (deg)	
	(mm)			100% to 75%	100% to 50%	100% to 75%	100% to 50%
In Air	57.73	215.60	0.268	294	306	137.5	138
Soil1	61.37	207.43	0.296	215	228	137.5	134.8
Soil2	61.49	207.13	0.297	228	228	137.5	135.6
Soil3	62.00	205.56	0.302	220	226	140.7	140.7

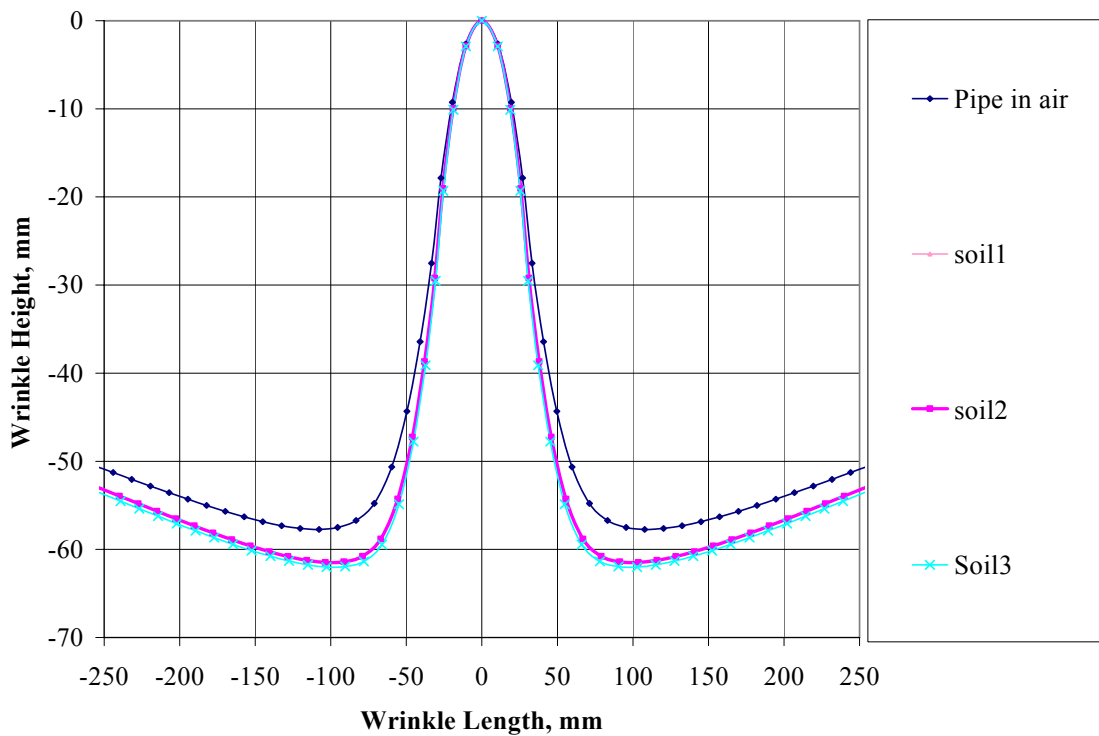


**Figure E.6: Wrinkle Height vs. Wrinkle Length**

The weld interaction criteria developed in this project focused only on the behavior of pipelines loaded in the air. Those studies indicate that the wrinkle shape aspect ratio ( $H/L_w$ ) play major roles in determining the normalized critical angle ( $\theta$ ) between a long seam weld and the wrinkle peak. The increasing  $H/L_w$  ratios result in increasing  $\theta$ , indicating a relationship between wrinkle shape,  $H/L_w$ , and wrinkle propagation around the circumference. More severe wrinkles form with higher aspect ratios - for higher  $H/L_w$ , the long seam weld must be further away from the wrinkle peak than for smaller  $H/L_w$ .

In the current study, for all analyzed cases the predicted normalized critical angle loaded in soil is relatively less than the one predicted for pipeline in air despite the increase of the wrinkle shape aspect ( $H/L_w$ ) for pipeline loaded in soil.

As demonstrated in the previous analyses, the wrinkle shape aspect ratio ( $H/L_w$ ) play major roles in determining the normalized critical distance ( $L/D$ ) between a girth weld seam and a wrinkle peak. The results indicate that the increase  $H/L_w$  ratios result in decreasing of  $L/D$ .

The predicted critical wrinkle –girth weld distance and the critical wrinkle-long seam weld angle for pipe loaded in air and in soil are listed in Table E.2

The deformed shapes of the pipe at the end of post buckling analyses for the pipe loaded in Soil1 and loaded in air are shown in Figures E.7 and E.8 respectively. For all cases analyzed the predicted, the local strains are higher for pipe in soil than the one predicted for pipeline in air; this is due to the external soil pressure. Figures E.9 to E.10 illustrate a sample of the deformed pipe in soil.

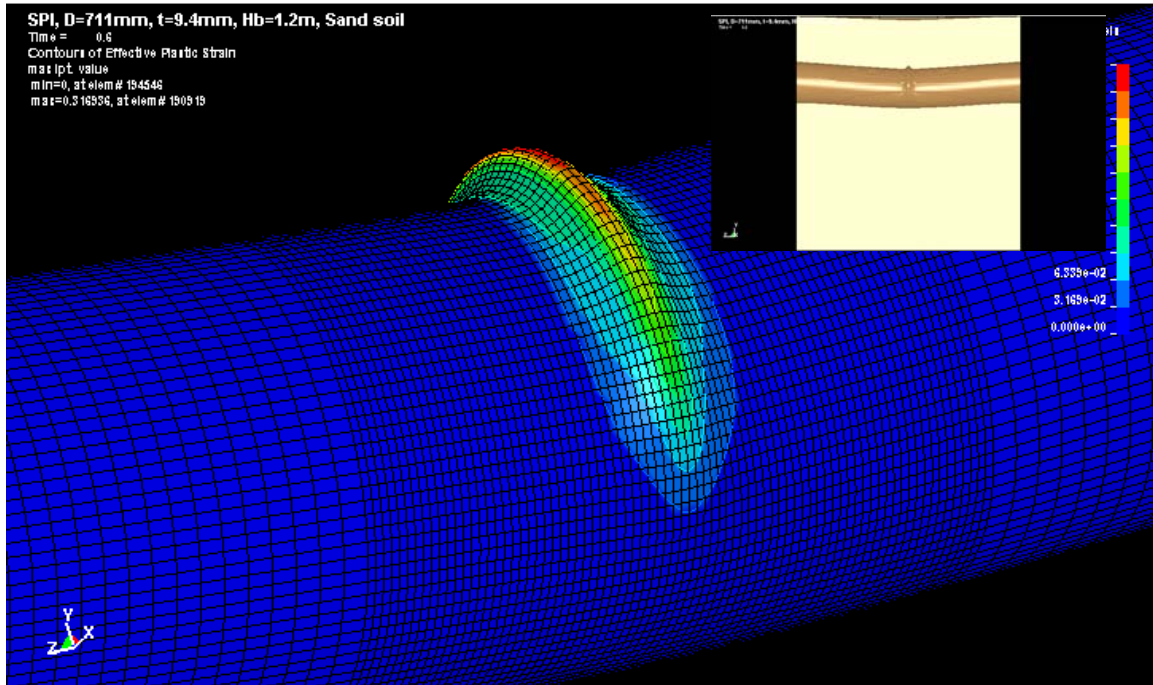


Figure E.7: Wrinkled Pipe Loaded in Soil (1)

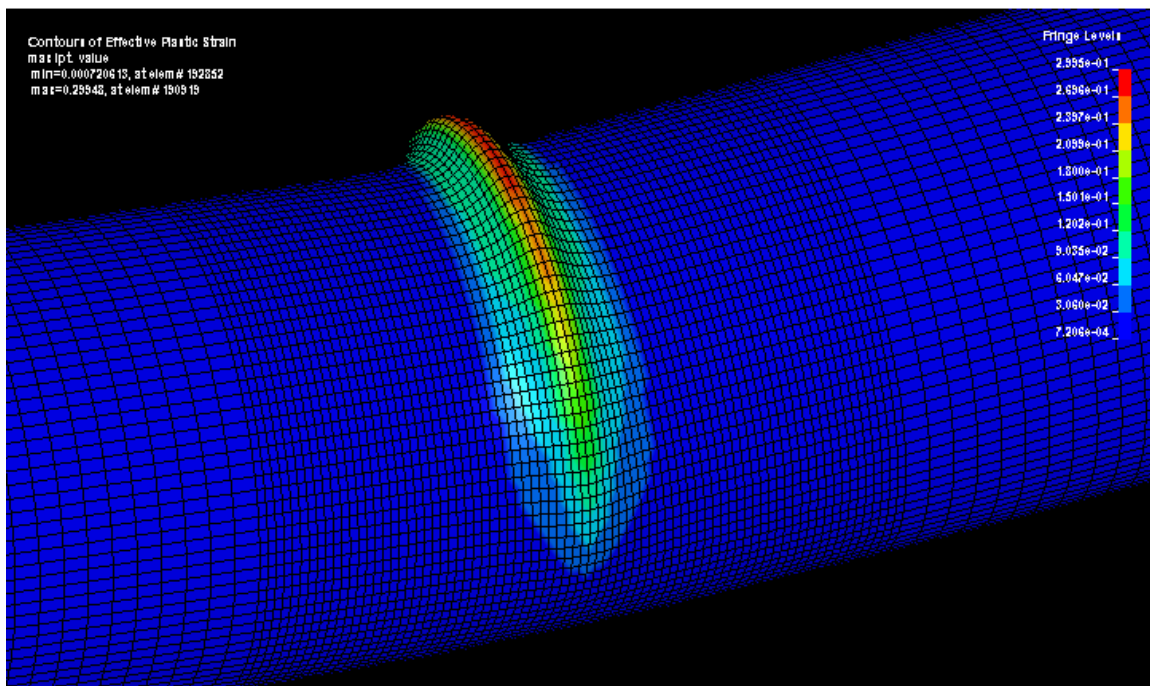


Figure E.8: Wrinkled Pipe in Air

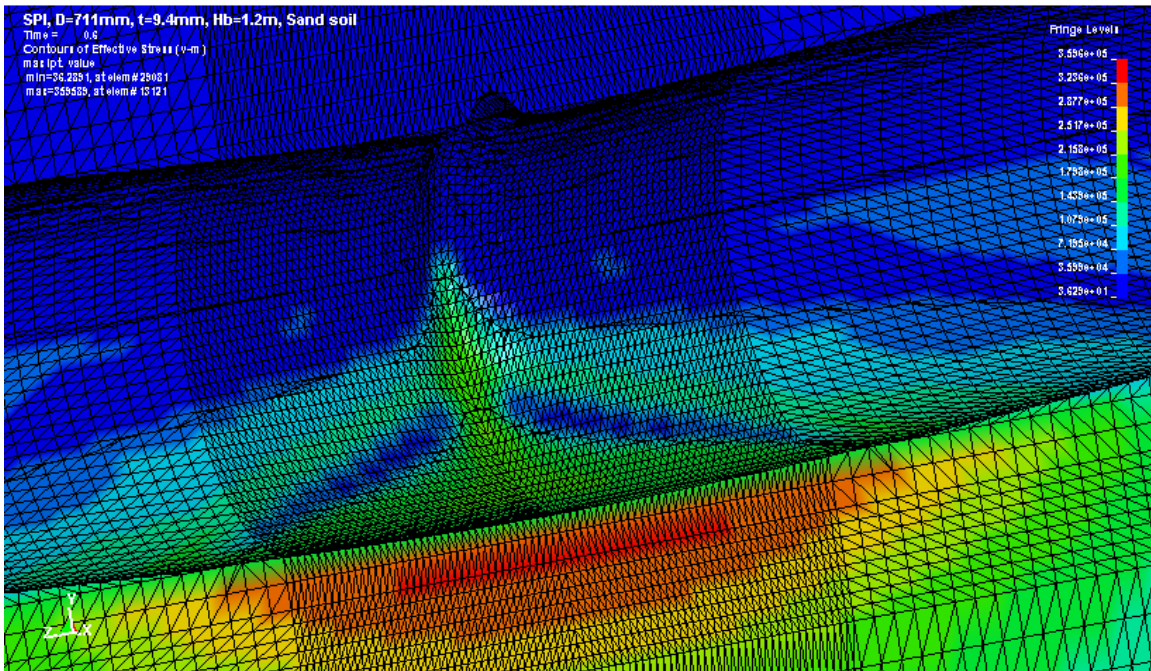


Figure E.9: Sample Soil Effective Stress Distribution

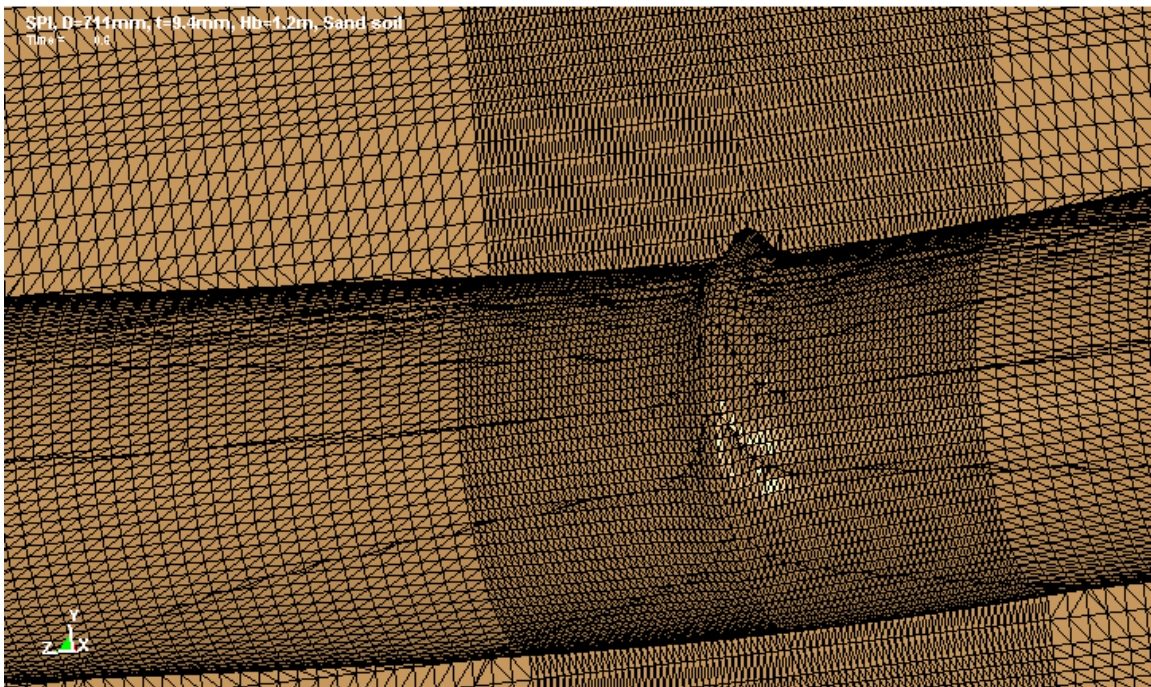


Figure E.10: Section through Soil Volume Illustrating the Wrinkled Pipe Print in the Soil

The effect of soil restraint on pipe behavior after wrinkle formation is also illustrated in Figure E.11. This figure illustrates the change in strain at the crest of the wrinkle due to two magnitudes of pressure fluctuation. The restraint offered by the soil is demonstrated by the differing behavior of the pipe in air as opposed to the behavior in the three soil types. These results also demonstrate the effect of wrinkle geometry on strain fluctuation since the wrinkle formed in any of the soils is larger (greater amplitude) than the wrinkle formed in air. For wrinkles of comparable size the strain fluctuations in air would be larger than those in soil.

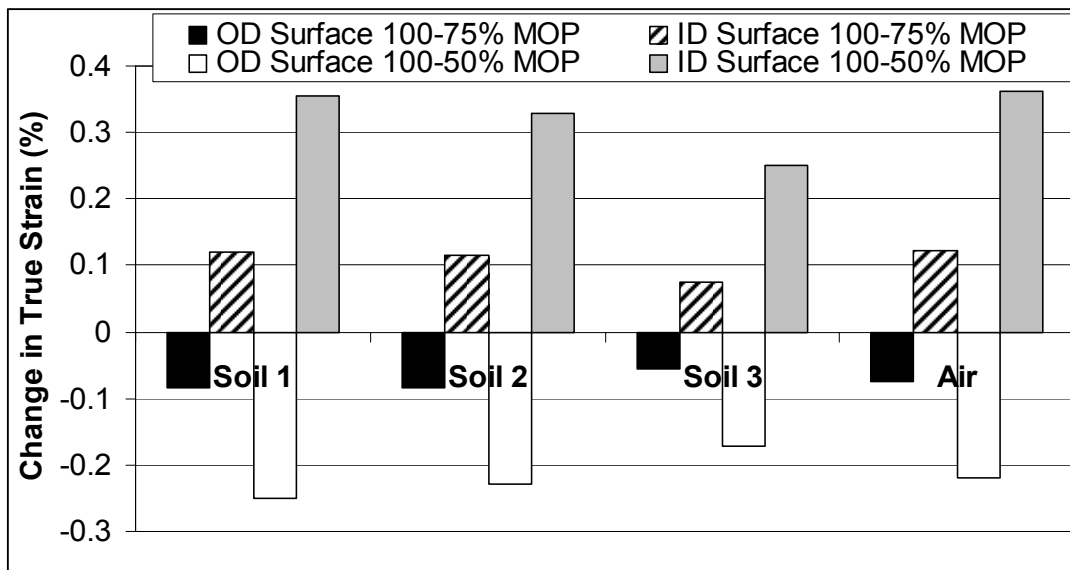


Figure E.11: Wrinkle Crest Change in Strain Due to Pipe Internal Pressure Fluctuations

### E.6 FURTHER WORK

The soil pipe interaction study developed on this section compare the response of the pipeline with and without soil restraint. It is noted that this study is comprised of one single pipe geometry and material, two soil types and one single type loading. This investigation is not expected to result in a comprehensive understanding of the effect of soil restraint; however, it will provide a reasonable bound on the potential effects of soil restraint for consideration in either damage assessment or in the direction of future research. Further work will be required to validate the procedures and investigate the effect of the following parameters:

- Effect of soil type and stiffness;
- Effect of pipe material behavior;
- Effect of Burial depth;
- Effect of the backfill Material;
- Effect of confining stress;
- Effect of the loading path;
- Effect of internal pressure and thermal load; and
- Effect of mesh refinement.

The soil restraint illustrated in these example applications demonstrated that the constraint offered by the soil can stabilize the pipe wall and thus:

- modify the shape of the wrinkle formed due to a given applied load or displacement, and
- reduce pipe wall stress fluctuations promoted by internal pressure changes.



**APPENDIX F**  
**APPLICATION OF THE DENT-WELD**  
**INTERACTION CRITERIA**

## F.1 RANGE OF APPLICABILITY OF DENT-WELD INTERACTION MODEL

The dent-weld interaction criteria presented in this document has been developed solely using finite element models based upon the modeling assumptions discussed in Appendix A and Section 3. It is subject to the following restrictions:

- Intended for plain restrained dents (i.e., rock dents on the bottom half of the pipe). Factors in addition to weld seams (i.e., corrosion related metal loss, gouges) have not been considered.
- Intended to compliment and not supersede criteria governing the acceptability of plain dents. For example, the strain based criteria in ASME B31.8 [F1] should first be used to determine that the strain level in the dent is acceptably low prior to evaluating the permissible dent-weld interaction distance.
- Intended to evaluate the long term performance of the dented pipe segment when subjected to normal operational pressure cycles. It should not be used for pipeline subjected to frequent and severe upset conditions such as “water hammer” events.
- Requires a detailed three dimensional profile of the dent from a “high resolution” inspection tool.
- The user has determined that the in-line inspection tool is sufficiently accurate to characterize the dent profile. In the case of tools that use mechanical finger technologies, the accuracy of the tool will depend upon the sensor spacing, the sensor stiffness and the speed of the tool.
- Does not predict the actual fatigue life of a dented pipe section, it is merely intended to provide guidance on the safe interaction distance measured from the peak of the dent to the seam weld location.
- Criteria was developed using the fatigue design curve for carbon steel welds in ASME Section 8, Div. III [F2] and is therefore limited to materials with an ultimate tensile strength less than 552 MPa (80 ksi).
- Assumed that the dent profile is nominally symmetrical around the dent peak and should not be used for significantly skewed dent profiles until further validation work can be carried out.
- The weld is assumed to be sound and free of manufacturing defects. The application of the long seam weld criteria to low frequency ERW pipe is not advisable given the potential for manufacturing defects (hook cracks, lack of fusion, etc.)
- Use of the criteria is subject to the approval of the applicable regulatory agency.

## F.2 EVALUATION OF THE INTERACTION OF DENTS AND LONG SEAM WELDS

- Step 1: Review the three–dimensional dent profile information supplied by the in-line inspection tool to determine that the dent profile is nominally symmetric either side of the dent peak in the circumferential direction.
- Step 2: Determine that the dent is acceptable from an ultimate strength perspective (i.e. the strain based criteria in ASME B31.8 [F1]).
- Step 3: If not generated automatically by the ILI tool software, generate a two-dimensional profile of the entire pipe circumference through the peak (maximum depth location) of the dent as shown in Figure F.1.

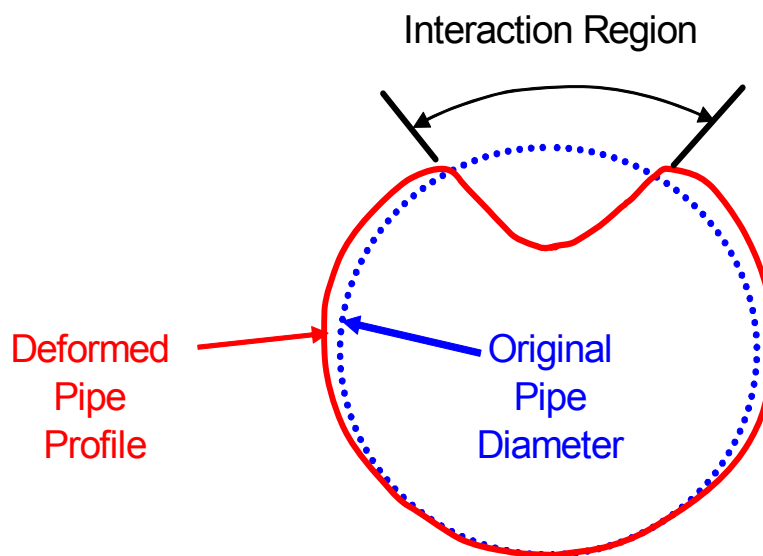


**Figure F.1: Circumferential Profile of the Pipe through the Dent Peak**

- Step 4: Determine the position of the weld seam. If the weld seam lies within the region of inward radial deflection (Interaction Region), the weld will interact with the dent to reduce the fatigue life of the pipe segment. If the weld is located outside of the Interacting Region the dent and weld do not interact.

## F.3 EVALUATION OF THE INTERACTION OF DENTS AND GIRTH WELDS

- Step 1: Review the three–dimensional dent profile information supplied by the in-line inspection tool to determine that the dent profile is nominally symmetric either side of the dent peak in the axial direction.
- Step 2: Determine that the dent is acceptable from an ultimate strength perspective (i.e., the strain based criteria in ASME B31.8 [F1]).

Step 3: If not generated automatically by the ILI tool software, generate a two-dimensional profile through the dent peak (maximum depth location) in the axial orientation as shown in Figure F.2.

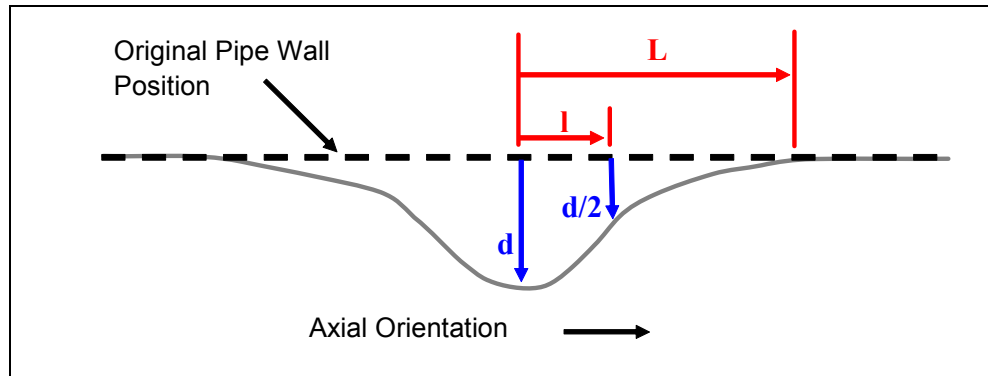


**Figure F.3: Profile through the Peak of the Dent in the Axial Orientation**

Step 4: Calculate the following parameters

Strength Ratio (SR):	The pipe material ultimate tensile strength (in practical terms the specified minimum ultimate strength) divided by 552 MPa (80 ksi)
Pipe D/t Ratio (D/t):	Nominal outside diameter (D) divided by the nominal pipe wall thickness (t).
Dent Depth (d):	Dent depth as a percentage of the pipe's nominal outside diameter
Depth/Length Ratio ( $d/\sqrt{L}$ ):	Depth of the dent (d) in mm divided by the square root of the length of the dent shoulder in mm (L).
Axial Sharpness ( $l/\sqrt{L}$ ):	Distance from the dent peak to the location of the half peak height (l) divided by the square root of length of the dent shoulder (L).

Step 5: Characterize the typical operating pressure spectrum of the pipeline system using a cycle counting algorithm [F3] (rainflow counting algorithm is recommended). The pressure spectrum used should be representative of the operation of the pipeline system over its entire service life assuming that the dent has been present for the entire time.

Step 6: Using the results from Step 4, determine whether the operation of the pipeline can be best describe as operating primarily (i.e. greater than 80% of the time) in one of the following pressure fluctuation ranges, defined in terms of maximum operating pressure (MOP):

- a. 75% to 100% MOP
- b. 50% to 100% MOP
- c. 25% to 100% MOP
- d. 0% to 100% MOP

Example 1: A steadily operating gas pipeline has a mean stress of 85% MOP and typical pressure cycle R-ratios (ratio of minimum to maximum pressure) of 0.9 generating typical pressure cycles from 80% to 90% MOP. This pipeline would be classified using the 75% to 100% MOP pressure fluctuation range.

Example 2: A liquid petroleum pipeline has a mean stress of 50% MOP and typical pressure cycle R-ratios of 0.5 generating typical pressure cycles from 33% to 67% MOP. This pipeline would be classified using the 25% to 100% MOP pressure fluctuation range.

If the pressure data is not available to characterize the typical pipeline operation then it would be conservative to assume that the pipeline typically operates in the 0% to 100% MOP range.

Step 7: Using the nominal operating pressure range, select the appropriate coefficients (A, B and C) from Table F.1 for each parameter calculated in Step 4 and calculate the minimum permissible interaction distance between the dent peak and the girth weld,  $I_{axial}$  (equation provides the distance in units of mm). If the distance between the dent peak and the weld is less than  $I_{axial}$  then they are considered to be interacting.

**Table F.1: Coefficients of Axial Interaction Distance Equation**

Pressure Range (% MOP)	Regression Equation Coefficients						Mean Error (mm)	Max Error (%)	Min Error (%)
	Coeff	SR	D/t	d	d/ $\sqrt{L}$	l/ $\sqrt{L}$			
75 – 100	A	415.82	0.02	66.46	265.25	-406.98	22	15	-11
	B	336.06	-4.56	-698.62	-350.33	1689.98			
	C	233.33	233.33	233.33	233.33	233.33			
50 – 100	A	87.16	-0.02	-157.18	-299.73	-7435.48	31	19	-12
	B	-252.71	2.23	1180.18	776.62	8277.58			
	C	-682.75	-682.75	-682.75	-682.75	-682.75			
25 – 100	A	183.85	-0.03	-167.01	-274.63	-8206.91	28	16	-9
	B	-225.83	4.11	1218.56	737.45	9402.45			
	C	-743.21	-743.21	-743.21	-743.21	-743.21			
0 – 100	A	-16.15	0.05	43.98	470.19	-7448.47	18	8	-4
	B	115.58	-10.07	-811.53	-600.68	10166.21			
	C	265.54	265.54	265.54	265.54	265.54			

$$I_{axial} = 1.2 \left[ A_{SR} (SR)^2 + B_{SR} (SR) + C_{SR} \right] + \left[ A_{D/t} \left( \frac{D}{t} \right)^2 + B_{D/t} \left( \frac{D}{t} \right) + C_{D/t} \right] + \left[ A_d (d)^2 + B_d (d) + C_d \right] + \left[ A_{d/\sqrt{L}} \left( \frac{d}{\sqrt{L}} \right)^2 + B_{d/\sqrt{L}} \left( \frac{d}{\sqrt{L}} \right) + C_{d/\sqrt{L}} \right] + \left[ A_{l/\sqrt{L}} \left( \frac{l}{\sqrt{L}} \right)^2 + B_{l/\sqrt{L}} \left( \frac{l}{\sqrt{L}} \right) + C_{l/\sqrt{L}} \right]$$

#### F.4 REFERENCES

- F1 American Society of Mechanical Engineers, ASME B31.8-2003, “Gas Transmission and Distribution Piping Systems.”
- F2 American Society of Mechanical Engineers, Boiler and Pressure Vessel Code, Section VIII, Division 3, “Alternative Rules for the Construction of High Pressure Vessels.”
- F3 ASTM Standard E 1049, “Standard Practices for Cycle Counting in Fatigue Analysis”, 1985, Reapproved 1997.



**APPENDIX G**  
**APPLICATION OF THE OVALITY-WELD**  
**INTERACTION CRITERIA**

## **G.1 RANGE OF APPLICABILITY OF OVALITY-WELD INTERACTION MODEL**

The ovality-weld interaction criteria presented in this document has been developed solely using finite element models and is based upon the modeling assumptions discussed in Section 4. It is subject to the following restrictions:

- Intended to consider the significance of ovality in pipe segments in the absence of secondary effects (such as dents, corrosion features, cracks).
- Intended to compliment and not supersede criteria governing the acceptability of ovality. For example, the allowable level of ovality will be limited by industry standards to ensure the prevention of pipe section collapse and the passage of in-line inspection tools (e.g. CSA Z662 [G1]). These criteria should be considered first and then the criteria developed herein should be applied to qualify the significance of any interaction with weld seams.
- Intended to evaluate the long term performance of the ovalized pipe segment when subjected to normal operational pressure cycles. It should not be used for pipeline subjected to frequent and severe upset conditions such as “water hammer” events.
- Requires information describing the largest and smallest diameter of the pipe segment and the relative position of the weld seam that may be derived from in-line inspection or field measurements.
- Assumes that the user has determined that the inspection data is sufficiently accurate.
- Does not predict the actual fatigue life of a ovalized pipe section, it is merely intended to provide guidance on the included angle about the centre of the maximum diameter within which the fatigue life of a weld will be significantly affected by the ovality.
- Criteria was developed using the fatigue design curve for carbon steel welds in ASME Section 8, Div. III [G2] and is therefore limited to materials with an ultimate tensile strength less than 552 MPa (80 ksi).
- The weld is assumed to be sound and free of manufacturing defects. The application of the long seam weld criteria to low frequency ERW pipe is not advisable given the potential for manufacturing defects (hook cracks, lack of fusion, etc.)
- Use of the criteria is subject to the approval of the applicable regulatory agency.

## **G.2 EVALUATION OF THE INTERACTION OF OVALITY AND LONG SEAM WELDS**

Step 1: Collect pipe minimum and maximum pipe diameter at a given ovalized pipe section and relative position of the weld seam in degrees around the pipe circumference using the pipe surface maximum diameter point as the zero angle reference.

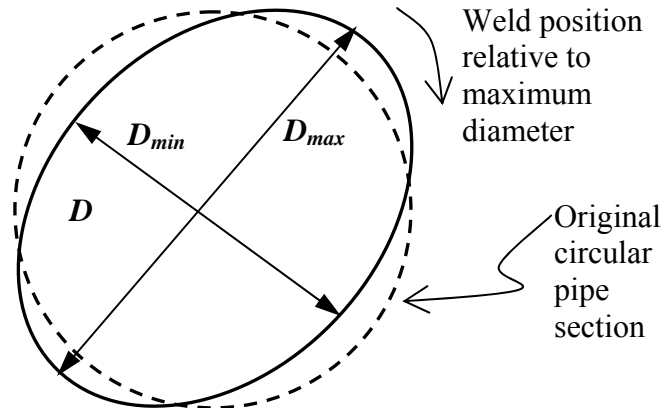


**Figure G.1: Ovalized Pipe Geometry**

Step 2: Calculate the ovality ( $\omega$ ) as defined as follows:

$$\omega = \frac{D_{max} - D_{min}}{D_{av}} \times 100$$

Step 3: Determine that ovality is acceptable from an ultimate strength perspective and ILI tool passage based upon applicable standard.

Step 4: Using Figure G.2, estimate the zero pressure residual ovality, based on the measured ovality, the internal pressure at the time of inspection, and the pipe D/t ratio.

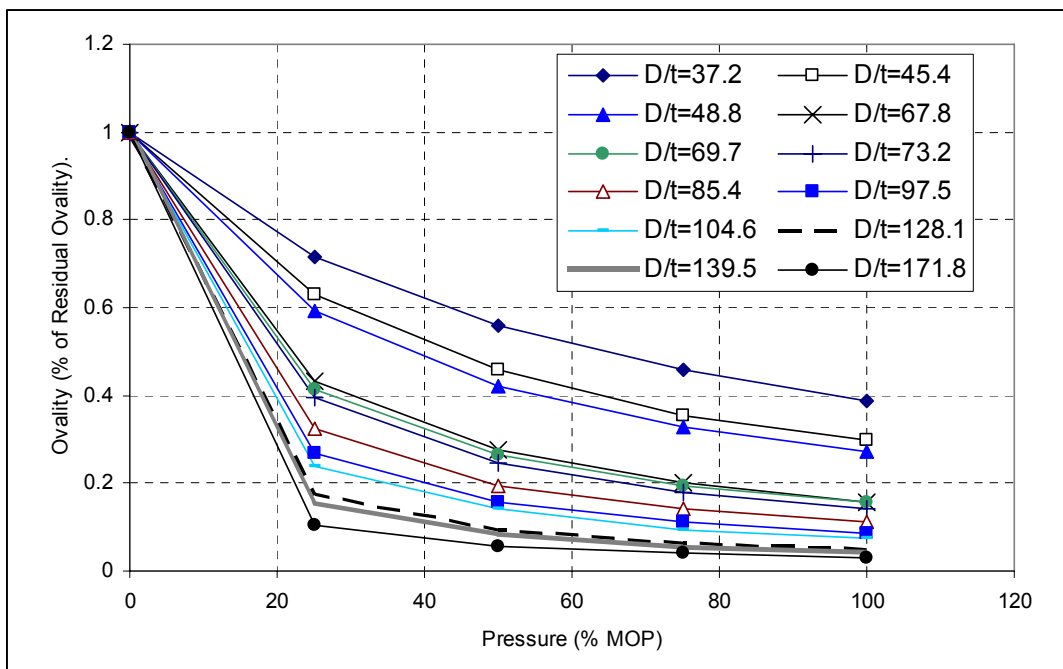


**Figure G.2: Residual Zero Pressure Ovality vs. Internal Pressure**

- Step 5: Characterize the typical operating pressure spectrum of the pipeline system using a cycle counting algorithm [G3] (rainflow counting algorithm is recommended). The pressure spectrum used should be representative of the operation of the pipeline system over its entire service life assuming that the ovality has been present for the entire time.
- Step 6: Using the results from Step 4, determine whether the operation of the pipeline can be best describe as operating primarily (i.e. greater than 80% of the time) in one of the following pressure fluctuation ranges, defined in terms of maximum operating pressure (MOP):
- e. 75% to 100% MOP
  - f. 50% to 100% MOP
  - g. 25% to 100% MOP
  - h. 0% to 100% MOP

Example 1: A steadily operating gas pipeline has a mean stress of 85% MOP and typical pressure cycle R-ratios (ratio of minimum to maximum pressure) of 0.9 generating typical pressure cycles from 80% to 90% MOP. This pipeline would be classified using the 75% to 100% MOP pressure fluctuation range.

Example 2: A liquid petroleum pipeline has a mean stress of 50% MOP and typical pressure cycle R-ratios of 0.5 generating typical pressure cycles from 33% to 67% MOP. This pipeline would be classified using the 25% to 100% MOP pressure fluctuation range.

If the pressure data is not available to characterize the typical pipeline operation then it would be conservative to assume that the pipeline typically operates in the 0% to 100% MOP range.

- Step 7: If the operating pressure ranges fall in the 0 to 25% MOP range no significant interaction zone exists.
- Step 8: Since ovality will always reduce the fatigue life of a pipe segment in the presence of fluctuating pressures, a target relative life fraction (*R.L*) should be selected which defines the acceptable fatigue life of the ovalized pipe relative to a circular pipe. This parameter can be set by the user or regulator to define the life reduction that would be acceptable for an ovalized pipe scenario. It is suggested that a value of 0.75 be used for *R.L*.
- Step 9: Based on Table G.1, determine whether the combination of parameters describing the ovalized pipe scenario ( $\omega$ ,  $D/t$ ,  $P.R.$ ,  $R.L$ ) represents a shaded cell. If the combination does not represent a shaded cell then no significant interaction zone exists for the scenario. If the combination represents a shaded cell proceed to Step 10.
- Step 10: Calculate the angle defining the zone of significant weld interaction using the critical angle,  $\alpha_{crit}$ , measured from the peaks of the ovalized using the following equation:

$$\alpha_{crit} = \beta \left( \left[ a \left( \frac{D}{t} \right)^2 + b \left( \frac{D}{t} \right) \right] + [c(\omega)^w + d(\omega)] + [e(R.L.)^2 + f(R.L.)] + g \right)$$

where the regression coefficients are summarized in Table G.2.

**Table G.2: Ovality - Dent Interaction Criteria – Significant Scenarios**

	D/t	37.1	45.4	48.8	67.8	69.7	73.2	85.4	97.5	104.6	128.1	139.5	170.8	
Ovality	P.R.	Relative Life (R.L)												
(%)	(% MOP)													
1	50	90	90	90	90	90	90	90	90	90	90	90	90	
		75	75	75	75	75	75	75	75	75	75	75	75	
		50	50	50	50	50	50	50	50	50	50	50	50	
	75	90	90	90	90	90	90	90	90	90	90	90	90	90
		75	75	75	75	75	75	75	75	75	75	75	75	75
		50	50	50	50	50	50	50	50	50	50	50	50	50
	100	90	90	90	90	90	90	90	90	90	90	90	90	90
		75	75	75	75	75	75	75	75	75	75	75	75	75
		50	50	50	50	50	50	50	50	50	50	50	50	50
2	50	90	90	90	90	90	90	90	90	90	90	90	90	
		75	75	75	75	75	75	75	75	75	75	75	75	
		50	50	50	50	50	50	50	50	50	50	50	50	
	75	90	90	90	90	90	90	90	90	90	90	90	90	90
		75	75	75	75	75	75	75	75	75	75	75	75	75
		50	50	50	50	50	50	50	50	50	50	50	50	50
	100	90	90	90	90	90	90	90	90	90	90	90	90	90
		75	75	75	75	75	75	75	75	75	75	75	75	75
		50	50	50	50	50	50	50	50	50	50	50	50	50
3	50	90	90	90	90	90	90	90	90	90	90	90	90	
		75	75	75	75	75	75	75	75	75	75	75	75	
		50	50	50	50	50	50	50	50	50	50	50	50	
	75	90	90	90	90	90	90	90	90	90	90	90	90	90
		75	75	75	75	75	75	75	75	75	75	75	75	75
		50	50	50	50	50	50	50	50	50	50	50	50	50
	100	90	90	90	90	90	90	90	90	90	90	90	90	90
		75	75	75	75	75	75	75	75	75	75	75	75	75
		50	50	50	50	50	50	50	50	50	50	50	50	50
4	50	90	90	90	90	90	90	90	90	90	90	90	90	
		75	75	75	75	75	75	75	75	75	75	75	75	
		50	50	50	50	50	50	50	50	50	50	50	50	
	75	90	90	90	90	90	90	90	90	90	90	90	90	90
		75	75	75	75	75	75	75	75	75	75	75	75	75
		50	50	50	50	50	50	50	50	50	50	50	50	50
	100	90	90	90	90	90	90	90	90	90	90	90	90	90
		75	75	75	75	75	75	75	75	75	75	75	75	75
		50	50	50	50	50	50	50	50	50	50	50	50	50
5	50	90	90	90	90	90	90	90	90	90	90	90	90	
		75	75	75	75	75	75	75	75	75	75	75	75	
		50	50	50	50	50	50	50	50	50	50	50	50	
	75	90	90	90	90	90	90	90	90	90	90	90	90	90
		75	75	75	75	75	75	75	75	75	75	75	75	75
		50	50	50	50	50	50	50	50	50	50	50	50	50
	100	90	90	90	90	90	90	90	90	90	90	90	90	90
		75	75	75	75	75	75	75	75	75	75	75	75	75
		50	50	50	50	50	50	50	50	50	50	50	50	50
6	50	90	90	90	90	90	90	90	90	90	90	90	90	
		75	75	75	75	75	75	75	75	75	75	75	75	
		50	50	50	50	50	50	50	50	50	50	50	50	
	75	90	90	90	90	90	90	90	90	90	90	90	90	90
		75	75	75	75	75	75	75	75	75	75	75	75	75
		50	50	50	50	50	50	50	50	50	50	50	50	50
	100	90	90	90	90	90	90	90	90	90	90	90	90	90
		75	75	75	75	75	75	75	75	75	75	75	75	75
		50	50	50	50	50	50	50	50	50	50	50	50	50

**Table G.2: Regression Equation Constants**

Parameter	Pressure Range (% MOP)		
	0% to 100%	25% to 100%	50% to 100%
<b>A</b>	<b>0.0008</b>	<b>-0.0003</b>	<b>-0.001</b>
<b>B</b>	<b>-0.334</b>	<b>-0.180</b>	<b>-0.166</b>
<b>C</b>	<b>-1.266</b>	<b>-0.414</b>	<b>-0.581</b>
<b>D</b>	<b>15.905</b>	<b>6.350</b>	<b>8.631</b>
<b>E</b>	<b>130.904</b>	<b>43.976</b>	<b>41.445</b>
<b>F</b>	<b>-88.533</b>	<b>-18.539</b>	<b>-12.040</b>
<b>G</b>	<b>21.166</b>	<b>18.295</b>	<b>7.814</b>
<b>Scale Factor <math>\beta</math></b>	<b>1.2</b>	<b>1.2</b>	<b>1.3</b>

Step 11: If the weld seam lies within the zone defined by the interaction angle, the weld will interact with the ovality to reduce the fatigue life of the pipe segment. If the weld is located outside of the Interacting Region the ovality and weld do not interact.

### **G.3 EVALUATION OF THE INTERACTION OF OVALITY AND GIRTH WELDS**

The development of a girth weld interaction criteria for ovality is not viable since both features extend around the entire pipe circumference. The criteria developed for long seam welds could be used to define areas in a girth weld that would have seen more severe cyclic loading and deserve additional attention during field inspection.

### **G.4 REFERENCES**

- G1 American Society of Mechanical Engineers, ASME B31.8-2003, "Gas Transmission and Distribution Piping Systems."
- G2 CSA Z662-03, "Oil and Gas Pipeline Systems", CSA.
- G3 ASTM Standard E 1049, "Standard Practices for Cycle Counting in Fatigue Analysis", 1985, Reapproved 1997.



**APPENDIX H**  
**APPLICATION OF THE WRINKLE-WELD**  
**INTERACTION CRITERIA**

## H.1 RANGE OF APPLICABILITY OF DENT-WELD INTERACTION MODEL

The wrinkle-weld interaction criteria presented in this document has been develop solely using finite element models and is based upon the modeling assumptions discussed in Section 5. It is subject to the following restrictions:

- Intended for plain wrinkles that are not considered to be growing. The primary fluctuating load considered in these interaction criteria is internal pressure. Wrinkles subjected to significant thermal load fluctuations or changed in soil loads promoting permanent deformations are outside the scope of this work.
- Factors in addition to weld seams (i.e., corrosion related metal loss, gouges) have not been considered in the development of these interaction criteria.
- Intended to compliment and not supersede criteria governing the acceptability of wrinkles. For example, criteria in ASME B31.8 [H1] should first be used to determine that the wrinkle is acceptable prior to evaluating the permissible wrinkle-weld interaction distance.
- Intended to evaluate the long term performance of the wrinkled pipe segment when subjected to normal operational pressure cycles. It should not be used for pipeline subjected to frequent and severe upset conditions such as “water hammer” events.
- Requires a detailed three dimensional profile of the wrinkle from a “high resolution” inspection tool that can provide a detailed three dimensional profile of the wrinkle.
- Assumed that the user has determined that the in-line inspection tool is sufficiently accurate to characterize the wrinkle profile. In the case of tools that use mechanical finger technologies, the accuracy of the tool will depend upon the sensor spacing, the sensor stiffness, the speed of the tool and the interaction of the calliper arms with the wrinkle feature.
- Does not predict the actual fatigue life of a wrinkled pipe section, it is merely intended to provide guidance on the safe interaction distance measured from the peak of the wrinkle to the seam weld location.
- Criteria was developed using the fatigue design curve for carbon steel welds in ASME Section 8, Div. III [F2] and is therefore limited to materials with an ultimate tensile strength less than 552 MPa (80 ksi).
- Assumed that the wrinkle profile is nominally symmetrical around the wrinkle peak and should not be used for significantly skewed wrinkle profiles or multiple ripple wrinkles until further validation work can be carried out.
- The weld is assumed to be sound and free of manufacturing defects. The application of the long seam weld criteria to low frequency ERW pipe is not advisable given the potential for manufacturing defects (hook cracks, lack of fusion, etc.)
- If the pipe segment surrounding the wrinkle is ovalized, the ovality-weld interaction criteria should be applied to further define the interaction zone.
- Use of the criteria is subject to the approval of the applicable regulatory agency.

## H.2 EVALUATION OF THE INTERACTION OF WRINKLES AND LONG SEAM WELDS

- Step 1: Review the three-dimensional wrinkle profile information supplied by the in-line inspection tool to determine that the wrinkle profile is nominally symmetric either side of the wrinkle peak in the axial direction and that a plane of symmetry can be defined through the longitudinal axis of the pipe.
- Step 2: Determine that the wrinkle is acceptable from the point of view of the applicable pipeline standard (i.e., ASME B31.8 [H1]).
- Step 3: If not generated automatically by the ILI tool software, generate a two-dimensional profile through the wrinkle peak (maximum wrinkle height location) in the axial orientation as shown in Figure H.1.

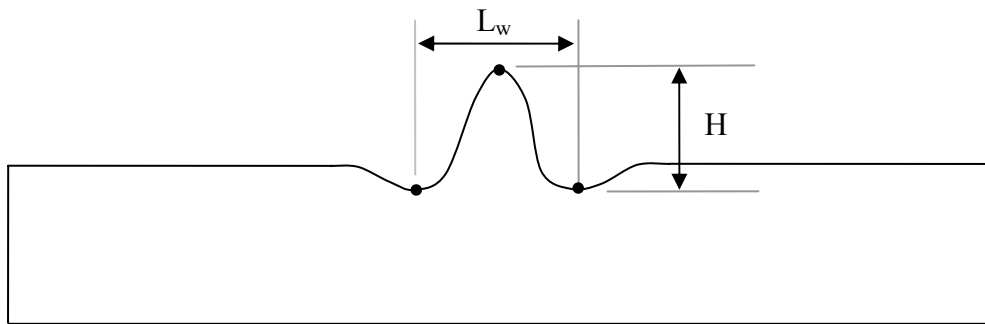


**Figure H.1: Profile through the Peak of the Wrinkle in the Axial Orientation**

- Step 4: Calculate the wrinkle shape ratio ( $H/L_w$ ) using the wrinkle height and length defined in Figure H.1.
- Step 5: Using the wrinkle aspect ratio ( $H/L_w$ ) and the material UTS calculate the angle ( $\theta$ ) defining the zone of long seam interaction with the wrinkle using the equation below:

$$\left(\frac{180}{\theta}\right)^2 = A \left(\frac{H}{L_w}\right)^B \frac{1}{SF}$$

where:  $A = 1.4492$  and  $B = -0.1049$   
 $\theta$  is the angular position from the wrinkle peak in degrees, as defined in Figure H.2  
 SF is the safety factor included in the criterion (1.2)  
 $H/L_w$  is the wrinkle shape ratio

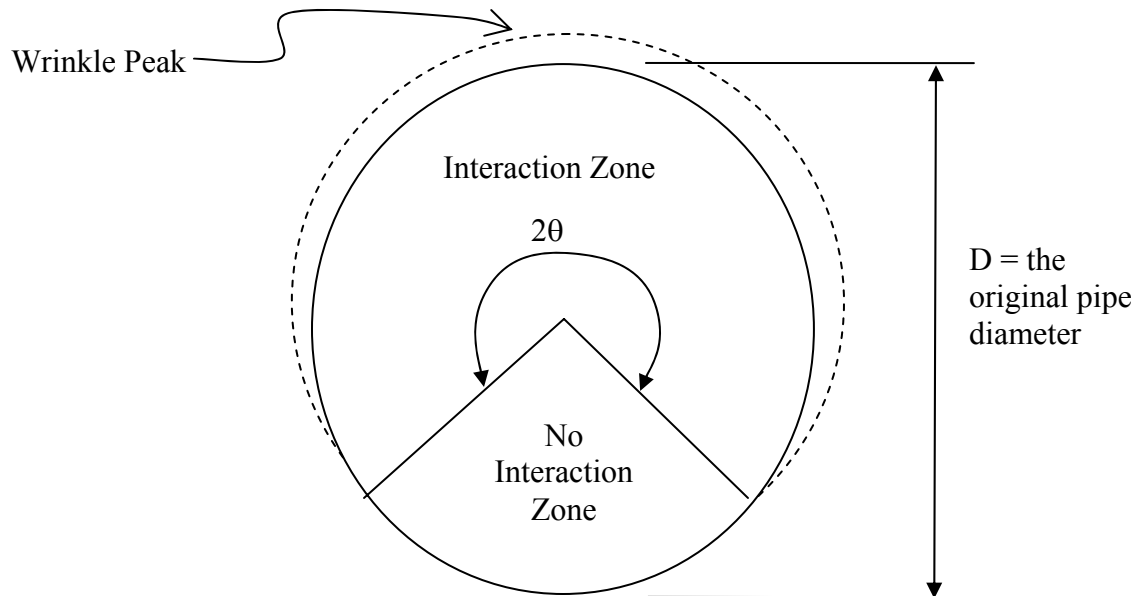


**Figure H.2: Wrinkle-Weld Interaction Angular Zone Definition**

Step 6: If the weld seam lies within the zone defined by the interaction angle ( $\theta$ ), the weld will interact with the wrinkle to reduce the fatigue life of the pipe segment. If the weld is located outside of the interaction Region the wrinkle and weld do not interact and can be considered independent pipe features.

### H.3 EVALUATION OF THE INTERACTION OF WRINKLES AND GIRTH WELDS

- Step 1: Review the three-dimensional wrinkle profile information supplied by the in-line inspection tool to determine that the wrinkle profile is nominally symmetric either side of the wrinkle peak in the axial direction and that a plane of symmetry can be defined through the longitudinal axis of the pipe.
- Step 2: Determine that the wrinkle is acceptable from the point of view of the applicable pipeline standard (i.e. ASME B31.8 [H1]).
- Step 3: If not generated automatically by the ILI tool software, generate a two-dimensional profile through the wrinkle peak (maximum wrinkle height location) in the axial orientation as shown in Figure H.1.
- Step 4: Calculate the wrinkle shape ratio ( $H/L_w$ ) using the wrinkle height and length defined in Figure H.1.
- Step 5: Characterize the typical operating pressure spectrum of the pipeline system using a cycle counting algorithm [H2] (rainflow counting algorithm is recommended). The pressure spectrum used should be representative of the operation of the pipeline system over its entire service life assuming that the wrinkle has been present for the entire time.

Step 6: Using the results from Step 4, determine whether the operation of the pipeline can be best describe as operating primarily (i.e. greater than 80% of the time) in one of the following pressure fluctuation ranges, defined in terms of maximum operating pressure (MOP):

- i. 75% to 100% MOP
- j. 50% to 100% MOP
- k. 25% to 100% MOP
- l. 0% to 100% MOP

Example 1: A steadily operating gas pipeline has a mean stress of 85% MOP and typical pressure cycle R-ratios (ratio of minimum to maximum pressure) of 0.9 generating typical pressure cycles from 80% to 90% MOP. This pipeline would be classified using the 75% to 100% MOP pressure fluctuation range.

Example 2: A liquid petroleum pipeline has a mean stress of 50% MOP and typical pressure cycle R-ratios of 0.5 generating typical pressure cycles from 33% to 67% MOP. This pipeline would be classified using the 25% to 100% MOP pressure fluctuation range.

If the pressure data is not available to characterize the typical pipeline operation then it would be conservative to assume that the pipeline typically operates in the 0% to 100% MOP range.

Step 7: Using the wrinkle shape ratio ( $H/L_w$ ), material UTS and the pressure range data (from Step 6) calculate the axial distance ratio ( $L_{ax}/D$ ) defining the zone of girth weld interaction with the wrinkle using the equation below:

$$\frac{L_{ax}}{D} = A \left( \frac{H}{L_w} \right)^B \left( \frac{552}{UTS} \right)^{0.0625} S_f$$

where:  $A=0.312$

$$B = -0.2922 * R - 0.1044$$

R is the pressure ratio = 0.25 for 75% to 100% MOP pressure fluctuation range  
 = 0.50 for 50% to 100% MOP pressure fluctuation range  
 = 0.75 for 25% to 100% MOP pressure fluctuation range  
 = 1.0 for 0% to 100% MOP pressure fluctuation range

SF is the safety factor included in the criterion (1.2)

UTS is the material minimum specified UTS in MPa

$H/L_w$  is the wrinkle shape factor

Step 8: If the distance between the wrinkle peak and the girth weld is less than  $L_{ax}$  then they are considered to be interacting. The interaction will serve to reduce the fatigue life of the pipe segment girth weld. If the weld is located outside of the interaction region the wrinkle and weld do not interact and can be considered independent pipe features.



#### **H.4 REFERENCES**

- H1 American Society of Mechanical Engineers, ASME B31.8-2003, “Gas Transmission and Distribution Piping Systems.”
- H2 ASTM Standard E 1049, “Standard Practices for Cycle Counting in Fatigue Analysis”, 1985, Reapproved 1997.